CONTENTS

Page

[1] Activities carried out in the frame of the Contract of Association EURATOM/IST and the Contract of Associated Laboratory.

[2] Activities performed in the frame of the Contract of Associated Laboratory, out of the Contract of Association EURATOM/IST.

1. INTRODUCTION

C. Varandas[1], F. Serra[2], L.O. Silva[3]

1.1. FOREWORD

This document describes the activities carried out in 2009 mainly in the frame of:

- The Contract of Association (CoA) signed in 1990 between the "European Atomic Energy Community" (Euratom) and IST, hereinafter referred to as Association Euratom/IST;
- The Contract of Associated Laboratory signed in 2001 by "Fundação para a Ciência e a Tecnologia" (FCT), hereinafter mentioned as Associated Laboratory (AL);
- Task Agreements with the European Fusion Development Agreement (EFDA);
- Contracts with the ITER International Organization (ITER IO);
- Projects of the general 7th Framework Programme of the European Unit;
- Projects of the European Space Agency (ESA);
- Projects funded by "Fundação para a Ciência e a Tecnologia".

"Instituto de Plasmas e Fusão Nuclear" (IPFN) developed in 2009 a very large variety of research, development, technology transfer, education, training and outreach activities in the main domains of our expertise: Plasma Physics and Engineering, Controlled Nuclear Fusion, Lasers and Photonics, Space and Advanced Computing. Some events should be underlined by their relevance: (i) maintenance of a very significant participation in the JET scientific exploitation (Figure 1.1); (ii) discussion and/or signature of the important contracts with F4E, ITER IO and ESA; (iii) increase of our collaboration with industry; and (iv) hiring of five Assistant Researchers in "Ciência-2009".

The quality of our research and development activities is well expressed by the scientific output presented in chapter 24 as well as by the international participation of several members of our staff in management bodies and in the organization of scientific conferences.

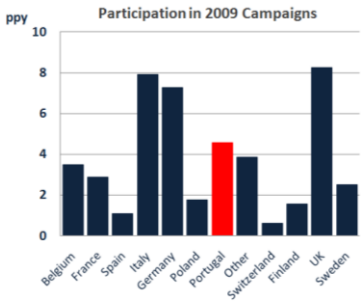

Figure 1.1 – Participation in the 2009 JET campaigns

1.2. ORGANIZATION

Figure 1.2 presents a block diagram of the IPFN organization. The scientific activity is organized in two Thematic Areas:

- Controlled Nuclear Fusion;
- Technologies of Plasmas and Intense Lasers.

and eight Scientific Groups:

- Experimental Physics on Magnetic Confinement Fusion Devices;
- Microwave Diagnostics for Fusion Plasmas;
- Theory and Modelling of Magnetic Confinement Fusion Plasmas;
- Control and Data Acquisition;
- Lasers and Plasmas;
- Gas Discharges and Gaseous Electronics;
- Quantum Plasmas;
- Fundamental Physics in Space.

1.3. ACTIVITIES ON CONTROLLED NUCLEAR FUSION

1.3.1. Introduction

These activities, carried out according to the Contract of Association Euratom/IST are described in chapters 2 to 12.

The CoA frames the Portuguese participation in the Euratom Specific Research and Training Programme in the Field of Nuclear Fusion Energy, hereinafter referred as Euratom Fusion Programme. This Programme has as its long-term objective the development of a prototype commercial fusion power plant. It is presently implemented through several Agreements, in particular: (i) Contracts of Association signed between Euratom and Institutions of the Member States of the European Union (EU) and Switzerland (Associates); (ii) the European Fusion Development Agreement (EFDA) and the Mobility Agreement, both signed by Euratom and its Associates; and (iii) the European Joint Undertaking for ITER and the Development of Fusion Energy (F4E), signed by Euratom, the EU Member States and Switzerland.

1.3.2. Main projects of the Association Euratom/IST

The work programme of the Association Euratom/IST included activities carried out in Portugal (mainly related with the tokamak ISTTOK) and abroad related with the operation and scientific exploitation of large and medium-sized tokamaks and stellarator (JET, ASDEX-Upgrade, TCV, and TJ-II) as well as with the design and construction of the next generation fusion devices (ITER

[1]President of IPFN.
[2]Vice-President of IPFN and Head of the Research Unit of the Contract of Association Euratom/IST.
[3]Vice-President of IPFN.

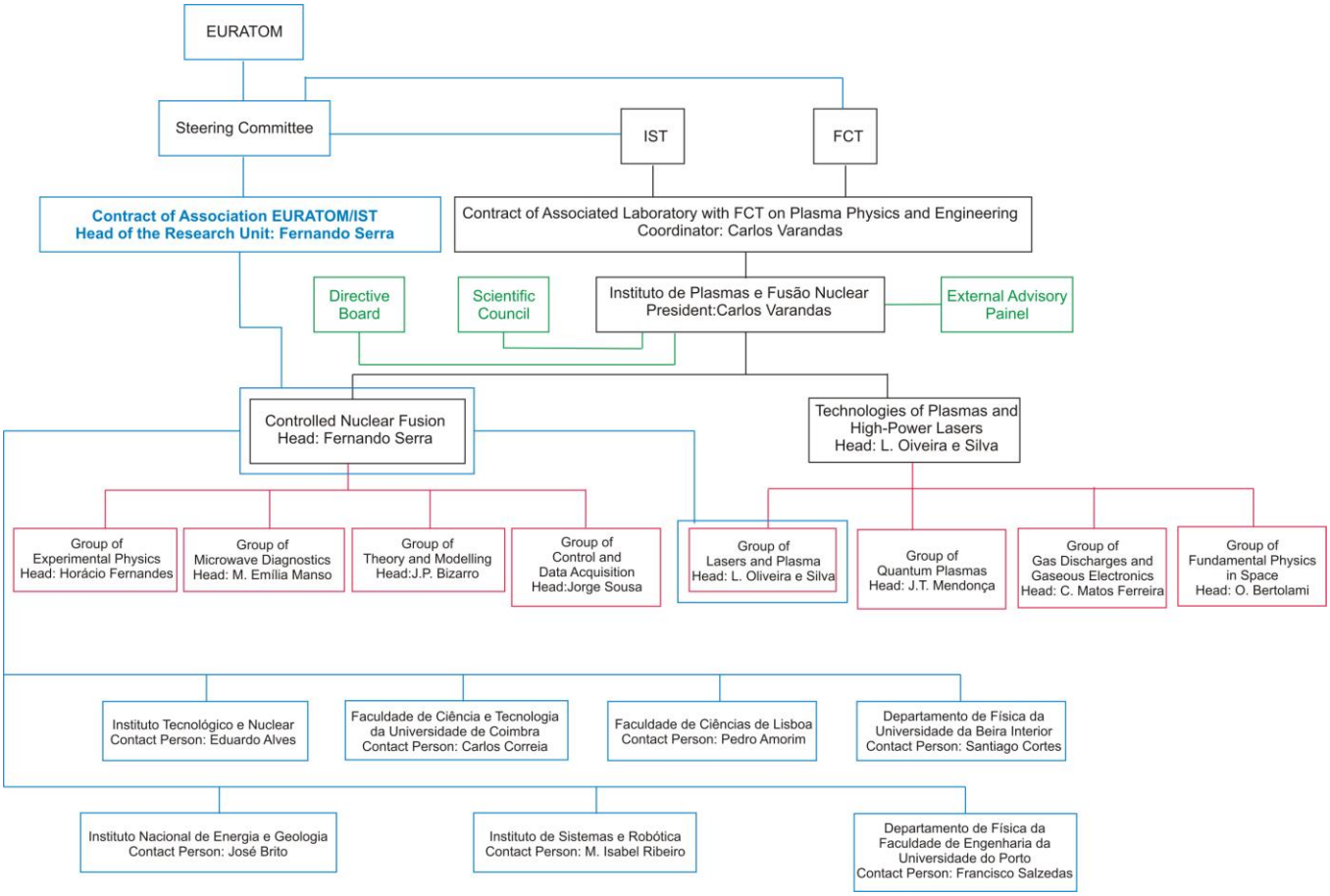

Figure 1.2 – Organization of IPFN

and W7-X). Its main projects in 2009 were:

- Tokamak ISTTOK;
- Participation in the ITER Project;
- Participation in the EFDA Programme;
- Participation in the collective use of the JET facilities by the EFDA Associates;
- Participation in the ASDEX-UPGRADE Programme;
- Participation in the TJ-II Programme;
- Participation in the COMPASS Project;
- Collaboration with the Association Euratom/CEA
- General activities on theory and modelling;
- Keep-in-touch activities on inertial fusion energy;
- Other fusion-related activities.

Table 1.1 presents information about the responsible person(s) and the Institutions involved in each project.

1.4. ACTIVITIES ON TECHNOLOGIES OF PLASMAS AND INTENSE PLASMAS

The activities carried out in the frame of this thematic area are described in chapters 13 to 23. The main projects in 2009 were:

- Plasma theory and simulations;
- New radiation sources from plasmas and optical physics;
- Laser-plasma accelerators and applications;
- High intensity laser science and technology;
- Coherent XUV sources and applications;
- Fast ignition and HiPER;
- Plasma Engineering Laboratory;
- Non-equilibrium kinetics and simulations of plasmas and afterglow plasmas;
- Modelling of plasma sources;
- Quantum plasmas;
- Fundamental physics in space.

Table 1.2 contains information about the responsible person(s) and the Institutions involved in each project.

Project	Responsible Person(s)	Collaborating Institutions	
		Portuguese	Other
Tokamak ISTTOK	Horácio Fernandes Carlos Silva	IPFN[3] UBI[4] CEI[5], CFA[6]	CIEMAT[7], IPP-Kharkov[8], UI[9], IFUR[10], IFUSP[11]
Participation in the ITER Project	Carlos Varandas Bruno Gonçalves	IPFN	EFDA CSU Garching
Participation in the EFDA Programme	Bruno Gonçalves Carlos Silva	IPFN	
Participation in the collective use of the JET Facilities by the EFDA Associates	Fernando Serra Bruno Gonçalves	IPFN, CEI, UBI	EFDA[12] CSU[13] Culham UKAEA[14]
Participation in the ASDEX Upgrade programme	Maria Emília Manso Fernando Serra	IPFN	IPP-Garching[15]
Participation in the TJ-II programme	Carlos Varandas Maria Emília Manso	IPFN	CIEMAT
Participation in the COMPASS Project	Carlos Varandas	IPFN	IPP.CR[16]
Collaboration with the Association Euratom/CEA	J. Pedro Bizarro	IPFN	
General activities on theory and modelling	J. Pedro Bizarro	IPFN	IFP[17], PT[18], DFRC[19]
Keep-in-touch activities on inertial fusion energy	J.T. Mendonça	IPFN	
Other fusion related activities	Carlos Varandas	IPFN	

Table 1.1 – Responsible person(s) and collaborating Institutions in the 2009 projects of the Association Euratom/IST

Project	Responsible Person(s)	Collaborating Institutions	
		Portuguese	Other
Plasma theory and simulations	L.O. Silva	IPFN, ISCTE[20], INESC-ID[21]	UCLA[22], UR[23], IC[24], RAL[25], MPIQO[26], PT[27]
New radiation sources from plasmas and optical physics	L.O. Silva J.M. Dias		
Laser-plasma accelerators and applications	L.O. Silva N. Lopes	IPFN, FCUL[28]	US[29], RAL, USa[30], OU[31]
High intensity laser science and technology	L.O. Silva G. Figueira	IPFN	
Coherent XUV sources and applications	L.O. Silva M. Fajardo	IPFN	LOA[32], PALS[33]
Fast ignition and HiPER	L.O. Silva J. Davies	IPFN	RLA, UPM[34], OsU[35], URLS[36], LULI[37]
Plasma Engineering Laboratory	C.M. Ferreira F.M. Dias	IPFN	US, RAL, OU
Non-equilibrium kinetics and simulations of plasmas and afterglow plasmas	C.M. Ferreira J. Loureiro	IPFN	UV-SA[38], LSGS[39], UP[40], LPTP[41], DFUM[42], RISSPO[43], IPT[44], FG[45], MU[46], BrU[47]
Modelling of plasma sources	C.M. Ferreira	IPFN, CFUM[48]	DFUC, CSI[49], LPGP[50], LPCE[51], LLAN[52], UV[53],
Quantum plasmas	J. Tito Mendonça	IPFN, UM[54]	RAL, UFF[55], UN[56], UAb[57], RUB[58]
Fundamental physics in space	Orfeu Bertolami	IPFN, CCTAE[59], UL[60]	ESA[61], JPL[62], ZARM BU[63]

Table 1.2 – Responsible person(s) and collaborating Institutions in the 2009 projects of the Associated Laboratory

[3] IPFN means "Instituto de Plasmas e Fusão Nuclear"
[4] UBI means "Universidade da Beira Interior"
[5] CEI means "Centro de Electrónica e Instrumentação da Faculdade de Ciências e Tecnologia da Universidade de Coimbra"
[6] CFA means "Centro de Física Atómica da Universidade de Lisboa"
[7] CIEMAT means "Centro de Investigaciones Energeticas Medioambientales y Tecnologicas"
[8] IPP- Kharkov means "Institute of Plasma Physics of the National Science Center" "Kharkov Institute of Physics & Technology".

[9] UI means “University of Innsbruck”.
[10] IFUR means “Institute of Physics of the University of Riga”
[11] IFUSP means “Instituto de Física da Universidade de São Paulo”
[12] EFDA means “European Fusion Development Agreement”
[13] CSU means “Close Support Unit”
[14] UKAEA means “United Kingdon Atomic Energy Authority”
[15] IPP-Garching means “Max-Planck-Institut für PlasmaPhysik”
[16] IPP.CR means “Institute for Plasma Physics – Czech Republic”
[17] IFP means “Istituto di Física del Plasma”
[18] PT means “Politécnico di Turino”
[19] DFRC means “Department de Recherches sur la Fusion Controlée”.
[20] ISCTE means “Instituto Superior de Ciências do Trabalho e Empresas”
[21] INESC-ID means “Instituto Nacional de Engenharia de Sistemas e Computadores – Investigação e Desenvolvimento”
[22] UCLA means “University of California Los Angeles”
[23] UR means “University of Rochester”
[24] IC means “Imperial College”
[25] RAL means “Rutherford Appleton Laboratory”
[26] MPIQO means “Max Planck Institute for Quantum Optics”
[27] PT means “Politécnico di Torino”
[28] FCUL means “Faculdade de Ciências da Universidade de Lisboa”
[29] US means “University of Strathclyde”
[30] USa means “University of Salamanca”
[31] OU means “Oxford University”
[32] LOA means “LOA/École Polytechnique”
[33] PALS means “Prague Asterix Laser System”
[34] UPM means “Universidad Politécnica de Madrid”
[35] OsU means “Osaka University”
[36] URLS means “University of Rome La Sapienza”
[37] LULI means “LULI/École Polytechnique”
[38] UV-SA means “Université de Versailles-Service d’Aéronomie”
[39] LSGS means “Laboratoire de Science et Génie des Surfaces”
[40] UP means “Université de Provence”
[41] LPTP means “Laboratoire de Physique et Technologie des Plasmas”
[42] DFUM means “Department de Physique, Université de Montréal”
[43] RISSPO means “Research Institute for Solid State Physics and Optics”
[44] IPT means “Moscow Institute of Physics and Technology”
[45] FG means “Fluid Gravity”
[46] MU means “Masaryk University”
[47] BrU means “Brno University of Technology”
[48] CFUM means “Centro de Física da Universidade do Minho”
[49] CSI means “Consejo Superior de Investigaciones Cientificas”
[50] LPGP means “Laboratoire de Physique dês Gaze t dês Plasmas”
[51] LPCE means “Laboratoire Plasmas et Conversion d’Énergie”
[52] LLAN means “Laboratoire dês Lésions dês Acides Nucléiques”
[53] UV means “Université de Versailles”
[54] UM means “Universidade do Minho”
[55] UFF means “Universidade Federal Fluminense do Rio de Janeiro”
[56] UN means “Université de Nice”
[57] UAb means “University of Aberdeen”
[58] RUB means “Ruhr Universtat Bochum”
[59] CCTAE means “Centro de Ciências e Tecnologias Aeronáuticas e Espaciais”
[60] UL means “Universidade Lusófona”
[61] ESA means “European Space Agency”
[62] JPL means “Jet Propulsion Laboratory”
[63] ZARM BU means “Bremen University”

2. TOKAMAK ISTTOK[1]

H. Fernandes, C. Silva (Heads), B.B. Carvalho, R. Coelho, B. Gonçalves, D. Alves, I. Carvalho, P. Carvalho, P.A. Carvalho, A. Duarte, P. Duarte, H. Figueiredo, J. Fortunato, R. Gomes, R. Henriques, R. Mateus, I. Nedzelskij, A. Neto, V. Plyusnin, T. Pereira, A. Soares, Y. Tashev, D. Valcárcel, C.A.F. Varandas

2.1. INTRODUCTION

This Project included in 2009 activities in the areas of:

- Study of fusion relevant materials;
- Real time control and data acquisition;
- Diagnostics;
- Plasma physics studies.

which have been carried out in the frame of:

- The General Support of the Contract of Association;
- The following EFDA Tasks:
  - Long-range correlations (WP08-09-TGS-01b);
  - Demonstration of liquid plasma facing components (WP09-PWI-06);
  - Physics of rotation in plasmas (WP09-TGS-02b);
  - Impurity flux in the boundary of fusion devices (WP09-TGS-02c).

2.2. STUDY OF FUSION RELEVANT MATERIALS[2]

The following tasks were performed in 2009:

- *Design and implementation of a vacuum chamber for degassing liquid metals and preparing high purity, oxide-free gallium*;
- *Preparation of gallium samples to be exposed to fusion plasmas* (Figure 2.1). The dynamics of gallium solidification process after high temperature degassing has been researched. It has been observed that this element may remains in liquid state down to -20º C (supercooling property) without freezing, requiring seeding by solid gallium to solidify at higher temperatures;

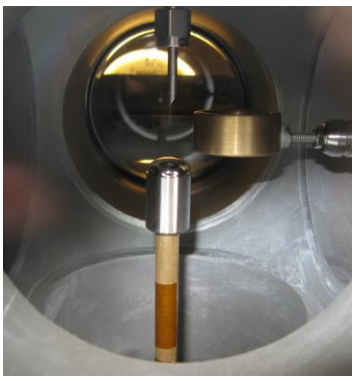

Figure 2.1 - Picture of the high purity gallium sample (and holder) to be exposed to the plasma.

- *Study of hydrogen retention in gallium* samples have been exposed to ISTTOK plasma during one week operation (~70 shots). Gallium hydrogen retention profiles (a few μm in depth) has been analyzed using ion beam techniques[3];
- *Exposure of several tungsten samples (wires and plates) to ISTTOK plasmas*, both during cleaning discharges and shots. Hydrogen retention has been investigated using ion beam techniques.

2.3. REAL TIME CONTROL AND DATA ACQUISITION

The following tasks were carried out in 2009:

- *Integration of three ATCA boards for control and data acquisition in ISTTOK.* Each board consists of 32 differential analog input channels, 18 bit resolution at 2 MSamples per Second (MSPS) with galvanic isolation;
- *Development of a link between the FireSignal System and the MARTe real-time executor using the HTTP MARTe interface.* This link allows configuration and data collection to the main database through FireSignal. Implementation and installation on ISTTOK tokamak, for the plasma position control system, using real-time tomography;
- *Use the tomography diagnostic for real-time plasma position control;*
- *Implementation of the tomographic algorithm Fourier-generic for control of the horizontal position of the plasma at ISTTOK.* The tomography plasma position was compared with three other diagnostics: the poloidal magnetic probe array, the cosine coil and the electrostatic (ES) probes. The cosine coil and ES probes are not absolutely calibrated, thus only a qualitative comparison was possible. The plasma position calculated by the tomography generally agrees with the other diagnostics, cross-correlating remarkably well with the cosine coil data (Figure 2.2). The tomography position control was successfully employed to maintain the plasma at the vessel axis with an error of the order of 1cm, which is the spatial resolution of the tomographic system;
- *Upgrade of the previous dsPIC controller board* to permit motor control capabilities and faster communication interfaces, allowing the future refurbishing of the ISTTOK slow control;

[1]Activities carried out in the frame of the Contract of Association Euratom/IST, the European Fusion Development Agreement and the Contract of Associated Laboratory, by staff of the Groups of Experimental Physics, Theory and Modelling and Control and Data Acquisition.
[2]Work in collaboration with Institute of Physics of the University of Latvia, ENEA-Frascati and "Instituto Tecnológico e Nuclear".
[3]Work made in EFDA Task WP09-PWI-06.

- *Upgrade of the vertical field power supply to provide currents from -500 A to 500 A.* The new power supply, built in site, is connected optically to the ATCA system, allowing the design of more complex controllers for the ISTTOK feedback, such as the tomography position feedback.
- *Development of the communication code between the plasma position controller and the stabilization power supplies* This communication protocol was designed to provide a fast (2 bytes×12 bit at 921.6 kbaud = 26 µs per command), simple (runs on a microcontroller) and yet reliable (has 4 bits of redundancy plus a parity bit in each byte) communication between the two systems. The plasma position controller normally hosts of the communications and the current power supplies reply with their status or with their measured current, depending on the command. When there is a major fault in the power supplies, they go to a safe state and send the corresponding error code. This communication protocol was tested successfully in ISTTOK and will be used in the COMPASS fast amplifiers.

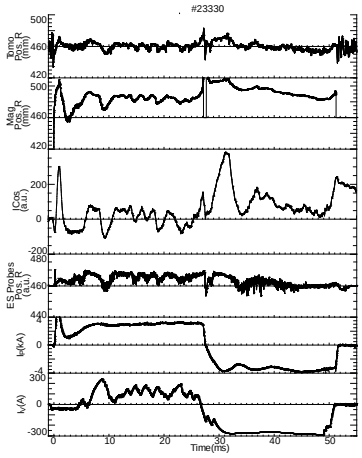

Figure 2.2 - Horizontal plasma position, determined by tomography, Mirnov coils (Mag), cosine coil (ICos) and electrostatic (ES) probes. The plasma current (I_P) and vertical field coil current (I_V) are also shown.

2.4. DIAGNOSTICS

The following activities have been made:

- *Installation and test of a 4-channel Cherenkov-type detector to investigate the energetic electrons characteristics*[4]. A prototype of 4-channel detector made of AlN poly-crystals with molybdenum filters was designed and used in the ISTTOK tokamak. Test-stand studies of filters with different thicknesses (1, 3, 7, 10, 20, 50 and 100 µm) have shown that they should allow the detection of electrons with energies higher than 69, 75, 87, 95, 120, 181 and 260 keV, respectively. Experiments in ISTTOK have shown that this detector is suitable to measure different fast electrons populations simultaneously (Figure 2.3). However, problems with the thickest deposits were found and therefore a new improved technique for Mo coating is required for future experiments. Furthermore, changes in the detector design are required to increase the detector collecting surface as well as its sensitivity;

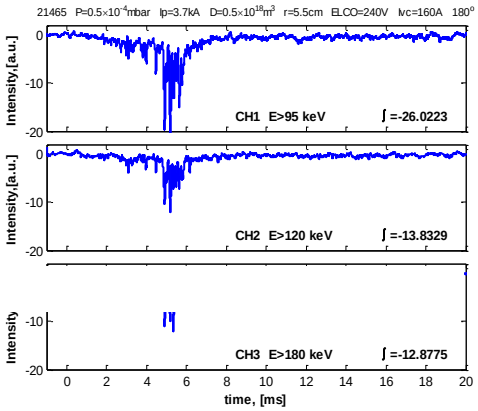

Figure 2.3 - Signals characterizing fast electron populations with different energies.

- *Design, construction and scientific exploitation of four multi-pin probe systems (Figure 2.4) installed at different poloidal positions (θ= 0º, 90º, 180º and 270º) in the ISTTOK edge plasma.* These probe systems permit the simultaneous determination of several plasma parameters including: floating potential, ion saturation current, turbulent particle flux, parallel flow and poloidal electric field. The properties of the fluctuations associated with these quantities can also be investigated as signals are recorded at 2 MHz. Such a probe system allows a comprehensive characterization of the edge plasma properties and the study of the poloidal asymmetries;
- *Installation of a diagnostic system to study the possible link between the SOL intermittent transport and the impurity influx from the wall.* The diagnostic consists of a graphite plate instrumented with Langmuir probes installed in a radially movable system to be exposed to the ISTTOK plasma. An optic system to measure with high temporal resolution the influx of impurities from that plate was also developed based on a photomultiplier tube and an interference filter. This diagnostic system allows the simultaneous measurement of the density fluctuations and the impurities influx in the same region with a high temporal resolution[5];
- *Design, construction and scientific exploitation of a mass-sensitive ion probe.* The mass-sensitive ion probe (MSIP) operation consists of the time-of-flight (TOF) analysis of burst ions excited by a short (µs-range) voltage pulse applied to small grid immersed into the plasma. The ions in the burst propagate along the magnetic field lines of the tokamak with velocities determined by the value of the applied voltage and by the ions mass/charge (m_i/Z_i) ratio. The grid bursts of ions, separated along some distance (TOF path) due to their different mass and charges, are detected by a retarding field energy analyzer (RFEA). The MSIP has been tested in SOL plasma of the

[4]Work in collaboration with Association EURATOM-IPPLM.
[5]Work performed in EFDA Task WP09-TGS-02C.

tokamak ISTTOK and results allowed the identification of ions such as H^+, C^{2+}, C^{3+}, O^+, O^{2+}, Cr^{2+} and Cr^{3+} (Figure 2.5). Results also indicate that the content of several impurity ions (mainly carbon and oxygen) in the SOL is comparable to that of the main ion;

- *Design and construction of low cost photodiodes for fluctuation studies.* A high gain (10^8) and medium bandwidth (50 kHz) transimpedance amplifier was designed and tested for line radiation detection to be used for fluctuation studies in the ISTTOK edge plasma;
- *Operation of the heavy ion beam diagnostic for fluctuations studies.* The nσ fluctuations measurements across the whole plasma cross-section have been performed with three Xe^+ beam energies: 22 keV, 24 keV and 26 keV. The symmetric top-bottom nature of GAM-like fluctuations has been identified.

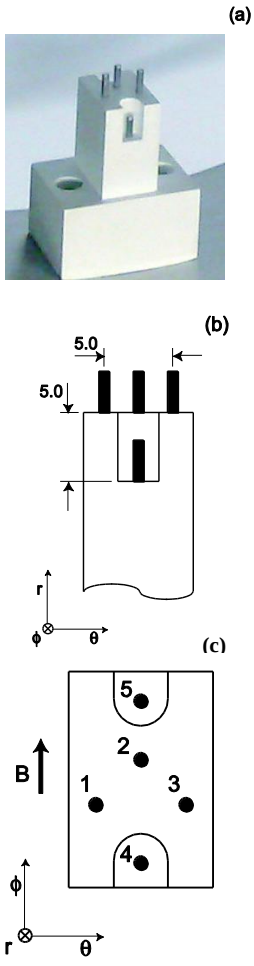

Figure 2.4 - Probe system used for the measurement of the poloidal asymmetries on the ISTTOK tokamak. The pins are cylindrical and measure either the floating potential or the ion saturation current. All lengths are given in millimeters.

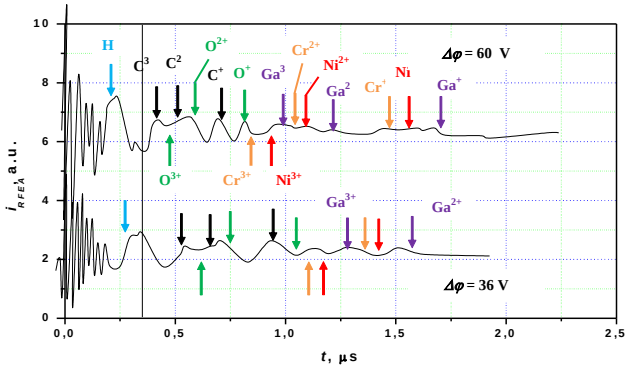

Figure 2.5 - Two mass-sensitive ion probe signals measured with $\Delta\varphi$ = 60 V, RFEA retarding potential U_{RFEA} = 50 V (top trace), and $\Delta\varphi$ = 36 V, U_{RFEA} = 10 V (bottom trace).

2.5. PLASMA PHYSICS STUDIES

Plasma physics studies have been carried out related with:

- Characterization of Geodesic Acoustic Modes;
- Study of the edge plasma poloidal asymmetries;
- Study of the parallel and poloidal flows in the ISTTOK edge plasma.

2.5.1. Characterization of Geodesic Acoustic Modes on the ISTTOK edge plasma[6]

The fluctuations in the ISTTOK boundary plasma have been investigated using two probe systems that allow the simultaneous measurement of the long distance correlation in the toroidal and poloidal direction as well as the radial structure of the fluctuations with high temporal resolution. It has been found previously that the floating potential fluctuations exhibit a significant toroidal correlation at large distances that can be attributed to the geodesic acoustic mode (GAM). *A detailed characterization of the GAM radial, poloidal and toroidal structure and its influence on turbulence and transport have been performed*, being the following observations reported: (i) Radially resolved measurements indicate that GAMs are localized just inside the LCFS position in a region with at least 1.5 cm of radial extension; (ii) GAM features such as the radial and poloidal structure are also in agreement with the theoretical predictions. The amplitude of the GAM density fluctuations shows a poloidal variation being smaller at the mid-plane position. At the plasma top, the amplitude of the GAM fluctuations in potential is typically 5 times larger than that in density. Furthermore, it was shown that GAMs have a finite wavelength in the radial direction ($k_r \approx 1.5$ cm^{-1}); (iii) The GAM amplitude and the long-range correlations are highly intermittent. Experimental evidence was found suggesting that GAMs modulate the long-range correlations and the ambient turbulent fluctuations (Figure 2.6). This result indicates that GAMs may regulate the turbulent fluctuations; (iv) The turbulent particle transport is small in the GAM dominated region as the phase

[6]Activities performed in the EFDA Task WP-08-09-TGS-01b.

between I_{sat} and E_θ fluctuations is modified in such a way that the time-averaged radial transport is reduced.
The comprehensive range of experimental observations performed allowed a clear identification of GAMs on the ISTTOK edge plasma and the conclusion that GAMs play an important role in controlling turbulence and the consequent transport. These findings provide also direct evidence of multi-scale physics in the regulation of transport mechanisms in the edge of fusion plasmas;

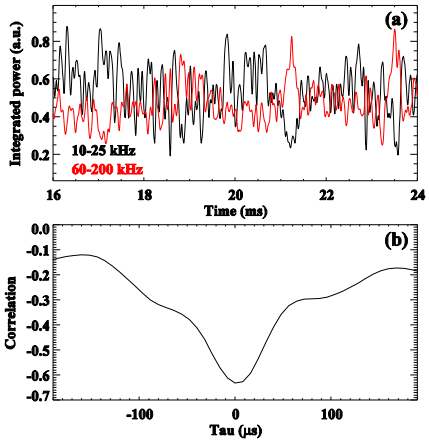

Figure 2.6 - (a) Amplitude of the V_f power spectrum in the range 10-25 kHz and 60-200 kHz. (b) Cross-correlation between V_f (10-25 kHz) and V_f (60-200 kHz).

2.5.2. Poloidal asymmetries in the ISTTOK edge plasma

For the typical toroidal field (B_T) direction used on ISTTOK (B×∇B drift direction upwards), *the edge plasma density and turbulent particle flux are found to be larger at the low field side and top of the device, suggesting an asymmetric transport.* Results indicate therefore that the constant pressure surfaces are not coincident with the constant magnetic flux surfaces. Strong poloidal asymmetries are also observed in the parallel flows, which is negative (relative to the B_T direction) at the high field side and positive in the other locations. Furthermore, large poloidal electric fields are identified, suggesting the existence of convective cells that can significantly modify the radial particle transport;

2.5.3. Study of the parallel and poloidal flows in the ISTTOK edge plasma[7]

A set of three probe arrays (radial, poloidal and gundestrup) was used during a large series of discharges on ISTTOK. Radial profiles (from near vessel position up to 3 cm inside the last closed flux surface, LCFS) of plasma flow, particle transport, density and radial electric field were obtained. Flow measurements provided by the gundestrup probe were tested for consistency with the results obtained from the other probes through the radial force balance equation. It was found that only in a limited region of the plasma (from the limiter up to 2 cm inside the LCFS) this validation is achieved for both plasma configurations, ohmic and edge biased. Further statistical analysis of the fluctuating edge plasma parameters allowed two other estimates for the plasma poloidal velocity: i) by the poloidal phase velocity of turbulence measured with poloidally separated probes using the two-point correlation method; ii) by the phase velocity derived from the two-point statistical dispersion relation of poloidally separated probes. As shown in Figure 2.7, a good agreement on a limited region of the edge plasma was found between these estimates and the measurements provided by the Gundestrup probe.

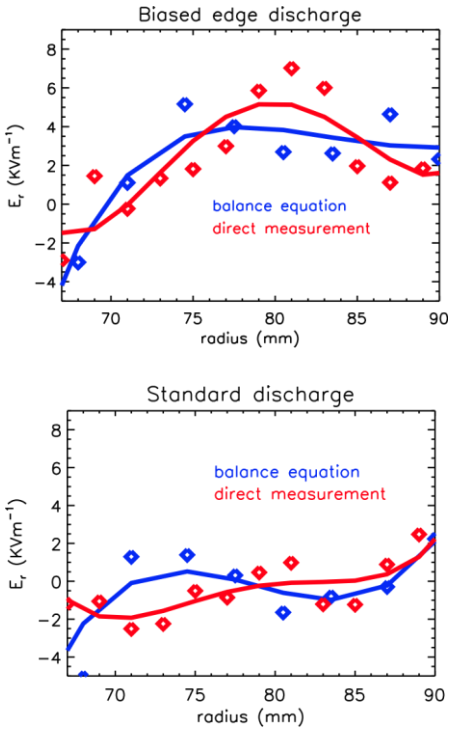

Figure 2.7 - Comparison of the measured radial electric field with that obtained from the force balance equation for discharges with and without electrode biasing.

[7]Work carried out in the EFDA Task WP09-TGS-02b.

3. PARTICIPATION IN THE ITER PROJECT[1]

C.A.F. Varandas (Head), B. Gonçalves (Deputy Head), J. Belo, J.P. Bizarro, L. Cupido, H. Fernandes, M.E. Manso, M.I. Ribeiro, J. Santos, F. Serra, A. Silva, A. Vale, P. Varela, R. Igreja, R. Patrício, J. Ricardo.

3.1. INTRODUCTION

The Portuguese participation in the ITER project included in 2009 activities in the areas of:

- Remote Handling;
- Control and Data Acquisition;
- Microwave Reflectometry;
- Theory and Modelling;
- Heating Systems;
- System Integration.

carried out in the frame of grants and contracts with Fusion for Energy and ITER International Organization as well as on the basis of voluntary contributions in preparation for further calls.

IPFN provided also technical support to the Portuguese industry aiming at its participation in the ITER project.

3.2. REMOTE HANDLING[2]

Remote Handling (RH) is an absolute required feature of ITER not only during nominal operation, but also during rescue and recovery situations. Among the various RH systems and sub-systems, a Transfer Cask System (TCS) has been adopted as the reference solution for the transportation of casks to/from vacuum vessel ports in all levels of the Tokamak Building (TB) and ports in the Hot Cell Building (HCB). The TCS is composed by a cask that enclosures the load, a pallet that holds the cask and an Air Transfer System (ATS) that is a mobile platform with a double set of pivoting drive wheels powered by electric motors, air-bearings and batteries on-board.

Developments and studies in the topic of path planning and trajectory following of the TCS/ATS inside the TB and HCB were performed in 2009.

The TCS path optimization algorithm developed in 2008 was improved, incorporating optimization criteria to maximize the clearance to the closest obstacles and to guarantee the smoothness of the path. *The algorithm was also extended to incorporate maneuvers*, i.e., path topologies where the TCS stops to change its orientation.

The proposed planning algorithm for the TCS was applied in the latest models of the TB and HCB. A total of 63 trajectories were calculated: 46 trajectories in TB (28 without maneuvers and 18 with at least a maneuver), and 17 trajectories in HCB. Figure 3.1 represents the set of optimal trajectories and the area spanned by the TCS in the Divertor level of TB. For each trajectory, the distance to the closest obstacle along the TCS motion is evaluated, together with the proposed TCS velocity profile along the path. The TCS velocity is proposed to be proportional to the distance to the nearest obstacle with a maximum speed of 20 cm/s when the minimum distance is above 1 meter. (Figure 3.2) displays a trajectory in the Equatorial level of TB with two maneuvers, and the corresponding evolution of the distance to the closest obstacle and the velocity profile. Statistical results on the set of trajectories, with emphasis on their length and time duration were evaluated.

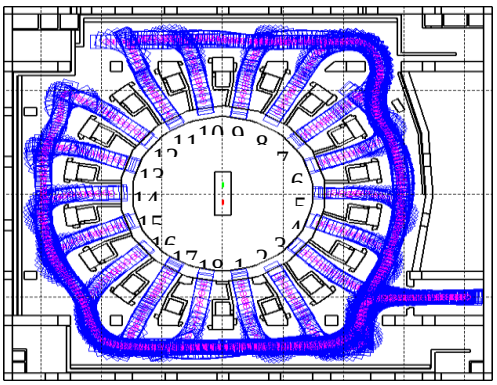

Figure 3.1 - Optimal trajectories for all ports of level B1 in TB (all spanned areas were obtained with 8500 mm x 2620 mm TCS).

The MATLAB simulator that supports the design and performance assessment of the trajectories was greatly improved and is now a powerful and flexible tool for the generation of optimal paths for the TCS, easily accommodating changes in the building models and infrastructures (e.g., cable trays), and in the TCS and ATS dimensions. This tool will be extremely useful to support the expected future developments in terms of ITER buildings and TCS/ATS design.

Preliminary trajectory results obtained before the grant starting date predicted that the doors' configurations in all levels of TB might raise problems in terms of optimal and safe trajectories to/from the lift and all VV ports. *These*

[1]Activities carried out in the frame of the Contract of Association Euratom/IST, F4E, ITER IO and the Contract of Associated Laboratory, by staff of the Groups of Experimental Physics, Microwave Diagnostics, Theory and Modelling and Control and Data Acquisition, in collaboration with Instituto de Sistemas e Robótica (ISR) and Active Space Technologies (AST). Contact Person: Maria Isabel Ribeiro (ISR) and Ricardo Patrício (AST).
[2]Work carried out in the frame of the F4E Grant Agreement, F4E-2008-GRT-016-01-(MS-RH), in collaboration with Astrium and Ciemat.

predictions were confirmed through deep studies on the three levels of TB using its latest CATIA model (March 2009). In 29 VV port cell doors (11 in level B1, 10 in level L1, 8 in level L2), out of 46, the door's configuration in the CATIA model of TB prevented the generation of a safe trajectory. *We proposed changes in the configuration of these doors,* including changes in the aperture direction, the aperture angle, the location and the length. IST proposal was accepted by IO and is now under incorporation in ITER building design, as illustrated in Figure 3.3 for the VV port cell 8 in level L1 of TB.

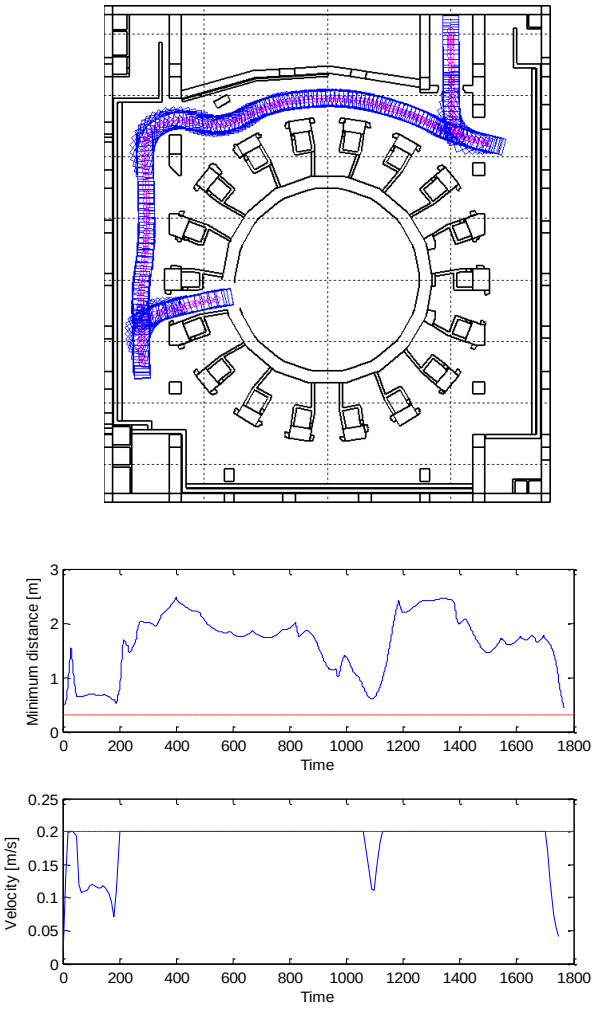

Figure 3.2 - (above image) Trajectory between the lift and the vacuum vessel port cell 10 in the level B1 of Tokamak Building; and, (below image) the minimum distance between the TCS and the nearest obstacle and velocity along the trajectory.

Studies on the location of parking areas, and the trajectories and the required maneuvers for parking were studied under the grant. A list of open issues related with the operation of the ATS/TCS was composed and provided to F4E. It will constitute future work within the group.

Preliminary results on the specification of a test facility for an ATS/TCS prototype were obtained. Based on the experience gained on the path generation topic, we compiled a list of tests that should be carried out in the test facility in what concerns the motion of the ATS/TCS. This will guide the specification of the building requirements.

Technical consultancy support was given to F4E in various aspects of the ATS design. In particular issues that require future design attention were raised: non uniform dimension of all cask envelopes for the same pallet dimension, order of the procedures in a TCS docking operation, ATS and pallet connection.

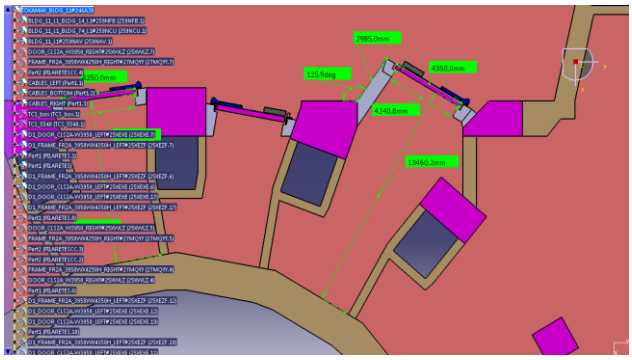

Figure 3.3 - IST proposal for port extension and door configuration changes in VV port cell 8 in level L1of TB.

3.3. CONTROL AND DATA ACQUISITION

The Portuguese activities on control and data acquisition for ITER consisted on the participation on:

- Fast Plant System Controller Project
- ITER Core LIDAR control and data acquisition

These are activities have been carried out in collaboration with other Association, namely CIEMAT for the Fast Plant System Controller and a consortium of Association lead by CCFE for the Core Lidar activities.

3.3.1. Fast Plant System Controller Project[3]

Development activities on the ATCA instrumentation platform were carried out targeting the IPFN participation on ITER projects, namely the implementation of a Plant System Simulator and the prototype of a Fast Control Plant System. The following activities were performed:

- *Preparation of the proposal for the participation on the Fast Control Plant System project for the ITER CODAC;*
- *Research and documentation of EPICS (Experimental Physics and Industrial Control System) integration including the Interface Development Environment configuration and base source code development for client/server application development;*
- *Development of the processes for software/hardware development and integration with EPICS;*

[2]Work performed in the frame of the ITER Contract nr 4300000061 in collaboration with CIEMAT.

- *Design and development of the electronic circuitry and software of an Intelligent Platform Management Controller (IPMC) based in the Intelligent Platform Management Controller Bus Protocol (IPMB),* to be integrated in the actual and future ATCA modules;
- *Initial study and development of an ATCA PCIe carrier/switch module.* This included the base specifications, ITER requirements, component analysis and commercial availability, design of schematics and layout.

Envisaging a general purpose fast controller design, several diagnostic use cases with demanding requirements were analysed as well as its interfaces with CODAC and sensors. Considerable amount of work was dedicated to characterize the ITER magnetic, microwave position reflectometer, LIDAR and IR cameras from the point of view of control and data acquisition needs. The work allowed to start elaborating the functional specifications and designing a technology neutral architecture for the Fast Plant System Controller (Figure 3.4).

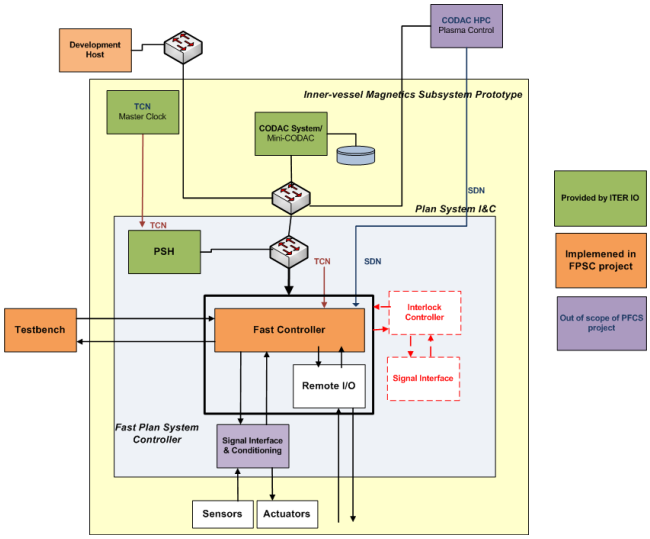

Figure 3.4 - Fast Plant system controller architecture (preliminary)

3.3.2. ITER Core LIDAR Control and data acquisition

The Association Euratom-IST joined the LIDAR Consortium Agreement and is actively involved in *continuing the specification of the ITER Control and Data Acquisition sub-system of the Thomson Scattering (Core LIDAR).*

3.4. MICROWAVE REFLECTOMETRY

The activities for ITER included in 2009:

- *Development of millimeter systems and digital circuitry* aiming at compact reflectometers with superior measuring capability;
- *Modeling of reflectometry experiments* in support of all reflectometry developments for ITER in particular in preparation for the design of PPR diagnostics to be carried out under next F4E tasks;
- *Demonstration of Plasma Position Reflectometry (PPR) technique for ITER* carried out on ASDEX Upgrade (AUG) in the frame of an EFDA Task[4];
- *Preliminary study of reflection from X mode lower cutoff on AUG a technique foreseen on ITER to probe the core plasma from the HFS*[4].

3.4.1. Development of advanced coherent reflectometers

Significant progresses have been made in 2009 concerning developments of electronics and millimeter wave techniques towards a full coherent compact reflectometer able to measure with the same equipment both density profiles and plasma fluctuations. So far, swept frequency FM-CW reflectometers relies on fast broad band tunable oscillators while the Hopping reflectometer uses fast frequency synthesizers being therefore separate equipments using different technologies. Recent developments made by the GMD for the JET (KG10) FM-CW diagnostic, brought the swept systems to use coherent detection although it still employs the standard swept tuned oscillator. The design and successful test in the laboratory of hoping systems capable of jumping from frequency to frequency in a microsecond scale will enable a Hybrid Reflectometer to be conceived. In Figure 3.5 results are shown of one of the first developed prototypes. Displayed are the control signal for the frequency synthesizers and the frequency error signal showing that frequency stabilization is achieved in 350 μs. Faster switching time is a major step toward a full coherent system and it will be first applied on the reflectometry diagnostic under development for the COMPASS tokamak.

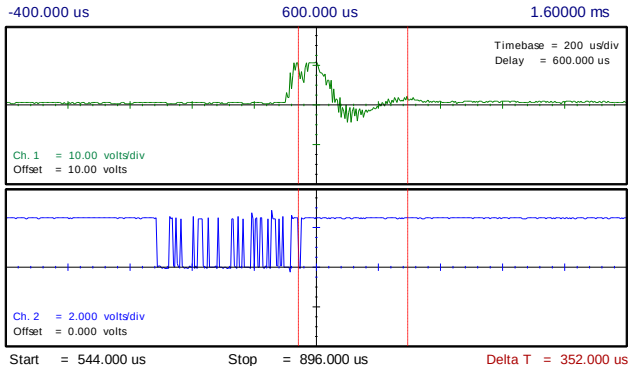

Figure 3.5 - Results of one of the first developed prototypes. Displayed are the control signal for the frequency synthesizers and the frequency error signal showing that frequency stabilization is achieved in 350 μs.

[4]See section 6.2.

3.4.2. Modeling of reflectometry experiments

A key tool for the progress of reflectometry is numerical simulation able to assess the measuring capabilities of present systems and to predict the performance of future ones, in machines such as ITER and DEMO. Main activities in 2009 were:

- Development of simulation tools to support the design of reflectometers;
- Participation in the European Reflectometry Code Consortium;
- Simulation in preparation for reflectometry experiments on ITER.

3.4.2.1. Development of simulation tools to support the design of reflectometers

A two-dimensional (2D) full-wave finite-differences time-domain (FDTD) code is being developed to simulate X-mode reflectometry in a comprehensive set of plasmas scenarios and experiments. Simulations are integrated with the output of a state-of-the-art turbulence code implementing thus a complete synthetic diagnostic capable of coping with the complex signature of turbulence in realistic experiments. The turbulence code used is a gyrofluid electromagnetic model with global geometry (GEMR). In Figure 3.6 it is depicted the electric field snapshot from a simulation of X-mode reflectometry, integrating the turbulence data given by a gyrofluid electromagnetic code with global geometry (GEMR). The X-mode wave-propagation code solves Maxwell equations using a finite-difference time-domain technique coupled to the ordinary differential equations of the motion or to differential equations describing the plasma behavior. The plasma current equation is handled through a novel solver (JE) that allows a direct FDTD implementation, which constitutes an improvement over the much slower Runge-Kutta solvers, traditionally used.

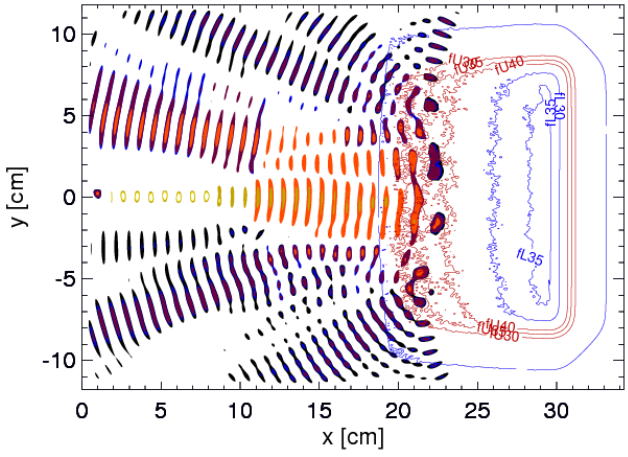

Figure 3.6 - Electric field snapshot from a simulation of X-mode reflectometry, integrating the turbulence data given by a gyrofluid electromagnetic code with global geometry (GEMR).

3.4.2.2. Participation in the European Reflectometry Code Consortium

Research was focused on the study of numerical schemes applicable to the EU 3D code under development in the frame of the EU Reflectometry Consortium. The JE solver tested in 2D, which is able to include collision effects, seems to be extendable to 3D. This approach to a synthetic diagnostic will provide a better understanding of the complexity associated with the reflectometry measurements that will appear when ITER reflectometry will be simulated. The solver proved to be quite fast and accurately described the physics involved. For high turbulence values when passing a current density limit, it becomes unstable (as happens also with the RK solvers) and with low external magnetic field can be noisy. The study of other JE schemes is underway.

3.4.2.3. Simulation in preparation for reflectometry experiments on ITER

Cumulative forward scattering (CFS) is being studied which is most likely to play an important role in ITER reflectometry and in large size fusion devices like JET or even AUG. In small and mid-sized devices with low levels of turbulence, scattering is accepted to be caused by Bragg backscattering in the vicinity of the oblique cutoff but under high turbulence conditions or long plasma paths as occurs in larger machines CFS can appear. To understand such complex phenomena the following activities were performed:

- *Evaluation of the forward scattering to Doppler reflectometry using a FDTD code;*
- *Simulation studies to as certain the enlargement and loss of coherence of the probing beam in Doppler reflectometry,* when propagated through a long path where turbulence may be able to induce forward scattering. In Figure 3.7 it is shown the results of numerical simulation displaying a snapshot of the electric field showing the effect of forward scattering on the coherence of the probing beam in a situation where no Bragg backscattering contributes to the reflected signal. The results of such a study will help the interpretation of the complex phenomena involved in forward scattering and will be used in comparisons with theoretical models in order to bring modelling and simulation closer.

3.5. THEORY AND MODELLING FOR ITER

3.5.1. Participation in the ITER scenario modelling working group

The Tungsten released from the ITER divertor wall during the current ramp up was calculated by the COREDIV code with different pumping efficiencies (recycling factors). *The total content was passed on to JETTO/SANCO code for the ITER scenario 2 plasmas.*

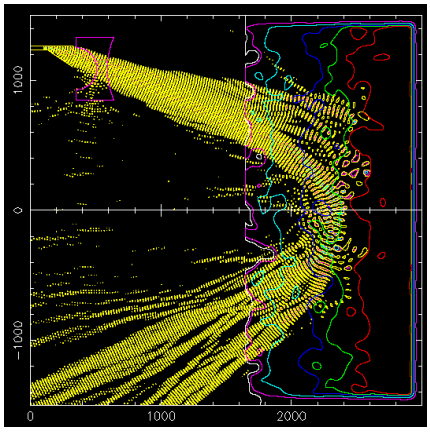

Figure 3.7 - Results of numerical simulation displaying a snapshot of the electric field showing the effect of forward scattering on the coherence of the probing beam in a situation where no Bragg backscattering contributes to the reflected signal.

The results were that the Tungsten would be removed from the plasma core in the H-mode due to an outward impurity convective velocity within the ETB. However with 0.1 % of Tungsten concentration in the plasma leads to a radiative collapse even before the H-L transition occurs.

The effect of the continuous pellet model with different flux rates on the power deposition on the ITER target divertor plates was studied using the EDGE2D/EIRENE code. The divertor power load decreases with the core deuterium flux from the pellets. Nevertheless for core fluxes higher then 6.0e22 1/s the plasma can reach the density limit for moderate H-mode plasma. Further work needed for the discrete pellet model using the edge core coupling code COCONUT.

Initial studies for the H-L transition with EDGE2D/EIRENE were done. Different increments in power and particle flux form the core were used to simulate the increase power trough the last closed flux surface found in the JETT simulation during the H-L transition. The divertor could in principle coupe with increase of power in the initial 5 ms after the H-L transition but a high increment of particle flux leads to a density limit disruption and a high increment of power crossing the separatrix can lead to power loads to the divertor greater than the safety limit and shorten the divertor life time. Further work is needed to change the boundary condition in the plasma core during the H-L transition and calculate again in a more self consistent way to evaluate the divertor power loads using the COCONUT code.

3.6. DESIGN OF A LH FAM LAUNCHER FOR ITER

The international collaboration set up under the moniker LH4IT for the *conceptual design of a possible LHCD system for ITER is ongoing*, wherein the option of a Fully Active Multijunction (FAM), an alternative concept predating the Passive Active Multijunction (PAM) initially proposed for ITER (DDD2001), is being assessed, aiming at improving directivity over the PAM for higher densities (n/n_{co} > 2). *A preliminary model of its waveguide structure was conceived* and its key components, bijunctions, 120º geometric phase shifters, λ/4 H-plane step transformers and E-plane step taper, were optimized to comply with the port-plug (dimensions) constraints while aiming for the best RF performance, and for use in further RF and coupling optimization studies. Preliminary results show that good coupling (RC <2%) is achieved for n/n_{co} >1.5 and good directivity for n/n_{co} >2 but, nevertheless, the PAM has better performance (most notably CD capability) for n/n_{co} <3, as expected.

3.7. SYSTEM INTEGRATION[5]

The Association Euratom-IST joined a group of Associates, led by CEA, on a winning F4E bid for the port plug integration. The Association Euratom-IST will be actively involved in the *development of CAD models, execution of the structural analysis and the computation of the effects of loads on the port plugs.*

[5]This activity is performed in collaboration with Active Space Technologies.

4. PARTICIPATION IN THE EFDA PROGRAMME[1]

B. Gonçalves (Head), C. Silva (Deputy Head) E. Alves, L.L. Alves, P. Belo, J.P. Bizarro, J. Brito, P. Carvalho, R. Coelho, P. Ferrão, A. Figueiredo, R. Gomes, M.E. Manso, R. Mateus, A. Pina, V. Plyusnin, J. Santos, A. Silva, C.S. Silva, F. Silva, C. Amador, J. Ferreira, H. Figueiredo, L. Guimarães, V. Livramento.

4.1. INTRODUCTION

The Portuguese participation in the 2009 EFDA programme included activities associated with:

- The collective use of the JET facilities by the EFDA Associates, which are described in chapter 5;
- The EFDA Tasks mentioned in Table 4.1.

in the areas of:

- Diagnostics;
- Materials;
- Plasma-wall interaction;
- Integrated tokamak modelling;
- Socio-economics research;
- Heating and current drive;
- Transport and MHD;
- Training.

The experimental work has been carried out at ISTTOK, AUG and COMPASS. The ITM related work has been carried out, mostly, at IST.

4.2. MATERIALS

4.2.1. Studies of material erosion and redeposition in ITER-relevant divertor target temperatures, plasma impact energies and divertor chamber geometries[2] (TW6-TPP-ERDEP)

This work reports on the results of the *study of tungsten and molybdenum metals exposed to high flux densities (~10^{24} D/m^2.s) and low temperature (T_e ~3 eV) deuterium plasmas in the Pilot-PSI irradiation facility*. The Pilot-PSI linear plasma generator produces plasma conditions that are expected to be typical at a detached ITER divertor strike point ($n_e \sim 10^{20}$ D^+ m^{-3}, $T_e < 5$ eV). In addition this experiment offers the possibility to measure the retention at high flux densities (~10^{24} D/m^2·s) rather than relying on extrapolations from ion beam or low-density plasma experiments and explore the influence of plasma impurities like carbon.

Task		Details in section
Reference	**Name**	
WP08-09-TGS-01b	Long-range correlations	2.5
WP08-09-DIA-01	AUG plasma position reflectometer	6.2
WP09-PWI-07	SEWG ITER Material mix	4.3
WP09-PWI-06	SEWG High-Z materials	2.2
WP09-ITM-TFL2	ITER scenarios and impurity control in the core and SOL	4.4
WP09-ITM-IMP3	Transport code and discharge evolution	4.4
WP09-ITM-TFL1	Task Force Leadership	4.4
WP09-ITM-ISIP	Infrastructure and software integration project	4.4
WP8-SER-INTF	Development of an integrated and interdisciplinary framework …	4.5
WP8-SER-ETM	EFDA times & fusion economics	4.5
WP08-09-MAT-WWALOY	Tungsten and tungsten alloys development	4.2
WP08-09-MAT-ODSFS	Ferritic steels development	4.2
WP09-PWI-05	SEWG High-Z Materials	4.3
WP09-PWI-08	SEWG Transient Heat Loads	4.3
WP09-TGS-02b	Physics of Rotation in plasmas	2.5
WP09-TGS-02c	Impurity influx in the boundary of fusion devices	2.4
WP09-HCD-02	Heating and current drive topical group	4.6
WP09-MHD-03	Sawtooth and NTM Physics and Control	4.4
WP09-PWI-01	SEWG Gas Balance and Fuel Retention	4.3
WP08-GOT-LITE	EFDA Training Programme	4.8
WP08-GOT-ETN-QPM	Quality Training	4.8
Contract nr. 042961 (FU06)	Microwave Diagnostics Engineering in preparation for ITER (MDEI)	4.8
TW6-TPP-ERDEP	Studies of material erosion and redeposition in ITER-relevant divertor target temperatures, plasma impact energies and divertor chamber geometries	4.2

Table 4.1 – EFDA Tasks with Portuguese participation

[1]Activities carried out in the frame of the Contract of Association Euratom/IST, the European Fusion Development Agreement and the Contract of Associated Laboratory, by staff of the Groups of Experimental Physics, Theory and Modelling and Control and Microwave Diagnostics

[2]Work in collaboration with the Association Euratom/FOM.

The deuterium trapping was investigated using D(^{3}He,p)α Nuclear Reaction Analysis (NRA) and Thermal Desorption Spectroscopy (TDS). The deposited carbon films were analyzed by proton micro-beam Rutherford backscattering (RBS) using the non-Rutherford $^1H^+$ cross section. The microstructure was analyzed using the electron microscopy.

The NRA studies reveal a D depth profile that is peaked at the surface and a measurable D retention at deeper regions (0.01 at. %) after only 40 s (2 discharges) of total plasma exposure time. This demonstrates the trapping of D that has diffused away from the ion implantation zone towards the bulk. The xy scan of the W targets shows an asymmetric D retention profile with the lowest retention values at the center of the target and the highest 6 mm off-center. Even in the regions of larger retention, the D concentrations were ≤ 0.06 at. %, (Figure 4.1). However, even where (~6 mm off-center) the retention reaches the maximum (~5×10^{15} cm^{-2}) the retention fraction is very low (10^{-5} to 10^{-6}).

The microstructure shows some differences from the centre to the borders particularly regarding the grain dimension (Figure 4.2). The small grains in the off center region offer a large are of grain boundaries where D diffusing from the high temperature region at the centre could find precipitating sites. Nevertheless the microscopy data do not reveal presence of any kind of D bubbles which is somehow expected due to the low retained concentration.

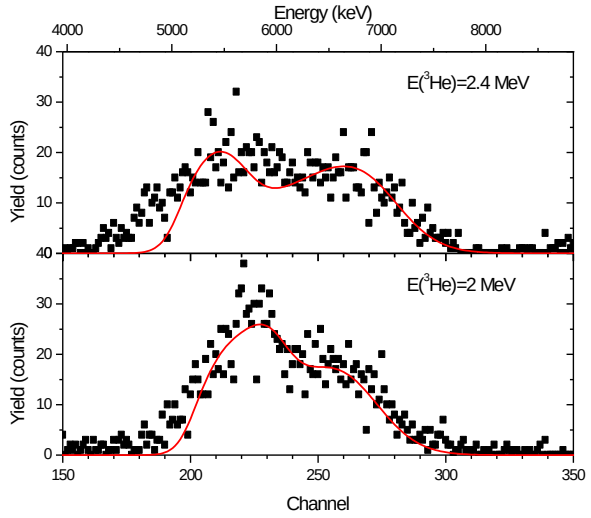

Figure 4.1 - Typical proton spectra from the D(^{3}He,p)α nuclear reaction for sample measured 6 mm off center with two beam energies. The solid line is the simulation obtained with the NDF code.

4.2.2. FeCrY/FeCrTiY composites for fusion applications (WP08-09-MAT-ODSFS)

Eurofer ODS steels based on the FeCrY or FeCrTiY systems are promising in the field of structural materials for nuclear fusion reactor applications. These materials must have low DBTT and sufficient creep strength up to ~750°C with reasonable fracture toughness.

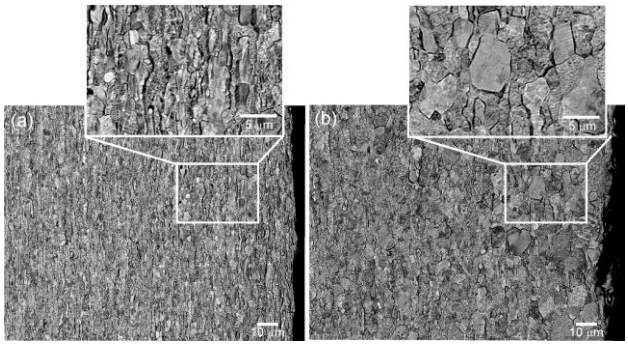

Figure 4.2 - Microstructure of a W sample irradiated for 160 s evidencing recrystallization with the grain changing from elongated, with an average size of ~1 µm at 6 mm off the center (a), to approximately equiaxed with an average size of ~3 µm at the most exposed region close to the center (b).

The present work involves *the production of FeCr-Y_2O_3 and FeCr- Ti_xY_yO nanocomposites by mechanical alloying of pure metals.* This is a new approach regarding previously published work, as it was realized that Y_2O_3 particles used as starting material convert to the Ti_xY_yO complex oxide during thermomechanical processing. Our approach is thus to a) form a metastable solid solution Fe(Cr,Ti,Y) and b) in-situ formation of the complex nanosized Ti-Y oxides during high temperature consolidation (Ti and Y reacting with O always present in the powders). This will enable finer oxide dispersion and lower consolidation temperature (e.g. by hot extrusion). The effect of high energy mechanical alloying on the transformation temperatures of Fe(Cr,Ti,Y) was investigated with thermal analyses. The characterization of the metastable solid solution with XRD, TEM and Mossbauer spectroscopy is under way[2] in collaboration with NIMP-Romania.

4.2.3. W-Ta composites for fusion applications (WP08-09-MAT-WWALLOY)

A W-Ta nanostructured alloy is promising as a candidate material for the first wall in nuclear reactors. Tungsten and tantalum have high resistance to plasma erosion and moderate tritium retention. *W-Ta alloys were produced by mechanical alloying and were subsequently consolidated by thermomechanical processes.* Two different batches were produced by mechanical alloying (Figure 4.3): W-10%at Ta and W-20%at Ta, both milled for several different times (15'; 30'; 1h and 2h) and consolidated by Spark Plasma Sintering at several temperatures (1510ºC and 1600ºC). All the powder batches and the consolidated samples were characterized by XRD, optical microscopy, SEM/EDS and microhardness measurements. The XRD

[2]In collaboration with NIMP - Romania.

patterns of the consolidated samples revealed that oxide formation did not occur. The SEM-BSE contrast clearly indicates the presence of a Ta rich phase in the SPS consolidated composites. Relatively high densification values, 81 to 88 % of theoretical density, were obtained after consolidation.

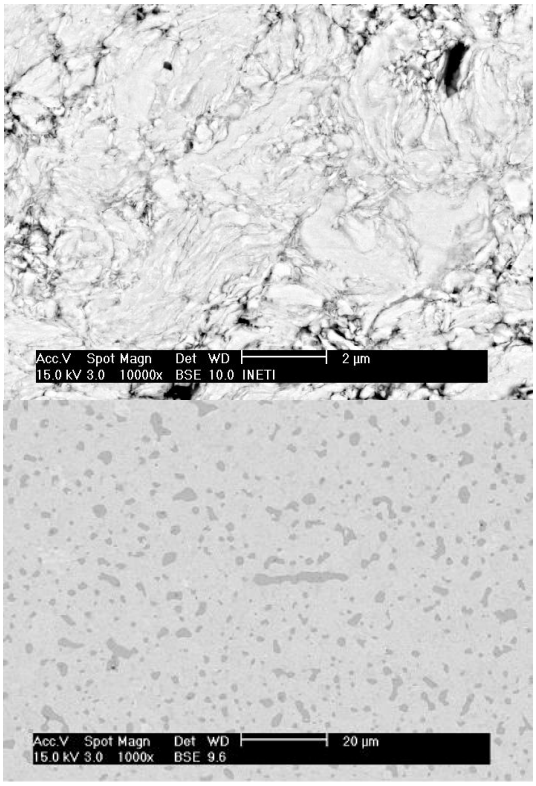

Figure 4.3 - Scanning electron microscopy pictures of Mechanical alloying of W-Ta20% for 2h at 200rpm produced a lamellar W, Ta nanostructured composite (a). The Spark Plasma Sintered samples resulted in a homogeneous fine composite (b).

4.3. PLASMA WALL INTERACTION

4.3.1. Characterization of retention as a function of wall materials foreseen for ITER[3] (WP09-PWI-01-01/IST/BS)

This task was performed in the domain of *irradiated refractory metals under ITER-like relevant conditions (flux ~10^{24} D/m^2.s and T_e ~2 eV). Additional W samples were irradiated in the Pilot-PSI device.*

The main results presented in this document follow the conclusions of the TW6- TPP-ERDEP report of 2008. Ion beam scans along the W target surface show 2-D special asymmetric retention profiles where the lowest retention values are measured at the centre of the target and the highest at 6 mm off-centre.

Additionally, the new retention measurements point to an increase/decrease of the D retention ratio when the W surfaces are previously polished/annealed before irradiation. These remarks are in agreement with other previous results.

4.3.2. D retention and microstructural changes in W and Mo targets exposed in the Pilot-PSI device (WP09-PWI-05-03/IST/BS)[3]

The aim of this work was to correlate the existing data (temperature, ion beam and thermal desorption spectroscopy) with possible induced microstructural changes observed by electron microscopy.

Besides the correlation between thermal profile and the D retention ratio, which grows up from a minimum in the centre of the samples (~1600 K) to maximum values in the border of the bombarded area (~1000 K), scanning grow electron microscopy (SEM) revealed that a smooth grain electron occurs in both W and Mo when the corresponding recrystallization temperature is reached.

Additionally, transmission electron microscopy (TEM) bright-field images obtained under the Bragg condition showed a mottled contrast in the grains compatible with the presence of a high density of self-interstitial dislocation loops and/or platelet clusters in the centre of the W samples (Figure 4.4.a). The corresponding irradiated Mo samples show the same mottle structures. Nevertheless, the produced contrast is much lower (Figure 4.4.b) in this case.

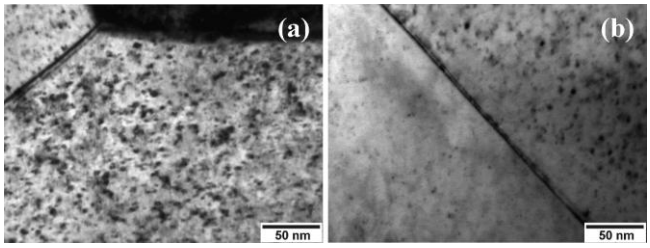

Figure 4.4 - Bright-field TEM images close to Bragg conditions for a) W targets and b) Mo targets.

4.3.3. Study of Be and C interdiffusion, arbide formation and compound sublimation (WP09-PWI-07-01/IST/PS; WP09-PWI- 07-01/IST/BS)

Carbide formation and corresponding microstructural changes induced by thermal treatments were studied in the Be:C system. C films of about 120 nm were evaporated in polished Be plates with an electron beam evaporator device for this propose. Afterwards, Be:C samples were annealed during 90 min in the 373 to 1073 K temperature range. Be/C interdiffusion and beryllium carbide formation evolution were checked by Rutherford backscattering (RBS) and X-ray diffraction (XRD).

It is evident from RBS spectra that the Be-C interface remains thinner in the 373 to 773 K temperature range. However, it strongly increase at higher temperatures, where Be and C backscattering yields are compatible with the presence of the Be_2C stoichiometry. At the same time, a strong superficial oxidation occurs.

[3]Work made in collaboration with the Association Euratom/FOM.

Most probably Be difuses through the carbide layer and oxidises at the surface.

Beryllium carbide formation at higher temperatures is ensured by the XRD patterns due to the presence of the characteristics Be_2C diffraction lines.

Scanning electron microscopy inspection did not reveal evidences of sublimation locations. Nevertheless, thermal treatments at higher temperatures induced the formation of blisters-like structures in large areas of the Be:C surfaces. Several cracks were preferentially observed in the base of these structures after the annealing route at 1073 K which may promote their partial removal.

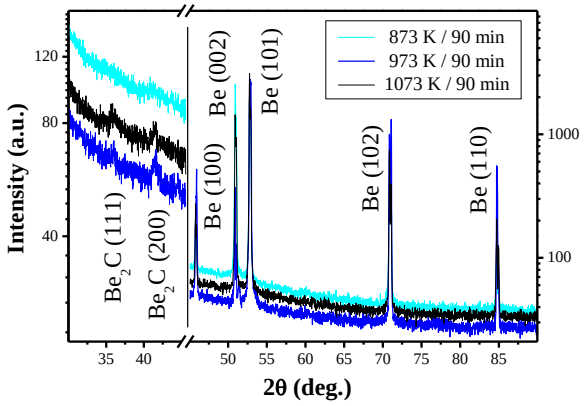

Figure 4.5 - XRD spectra of Be:C samples. Beryllium carbide (Be_2C) is formation at temperatures higher than 873 K.

4.3.4. Measurements of power and particle fluxes (including runaway fluxes) (WP09-PWI-08-01)

Experiments at TEXTOR have been postponed to the end of 2009 or early 2010 due to prolonged shutdown. The main aim of these studies is documenting MGI and runaway electrons data and elaboration of the effective methods for mitigation of disruptions and concurrent suppression of runaway electrons in a view of ITER operation scenarios. Besides the work on disruptions and runaway electrons, *the studies on interaction of fast ions with PFC have been initiated in order to compare the experimental data from JET with that obtained in other machines.* It is envisaged to assess the trends in this phenomenon in view of ITER operation parameters.

4.4. INTEGRATED TOKAMAK MODELLING

The ITM-TF has a long-term commitment to provide an integrated modelling infrastructure and whole discharge modelling tools in view of developing a comprehensive package for ITER plasma simulation exploitation. During 2009 the ITM-TF activities entered a notable production phase with a stable release of the KEPLER simulation orchestrator and testing of many contributed modules with associated actors. IPFN staff has contributed to the following ITM-TF related activities:

- Task Force Leadership
- Impurity control in the core and SOL
- Synthetic diagnostics – 3D reflectometry modelling framework
- CPOs management in UAL actors and specialized actors
- Maintenance and continuing development of the ETS
- 3D simulations on critical NTM island width

4.4.1. Task Force Leadership (ITM-09-TFL1)

Cast within the charges of deputy Task Force Leader, a dedicated coordination of the activities of the Experimentalists and Diagnosticians Resource Group was given. The later comprised coordinating and assisting the development of machine descriptions and data mapping by the experimental devices engaged with the ITM-TF. The consolidation of the coverage of machine descriptions and data mapping files for European fusion devices allowed for the first trials of code validation exploiting a full chain of experimental data retrieval. Supervision was also given to the plasma control related activities and associated working sessions as well as for collaboration efforts with other EFDA working groups. Coordination of 3D machine descriptions was initiated and first contacts with 3D CAD experts to set forth strategies for developing defeatured 3D wall meshes were taken. Assistance to the ITM-TF Leader and support for the 2009 overall activities also comprised support on the elaboration of Progress Report Tables, joint coordination with FZJ-Juelich of the ITM-TF General Meeting (GM) including setting up and manage the content of the GM website, assistance to the drafting of support actions and the 2010 Workprogramme and revision of the 2010 Call for Participation.

4.4.2. Impurity control in the core and SOL (ITM-09-TFL2-ISM-T3)

Development of improved set of ITER reference scenarios (ITM-09-TFL2-ISM-T5)

The Tungsten released from the ITER divertor wall during the current ramp up was calculated by the COREDIV code with different pumping efficiencies (recycling factors). The total content was passed on to JETTO/SANCO code for the ITER scenario 2 plasmas. The results indicated that Tungsten would be removed from the plasma core in the H-mode due to an outward impurity convective velocity within the ETB. However, a 0.1 % of Tungsten concentration in the plasma cores leads to a radiative collapse even before the occurrence of the L-H transition. The effect of the continuous pellet model with different flux rates on the power deposition on the ITER target divertor plates was studied using the EDGE2D/EIRENE code. The divertor power load decreases with the core deuterium flux from the pellets. Nevertheless, for core fluxes higher then 6.0e22 *1/s* the plasma can reach the density limit for moderate H-mode plasma. Further work is needed for the discrete pellet model using the edge core coupling code COCONUT.

Initial studies for the H-L transition with EDGE2D/EIRENE were done. Different increments in power and particle flux from the core were used to simulate the increase power through the last closed flux surface found in the JET simulation during the H-L transition. The divertor could in principle cope with increase of power in the initial 5 ms after the H-L transition but a high increment of particle flux leads to a density limit disruption and a high increment of power crossing the separatrix can lead to power loads to the divertor greater than the safety limit and shorten the divertor life time. Further work is needed to change the boundary condition in the plasma core during the H-L transition and repeat the calculation in a more self consistent way to evaluate the divertor power loads using the COCONUT code.

Heating and Current Drive mix in ITER baseline design by means of predictive modelling was addressed. Assessment of the plasma performance with respect to H&CD mix for reference ITER Scenarios 3 and 4 was initiated. Although there are still good enough models for many of the important physical processes, preliminary results indicate that it may be difficult to maintain hybrid and advance scenarios for the full 1000 second ITER pulse. Additionally, the projected Q=10 for these scenarios will be difficult to achieve without a very hot pedestal. This has a huge impact on edge MHD stability. Ongoing activities involve exploring the more optimistic Q=5 operation at the cost of even lower duration.

4.4.3. Synthetic diagnostics – 3D reflectometry modelling framework (ITM-09-TFL2-EDRG-T5)

A novel solver (JE) to handle the plasma current equation has been tried allowing a direct FDTD implementation, which constitutes an improvement over the much slower Runge-Kutta solvers, traditionally used. Such numerical scheme can be used to develop a 3D code including collision effects. The solver proved to be quite fast and accurately described the physics involved. For high turbulence values, when passing a current density limit, it becomes unstable (as the RK solvers) and with low external magnetic field can be a noisy. The study of other JE schemes is underway.

4.4.4. CPOs management in UAL actors and specialized actors (ITM-09-ISIP-T7)

A strong effort was provided for the ITM-09-ISIP-T7 task dedicated to CPOs management in UAL actors and specialized actors. In particular, special focus was given to: discussion and agreement on the requirements for the CPOs management; upgrading FC2K regarding the iterations on a CPO by actors code (rather than increment the CPO run within a workflow, output of actors increase the CPO occurrence); upgrading UALInit and UALCollector to account for multiple CPO occurrences within a single workflow; testing possibility for actors to act upon a single CPO time slice rather than acting upon the full CPO. Some support was given for the handover of the task dedicated to the support and simulated workflow testing of the data and workflow relational database. Database querying tools was considered at the project leadership level to be less urgent therefore was postponed to 2010. No assistance was asked for to accomplish the implementation of the catalogue database access within the UAL. Administration of the collaborative software was reallocated in another Task.

4.4.5. Maintenance and continuing development of the ETS (ITM-09-IMP3-T1).

Use of the modules and interfaces, comparison with existing 1D codes and experiment (validation and verification) (ITM-09-IMP3-T2)

Dedicated testing of ETS solvers was pursued. Ohmic heating power density calculation was incorporated in the *analytics* module, consistent with the *main_plasma* ETS module internal calculation, allowing for testing the solvers at lower temperatures for which ohmic heating plays a role. Automatic tools have been development to extent the capability of the ETS framework to periodically test itself and generate accuracy and verification reports. To be able to easily extent these tools, technologies like XML and python, within the ITM development framework, have been used. Shell scripts have been written to execute automatically batches of ETS runs from a set of XML and Fortran 90 files and Python scripts were created to process the output of ETS runs, which extract from the output files created by the *solver test* workflow profiles of chosen variables at selected instants, their time evolution, and their absolute or relative errors. Scripts to make plots of these post-processed data have also been prepared. Convergence tests using several solvers in the *solver_test* workflow were performed and discussed within the ETS team. Tests with temperatures typical of JET, ITER and DEMO at different time steps and grid sizes were initiated.

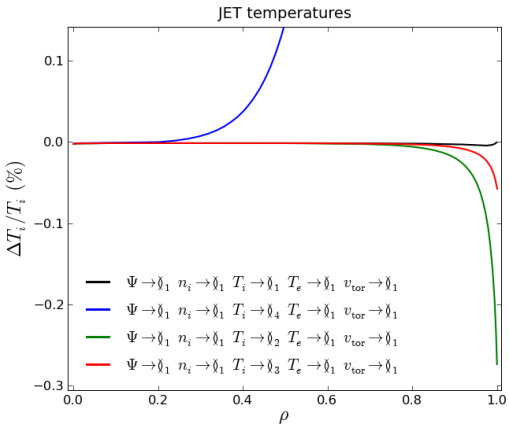

Figure 4.6 – Verification of boundary conditions on the ETS. An error in constant thermal flux conditions (blue curve) was identified and corrected.

Participation in some ETS tasks, related with the development of Consistent Physical Objects (CPOs) and with the V&V of case-study solutions for the ETS. In particular, we have collaborated in (i) the development of a schema/xsd and of the corresponding xml file to describe a set of V&V tests; (ii) the development of a Python script for automatic generation of ETS xml input files from a V&V xml description (iii) the development of an ETS V&V test version based on the solver_test and the new eq_ets_test version (August 2009), that reads ETS V&V input data files.

4.4.6. 3D simulations on critical NTM island width (WP09-MHD-03)

The onset and growth of neoclassical tearing modes (NTM) in a tokamak discharge is known to limit the plasma beta, deteriorate plasma confinement and ultimately lead to plasma disruptions. It is therefore quite crucial to understand fully the mechanisms determining the characteristic critical island width above which the NTM is unstable. In particular, assessment of the dependence on transport coefficients, magnetic shear, Lundquist number and fraction of bootstrap current may provide valuable information to assist the prediction of stable operational regimes or regimes where the destabilization threshold is raised significantly. A Full MHD 3D code solving magnetic field, plasma velocity and pressure dynamic non-linear equations with bootstrap current drive (XTOR code) was used for interpreting experimental evidence of the onset of the n=1 NTM on JET advanced scenario discharges. The simulations attempted to reproduce realistic ratios of perpendicular to parallel thermal conductivities and resistive diffusion to energy confinement times. Analysis of one particular shot (#72668) evidenced the competing roles of stabilizing curvature and bootstrap drive, mitigated both by an increasing magnetic shear provides a destabilizing role as the plasma current density diffuses during the discharge.

4.5. SOCIO-ECONOMICS RESEARCH

4.5.1. Development of an integrated and interdisciplinary framework to promote the understanding of the socio-economic-technical system of fusion energy

The following activities were performed:

- *Characterization of the data and tools used by the Associates in their socio-economic research*

IST contacted the other associates and identified three types of methodologies used in their socio-economic research: technical models to estimate social impacts, such as TRACT to evaluate accidents scenarios or irradiation of materials; technical models to estimate economic impacts, such as PROCESS, TIMES or ExternE; social techniques, like workshops or focus groups discussions to identify social variables like awareness or acceptability of fusion energy.

- *Assessment of the state-of-the-art concepts and methodologies, definition of a draft roadmap on designing an integrated framework providing a holistic view*

A new field of scholarship is emerging to seek solutions to this type of problems my mixing technologies and tools from the different fields, called Engineering Systems. The idea is to bring together knowledge from engineering, management and social sciences and integrate their methodologies and develop joint cross-cutting tools in areas as interface of humans and technology, design and implementation, networks and flows, policy and standards, uncertainty and dynamics.

- *SWOT analysis of the data and tools to address issues as defined above*

No specific threat or opportunities have been identified for the different tools, except in the case of EFDA-TIMES where it has been acknowledge that the funding has been decreasing and it is necessary to expand its capabilities.

- *Development of a dialogue with associates aimed at understanding the Fusion system structure and developing trade-offs among strategic options*

From the dialogue with other associates it has been recognized that the integration of economic and social studies it is not easy. For example, it may be very difficult to quantify social findings as awareness and willingness for acceptability or using economic and technical findings to communicate with people, since economic and technical literacy is generally low for the general population. It has also been recognized that EDFA has to provide a vision and strategy for the socio-economic studies, such as when to inform and who should be informed (general public, civil society)

- *Establishment of a framework that may support the development and governance of complex fusion infrastructures in a context of global uncertainty (e.g. economic conditions, cost of fuels, economic and environmental policies)*

The new framework is based on the integration closing the information loop between social and technical-economic studies, creating a decision making tool where different scenarios can be generated and communicated (using for example EFDA-TIMES) and using these scenarios in focus groups discussions to inform, make multi-criteria decisions and design policies and use these information from different stakeholders to generate new and more accurate scenarios.

4.5.2. WP8-SER-ETM, EFDA times & fusion economics

According to the Task Agreement of the EFDA Work Program for 2008 & 2009 for Socio-Economic Studies: EFDA-TIMES & Fusion Economics, IST had 3 tasks:

- *Check the CHP (combined heat and power) data for incorrect modelling of total efficiencies*

The existing CHP plants are producing double of the efficiency defined in the template files. This is because

the CHPR~FX parameter is defined as 1, and the CEH parameter is defined as 0. CHPR~FX defined as 1 means that the process produces exactly the same amount of heat and electricity. CEH defined as 0 means that the efficiency defined in the template corresponds only to the efficiency of the electricity conversion process. Therefore, the process will produce the amount of electricity that it can given the efficiency, and then produce the same amount of heat. This is why the output is the double of what we are defining. To solve this problem, the CEH value should be set to 1.

For the new CHP plants, the CHPR~FX is higher than 1, which means that for each unit of electricity, the process produces more than 1 unit of heat. This, combined with the efficiencies defined in the templates for the electricity production process (with CEH defined as 0) results in total efficiencies higher than 100%.

To solve this, there are several options: (i) Lower the CHPR~FX so that the total efficiency in the templates is lower than 100%; (ii) Lower the efficiency of the electricity conversion part of the process that is defined in the templates; (iii) Change CEH to 1, so that the efficiency in the templates becomes the total efficiency one of these options must be chosen based on available data for the CHP plants. Usually, the thermal efficiency is lower than the electricity efficiency and so CHPR~FX should be lower than 1. Furthermore, the efficiencies defined in the new CHP plants are acceptable values for the electricity production part of the process. So, most likely option 1 should be chosen. However, good data is needed to introduce acceptable values for the heat to electricity ratio.

- *Check the PRC_CAPACT coefficients for new heat plants (ELC sector) for their consistency with the provided cost data*

Given that the CAPACT value is defined as 1 in all Heat processes, this means that the installed capacity would also be defined in PJ. Therefore, to be correct, the investment and fixed costs would be in M$/PJ.

If the prices in the model are in M$/PJ, the following table shows what these prices would be in regular units (M$/GW), as well as how they compare with the prices for the same technologies for electricity production.

	Heating		Electricity	
	Investment	Fixed	Investment	Fixed
Input	M$/GW	M$/GW	M$/GW	M$/GW
NGA	3468.96	126.144	780	10
OIL	3468.96	126.144	599	4
BIO	10406.88	204.984		
COA	3468.96	126.144	1500	40
GEO	378.432	78.84	2600	100

From the table, one can see that, generally, the heating prices would be quite higher than the electricity production technologies. This suggests that the prices in the excel files might already in M$/GW and therefore, the CAPACT coefficient should in fact be 31.536.

It should be stated, however, that no good data has been found for the costs of heating technologies and, therefore, there is no certainty of this. Also, the prices in the model seem very low (compared to the electricity production technologies), something that would favor this instead of CHP plants.

- *Check the UC constraint TUC_HydShr1 for its correctness and consistency*

The UC constraint TUC_HydShr1 was not well implemented. The following table shows how the constraint should be implemented in order to make sure that the limits for run-of-river hydro power are respected. The table presented should be placed in the Scen_Potentials.xls file, in the UserConstraints spreadsheet.

4.6. HEATING AND CURRENT DRIVE

The new ITM-flush libraries were implemented on the JAMS-ITC graphical interface to use the different options of equilibrium solvers: experimental equilibrium from EFIT; from an eqdisk file (which can be from different solvers) or calculated from the JETTO/SANCO simulations.

4.7. TRAINING

4.7.1. Participation in the Quality and Project Management training programme (WP08-GOT-ETN-QPM)

The Association is part of the network that prepared and signed the TA WP08-ETN_QPM in order to design and implement the training program that will allow a significant increase on the Associations' Quality and Project Management capabilities. The 2009 activity was limited to the selection of a trainee and the establishment of a common basis for the training programme.

4.7.2. LITE (WP08-GOT-ETN)

LITE is an EFDA Goal Oriented Training Program (GOIT) on Lower-hybrid and Ion cyclotron Technology involving IST, CEA, ENEA, ERM and IPP, in which IST participates with one trainee and one mentor. The main objective of LITE concerning IST is to provide its trainee, an RF physicist oriented for LH antennas, with the necessary knowledge and skills to accompany the various aspects involved in the construction of a LH antenna, its transmission line and transmitter, from physics basis and conception to testing, going through the RF design and optimization of each of its multiple components. During 2009, the activity carried out was mainly oriented towards the design and RF analysis of LH launchers for ITER and TORE SUPRA.

4.7.3. Microwave Diagnostic Engineering (Contract no 042961 (fu06))

This project covers a training programme on Microwave Diagnostics Engineering for ITER carried out by a

consortium of four Euratom Associations, coordinated by IPFN/IST. The project is dedicated to four trainees with home institutes at IST, CIEMAT and IPP Greifswald. The training activities of both the IPP trainee and the two IST trainees (one senior and one young trainee) were completed in 2009 and the CIEMAT trainee, who joined the project in a latter phase, is still going on. Regarding the trainees from IST, the work of the senior trainee was focused in Multiple Input Multiple Output (MIMO) techniques which are used in telecommunications and he performed an innovative study of the application of MIMO technique to improve communications with diagnostics implemented in nuclear fusion devices. The young trainee worked in 2010 on the fast reconstruction of density profiles from reflectometry diagnostics for plasma position feedback purposes. He investigated the accuracy of several sets of Neural Networks (NN) and applied the study to profile quality validation and automatic plasma position tracking. In Figure 4.6, the plasma position (magnetic separatrix) derived from the magnetic diagnostics is depicted (black line). In blue and red the lines were obtained from reflectometry using two of the developed methods to track the plasma position.

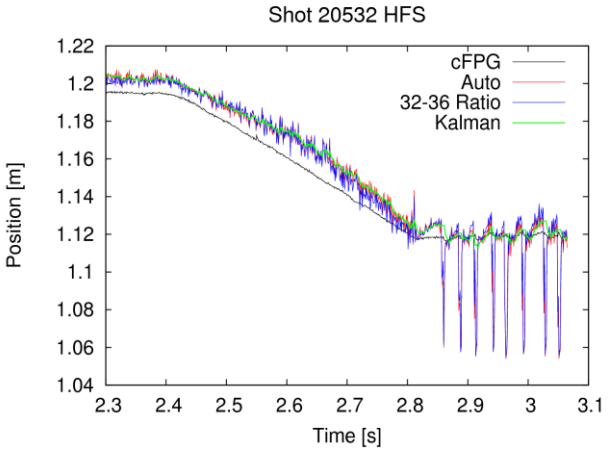

Figure 4.6 - In black plasma position given by the magnetic diagnostics and in blue and red two of the developed methods for tracking the plasma position.

5. PARTICIPATION IN THE COLLECTIVE USE OF THE JET FACILITIES BY THE EFDA ASSOCIATES[1]

F. Serra (Head), B. Gonçalves (Deputy Head), P. Belo, J.P. Bizarro, R. Coelho, S. Cortes, L. Cupido, A. Figueiredo, A. Fonseca, M.E. Manso, F. Nabais, M.F. Nave, I. Nedzelski, I. Nunes, V. Plyusnin, F. Salzedas, C. Silva, J. Sousa, C. Varandas, P. Varela, D. Alves, , J. Bernardo, P. Carvalho, N. Cruz, A. Fernandes, J. Ferreira, J. Figueiredo, L. Meneses, A. Neto, R. Pereira, J. Vicente.

5.1. INTRODUCTION

The Association EURATOM/IST has continued its participation in the collective use of the JET facilities, in the frame of EFDA through the "JET Operation Contract" and the "JET Implementing Agreement".

The main activities in this project were related with:

- Operation;
- Experimental physics ;
- Theory and modelling ;
- Plasma Engineering and Systems Integration.

5.2. OPERATION

Three members of the IST/IPFN staff have been working in the JET Operation Team:

- One Physicist has continued to work in the JET "Plasma Operation Group", as a Session Leader for the Campaigns;
- One Physicist has been working in the "Plasma Operation Group" as a Plasma Control expert in the framework of the Plasma Control Upgrade activities;
- One Physicist has carried on his work in the Reflectometry and LIDAR Diagnostic Group, being responsible by: (i) maintenance of the X-mode correlation reflectometer (KG8b); (ii) the analysis and validation of the signals of the KG8b X-mode correlation reflectometer and the KG3 O-mode fluctuation reflectometer.

In addition, *during JET experimental campaigns one Physicist has been seconded to perform duties as Session Leader for the experiments.*

5.3. EXPERIMENTAL PHYSICS

IST was strongly involved in the JET scientific exploitation through *the participation in the 2009 experimental campaigns (19 Researchers amounting to a total manpower of 1060 days) and activities on data analysis and modelling.*

5.3.1. Assessment of the influence of magnetic field ripple on JET intrinsic rotation

An extrapolation of experimental data from several machines, known as the Rice's scaling (J. Rice et al., NF 2007), has suggested that intrinsic plasma rotation in the co-current direction, will be important in ITER. However, an effect that is still needed to be accounted for when making predictions for ITER comes from the toroidal ripple in the magnetic field. Using the unique capability of JET to monotonically change the amplitude of the ripple, without modifying other relevant equilibrium conditions, *the effect of the ripple on the angular rotation frequency of the plasma column was investigated under the conditions of no external momentum input.* In order to separate ripple fast-ion effects from thermal ion effects and to test existing ripple transport models, plasma rotation was measured in Ohmic and in ICRF heated plasmas with ITER relevant ripple levels. Experiments were performed in deuterium for plasma current values of 1.5 and 2.1 MA, with an average toroidal field at the centre of $<B_T>$=2.2 T and, toroidal field ripple values (at R=3.80m, Z=0 m) ranging from δ=0.08% to δ=1.5% The ICRF experiments were performed with hydrogen minority heating using a dipole antenna phasing, ICRF powers up to 4 MW, and cyclotron resonances near the plasma core, or on the high field side of the plasma. It was concluded that ripple has a significant effect on the intrinsic plasma rotation. In both Ohmic and ICRF heated plasmas ripple causes counter rotation (Figures 5.1 and 5.2 for plasmas with ICRF), indicating a strong torque due to non-ambipolar transport of thermal ions and in the case of ICRF also fast ions. At ITER-relevant ripple values of δ=0.5%, JET plasmas with ICRF heating are hardly rotating, while at δ=1%, both L- and H-modes are observed to counter-rotate. These results do not fit Rice's inter-machine intrinsic rotation scaling. JET results suggest that ripple will affect rotation in ITER and, it should be taken into account in extrapolation from present data.

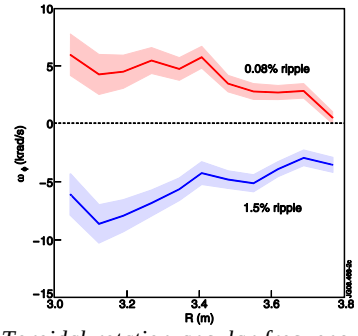

Figure 5.1 - Toroidal rotation angular frequency profiles from CXRS measurements for ICRF heated H-mode plasmas with I_p=1.5 MA, $<B_T>$=2.2 T, P_{ICRF}~3 MW for two ripple levels. Top: pulse # 74688 with δ=.08% and P_{ICRF}=3.1 MW; bottom: pulse # 74686 δ=1.5% and P_{ICRF}= 2.9MW. The plasma centre is at R_0=3.02 m, the ICRF resonance is slightly off-axis on the high-field side at R_{res}= 2.71 m.

[1]Activities carried out in the frame of the Contract of Association Euratom/IST, the European Fusion Development Agreement and the Contract of Associated Laboratory, by staff of the Groups of Experimental Physics, Theory and Modelling and Control and Data Acquisition.

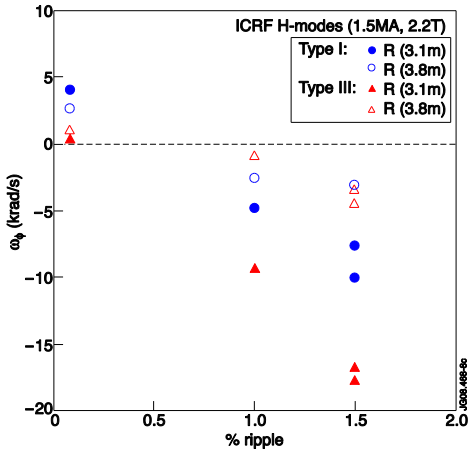

Figure 5.2 - Toroidal rotation angular frequency as a function of ripple for ICRF pulses with 1.5 MA, with resonance slightly off-axis on the high field side (R_{res}=2.71 m), for the centre (3.1 m, solid symbols) and the edge (R=3.8 m, open symbols). These are H-mode pulses, circles are measurements during type I ELM phases, while triangles are during type III-ELM phases.

5.3.2. Rotation studies of JET discharges with no momentum input

In present day tokamaks, rotation is mostly driven by NBI torques, while in an alpha-heated reactor the momentum input is expected to be small. Even in reactors with high NBI power, the torque is still expected to be small. Since rotation and rotation shear are important for plasma performance, alternative sources of plasma rotation need to be found and understood. The work on the scientific co-ordination of the JET intrinsic rotation database and execution of experiments aimed at measuring and understanding rotation in JET plasmas with no momentum input has therefore continued. During 2009 *emphasis was given on measuring rotation in plasmas with lower-hybrid current drive (LHCD), and in H-mode plasmas obtained with pure ion-cyclotron radio-frequency (ICRF) heating.* In addition, *the experiments to study the effect of the magnetic field ripple on the intrinsic rotation were completed.* Toroidal angular frequency profiles were obtained from charge exchange recombination spectroscopy of C^{+6} during short neutral beam injection (NBI) pulses (P_{NBI}~1.3 MW). Rotation analysis was complemented by the analysis of MHD modes frequency and direction of propagation. In the standard JET low ripple configuration the plasma edge of JET plasmas rotates in the co-current direction independent of the heating scheme used. The core of the plasma however may be either rotating in co or counter current direction. The observed toroidal angular frequencies are small, <10 krad/s, typically one order of magnitude smaller than in JET plasmas with NBI heating. Preliminary data analysis appears to indicate that with LHCD core co-current rotation might only be observed in pulses with good core LH wave penetration. Further experiments will be necessary to confirm this and to study the effect of magnetic shear. With ICRF heating counter-rotation has been experimentally associated with low plasma current (I_p<1.7 MA), low density regimes such as in L-mode and H-modes with type III ELMs, and the observation of MHD modes that displace fast ions such as TAE modes. The range of Mach-Alfven numbers observed with ICRF heating (Figure 5.3). Intrinsic rotation at JET shows no correlation with input power or with beta.

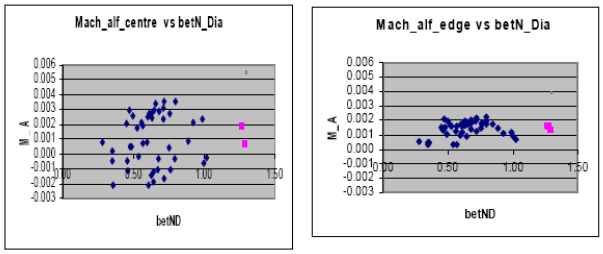

Figure 5.3 - Mach-Alfven numbers versus diamagnetic beta normalised for JET plamas with ICRF heating, for the plasma centre(R= 3.1m, on the left) and the edge (R=3.8 m, on the right). Kites show L-modes, while squares show an H-mode with P_{ICRF}=9 MW. Positive values indicate co-current, negative values counter-current rotation.

5.3.3. High delta configuration plasmas

High delta configuration demonstrated good confinement at Greenwald densities for 2.5MA. The operation of this configuration was demonstrated up to 3.5MA. Low delta configurations optimised at 2.5MA showed degraded confinement and ELM behaviour between 3.5MA and 4.3MA. Better ELM behaviour was found with corner configuration and optimised gas. 4.5MA was demonstrated but with H factor ~0.9. S1-2.4.16 demonstrated reduced target surface temperature with sweeping for both low and high delta.

5.3.4. NTM studies

An innovative method for real-time mode number analysis based on recursive filtering tested on JET magnetic signals. Discharge plan for Polarization current probing on NTM stability was prepared (experiment not possible in timeline constraints). Numerical studies on (2,1) NTM threshold island width in advanced scenario JET shots were performed yielding good qualitative agreement with observations.

5.3.5. Kalman filter application to TAE studies

Routine studies are performed at JET using a new set of antennas to excite Toroidal Alfven Eigenmodes (TAEs). A TAE resonance footprint is observed in the plasma response measurement when there is a noticeable variation in both the amplitude and the phase of the response with respect to the excitation. *The standard dual-phase lockin method,* implemented in JET using hardware synchronous detectors, *is compared to a linear Kalman filter non-stationary single harmonic estimator and to an Extended Kalman Filter frequency tracker for real-time resonance identification.* The fully digital linear

Kalman filter approach is shown to provide comparable results to the hardware dual-phase lockin approach in terms of signal-to-noise performance and introduced delay in the estimation of both the instantaneous amplitude and instantaneous phase of the plasma response with respect to the applied excitation. In the case when the estimation of the instantaneous amplitude suffices for the real-time resonance identification it is shown that the reference waveform is not required and that this particular Extended Kalman Filter implementation is capable of tracking the excitation frequency as well as perform harmonic estimation (Figure 5.4).

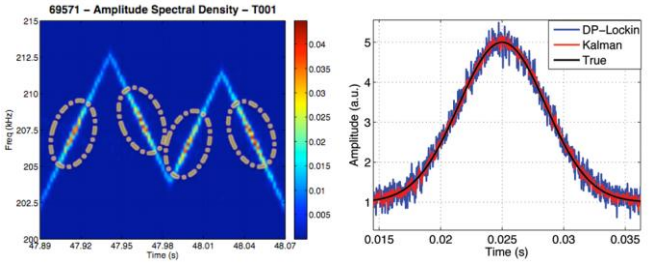

Figure 5.4 - TAE excitation with sweeping frequency indicating maximum response when crossing TAE resonances. Simulated amplitude response using 19th order FIR Low pass filtering and the Kalman filter evidence the excellent compromise of the latter at removing noise in the synchronous detection at very high throughput.

5.3.6. Radial correlation reflectometry analysis in JET

A simple "equilibrium" has been added to the correlation reflectometer analysis tool to be used with very simple plasmas for which EFIT cannot run. *A companion utility to the Correlation reflectometer analysis tool has been developed* to preview the cutoff location of all Correlation reflectometer channels given the toroidal magnetic field and an approximate density profile, which is needed in the planning phase of the experiments to know at which radial positions measurements can be expected. *Some upgrades to the correlation reflectometer analysis tool have been made*, to improve data reading from magnetic coils diagnostic and to use the new density profiles from the profile reflectometer. Correlation reflectometer data quality has been addresses, namely concerning data calibration.

Analysis of data from the correlation reflectometry diagnostic was made, including assistance in planning and control room analysis of particular experiments. Measurements and a qualitative interpretation of the radial correlation reflectometer results consistent with changes observed in other plasma signals (Figure 5.5). Correlations observed between variations in confinement, measured by the energy confinement time; in the turbulence level inferred from significant variations of the reflectometer correlation length at nearby radial positions; and in collisionality. Correlation lengths correctly reflected confinement changes in presence of ITBs.

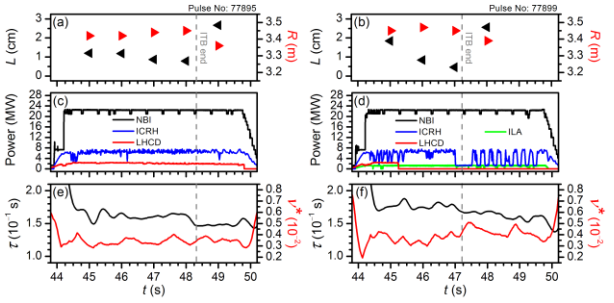

Figure 5.5 - For JET pulses (a,c,e) #77895 and (b,d,f) #77899 (B=2.7 T, I_p=1.8 MA, n_e=4×10^{19} m^{-3}) it is shown (a,b) the reflectometer correlation length (left) and cutoff position (right), (c,d) the heating power, and (e,f) the energy confinement time (left) and collisionality (right). The dashed lines mark ITB termination.

5.3.7. ELM transport in the JET far-SOL

The ELM filamentary structure in the JET scrape-off layer (SOL) has been further investigated using a multi-pin reciprocating Langmuir probe system. The far SOL plasma parameters have been compared during Type I and Type III ELMs. The main difference between the two ELM types appears to occur in the first ~300 μs of the ELM, where the parameters measured by the probe have higher amplitudes for Type I ELMs. Probe data has been compared with a model for the filament radial propagation. It is confirmed that the fast filaments observed at the beginning of Type I reach the wall with a large fraction of the pedestal density and temperature.

The peak particle flux, Γ, of the first ELM filament is significantly larger than the background (inter-ELM) value. The ratio $\Gamma_{peak}/\Gamma_{inter\text{-}ELM}$ is typically ~50 in the far-SOL for small Type I ELMs. This ratio increases significantly with the ELM size, being as large as 1×10^{3} near the limiter radial position for medium size Type I ELMs (Figure 5.6). The ion flux to the main chamber PFCs in the inter-ELM phase is typically below 1×10^{21} $m^{-2}s^{-1}$ for Type I ELMs and reaches ~3×10^{24} $m^{-2}s^{-1}$ in the ELM filaments. In spite of the time between ELMs being much longer than the ELM duration, the particle fluence is in general larger in the latter period. The fluence during the ELM (τ_{ELM} ≈ 3 ms) is typically ~5×10^{20} m^{-2} while during the inter-ELM period ($\tau_{inter\text{-}ELM}$ ≈ 50 ms) it is roughly ~5×10^{19} m^{-2}. Most of the particle flux to the main chamber PFCs thus occurs during ELMs.

The radial velocity associated with ELMs has been measured in different devices using a large variety of experimental techniques and a wide range of velocities have been reported. Part of this disparity may be traced to the variations in temporal and spatial resolution amongst the various diagnostics. Probes allow localized measurements with high temporal resolution and therefore are ideally suitable to study the detailed ELM structure. A radial velocity averaged over different time scales has been derived and its shown in Figure 5.7. For small Type I ELMs large velocities are obtained, ~0.8 km/s, for short time scales, 10 μs. As the averaging time

is increased the velocity quickly decreases, reaching ~270 m/s for a 100 μs average. For larger times, the radial velocity decreases slowly, attaining a value of ~170 m/s for an averaging time of 1 ms. Measurements performed with an integration time larger than 0.1 ms are therefore expected to give a modest radial velocity. The 0.1 ms time scale corresponds typically to the filament duration.

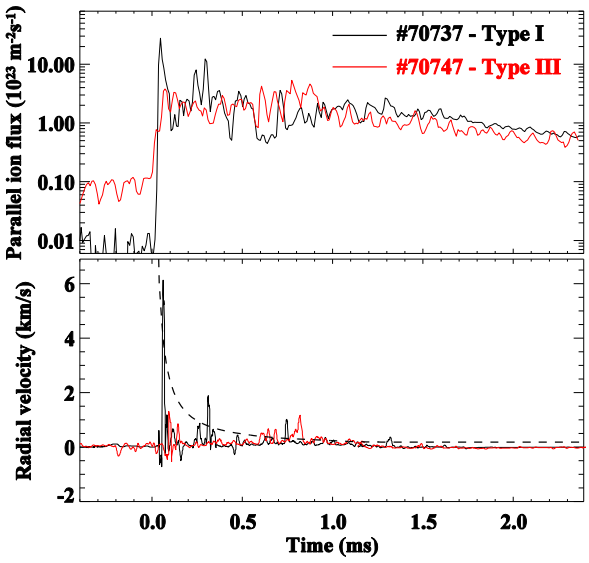

Figure 5.6 - Time evolution of the ion flux and radial velocity for a Type I and a Type III ELMs. The dashed line represents the radial velocity estimated from the time of flight assuming that all the filaments are release at the beginning of the ELM magnetic activity.

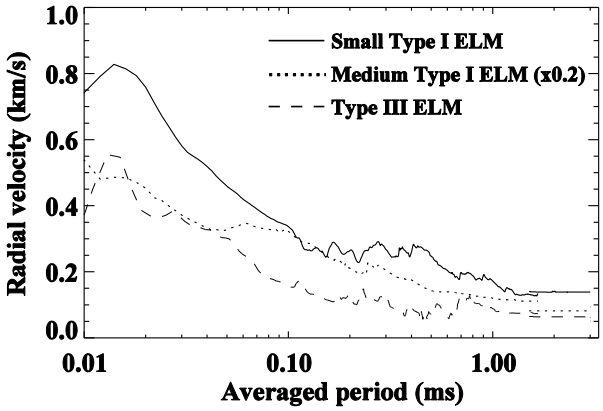

Figure 5.7 - Time averaged radial velocity as a function of the time-scale for three ELMs with different amplitude (small Type I #58749, medium Type I #70737 and Type III #70747).

5.3.8. Mitigation of disruption loads for ITER & Optimization of massive gas injection for disruption mitigation

Experiments on massive gas injection (MGI) have been continuing at JET in order to investigate capabilities of fast Disruption Mitigation Valve (DMV) to mitigate disruptions loads and suppress runaway electron generation. Up to 2×1023 atoms of neon and argon or their mixtures with deuterium have been injected into ohmic and neutral beam heated plasmas. A reduction of the heat loads caused by the fast energy loss during the thermal quench is achieved, if the radiation before and during the thermal quench is enhanced by the injected impurities. A maximum of 50% of the thermal energy is radiated during this phase in the JET experiments. An analysis of JET disruptions shows that runaway electrons have been generated in significant amount of all disruptions occurring in x-point configurations. By the injection of Ar/D2 or Ne/D2 mixtures the runaway generation was successfully avoided due to the suppression of the Dreicer mechanism. However, injection of pure argon led to runaway generation even at low toroidal magnetic fields, while pure neon injection demonstrated lower tendency to generate runaways. The pure gas injections are characterized by the much lower fuelling efficiency, ranging around 2 − 5%. Obviously, that was not enough to provide the necessary plasma density increase in order to suppress the runaway generation. The experimental data obtained in the recent experiments on disruptions and runway electrons in JET (2008-2009) has been added into existing data base on disruption generated runaway electrons.

Although, runaways can be safely avoided by MGI in JET disruptions, the density reached by MGI is still a factor 50 below the critical density for avalanche suppression, which is essential in ITER. Large runaway currents are expected to be generated in ITER disruptions, because of the strong amplification of the number of runaway electrons by the avalanche process. The energy deposited on PFC by such a runaway beam ranges between 30 − 200 MJ, depending on the conversion of magnetic to kinetic energy.

5.3.9. Development of the ITER Ion Cyclotron Technique for Wall Conditioning at JET

Experiments on ICRF plasma production in JET with the aim of developing the ITER Ion Cyclotron technique for Wall Conditioning (ICWC) scenario have been accomplished. ITER ICWC scenario has been simulated experimentally in JET at the same ratio between toroidal magnetic field and heating frequency as it is considered for ITER. Reliable plasma production and safe operation of ICWC in JET has been demonstrated. The experimental data on ICRF plasma production methods in large tokamaks has been significantly extended. This data is under detailed analysis now, especially, in relation to coupling efficiency and plasma conditioning properties. It was also shown that the limit to the frequency for safe operation appears less severe than originally proposed and will not prevent ICWC in ITER.

5.3.10. Characterisation of new ICRH antenna

Characteristics of new ICRH antenna (ILA) have been studied in H-mode and L-mode plasmas in JET. Despite

the high radiated power density small deleterious effect on impurity production was observed. Analysis of the data on fast ions at ICRH with ILA has been performed. First observation of energetic ions with ILA was reported.

Large source of metal impurities in JET plasmas has been found during a study of the metal impurities behavior depending on the loss of high-energy ions at their interaction with PFC. Increase of the fast ions loss has been observed at the presence of different MHD instabilities and with the increase of applied heating power. The enhancement of fast ions losses during MHD instabilities resulted in the deterioration of the plasma performance due to an increase (by more than 10 times) in the metal impurities concentrations resulting from the interaction of lost fast ions with PFC. Observed radiation losses was found to increase by more than 5 times. Interaction of lost high-energy ions with PFC and active elements of the heating systems sometimes resulted in deterioration of the heating systems performance till to their complete switch-off by protection systems.

5.3.11. Momentum pinch

IPFN has contributed to the analysis and modelling of experimental data, obtained from carefully executed experiments during JET experimental campaigns. Results show evidence that, under certain plasma conditions, a momentum pinch exists, which confirm other machine findings. Crucial to the analysis of momentum transport is the robustness of the modelling used to quantify the amount of injected torque into the plasma. To increase the confidence in the results, a sensitivity assessment of the NBI torque deposition was done with respect to the uncertainties of the measured plasma parameters. The results confirm initial estimations. New experiments were done with the purpose to quantify the parametric dependence of the momentum transport coefficients on various plasma quantities, which are essential to validate recent theoretical models, and to guide ongoing theoretical work that is being done in this area. After the quality evaluation of the data gathered, data and modelling analysis has started.

5.3.12. Highly spatially resolved measurements of JET edge toroidal rotation in Type-I ELMy H-mode plasmas

The main goal of the analysis, which is presently continuing, is *to obtain a relation of the variation of the toroidal rotation at the top of the pedestal, and its shear, with the ELM frequency (f_{ELM}).*

In order to investigate the influence of v_φ on the in the f_{ELM}, (Figure 5.8a) show the f_{ELM} as a function of v_φ. Data indicate that the ELM frequency is increasing as the rotation decreases and reaches values close to zero for δ_r = 0.75% (▲). However, for the higher ripple case (δ_r=1%), the data indicate that the f_{ELM} is decreasing as the rotation increase in the counter-current direction, which could indicate that the ELM frequency is linked to the amplitude of v_φ and not the direction of the velocity. In order to verify this assumption, the f_{ELM} was plotted as a function of the absolute value of v_φ (Figure 5.8b). It is clear in this figure that $|v_\varphi|$ is directly influencing the ELM frequency, and that as the rotation is decreasing the ELM frequency is increasing.

The profile of the plasma radial electric field (E_r) and hence the $\omega_{\mathbf{ExB}}$ shearing rate has been recognized as key factor to reduce turbulent transport and stabilization of MHD activity. In that sense, E_r and hence the ω_{ExB} shearing rate has been analyzed for discharges with low and high TF ripple value. Although $\mathbf{E}_r$ and $\omega_{\mathbf{ExB}}$ have been calculated using JETTO simulations, an analysis using the code MISHKA-I and MISHKA-FLOW is ongoing in order to fully understand the effect of plasma rotation in the MHD stability.

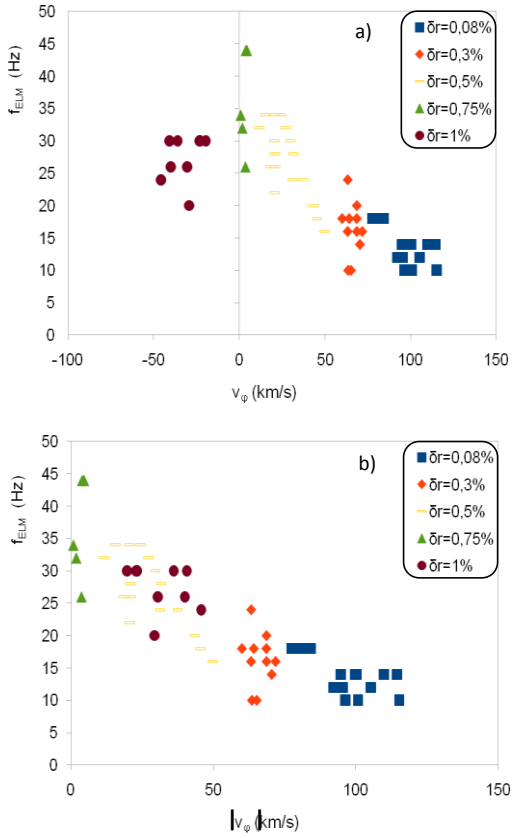

Figure 5.8 – a) f_{ELM} as a function of V_φ^{ped} and b) $|V_\varphi^{ped}|$

5.4. THEORY AND MODELLING

5.4.1. ITG modelling

JETTO and GLF23 codes were used to model S2 and T experiments. In particular, GLF23 was used to model different ion heating conditions (with various ICRH power deposition profiles between the two cases of on- and off-axis deposition) and points on the ITG plot ion energy flux vs. stiffness for different plasma rotations were obtained.

5.4.2. Momentum pinch

Analysis of experimental data has reconfirmed that, under certain plasma conditions, momentum pinch exists. *TRANSP was used* to quantify the amount of injected

torque, and JINTRAC for momentum transport analysis. To increase the confidence in the results, mainly due to experimental data uncertainty, *a sensitivity assessment of the NBI torque deposition was done*, confirming initial estimations. Parametric analysis will is ongoing.

5.4.3. Fast Ion Losses

The influence of Alfvén eigenmodes (Core-Localized TAE and High-m Global TAE) *on redistribution and loss of fast ions in the Advanced Tokamak Scenario has been investigated in JET dedicated experiments.* Temporal evolution of the spatial structure of Alfvén eigenmodes present in the plasma during q-profile evolution has been calculated with the MISHKA code. On the other hand, fast ion losses with resolution in energy and the pitch-angle were measured with a scintillator probe, while the internal redistribution of the fast ions was analysed by measuring the temporal evolution of the radial profiles of γ-ray emission coming from the fast ions colliding with main impurities, Be and C. By correlating the measurements above, it is possible to assess the effect of Alfvén eigenmodes on redistribution and loss of fast ions. It is found that the TAE localized in the core of the plasma cause a severe redistribution of the fast ions in the plasma centre, leading to a flattening of the vertical profile of γ-ray emission (Figure 5.9).

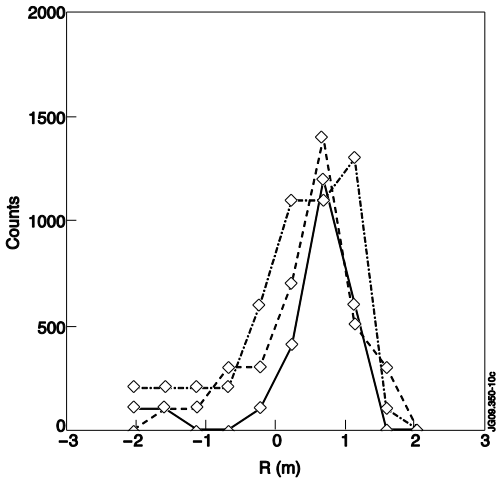

Figure 5.9 - Vertical profile of γ-ray emission. Solid line and dashed line: Before the onset of Core-Localized TAE. Dashed-dotted line: after the onset of Core-Localized TAE.

Aside from it, the Core-Localized TAE also cause enhanced loss of fast ions, with the number of losses increasing with time as the Core-Localized TAE moves radially outward (Figure 5.10). The red line corresponds to 7.2 MeV alpha particles which are not correlated with TAE activity. The blue line corresponds to a mix of alpha particles with energies E= 2.0 MeV and 3He ICRH accelerated ions ions with energies E= 2.3 MeV. At this range of energies, the fast ions interact with the Core-Localized TAE and an increased in the number of losses is measured by the scintillator probe.

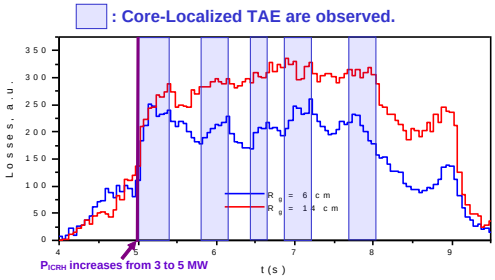

Figure 5.10 - Temporal evolution of fast ion losses with Rg= 6 cm (blue) and Rg= 14 cm (red). The periods of time at which Core-Localized TAE are observed are shadowed.

5.4.4. Interaction of lost fast ions with plasma facing components in JET

An interaction of escaping high-energy ions with plasma facing components (PFC) in JET resulted on large increase of metal impurities in plasma. The loss of energetic ions was found to cause the increase by about 100% of the Ni concentration following saw-tooth crashes. The excitation of MHD instabilities, like fishbones and kink-ballooning modes, also resulted in a significant loss of energetic ions and impurities release.

Figure 5.11a) and 5.11b) present detrimental impact of fast ions loss due to fishbone instability onto the plasma performance in discharge #77894 (B_0= 2.7 T, I_{pl}= 1.8 MA, H-minority heating scenario in D plasma (total $P_{ICRH} \cong$ 8.3 MW, P_{NBI}=22 MW, P_{LHCD}=2.6 MW)).

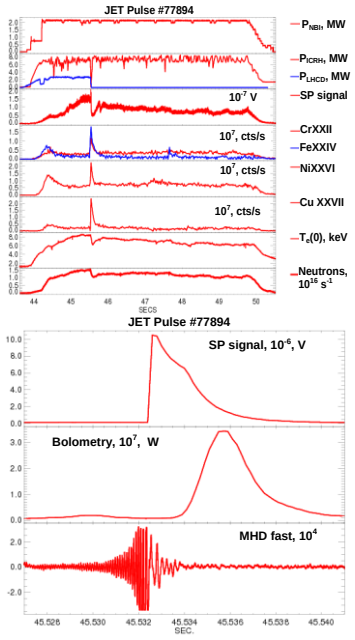

Figure 5.11 - JET pulse #77894 ('Advanced Tokamak' regime) with observed bursts of impurities and fast ions loss due to MHD event (chart a) identified as fishbone instability (chart b).

High amplitude fishbone (Figure 5.11b)) resulted in very large loss of fast ions, followed by intense impurities influx and radiation spikes, leading to a switch-off of the LHCD system for protection. Such events – MHD instabilities and intense fast ions loss – have been observed in AT regimes in JET, resulting in the loss of plasma performance and, in several cases, leading to disruptions. Frequently observed coincidence of intense fast ions loss, release of metals and deterioration of heating systems performance demonstrates the direct impact of fast ions loss on technical aspects of tokamak systems operation.

Progressive trends in the release of metal impurities depending on fast ions loss values have been found in many regimes. Most significant effect of high-energy ions loss on impurity production is observed in AT regimes (Figure 5.12 (a-c)), note the logarithmic scaling). Sometimes metal impurities concentrations peaked up till to 2 orders of value at the 10 times increase of high-energy protons and deuterons loss.

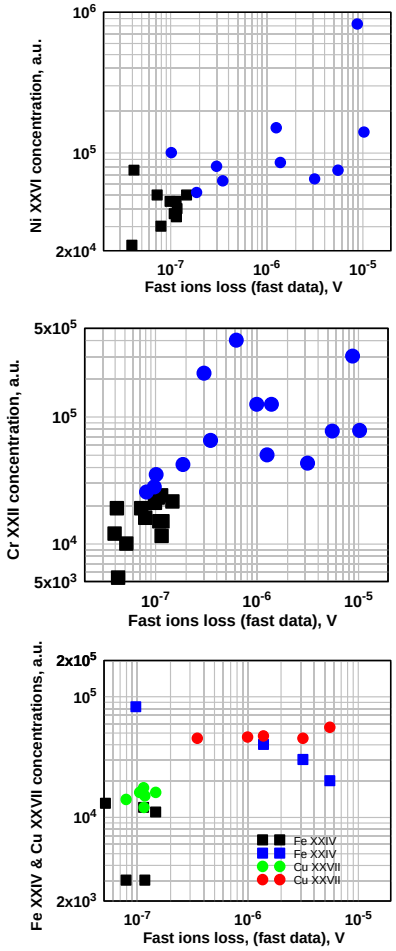

Figure 5.12 - Enhancement of metal impurities production (Ni – a, Cr – b and Fe and Cu – chart c) due to interaction of large populations of fast ions escaping from plasma at MHD instability (fishbones and kink-ballooning modes).

5.4.5. Impurity transport in high pedestal Te H-mode plasma

Simulations on impurity transport in the SOL were done for the ILW and seeded Neon experiments using JETTO/SANCO. It was found that, while Te at the target plates decreases, radiation does not increase significantly with Neon. These plasmas are also more transparent to the deuterium in the SOL, with deuterium throughput reaching 20% of the deuterium inlet gas.

5.4.5.1. Connection with ELMs

Simulations with JETTO/SANCO also suggest that the slowly increase of the Z_{eff} observed experimentally before the first ELM is due to the Carbon released from the walls. The 1st ELM leads to a fast impurity penetration into the plasma core, observed in the Z_{eff} signal, when the impurity density at the edge is lower than in the plasma core (positive impurity density gradient scenario). In a negative impurity density gradient scenario, this ELM would remove impurities from the plasma core.

5.4.5.2. Effect of extrinsic impurity seeding

Simulations with EDGE2D/NIMBUS suggest that when the extrinsic gas inlet rate is kept unchanged, the impurity concentration in the plasma core decreases with increasing deuterium inlet rate, in agreement with experimental observations. These experiments also indicate that the total radiation in high density plasmas doesn't increase with an increasing extrinsic impurity inlet rate. Similar results were also found in the EDGE2D/NIMBUS simulations although only at a higher radiation fraction. One should note that, although the radiation did not increase, the electron temperature at the targets decreased significantly with the extrinsic impurity inlet rate and Zeff in the plasma core did not increase significantly. One possible explanation might be that the impurity seeding leads to a reduction of Carbon released from the walls when the plasma is close to detachment.

5.5. PLASMA ENGINEERING AND SYSTEMS INTEGRATION

The activities on Plasma Engineering and Systems Integration consisted of:

- Voluntary activities on the improvement of diagnostics and plasma control systems;
- Participation in JET Enhancements projects;
- Participation in JET Fusion Technology Programme.

The voluntary contributions to the improvement of diagnostics and plasma control systems were the following:

- *Installation and test of Beam Profile Monitor of the Lithium beam diagnostic;*
- *Development of a new error field correction coils controller;*
- *Upgrade of the microwave reflectometry data acquisition system.*

Concerning the JET-EP project, the Association EURATOM/IST have been in charge of the following contracts in 2009:

- Data acquisition for the neutron camera diagnostics enhancements (DNG-G)[2];
- Data acquisition for the gamma ray spectroscopy (GRS)[3];
- ATCA hardware platform for the Plasma Control Upgrade project (PCU-VS)[4];
- Development of a Digital Link for the Vertical Stabilization controller (PC2-VS)[5];
- Real-Time Measurement & Control Diagnostics & Infrastructure[6];

For the JET Fusion Technology Programme, the Association Euratom/IST participated in the *Post-mortem analysis and simulation of the JET outer poloidal limiters tiles*[7].

5.5.1. Installation and test of Beam Profile Monitor of the Lithium beam diagnostic

The Lithium Beam Probe (LBP) is widely used for measurements of the electron density in the edge plasma of magnetically-confined fusion experiments. The quality of LBP data strongly depends on the stability and profile shape of the beam. The main beam parameters are: beam energy, beam intensity, beam profile, beam divergence and the neutralization efficiency. For improved monitoring of the beam parameters, *a Beam Profile Monitor (BPM) from the National Electrostatic Corporation (NEC) has been installed in the Li beam line at JET.* In the NEC BPM, a single grounded wire, formed into a 45º segment of a helix, is rotated by a motor about the axis of the helix. During each full revolution, the wire sweeps twice across the beam to give X and Y profiles. This work allowed the optimization of the beam intensity up to 1 mA, 1 cm size at energy of 50 keV. Experiments with Li beam diagnostics have been performed over all C27 Campaign.

5.5.2. New Error Field Correction Coils Controller

The Error Field Correction Coils have played a big part in the recent experimental program of JET campaigns. The DFAS, old TAE amplifiers, which were driving the EFCCs were replaced by the PRFA amplifiers which were formerly the circuit actuators of the old vertical stabilisation system. PRFA has brought higher current capability (hence higher magnetic field) over the DFAS at the expense of a lower bandwidth. Along with these improvements *a new controller has also been developed, deployed, commissioned and operated in recent JET operation.* In terms of hardware implementation the present setup comprises a VME crate hosting a Motorola 5100 PowerPC with ATM card, a MPV956 (Analog I/O - ADC & DAC) board, a MPV922 (Digital I/O) board and a VPLS/CTTS (Timing system) board. The controller software is the first MARTe-based application running on the VxWorks real-time operating system. In order to operate the EFCCs the session leaders are provided with a graphical user interface (Level-1) for programming the (PID controlled) target current waveforms flowing in the coils in either "n = 1" or "n = 2" configurations. The controller allows for the setup of a variable number of time windows and provides a very complete and flexible waveform generator suitable for either DC and AC operation including frequency, amplitude and offset sweeps.

5.5.3. Microwave reflectometry

The microwave correlation reflectometer control and data acquisition system has been upgraded. It is now capable of controlling and acquiring up to 20 measures during JET discharges with microwave control software totally linked to the VME acquisition. With the current upgrade the system can independently control up to 128 measures acquired in the VME system up to its memory limit. The remaining measures can be acquired in a parallel system. By making control and acquisition independent it is now possible to acquire frequency sweep and steady frequency measures, completely programmable using level-1 GUI interface.

5.5.4. Data acquisition for the neutron camera diagnostics and for the gamma ray spectroscopy

The following tasks were performed:

- *Installation of the ATCA controller and data acquisition boards,* 24-channel@250MSPS system for DNGG and 8-channels@400MSPS for GRS (5.13);
- *Assembling of the spare 400 MSPS board for GRS*;
- *Production and installation of 16 channels settable gain pre-amplifiers*;
- *Development and improvement of the FPGA code of the 8-4 channels @ 400MHz ATCA digitizer (TRP400) and @ 250MHz ATCA digitizer (TRP250),* including the development of the global firmware, with optional modules to be selected according to the project and digitizer requirements. In agreement with the requirements and foreseeing interleaved architectures all modules work now with parallelized data. The pulse storage module and the pulse processing module based on the trapezoidal filter were developed, in addition to improvements in the main modules;
- *Fully integration of the GRS (KM6S) and DNG-G (KN3G) in the JET CODAS infrastructure, both for diagnostic configuration user-interface and data collection.* During the C27 experimental campaign, the systems proved to reliably acquire large amounts of data to the JET database and run for several consecutive weeks without the need of intervention;
- *A Data Validation assessment occurs at JET* to analyze and validate the C27 results on the DNGG count rate on the test channel, which was very low;

[2] JW7-OEP-IST-28A
[3] JW6-OEP-IST-24A
[4] JW5-OEP-IST-22B
[5] JW7-OEP-IST-32A
[6] JW8-OEP-IST-39
[7] JW9-FT-3.47

- *Development, analysis and improvement of the trapezoidal and noise filtering algorithms* (FPGA code) and its feasibility at 400 MSPS using the GRS and DNGG pulse data files from JET as input to the digitizer through a Waveform Generator;
- *Development of a Graphical User Interface with real time spectra plot capability.*

IST also provided the Project Leader for the data acquisition for the neutron camera diagnostics project.

Figure 5.13 – GRS data acquisition

5.5.5. ATCA hardware platform for the Plasma Control Upgrade

The following tasks were performed:

- *Finalization of the specifications for the controller and experimental features of the vertical stabilization (VS).* A rather complex CODAS configuration user-interface was designed and commissioned together with the JET team. Besides the required support for running the plasma pulses (where VS is an essential system), a large set of experimental features was added: (a) time based scenarios which allow to change control scheme; (b) real-time time velocity estimator switching; (c) several types of vertical kicks, which can act combined and synchronous to plasma events; (d) divertor based kicks. These experimental features were commissioned in the laboratory, using plasma and plant simulators, and in the live system;
- With the Enhanced Radial Field Amplifier (ERFA) already on site *the amplifier was fully characterized and tested against a large amount of possible scenarios;*
- Once ERFA was tested, *the experimental C27 campaign started with the choice of the number of turns for the coils in the EFA circuit.* Two weeks of experimental campaign and data analysis were dedicated for this action. The system was then ready to be used and successfully run for more than 1500 plasma pulses during several weeks of operation. It guaranteed the required 50us control cycle time and permitted at the same time to explore a large set of experimental features, providing a very good combination between scientific and technological development; (iv) development of a Graphical User Interface for testing the ATCA-GPIO boards; (v) twelve additional ATCA-GPIO boards, 400 ADC modules and 3 RTM boards were produced, tested, commissioned on the laboratory and successfully installed for operation. Test and repair of the remaining faulty boards was also performed and (vi) a new solution for data streaming which doesn't compromise real-time performance was also developed and presented at the 7th IAEA Technical Meeting.

5.5.6. Plasma Control Upgrade Phase 2 – Digital Link for the Vertical Stabilization controller

The Digital Link is a bidirectional full-duplex link and allows also the monitoring and the digital close loop control of the ERFA amplifiers. The Digital Link provides an error-free digital interconnection between the ATCA VS System and the Enhanced Radial Field Amplifier (ERFA) of JET (Figure 5.14). It was designed to replace the analogue connection feed by DACs. The following tasks were performed:

- *Development of an Optical Gigabit Serial Link (OGSL) card* to interface between the ATCA Digital Link optical connection and the ERFA control circuitry;
- *Development and deploying of the FPGA code of the Digital Link for the ATCA-MIMO-ISOL board of the ATCA Vertical Stabilization (VS) System,* including an Aurora endpoint with FIFOs, CRC and Parity Bit generator engines interconnected to a DMA and PCI Express blocks.

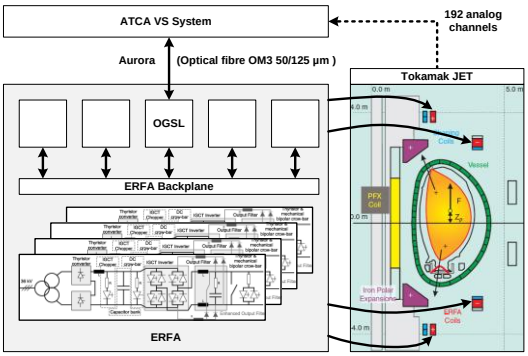

Figure 5.14 - ATCA VS system and ERFA interconnection.

5.5.7. Real-Time Measurement & Control Diagnostics & Infrastructure

The goal of this project is to expand the JET real-time diagnostics and control capabilities required to fulfill the programmed objectives of JET in the proposed FP7 phase of operation dedicated to the preparation of ITER. The contract signed in December 2008 specifies the following tasks to be developed, which are in progress:

- *Improvement of the real-time measurement capabilities of FIR Interferometry (KG1).* The new PL6 laser and FIR twin cavity, on loan for UKAEA/Culham, were installed in the new Laser Class 4 Lab in J1 building. The new lasers successfully restarted operation, after some delays caused by a major failure from a power supply oil leak. The power of 220mW was obtained in one FIR cavity which is about 90 % of the original setup, almost 20 years old. For the new DAQ system for the new KG1 channels the planned extension of the present KG1rt was suspended in order to discuss an alternative method proposed by CEA. This solution runs in dedicated hardware based on FPGAs to calculate the line density by a new algorithm. This system is being presently tested in JET in a prototype connected to KG1 channels 3 and 4;
- *Improvement of the real-time measurement capabilities of some of the Neutron Diagnostics* (Total Neutron rate KN1, Hard X-ray rate KH1, 14 MeV neutron rate-KM7). The final specifications for the Total Neutron rate, KN1, diagnostic upgrade and the new real-time NPLN calculation) were developed. A partial Design Note with the KN1 diagnostic upgrade and the new real-time NPLN calculation has been discussed and approved in the EP2-RTM project board;
- *Expansion of the real-time JET Network Infrastructure to accommodate the extra real-time Diagnostics* required for FP7 either by exploiting recent network technologies or by extending existing ATM, including the development and implementation of a Real-Time Network prototype. An evaluation study of present technologies in high performance networks with relevance to real-time control has been started. A draft of the planned evaluation prototype network has been presented and the basic benchmark test methodologies.

IST also provided the Project Leader.

5.5.8. KK3F CADAS Enhancement

IST/IPFN developed *error analysis and correction of the data acquisition software for this Project.*

5.5.9. Post-mortem analysis and simulation of the JET Outer Poloidal Limiters tiles

The JET Outer Poloidal Limiters (OPL) limiters comprise about 50 pairs of tiles in a poloidal stack, each of which has a plasma facing surface about 25 mm (poloidal) by 350 mm (toroidal) and is about 50 mm thick. *Standard CFC and W coated tiles overlaid with a 10 micron layer of C on top were studied with RBS/PIXE* to understand the erosion/re-deposition processes occurring in this region of the reactor chamber. *The surface morphology was assessed with SEM and the retention of hydrogen isotopes in the tiles with NRA and ERDA techniques.* This is mostly 2H from the fuelling gas, but 3H is also present as a result of 2H-2H fusion reactions and 1H coming from the atmospheric exposure.

Enhanced erosion was observed at the center of the tile and redeposion more close at their ends. A significant amount of D was incorporated within the deposited layers together with the plasma impurities (Figure 5.15). The impurities are coming from the inconel components of the chamber wall. The results also suggest that the fuel retention occurs during the re-deposition of the plasma impurities. The divertor tiles are permanently exposed to a high flux of plasma particles and heat loads. The major impurities are Ni and Be together with oxygen, Figure 5.16. The amount of oxygen is consistently higher in the divertor tiles compared to the OPL ones. The surface of the divertor tiles is destroyed and develops a spongy like structure which contributes to an increase of fuel retention.

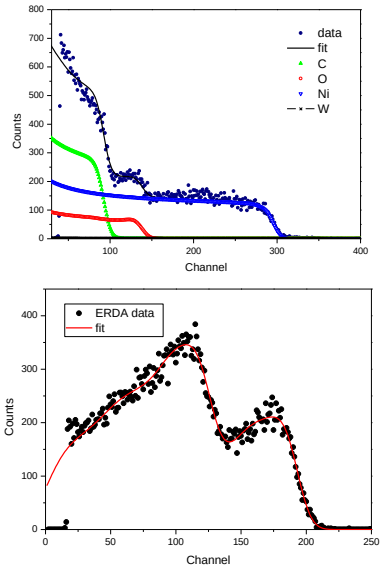

Figure 5.15 - RBS spectrum (above) showing the profile of the impurities in a poloidal tile and the ERDA spectra (below) with the 2H and 1H incorporated in the tile.

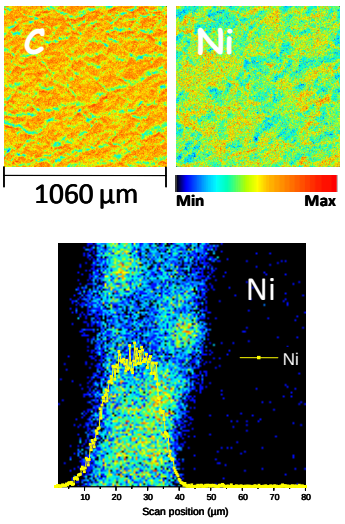

Figure 5.16 - Distribution maps for the major impurity in a divertor tile. The solid line is the depth profile extracted from the RBS data.

6. PARTICIPATION IN THE ASDEX UPGRADE PROGRAMME[1]

M.E. Manso (Head), F. Serra (Deputy Head), D. Borba, R. Coelho, L. Cupido, L. Fattorini, I. Nunes, V. Plyusnin, T. Ribeiro, F. Salzedas, J. Santos, A. Silva, F. Silva, P. Varela, A. Combo, S. Graça, L. Guimarães, L. Meneses.

6.1. INTRODUCTION

This project included in 2009 activities on:

- New microwave reflectometry techniques;
- Modelling and scientific exploitation of reflectometry diagnostics for plasma physics studies namely to study MHD modes;
- Other plasma physics studies concerned the development of the ICWC technique;

which has been carried out in the frame of:

- The General Support of the Contract of Association;
- The EFDA Task WP08-09-DIA-01, AUG Plasma Position Reflectometer.

6.2. MICROWAVE REFLECTOMETRY

6.2.1. Operation and hardware issues

The operation of the fixed frequency and hopping systems for fluctuation measurements was severely limited due to hardware problems. The Q band channel stop operating due to severe damage of the mixer and multiplier most likely caused by excessive plasma radiation. Also, the data acquisition for the fluctuation channels which presented problems since more than two years requiring extensive maintenance, stop working. *A new data acquisition system to replace the old one is presently being developed by IPP*.

In addition the operation of the FM-CW profile reflectometry system continued to be strongly limited due to the increased degradation of key microwave components following 15 years of continuous operation plus the damage of two HFS channels caused by stray high ECRH radiation. With the limited operation density profiles could only be obtained at the LFS and at low density. They display the *high quality of reflectometry profile data being obtained automatically using the burst-mode analysis technique. A clear reflection from X mode lower cutoff was detected* which from our knowledge was never seen before in any other fusion device. This is an important finding once the lower cutoff has been proposed for ITER to access the core plasma from the HFS. *The few operational swept FM-CW channels were also used in fixed frequency mode* providing important measurements of the Alfven wave cascades.

6.2.1.1. Refurbishment the FM-CW diagnostic

In view of the degradation of the FM-CW diagnostic and its importance for the EFDA Task on Plasma Position Reflectometry demonstration for ITER as well as for next EFDA tasks on Real Time density profiles (in preparation for the ITER advanced scenarios), *a conservative proposal for the refurbishment of diagnostic was elaborated which keeps most of the existing system.*

The refurbishment has two main purposes: (i) to make the front end at the HFS channels compatible with the levels of ECRH stray radiation reaching the antennas. A novel design has already been successfully tested at the laboratory; (ii) to repair the damage channels equipping them with modern electronics such as the one developed by IPFN for the JET FM-CW KG10 diagnostic.

6.2.2. Data processing for density profile evaluation Bayesian analysis techniques

One key objective in ASDEX Upgrade is to obtain a combined density profile using data from Li-beam, Thomson Scattering, and Reflectometry diagnostics. Recently, the Li-beam data processing has included Bayesian analysis which allows reaching the profile edge pedestal, although at the cost of decreasing accuracy. Comparison of measurements from Li-beam with reflectometry (which provides stand alone edge pedestal measurements) is very important to assess the relative performance of the two diagnostics. For this purpose *several software utilities were developed that make possible to compare a large number of shots in a fairly easy way*, including among other tools the extraction of the Li-beam data, the calculation of an equivalent O-mode group delay for comparison with Reflectometry.

6.2.2.1. Density profiles from reflectometry in AUG level-2 shot files

Following the decision of the ASDEX Upgrade to include fitted profiles from reflectometry and corresponding edge pedestal data into level-2 AUG shot files, *software has been developed to update the level-2 shot files structure used by Reflectometry.*

6.2.2.2. Reflection at lower cutoff

A software tool to invert X-mode data from lower cutoff operation has been developed and is currently being tested for the inversion of the density profile. It will also allow the calculation of an equivalent O-mode group delay to compare with the simultaneously group delay measurement performed with the O-mode channels. The extent of the overlap region between X and O mode data as well as the possibility of cross-correction of data are being assessed. A comprehensive analysis of the cutoff reflection can be made with these algorithms as soon as more FM-CW data is available.

[1]Activities carried out in the frame of the Contract of Association Euratom/IST, the European Fusion Development Agreement and the Contract of Associated Laboratory, by staff of the Groups of Microwave Diagnostics, Theory and Modelling and Control and Data Acquisition, in collaboration with the ASDEX-Upgrade Team. Contact Person: G. Conway

6.2.3. Real time plasma position demonstration for ITER[2]

The full demonstration of real time Plasma Position technique proposed for ITER is being carried out in collaboration with IPP. In 2009 the activities performed were mainly related to the *development of the real-time (RT) data acquisition and data processing hardware. The final design of the dedicated high data throughput acquisition system was completed and all components were procured and delivered. A dedicated interface board was designed, manufactured and tested.* All physical components were assembled and at this stage only a small fraction (internal data buffering block) of the data acquisition on-board control FPGA remains to be programmed. The implemented block functionality has been successfully tested either experimentally in the laboratory or validated using a "post-placement and routing" FPGA simulator. On the software development side, the RT patching of the host operating system (OS) was completed and the critical system response time to hardware (acquisition system) interrupts was benchmarked, satisfying the RT design requirements. The low level software framework was completed and the software to integrated the diagnostic in the ASDEX Upgrade (AUG) RT diagnostic network initiated. The adaptation of the existing RT neural networks code to invert the density profiles is underway. The system will be integrated in 2010 in the AUG RT diagnostic network.

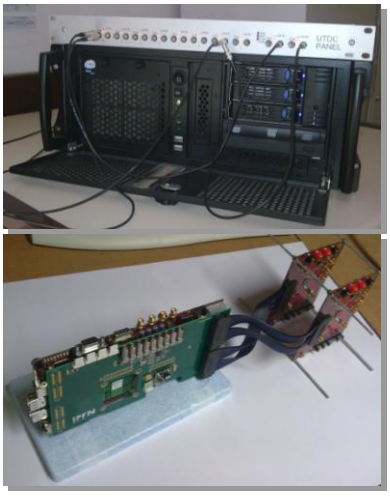

Figure 6.1 - Dual Quad-core data acquisition and real-time data processing diagnostic workstation (above), and 8 channels, 12 bit, 100 MSPS PCIe 8x data acquisition system (below).

6.2.4. Reflectometry at X mode - lower cutoff for ITER

Reflectometry operating at the X mode lower cutoff has been proposed for ITER to access the core plasma from the HFS but it has never been demonstrated in fusion plasmas. On ASDEX Upgrade *a clear signal from the low cutoff reflection (LCO) was detected (Figure 6.2)* which was confirmed by a numerical analysis of the electromagnetic access. *Inversion algorithms are being developed* to extract automatically the density profile and a 2D full wave code using a GEM code that provides realistic turbulence in ASDEX Upgrade (AUG) is being adapted, to study the LCO reflection in ITER relevant plasma scenarios.

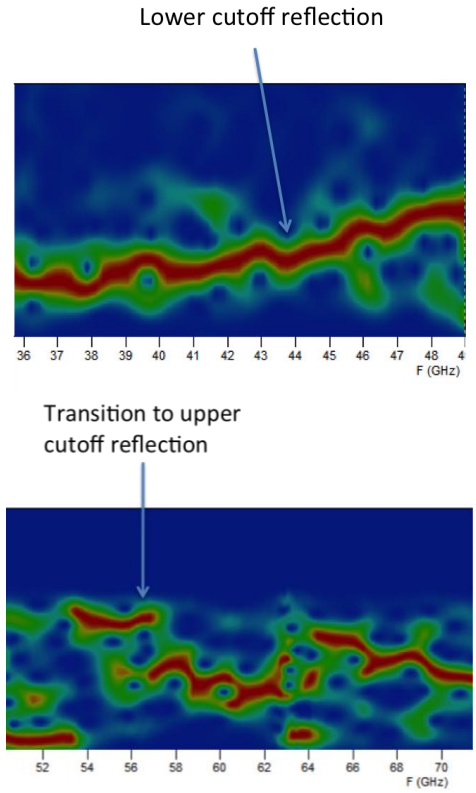

Figure 6.2 - Spectrogram of the reflectometry signal obtained in AUG shot # a standard H-mode em LSN configuration with Ip= 1.008MA; ne_{max}= 9.14x10^{19}m^3; Bt= -2.498 T; q_{95}= 4.586. Reflection from X mode lower cutoff occurs up to F = 56 GHz and beyond this value the reflection changes to the upper cutoff in agreement with the electromagnetic access conditions.

6.2.5. Study of magnetic modes

The radial eigen function of the n=4 TAE mode was studied as well as edge MHD modes in H-mode discharges using hopping and fixed frequency reflectometers. First results on poloidal velocity of edge MHD modes were deduced using the poloidal correlation technique. A PhD thesis on MHD and fast particle mode studies at IST University with joint supervision of IPFN/IPP was completed.

HFS/LFS asymetries of Alfvén Cascades (AC) could be detected using the HFS/LFS channels of the FM-CW reflectometer operating in fixed frequency. A study of the wave propagation shows that the coherent and recurrent frequency spectra typical an Alfvén cascade signatures were obtained in the absence of a cutoff layer and/or interferometric operation. Two different possibilities are

[2]Work performed in the EFDA Task WP08-09-DIA-01

being investigated with the support of numerical modelling: modulation of a resonant Bragg backscattering response by an Alfvén mode structure located at the centre of the plasma; (ii) radial movement of a turbulent wavefront, which induces a Doppler effect representative of its velocity at the location where the Bragg backscattering occurs. *Those two situations are being modelled and simulated using an O-mode full-wave Maxwell finite-differences time-domain code.*

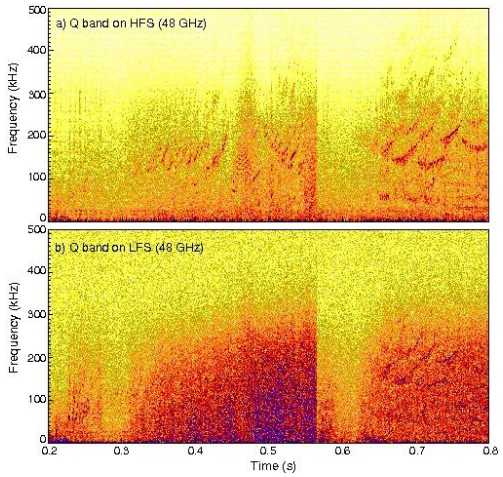

Figure 6.3 - Time-frequency spectrogram of (a) Q band signal on High Field Side (HFS) and (b) Q band signal on Low Field Side (LFS) for ASDEX Upgrade shot 25528. The Alfven Cascades (ACs) are clearly visible and the different slopes of the ACs give information on the evolution of $q_{min}(t)$. The asymmetry between HFS and LFS is being investigated.

6.3. PLASMA PHYSICS STUDIES

6.3.1. Further development of ICWC technique in AUG in support of ITER[3]

Ion Cyclotron Wall Conditioning (ICWC) plasma was reliably produced in widely-variable conditions at π- and π/2-phasing of the antenna straps. Antenna-plasma coupling (f=30 MHz) increased (up to 50–60%)(i) at higher applied RF power, (ii) on shifting the fundamental resonance $\omega=\omega_{cH+}$ from the vessel axis (B_T=2.0 T) towards antenna side (B_T=2.4 T), (iii) at antenna operations with π/2-phasing compared with π-phasing. *The preliminary assessment of surface isotopic exchange (D/H) using (He+H_2) ICWC plasmas shows the benefit from operation at higher coupled RF power and lower gas pressure*. Desorption of deuterium from the wall during both the ICW discharge and the post-discharge, occurs in the form of HD and D_2. However, a large fraction of the injected gas was found to be retained by AUG plasma facing components. In particular, He retention was observed during He containing ICWC discharges, in agreement with the observed He storage in W materials by He glow discharges in laboratory experiments.

[3]Work performed in the EFDA Task WP08-HCD-02-02.

7. PARTICIPATION IN THE TJ-II PROGRAMME[1]

C. Varandas (Head), M. Manso and C. Silva (Deputy Heads), D. Baião, L. Cupido, H. Fernandes, L. Guimarãis, T. Madeira, I. Nedzelskij and A. Silva

7.1. INTRODUCTION

This Project had in 2009 three research lines:

- Microwave reflectometry;
- Edge physics;
- X-ray diagnostics.

7.2. MICROWAVE REFLECTOMETRY

This research line included turbulence studies based on data from reflectometer hopping systems aiming at investigating the parameters that control the radial electric field in the TJ-II stellarator leading to improved confinement.

The 2009 work was focused on the *development of a new hopping system with two major improvements: switching speed and coordinated gain control.* The overall design and simulations were performed and a preliminary study leads to a design employing the latest PLL technology but requiring a fast control and configuration architecture, based either on a small FPGA or a large CPLD device. While switching times with previous hopping systems were in the millisecond scale with the novel configuration switching times below 10 micro seconds seems to be possible.

That is a major achievement and advantage for plasma physics studies because it opens the possibility of tracking faster plasma phenomena and enables also to scan the plasma radially prior and/or in between fluctuation measurements. Radial scan provides an estimation of the density profile to localize the regions where turbulence characteristics such as correlation parameters are being measured. It is expected to have a prototype for TJ-II ready for testing in 2010.

7.3. EDGE PHYSICS

7.3.1. Introduction

This research line included activities in:

- Multi-scale physics mechanisms at the L-H transition;
- Development of a radial array of probes;
- Test of a 5-channel retarding field analyzer probe.

7.3.2. Multi-scale physics mechanisms at the L-H transition

The main focus of this work was the *discovery of the amplification of multi-scale physics mechanisms and the dominant role of long-range correlations when approaching plasma conditions in which the edge transport bifurcation develops spontaneously in the TJ-II stellarator.*

It was previously found that the degree of long-range coupling for potential fluctuations is significant in the low confinement regime and strongly intermittent. This potential correlation is observed to increase significantly at the bifurcation point to about 0.8, matching the evolution of inverse of the H_α radiation (Figure 7.1). Once in the improved confinement regime, the long-range cross-correlation of the potential fluctuations decreases on the time scale of the energy confinement time.

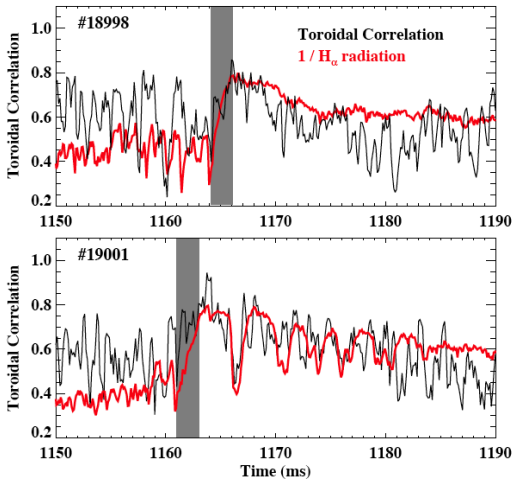

Figure 7.1 - Time evolution of the potential long-range correlation together with the evolution of inverse of the H_α radiation.

The dynamic interplay between the different frequency ranges of the potential spectra has also been investigated. Experimental results show that the integrated power in the low (below 25 kHz) and high (above 60 kHz) frequency ranges are approximately anti-correlated; thus, as the low frequency fluctuation power increases the power in the high frequency range decreases. This result is consistent with the idea of an inversed energy transfer between broadband turbulence and low frequencies (i.e. between different plasma scales), providing a mechanism for the development of long-range correlations.

7.3.3. Development of a radial array of probes

The main purpose of this research line was the *design, construction and test of a multi-pin array of Langmuir probes.* This probe allows the simulatenous measurement of the turbulent particle flux and the radial profile of the edge quantities with high spatial (down to 3 mm) and temporal (only limited by the data acquisition) resolution.

[1]Activities carried out in the frame of the Contract of Association Euratom/IST and the Contract of Associated Laboratory, by staff of the Groups of Experimental Physics and Microwave Diagnostics, in collaboration with the TJ-II Team. Contact Persons: Joaquin Sanchez, Carlos Hidalgo and Maria Ochando

7.3.4. Test of a 5-channel Retarding Field Analyzer Probe

A 5-channels RFEA has been elaborated, built and successfully tested in TJ-II plasmas. Ion temperatures in the order of 10 eV have been observed 1.5 cm outside the last closed flux surface. Degradation of the probe signals did not allow the RFEA operation deeper into the plasma. *The RFEA has been redesigned to 3 channels with the addition of two single Langmuir probes* to allow the simultaneous determination of the plasma electron density and temperature.

7.4. X-RAY DIAGNOSTICS

The main goal of this project was the successful implementation of two soft X-rays prototypes for electron temperature measurements, based on the two-filters method. Each of the prototypes consists of two detectors and two Beryllium filters with different thicknesses (Figure 7.2).

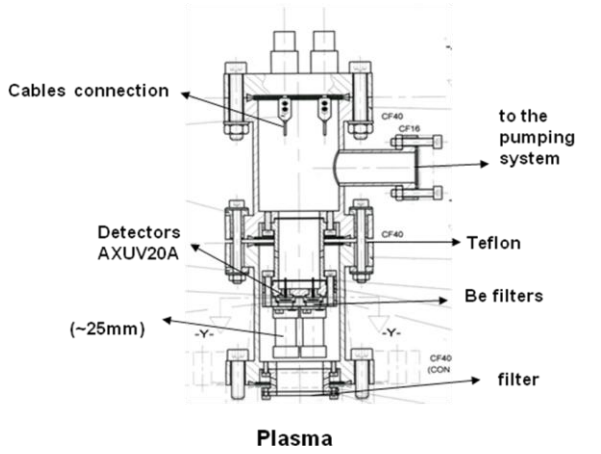

Figure 7.2 - Schematic illustration of the multi-channel electron temperature diagnostic for high density plasmas in TJ-II.

The average electron temperature was successfully determinate using Ge-detector (with a 50 μm Be filter), enabling the use of chord integrated flux signal for simulating the two-filters method and at the same time estimate T_e from the soft X-spectra. The electron temperature obtained with the two-filters method was found to be in good agreement with the one obtained with the PHA diagnostic, in spite of the different detection geometry (Figure 7.3).

These results indicate that it is necessary to use filters that completely cut the oxygen lines, namely thicker than 33 μm, to correctly estimate the electron temperature. Nevertheless, thinner filters can be used to give evidence on the presence of different amounts of oxygen and that may help to determine the plasma effective atomic number (Z_{eff}). Based on these results, the second phase of the project was initiated, with the design and implementation of two systems of global detectors, each with four filters of different thicknesses.

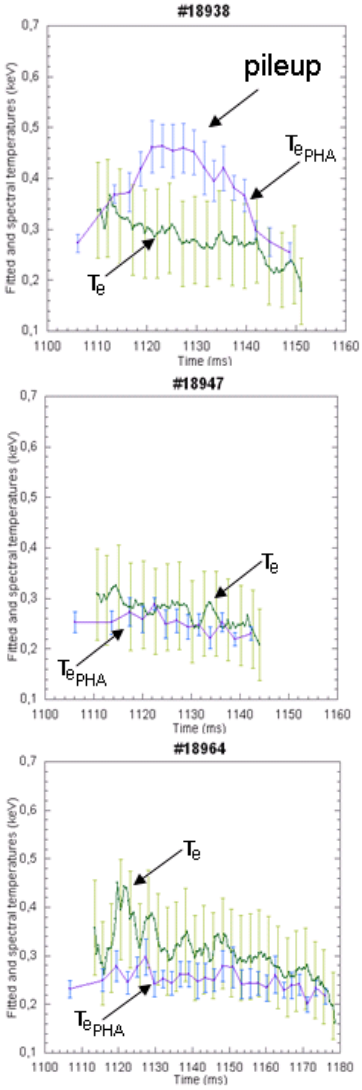

Figure 7.3 - Comparison of the electron temperature results obtained with the two-filters method with and from the PHA spectrum.

8. PARTICIPATION IN THE COMPASS PROGRAMME[1]

C. Varandas (Head), H. Fernandes and M.E. Manso (Deputy Heads), B. Carvalho, C. Silva, J. Sousa, A. Batista, J. Fortunato, D. Valcárcel, I. Carvalho, B. Santos, T. Pereira, A. Duarte, H. Alves.

8.1. INTRODUCTION

The 2009 Portuguese participation in the COMPASS project was centred in:

- Control and data acquisition system;
- Reflectometry diagnostic;

and has been carried out in the frame of:

- The General Support of the Contract of Association;
- The EFDA Task Agreement WP08-09-TGS-01b;
- Two contracts between IST and IPP-Prague.

8.2. CONTROL AND DATA ACQUISITION SYSTEM[2]

IST participated in the final design and assembly of the COMPASS control and data acquisition system and the development of the main hardware based on ATCA. The following activities were performed:

- *Implementation of a library for tokamak plasma control* consisting on several specialized modules integrated on the MARTe real-time software and executed during a plasma discharge was implemented (Figure 8.1). The modules were tested offline and are ready to be tested on a real plasma discharge environment;
- *Development of the module for the communication between the software and the energetic system* (fast amplifiers supplied by IPFN and being commissioned on COMPASS). The module was successfully tested, driving the fast amplifiers and power supplies during a plasma pulse, generating programmed currents on the plasma control circuits;
- *Design of other modules to perform the management of the real-time system and control.* In particular a generic controller was developed allowing generating programmed waveforms, performing feedback and feed-forward control. The plasma current and position measurement module was also developed and tested offline;
- *Training of IPP staff* on the configuration and use of the control and data acquisition software for the COMPASS operation;
- *Production and installation of 256 galvanic isolated 18-bit ADC channels, sampling at 2 MSPS@18-bit and 16 fast DAC channels on the ATCA data acquisition system,* targeting the plasma/machine diagnostics;
- *Development, test and installation of the FPGA code for Data Acquisition* for the ATCA-IO-Control boards developed at IPFN;
- *Development of the device drivers for the Linux OS and the Firesignal Node and its integration in the COMPASS Firesignal CODAC*;
- *Installation of a timing and synchronization system PC-based unit* (including PCI-EPN cards developed in-house) for managing event distribution and synchronization (triggers, clocks and gate signals) of all devices during experiments. The unit was connected to the COMPASS control and data acquisition system and successfully tested;
- *Development of a module to provide multiple optical I/O to the PCI-EPN modules*;
- *Development, test and installation of the FPGA and DSP codes, the Linux device drivers and the Firesignal Node* for the new Timing and Synchronization System based on the timing and event transport concept;

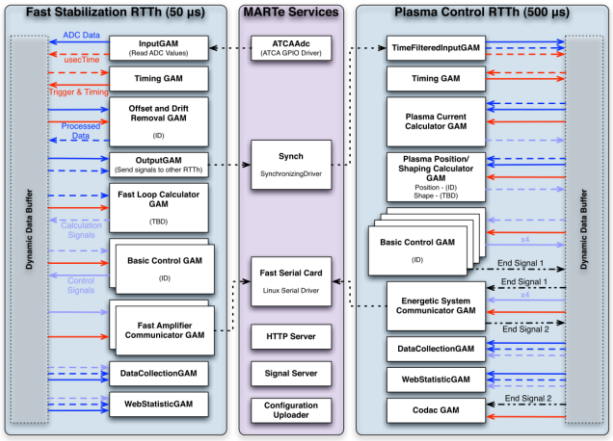

Figure 8.1 - Library of modules for COMPASS.

- *Development and integration in the COMPASS control system of a "Local Control Panel"* for viewing and management of the gas injection, baking, vacuum and puffing variables (Figures 8.2 and 8.3), based on Java and RXTX libraries;
- *Connection and successful testing at low power of the fast amplifiers for radial and horizontal plasma positioning* (Figure 8.4) being built by IPFN (currents of -5 kA to 5 kA) to the ATCA control system;
- *Testing and repair of 14 COMPASS ATCA-MIMO-ISOL and one ATCA-CONTROLLER-PCIe boards.*

[1]Activities carried out in the frame of the Contract of Association Euratom/IST, European Fusion Development Agreement (EFDA) and the Contract of Associated Laboratory, by staff of the Groups of Microwave Diagnostics and Control and Data Acquisition, in collaboration with the COMPASS team.
[2]Contact Person: Martin Horn.

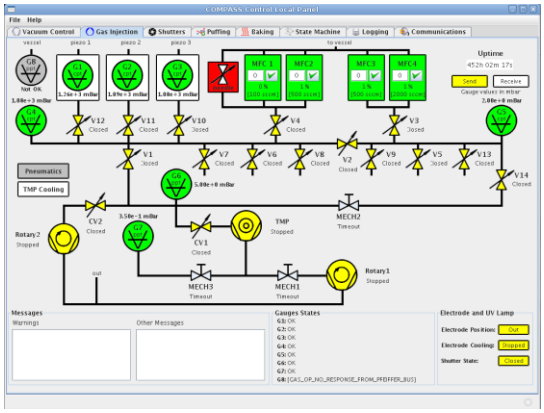

Figure 8.2 - Gas injection control on COMPASS.

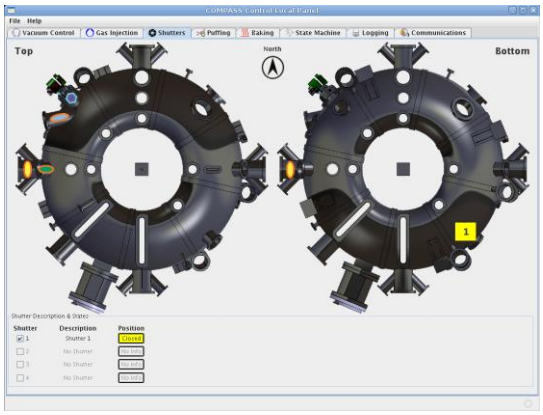

Figure 8.3 - Shutters control on COMPASS.

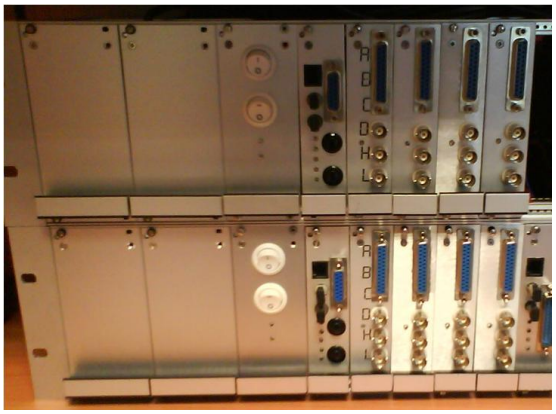

Figure 8.4 - Fast amplifiers for radial and horizontal plasma positioning.

8.3. REFLECTOMETRY DIAGNOSTIC[3,4]

The following tasks were performed:

- *Beginning of the development of the dedicated data acquisition system* with 16-channel at 250 MSPS;
- *Beginning of the development of the modified FPGA code* for the specificities of the reflectometry diagnostic;
- *Finalization of the design of the microwave reflectometry system*. The system aims at: (i) performing the edge pedestal plasma survey; (ii) measuring the correlation properties of plasma turbulence and (iii) studying fast transient events. The first phase of the project includes the first two lower frequency bands. One critical item is the quasi optical combiners that will combine the different frequency bands in a pair of transmitting/receiving oversized waveguides with out-vessel antennas, vacuum windows and two complex transmission lines, thereby reducing the access to the tokamak. An assessment of the design proposed by IRE NASU (Institute for Radiophysics & Electronics from the National Academy of Sciences of Ukraine) Kharkov was made. The equipment will be developed at IRE in collaboration with IPFN.

Concerning microwave/millimetre waves, the FM-CW reflectometry system at COMPASS will use for the first time an advanced hybrid configuration incorporating novel designs ranging from millimetre wave to digital technologies. The first prototype (Figure 8.5) that was successfully tested in the laboratory opened the possibility of having during the same discharge fast hopping fixed frequency measurements interleaved with broadband sweeping for density profile. The system performance will be improved benefiting both from ultra fast sweeping and phase coherent detection for fluctuation measurements.

Figure 8.5 - First prototype of an Hybrid frequency synthesizer / swept frequency generator, employing the first generation of PLL boards (2001) and first version of the FPGA ramp generator (2004) assembled together but loaded with a specific FPGA configuration controlling software as the proof of principle of the performance of an hybrid signal generator design.

[3]Contact Person: Jaromir Zajac.
[4]Work made in the EFDA Task Agreement WP08-09-TGS-01b.

9. COLLABORATION WITH THE ASSOCIATION EURATOM/CEA[1]

J.P. Bizarro (Head), M. Manso and R.V. Mendes (Deputy Heads), J.H. Belo, F. Briolle, F. Cipriano, R. Coelho, S. Cortes, F. Silva, D. Alves, J. Bernardo.

9.1. INTRODUCTION

This project had five research lines in 2009:

- RF studies of Tore Supra´s LH PAM Launcher;
- Transport studies;
- Plasma diagnostics;
- Stochastic solutions of equations for turbulence studies;
- Use of random sampling techniques for signal reconstruction.

Moreover, IST and CEA have also carried out joint activities on plasma rotation and training on lower hybrid and ion cyclotron technologies, which are described in sections 5.3.12 and 4.7.2.

9.2. RF STUDIES OF TORE SUPRA´S LH PAM LAUNCHER

Studies for the RF validation of the TORE SUPRA ITER-like LH PAM launcher were carried out via detailed numerical modelling of its 16 different modules, each including a raised cosine TE_{10} taper, a TE_{10} to TE_{30} mode converter, 3 main waveguides (stacked in the vertical direction), 3 E-plane step tapers and 3 E-plane 270° bijunctions, the latter employing internal geometric phase shifters (with λ/4 step transformers) in both output arms to create an extensive RF characterization at f_0=3.7 GHz, the design frequency, as well as over a relatively broad bandwidth around f_0. The launcher passed its main low-power RF validation tests, besides vacuum and hydraulic leak tests, whereas the first validations on plasma are in agreement with predictions. *Comparisons between this extensive numerical RF characterization and the corresponding low RF power measurements are in progress.*

9.3. TRANSPORT STUDIES

These studies had included in 2009:

- *Description of ITB oscillations in terms of a reduced set of ODEs;*
- *Extension of the reduced model analysis to the determination of ITB steady state bifurcations and identification of the transport parameters relevant to ITB dynamics.*

Facing the multiple phenomena known to play a role in ITB formation in different machines, a specific set-up has been chosen for the analysis, namely the ITB channeled through the electron temperature, typically observed in TORE SUPRA discharges, where the ITB cyclic behavior has been well identified and documented. One dynamics has been identified with the energy transport equation and reduced to an ODE form, but the analysis of the second equation for the expected planar ODE system, which was previously thought to be related with the current diffusion equation, has shown some subtleties and demands additional efforts.

9.4. PLASMA DIAGNOSTICS

9.9.1. Application of tomographic techniques to reflectometry data

Many signals in Nature, technology and experiment have a multi-component structure. *By spectral decomposition and projection on the eigenvectors of a family of unitary operators, a robust method has been developed to decompose a signal in its components.* Different signal traits may be emphasized by different choices of the unitary family. The method was illustrated in simulated data and on data obtained from plasma reflectometry experiments in TORE SUPRA. This technique was also shown to be appropriate to obtain the instantaneous phase derivative of the signal components.

Figure 9.1 shows the components of a reflectometry signal obtained by this method. Figure 9.2 presents the phase derivative of the second component

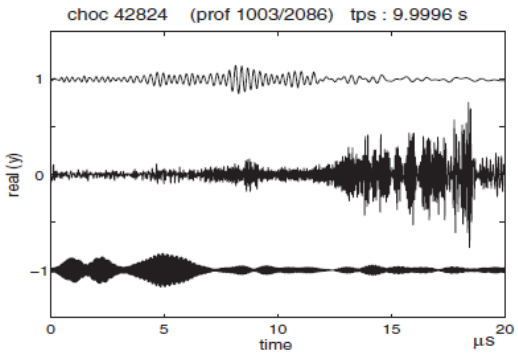

Figure 9.1 - Components of a reflectometry signal

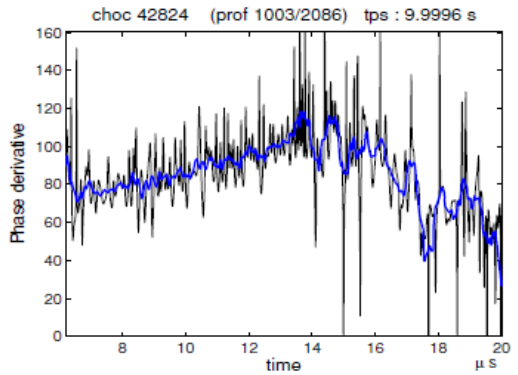

Figure 9.2 - Components of a reflectometry signal

[1]Activities carried out in the frame of the Contract of Association Euratom/IST and the Contract of Associated Laboratory, by staff of the Groups of Microwave Diagnostic and Theory and Modelling, in collaboration with the TORE SUPRA team.

9.5. STOCHASTIC SOLUTIONS OF EQUATIONS FOR TURBULENCE STUDIES

Stochastic solutions were obtained for the Maxwell-Vlasov equation in the approximation where magnetic field fluctuations are neglected and the electrostatic potential is used to compute the electric field. This is a reasonable approximation for plasmas in a strong external magnetic field. Both Fourier and configuration space solutions are constructed. Solutions were also obtained for magnetohydrodynamics.

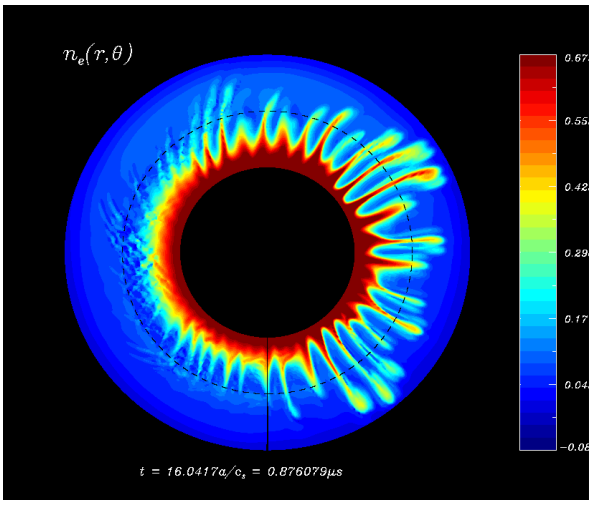

Figure 9.3 - Visualisation of the tokamak ELM burst. Poloidal plane cross section of the normalised electron density during the maximum growth phase. The radial domain is stretched by a factor of 2 for better visualization.

In addition, stochastic solutions were proposed as a basis for the development of numerical codes for localized solutions in configuration or Fourier space and for parallel computation with domain decomposition.

The stochastic solution technique was also extended to other nonlinear partial differential equations.

Figure 9.4 shows a sample path of the stochastic process associated to Poisson-Vlasov in an external magnetic field.

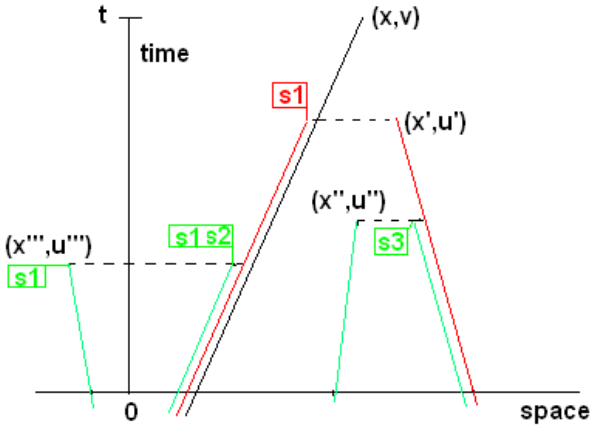

Figure 9.4 - Sample path of the stochastic process

9.6. USE OF RANDOM SAMPLING TECHNIQUES FOR SIGNAL RECONSTRUCTION

Reconstruction by irregular sampling and sampling at rates below the Nyquist rate are important for the experimental characterization of dynamical systems. *For the space of functions that can be approximated by chirps, a reconstruction theorem by random sampling at arbitrary rates was obtained.* Figure 9.5 compares the reconstruction of a 3-chirp signal by random sampling at ¼ the Nyquist rate of the smallest frequency with the (meaningless) reconstruction at regular sampling of the same signal

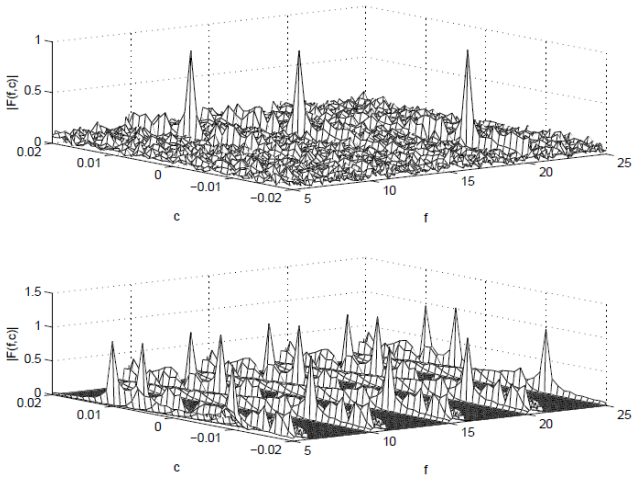

Figure 9.5 – Comparation of the reconstruction of a 3-chirp signal.

10. GENERAL ACTIVITIES ON THEORY AND MODELLING[1]

J.P. Bizarro (Head), R. Coelho (Deputy Head), J. Belo, P. Belo, A. Figueiredo, F. Nabais, F. Nave, A. Neto, V. Plyusnin, T. Ribeiro, J. Santos, F. Serra, F. Silva, A. Duarte, J. Ferreira and P. Rodrigues, J. Weinholte.

10.1. INTRODUCTION

This project included in 2009 three research lines:

- 3D simulations on critical NTM island width;
- Real-time signal processing;
- Conformal tokamak geometry for turbulence computations.

10.2. 3D SIMULATIONS ON CRITICAL NTM ISLAND WIDTH

The onset and growth of neoclassical tearing modes (NTM) in a tokamak discharge is known to limit the plasma beta, deteriorate plasma confinement and ultimately lead to plasma disruptions. It is therefore quite crucial to understand fully the mechanisms determining the characteristic critical island width above which the NTM is unstable. In particular, assessment of the dependence on transport coefficients, magnetic shear, Lundquist number and fraction of bootstrap current may provide valuable information to assist the prediction of stable operational regimes or regimes where the destabilization threshold is raised significantly. *A Full MHD 3D code solving magnetic field, plasma velocity and pressure dynamic non-linear equations with bootstrap current drive (XTOR code) was used for interpreting experimental evidence of the onset of the n=1 NTM on JET advanced scenario discharges.* The simulations attempted to reproduce realistic ratios of perpendicular to parallel thermal conductivities and resistive diffusion to energy confinement times. Analysis of one particular shot (#72668) evidenced the competing roles of stabilizing curvature and bootstrap drive, mitigated both by an increasing magnetic shear provides a destabilizing role as the plasma current density diffuses during the discharge.

10.3. REAL-TIME SIGNAL PROCESSING

An accurate detection and tracking in real-time of deleterious plasma instabilities and their space-time characteristics is an essential component of feedback control schemes. One such mode is the toroidal Alfvén eigenmode. The resonant wave-particle interaction between these modes and the fusion born alpha particles may lead both to the destabilization of the modes and to the stochastization of the alpha particles orbit, with a consequent particle and energy confinement loss and possible damage to the first wall. Assessing the damping/growth rates, frequency and wavenumber analysis of TAEs may therefore provide valuable information on bulk plasma stability and fast particle confinement losses. The prospects for a real-time synchronous detection of TAE modes excited by the TAE antenna using recursive filtering software techniques were therefore investigated with Kalman filters (KF).

Two approches were proposed: synchronous I-Q detection assisted by the excitation signal and an extended algorithm where both signal and frequency synchronous are estimated. The latter builds on previous studies on the real-time tracking and toroidal mode number identification of magnetic fluctuation signals based on recursive filtering techniques and relies on the use of the Extended Kalman Filter (EKF). The filtering implementation of a lock-in amplifier is shown to require no knowledge about the TAE antenna excitation waveform (only excitation frequency) and, if one can use solely the amplitude of the plasma response to extract the damping/growth rates, is a powerful method providing adaptively, as a parallel product, a high quality frequency estimator. Much higher sampling rates and higher robustness and usage flexibility as opposed to traditional FIR/IIR approaches were evidenced (Figure 10.1) where a comparison between KF and traditional dual-phase lockin amplifier assisted by FIR filtering).

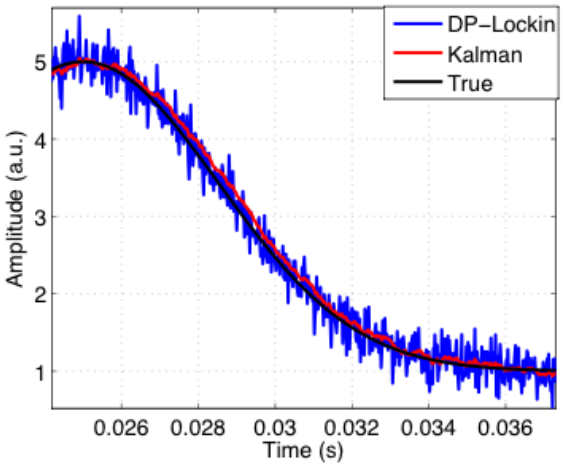

Figure 10.1 – Estimated amplitude from simulated plasma response to TAE excitation from fast sweeping TAE antenna, as measured by magnetic coils

[1]Activities carried out in the frame of the Contract of Association Euratom/IST and the Contract of Associated Laboratory, by staff of the Group of Theory and Modelling.

10.4. CONFORMAL TOKAMAK GEOMETRY FOR TURBULENCE COMPUTATIONS

A novel geometrical treatment has been introduced to address the discrete grid mesh deformation inherent to tokamak field aligned coordinate systems under strong shaping typical of the tokamak edge region. A consistent combination of magnetic field aligned and conformal coordinates is used. This allows an efficient treatment of the dynamics along the magnetic field lines while enforcing the necessary isotropicity in the plane perpendicular to it at the grid spacing level, best representing the turbulence physical properties. Such geometry is being implemented in both gyrofluid and gyrokinetic models for turbulence computations.

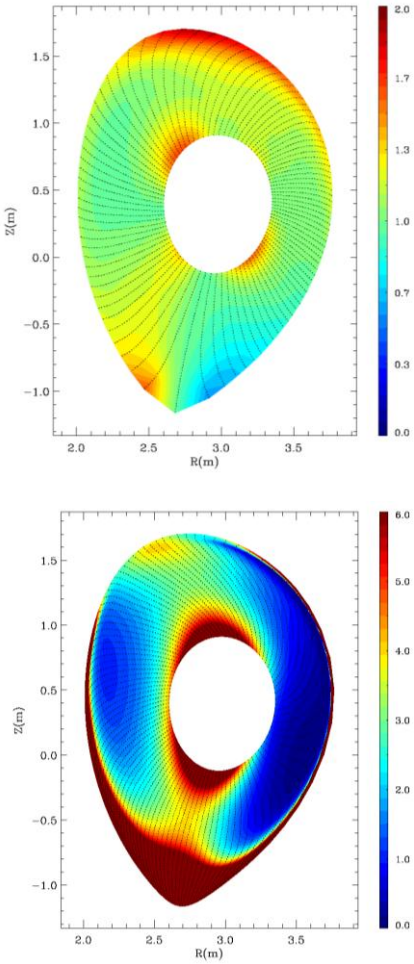

Figure 10.2 - Contour plots of the grid conformality defined as the ratio between each side of the mesh perpendicular to the magnetic field for (right) the novel conformal coordinates and (left) the standard symmetry coordinates on a typical ASDEX Upgrade equilibrium magnetic field. The latter shows much bigger deformation, which affect spuriously turbulence simulations. Note the different color scales used for each plot. In the right plot the same color is used for values greater than 6.0.

10.4.1. Synthetic full-wave reflectometry diagnosis of gyrofluid turbulence

Synthetic full-wave reflectometry diagnosis of gyrofluid turbulence simulations was performed successfully using the GEMR (turbulence) and REFMULX (reflectometry) codes. GEMR simulated turbulent edge plasmas with parameters typical of an L-mode ASDEX Upgrade scenario were probed with REFMUL code. In Figure 10.3 it is depicted the Wave field contour snapshot of a REFMULX full-wave frequency sweep simulation in the band 30-40GHz on the density and magnetic field provided by GEMR. This activity is ongoing and comparisons with the experiment reflectometry data from the ASDEX Upgrade are foreseen.

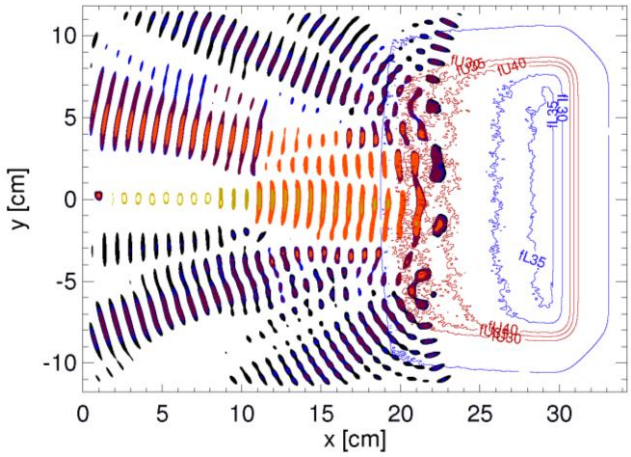

Figure 10.3 - Wave field contour snapshot of a REFMULX full-wave frequency sweep simulation in the band 30-40GHz on the density and magnetic field provided by GEMR.

10.4.2. Nonlinear computation of edge localised ideal ballooning modes

Gyrofluid computations of edge localised ideal ballooning modes (ELMs) have been performed. Although the main underlying instability at experimentally relevant parameters is the ideal ballooning instability, the main saturation process is the energy exchange with broadband turbulent dynamics in the drift wave/ITG regime, which the instability itself generates. As a result, the system falls outside both the magneto-hydro-dynamics (MHD) and collisional Braginskii frameworks, on which most of previous approaches have been based.

11. KEEP-IN-TOUCH ACTIVITIES IN INERTIAL FUSION ENERGY[1]

J. T. Mendonça, (Head), J. Davies, J. M. Dias, M. Fajardo, G. Figueira, R. Fonseca, A. Guerreiro, C. Leitão, N. Lopes, A.M. Martins, D. Resendes, J.A. Rodrigues, L.O. Silva

11.1. INTRODUCTION

The main results obtained on keep in touch activities on inertial fusion energy during 2009 have been obtained along four different lines in ICF research:

- Fast ignition and ICF theory;
- High intensity photonics;
- Plasma accelerators and intense radiation sources;
- Quantum plasmas.

11.2. FAST IGNITION

Continuation of code development and theory for fast ignition and IFE theory. The PIC code Osiris is now being applied to modelling fast ignition physics, including laser channelling and fast electron generation. Our fast electron hybrid code is being developed so that it can be used to model fast ignition using density and temperature profiles taken from hydrocode modelling of the compression, including more accurate models for the collision coefficients and electrical and thermal conductivities.

11.3. HIGH INTENSITY PHOTONICS

Demonstration of diode-pumped optical parametric amplification: an Yb:glass regenerative amplifier was successfully operated to the mJ level at 1 Hz repetition rate. A preliminary test of multipass amplification was also carried out, allowing the identification of some issues to be addressed in 2010. An experiment on multipass amplification in Yb:YAG and Yb:KYW is scheduled for May 2010.

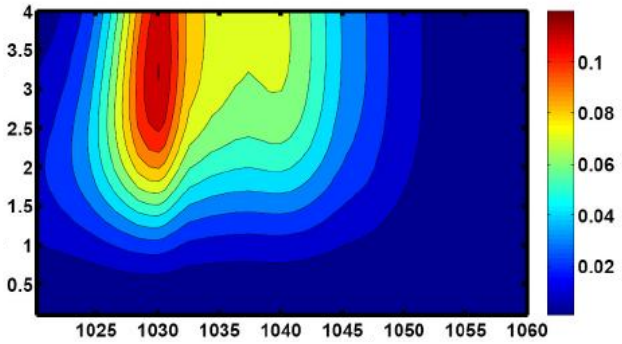

Figure 11.1 - Calculated output energy (Joules, color bar) for a diode-pumped 8-pass Yb:KYW amplifier as a function of crystal length (vertical scale, in cm) and seed central wavelength. The numerical code takes into account the full pump and seed pulse parameters, and the optical, material and thermal properties of the gain medium.

11.4. PLASMA ACCELERATORS AND INTENSE RADIATION SOURCES

The activities on this topic have covered the following aspects:

- *Guiding of high power laser pulses in plasma channels*

An experiment was performed in order to test guiding in field ionization plasma channels. Preliminary results show guiding but with low coupling efficiency at the channel entrance.

- *High power guiding demonstration, longer channels (>10 cm) demonstration, small diameter plasma channels (<200 micrometers).* A new structured gas cell device able to produce 8 cm plasma channels was built and tested using a test facility for testing plasma channels at the Laboratory for Intense Lasers. The first prototype was able to produce 8 cm plasmas, however the existing setup doesn't allow triggering the simmer discharge (essential for uniformity of 8 cm plasmas) after the gas feeding. The premature deployment of the simmer discharge results in a parasitic discharge reducing the plasma heating and the depth of the density profile during expansion. With the collaboration of the MFE experimental group we tested the channel formation on a static longitudinal magnetic field. The preliminary results point, as expected, to the need for increasing the magnitude of the magnetic field by using a pulsed kA discharge to increase the field to the order of 10 T. These aspects will be improved in the next experiment. The development of smaller diameter plasma channels was postponed due to the unavailability of funds to purchase an electron gun.

11.5. QUANTUM PLASMAS

New activities in the field of quantum plasmas:

- *Exploitation of the analogy between ionization dynamics in an ultra cold Rydberg gas and the fast ignition model for inertial fusion;*
- *Development of a new experimental facility on laser cooling and trapping, with additional capabilities for plasma formation and diagnostics.*

[1]Activities carried out in the frame of the Contract of Association Euratom/IST and the Contract of Associated Laboratory, by staff of the Groups of Lasers and Plasmas and Quantum Plasmas.

12. OTHER FUSION-RELATED ACTIVITIES[1]

C. Varandas (Head), M.P. Alonso, E. Alves, J. Brito, P. Carvalho, H. Fernandes, M.E. Manso, A. Silva, R. Silva, J. Sousa, V. Livramento, A. Neto, D. Nunes.

12.1. INTRODUCTION

This project concerns:

- The collaboration of IST/IPFN with Brazilian Institutions;
- The participation in the W7-X Project;
- The participation in the TCV programme;
- Other activities on data acquisition and real-time plasma control;
- Fusion materials studies;
- Education and training;
- The organization of scientific meetings;
- The Portuguese participation in the management of the International Fusion Programme and Projects;
- The outreach activities.

12.2. COLLABORATION WITH BRAZILIAN INSTITUTIONS[2]

12.2.1. Introduction

IST/IPFN has collaborated with:

- Laboratório de Plasmas do Instituto de Física da Universidade de São Paulo (LP-IP-USP);
- Laboratório Associado de Plasmas do Instituto Nacional de Pesquisas Espaciais (INPE).

The research activities were focused on control and data acquisition, microwave reflectometry and Thomson scattering diagnostic.

IST/IPFN staff has actively collaborated with LP-IP-USP in the IAEA Joint Research Experiments, made in May 2009, on TCA/Br.

12.2.2. Microwave reflectometry for TCA/Br[2,3]

The development, installation and commissioning of the ultra fast FM-CW system for TCA/Br was completed. Figure 12.1 shows the k and ka band frequency combiner/decombiner sections and Figure 12.2 depicts a view of the vacuum flange with the antennas plus tilting mechanism to optimize reception. *The first results were obtained both in ultrafast and fixed frequency operation* showing the high performance of the diagnostic. However, some limitations were found in the signals detected above 33 GHz due to a problem in the transmission line combining the two fundamental frequency bands. This is caused by an impedance mismatch which affects the performance of the combining coupler. *A new combiner/decombiner module was developed* and tests in the laboratory reveal the good performance of the new device able to cope with impedance mismatches. Its installation in TCA/Br is expected to occur.

Figure 12.1 - View of the and Ka bands frequency combiner/decombiner sections of the TCA/Br reflectometer.

Figure 12.2 - View of the vacuum flange with the antennas and tilting micrometer mechanism to optimize the antennas reception angle.

The O-mode reflectometer in the frequency scanning mode was used to study the plasma density oscillations during local Alfvén wave (LAW) excitation in TCA/Br at the frequency fA = 5 MHz. It was found that the spectrum of the reflectometer output signal, which consists mainly of the 'beat' frequency fB, is modified by the LAW excitation, and two additional frequency peaks appear (Figure 12.3), which are symmetrical in relation to the LAW excitation frequency f = fA ± fB. This result opens the possibility to improve the efficiency of the studying the LAW induced density oscillations. The symmetry of these frequency peaks yields the possibility of finding the microwave frequency at which the reflectometer cutoff layer coincides with radial position of the LAW resonance zone in the TCA/Br tokamak.

12.2.3. Data Acquisition systems

Continuing the commitment of IPFN of supplying state-of-the-art data acquisition systems for fusion experiments, the following tasks were performed:

- *Installation of a PCI-TR512 data acquisition system in ETE* composed by 6 computers, 24 data acquisition boards, 192 channels.

[1]Activities carried out in the frame of the Contract of Association Euratom/IST and the Contract of Associated Laboratory.
[2]TCA/Br is a tokamak of the "Laboratório de Plasmas, do Instituto de Física, da Universidade de São Paulo".
[3]Contact Person: Ricardo Galvão".

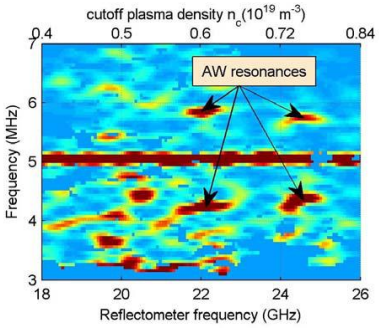

Figure 12.3 - Shot #24508. Spectrogram of the reflectometer signal during AW excitation at time t=72.6ms. The scanning frequency is shown at the bottom x-axis, and the corresponding cutoff plasma density is shown at the top.

- *Installation of 4 PCI-TR512 data acquisition boards (32 channels) in TCABR* to be used during "Joint Experiment" activities.
- *Development of a dedicated data acquisition systems for the reflectometry TCA/Br system.* The ATCA based data acquisition system, resultant from the development of the data acquisition system for the ASDEX-UPGRADE, was installed in the TCAbr tokamak in the first quarter of 2009. The following actions were carried out: *(i) production and test of a 250 MSPS ATCA Transient Recorder; (ii) changes in FPGA code of the ATCA 250 MSPS digitizer to comply with the requirements of the TCA/Br microwave reflectometry diagnostic; and (iii) integration of the diagnostic specific FPGA code on the digitizer and the specific software on the FireSignal data acquisition platform.*

12.2.4. Thomson scattering diagnostic

The first phase of the Thomson scattering (TS) diagnostic (Figure 12.4) was concluded with success. This diagnostic allows to measure, in a routine mode, the electron temperature in the plasma center for any instant during the discharge.

In the first phase of this international collaboration, the TS diagnostic uses a Neodymium: Glass laser with 5 Joules per laser pulse and a first generation polychromator with three pairs of interference filters and avalanche photodiodes. It measures 90º scattered radiation in a single volume of observation (18 cm length and 2 mm diameter) with a single laser pulse to obtain the instant plasma electron temperature. All the digitalized raw data are stored in a local hard disk of a personal computer. We concluded an algorithm for obtaining the electron temperature using the values achieved in the relative calibration made with a filament lamp and a monochromator and an optical ray-tracing study for a new collecting lens. During 2009 more than 200 electron temperature measurements were carried out with no change in any diagnostic parameter. The determined electron temperatures varies from 50 eV up to 600 eV and are in agreement with those provided by the electron cyclotron emission diagnostic for purely ohmic discharges and gives indications to be able to contribute effectively to the Alfvén heating program of this tokamak (Figure 12.5).

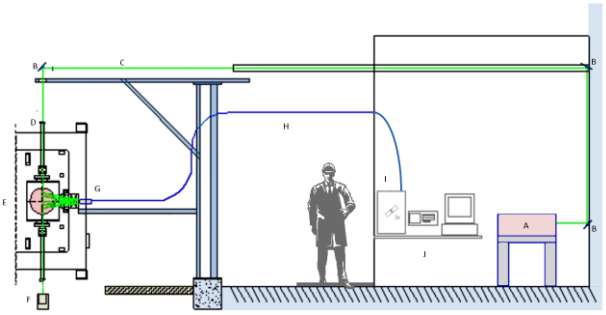

Figure 12.4 - The TS diagnostic lay-out at the TCABR tokamak with approximate sizes: (A) laser; (B) mirrors; (C) laser delivery system; (D) focusing lens; (E) tokamak's poloidal section; (F) laser's dump; (G) collecting lenses; (H) single optical fiber; (I) polychromator; (J) digital oscilloscope and PC data acquisition. The plasma is represented as a pink disk and the future collection lens is shown.

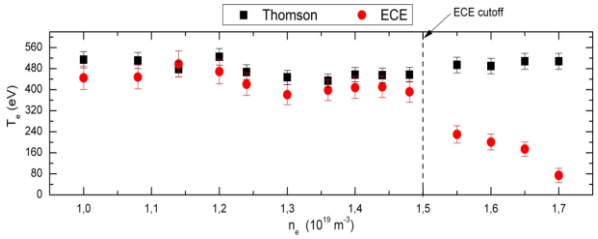

Figure 12.5 - Electron temperature obtained by the TS diagnostic compared with the values from the electron cyclotron diagnostic (ECE) in the same shots. The right side shows the electron temperature results obtained from the TCABR plasma center with Alfven heating and with a consequent added increase in the plasma density.

12.3. COLLABORATION WITH IPP GREIFSWALD[4]

IST/IPFN has performed the *conceptual design of a long duration integrator/ADC module for the ATCA-GPIO board targeting the W7-X requirements.*

12.4. PARTICIPATION IN THE TCV PROGRAMME[5]

This project has two research lines:

- X-ray diagnostics;
- Real-time plasma control.

12.4.1. X-ray diagnostics

The following tasks were performed:

- *Manufacturing a pre-amplifier pulse conditioner to the input characteristics of the DSP*, aiming at lifting the data acquisition limitations of the real-time application. This filter allowed: (a) to restore the signal baseline, (b) to amplify the input signal in order to use the total input voltage range of the ADC, (c) and to reduce the noise due to the DCDC converter of the preamplifier;
- *Time analysis of the system clock and triggers* for correct synchronization between VME modules and TCV plant;

[4]Contact Person: Andreas Werner.
[5]Contact Person: Basil Duval.

- *Installation of a new OS/tools and analysis/implementation of network protection and log tools* to avoid possible network attacks to the system.

12.4.2. Real-time plasma control

The new Advanced Plasma Control System (APCS) was *successfully integrated in the main TCV control system and routinely used during the TCV operation.*

In the second phase of the project several tasks were performed including:

- *Initial design of new algorithms for the plasma vertical control* including the necessary corrections to the analogue version due to some divergence phenomena related with noise that appears in the digital implementation;
- *Characterization of the APCS channels input and study of methods for noise reduction* to improve control performance;
- *Upgrade to the system control state machine* with enhanced logging system and error states definition;
- *Design and integration of development tools for daily operation and algorithm development.* Identification of error conditions and their resolution, and continuous system monitoring with alarms.
- *Testing of the tools and the quality of their integration on TCV* by running the APCS system with data acquired in TCV discharges;
- *Adaptation of the vertical plasma control to the APCS* using a single Processor card consisting of 4 DSP modules in the "Fast Data Mover" together with the development new algorithms that drive the TCV coil amplifiers more efficiently;
- *Development and testing of a new plasma vertical control observer* using non-integrated magnetic signals and a Matlab simulation for the new observer (Figure 12.6)
- Support to the TCV Control Group on the use of the APCS.

12.5. OTHER ACTIVITIES ON DATA ACQUISITION AND REAL TIME PLASMA CONTROL

The following development activities were performed:

- *Study of the ATCA Shelf Manager unit configuration and host communication* with application on the system fans speed adjust;
- *Design of the new version of the PICNODE card*, which is currently in the final stages of the PCB routing process. A prototype is planned to be assembled and tested, allowing for later production of these cards, which will be used in slow control systems.

The following activities for Prototype assembling and production occurred:

- *Micro-welding, printed circuit boards repairing and manual assembly of prototypes*;
- *Programming and maintenance of the Pick & Place and BGA rework machines* used for the assembly of complex prototypes;
- *Implementation of a component database* for stock control and manufacturing processes organization.

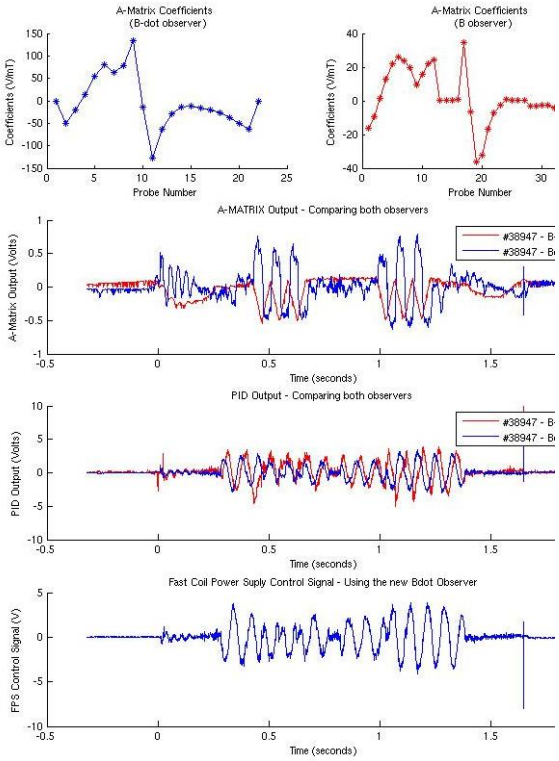

Figure 12.6 - New vertical observer

12.6. FUSION MATERIALS STUDIES

This Project included in 2009 four research lines:

- Study of a new batch of beryllium pebbles;
- Consolidation of Cu-nDiamond nanocomposites;
- Study of Cu/Graphite and Cu/Diamond interfaces reinforced with chromium;
- Development of microdiamond composites for fusion applications.

12.6.1. Study of a new batch of beryllium pebbles

The He cooled blanket design imposes the use of neutron multiplier materials like beryllium. However the use of Be in fusion reactors is hindered by its oxidation behavior and tritium retention. Furthermore, beryllium becomes brittle and swells under neutron irradiation. Since within small pebbles the temperature differences are small, and thus the stresses caused by thermal gradients and different swelling rates (swelling is temperature dependent) are considerably reduced beryllium is used in pebble beds.

Several Be pebbles were measured from different suppliers to assess the presence and distribution of impurities with particular emphasis on those with high activation neutron cross section. The quantitative results are an average over the analysed surface and the probed depth, that, in the case of Be bombarded with 2 MeV protons, is close to 50 μm. The results for one particular pebble are shown in Figure12.7.

In order to obtain a representative result of the impurity concentration in the pebbles *we took randomly 6 pebbles*

from each batch of samples and made a solution with acid digested for further PIXE analysis. The results are presented in the table and it is worth to notice that, within the sensitivity limits impurities of the technique, impurities of major concern e.g. Co, U, Mg, Si, Al Nb, were not detected.

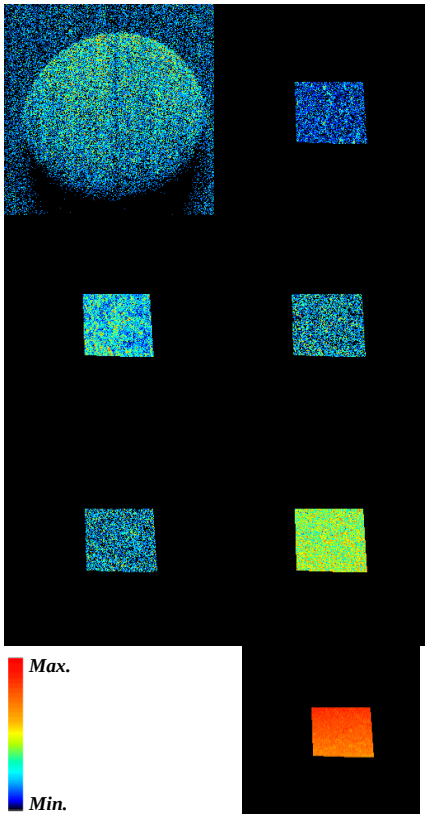

Figure 12.7 - Be distribution map obtained from the RBS spectrum for the Be GVT 4 pebble (top left) and maps showing the raster scan area chosen to perform PIXE quantitative analysis with the main impurities distribution in that area.

Sample	Ca	Ti	Cr	Mn	Fe	Ni	Cu	Zn	Mo
GVT1(FZK)	48	37	132	20	443	58	25	7	
GVT2(FZK)	5		43	15	132	9	14	6	44
GVT3(FZK)	20	140	218	40	854	112	29	6	15
GVT4(NGK)		97	29	32	479	80	44	3	9
GVT5(NGK)	90	212	57	42	511	101	41	34	19

Table 12.1 - Thin target PIXE quantitative results obtained after sample acid digestion. The results are in µg/g.

12.6.2. Consolidation of Cu-nDiamond nanocomposites

Due to their interesting properties copper-based materials have been considered appropriate heat-sinks for first wall panels in nuclear fusion devices. The concept of property tailoring involved in the design of metal matrix composites has led to several attempts to use nanodiamond (nDiamond) as reinforcement. In the present study, *powder mixtures of copper and nDiamond with 20 at.%C were mechanically alloyed and consolidated via hot extrusion or spark plasma sintering.* TEM analysis of the consolidated samples showed bonding between the copper grains and nDiamond particles. Microhardness values revealed significant differences between the consolidation processes and when compared to the as-milled powder. Density measurements indicate that the results depend on the consolidation route with superior results for hot extrusion. Further optimization of consolidation parameters is currently underway aiming at future exposure experiments to cyclic plasmas in a tokamak reactor.

12.6.3. Study of Cu/Graphite and Cu/Diamond interfaces reinforced with chromium

The reinforcement of a copper matrix with graphite or nanodiamond enables tailoring of composite properties, and increase the performance demanded for long term application in nuclear fusion devices. In order to improve copper adhesion to carbon phases, chromium can be incorporated, resulting in segregation of this carbide former to the reinforcement/metal interface and subsequent formation of a chromium carbide interlayer. In the present study, *powder mixtures of Cu/Graphite and Cu/nDiamond were mechanically alloyed with 0.1 wt% Cr for different milling times.* Consolidation was carried out via spark plasma sintering. Cr incorporation increased the hardness of the materials. The SPS consolidation process demonstrated to be efficient in terms of powder densification.

12.6.4. Development of W-microDiamond composites for fusion application

Nanostructured W-MicroDiamond composites are promising for first wall nuclear reactors due to their favourable thermal conductivity, mechanical strength and radiation resistance. Tungsten has high resistance to plasma erosion and moderate tritium retention and diamond has extremely high thermal conductivity. *W-microDiamond composites were produced by mechanical alloying and were subsequently consolidated by thermomechanical processes Short milling times (2 or 4 hours) minimize contamination by the milling media.* The present work shows that milling at 200 rpm for 4h followed by SPS at 1150ºC represents the best combination of processing parameters to obtain dense W-microD nanostructured composites. However, consolidation induced significant carbide formation.

12.7. EDUCATION AND TRAINING

Besides *the collaboration in Portuguese 2nd and 3rd cycle programmes*, IPFN integrated the international network responsible for the first three years of the *joint Ph.D. Programme on Fusion Science and Engineering*, promoted by IST, the University of Padova and the University of Munich.

IST was responsible for the lectures on Plasma Diagnostics and Control and Data Acquisition, given in Lisboa, in February 2009.

12.8. ORGANIZATION OF SCIENTIFIC MEETINGS

The following tasks were performed in 2009:

- Organization, in collaboration with Instituto Tecnológico e Nuclear, of the "*14th International Conference on Emerging Nuclear Energy Systems – ICENES 2009*, Ericeira, June 29th to July 23rd, 2009 http://www.icenes2009.itn.pt/;
- Organization of the *21st International Conference on Numerical Simulation of Plasmas*, Lisbon, October 6th to 9th, 2009, http://icnsp09.ist.utl.pt/;
- Organization, in collaboration with Laboratório de Instrumentação e Física Experimental de Partículas (LIP), of the *2010 IEEE/NPSS Real-Time Conference*, to be held in May 2010, at IST;
- Organization of the *27th Symposium on Fusion Technology*, to be held in Porto, in September 2010.

12.9. OUTREACH ACTIVITIES

The outreach activities included in 2009:

- *Promotion of science to secondary school students:*
  - Talks in portuguese high schools about nuclear fusion energy ;
  - ~30 visits of high-school students to the ISTTOK laboratory ;
  - Participation in the *Ciência Viva* summer project, hosting high school students for a week in July 2009.
- *Elaboration of the Annual Report;*
- *Invited Talks and Seminars:*
  - C. Varandas, "Research and development physics and technology issues towards fusion energy", *IAEA Joint Experiments*, São Paulo (May 2009);
  - C. Varandas, "Strategy for the development of nuclear fusion as an energy source", *11th International Conference on Energy and Environment*, Hurghada, March 2009;
  - M.P. Alonso "Nuclear Fusion", BEST Summer Course "All you need is Physics", IST, August 2009;
  - G. Figueira, "Lasers and plasmas" (inc. IFE), BEST Summer Course "All you need is Physics", IST, August 2009.
- *Articles and membership of editorial boards:*
  - C. Varandas, "A física e a energia", Gazeta de Física 32(1), 2009;
  - G. Figueira is the assistant editorial director of "Gazeta de Física", the official journal of the Portuguese Physical Society.
- *Corporate image, media and public relations:*
  - Creation of a new homepage for IPFN: http://www.ipfn.ist.utl.pt/;
  - Creation of IPFN's corporate image and public information team ;
  - Media interviews: portuguese newspapers, radio and television stations.
- *Media accounts of the activities of the Association:*
  - "Cientistas obtêm alumínio transparente como acontece nos núcleos de planetas gigantes", in *Público* (Jul 29, 2009).
  - "Fusão nuclear: Técnico assina contrato de um milhão de euros com megaprojecto de fusão nuclear", in *Correio do Minho* (Oct 7, 2009).
  - "IST ganha 2,5 milhões de horas no maior supercomputador Europeu", in *Ciência Hoje* (Feb 3, 2009);
  - "Fusion research in Brazil", in *EFDA Fusion News* (Oct. 2009).

12.10. PARTICIPATION IN THE MANAGEMENT OF INTERNATIONAL FUSION PROGRAMMES AND PROJECTS

Several members of the IST staff have been involved in the management of the EURATOM Fusion Programme (EFP) as well as on Ad-Hoc Groups and Scientific Committees of the EFP and other Fusion Programmes:

- *Prof. Carlos Varandas* is:
  - Chairman of the F4E Governing Board
  - Member of the Consultative Committee for the Research and Training Programme on Nuclear Energy-Fusion (CCE-FU);
  - Member of the Group of Chairmen (GoC);
  - Member of the Scientific and Technical Committee (STC) of the EURATOM Treaty;
  - Member of the EFDA Steering Committee;
  - Member of the EURATOM Delegation to the ITER Council;
  - Member of the EURATOM Delegation to the Steering Committee of the Broader Approach.
- *Prof. José Tito Mendonça* is member of the Inertial Fusion Energy Coordinating Committee.
- *Profª Maria Emília Manso* is:
  - Member of the Programme Committee of the ASDEX-Upgrade Project;
  - Chairperson of the International Advisory Board on Reflectometry;
  - Coordinator of the Cluster of EURATOM Associations for the development of the Plasma Position Reflectometer for ITER.
- *Prof. Fernando Serra* is member of:
  - F4E Governing Board;
  - CCE-FU;
  - Ad-Hoc Group from STAC for the Monitoring of W7-X Project;
  - ITPA (International Tokamak Physics Activity) Topical Group on Diagnostics;
  - Ad-Hoc Group from STAC for the COMPASS-D Project;
  - International Board of Advisories of the COMPASS-D Project.
- *Prof. António Cruz Serra* was member of the F4E Executive Committee until July 2009;
- *Prof. Pedro Girão* is member of the F4E Executive Committee since July 2009;
- *Prof. Horácio Fernandes* is member of the F4E Technical Advisory Panel.

13. PLASMA THEORY AND SIMULATIONS[1]

L.O. Silva (Head), R.A. Fonseca, F. Peano, M. Marti, P. Abreu, L. Gargaté, J. Vieira, S.F. Martins, F. Fiúza, J.L. Martins, N. Shukla, P. Alves.

13.1. INTRODUCTION

The work in this field was developed along the following main topics:

- Towards OSIRIS 3.0: performance optimization for state of the art computing systems;
- Effect of random frequency fluctuation in multiple beams on laser wake field generation;
- EAT for thermal fluctuations;
- Ion acceleration from ultra intense lasers interacting with solid hydrogen targets: a parametric study of the ELI regime;
- Enabling OSIRIS on the Bluegene architecture;
- A full relativistic PIC code in CUDA enabled hardware;
- Direct visualization in PIC codes;
- Magnetic field amplification in Supernova Remnant Shocks by the Non-resonant kinetically driven streaming instability;
- Implementation of a particle-tracking algorithm in QuickPIC;
- Polarized beam acceleration;
- Laser-plasma accelerators ride on Einstein's shoulders;
- Modeling laser-wakefield acceleration experiments in OSIRIS;
- Relativistic collisionless shocks with state-of-the-art PIC simulations;
- Astrophysics in the laboratory with fireball beams;
- Generation of relativistic shocks in fast ignition scenarios;
- Efficient Raman amplification into the PetaWatt regime;
- Numerical modeling of radiation from Weibel scenarios;
- Comparison of radiation cooling models for particle-in-cell simulations;
- Enhancement of the electromagnetic Weibel instability due to ion streaming;
- Magnetic field generation via the Kelvin-Helmholtz Instability.

13.2. TOWARDS OSIRIS 3.0: PERFORMANCE OPTIMIZATION FOR STATE OF THE ART COMPUTING SYSTEMS

OSIRIS 2.0 is a state of the art, fully relativistic massively parallel particle in cell code, that is widely used in kinetic plasma modeling for many astrophysical and laboratory scenarios. Current code capabilities allow it to be used for large scale, one-to-one, numerical experiments. However, modeling these scenarios requires state of the art computing systems, capable of handling up to ~ 10^{10} grid cells and ~10^{11} particles for over ~10^{7} iterations (Figure 13.1). Moreover, efficient use of these systems is critical, requiring high floating point efficiency and parallel scalability to ~10^{5} cpus.

OSIRIS now has a high performance vector SIMD module for the particle advance and current deposition, which are responsible for over 90% of the total loop time. The SIMD code was written for the Intel SSE3 architecture, which is available on all current x86 systems, such as the Cray XT4 and XT5 systems. The vectorization strategy used will be easily applied to the Altivec/VMX architecture that will be present on the new BlueWaters system. Currently we achieve floating point efficiencies of up to 70%, allowing us to push up to 22.5 million particles per second in 2D, and 13.7 million particles per second in 3D in a single computing core, representing a speedup of up to 3.8 times of the reference fortran code.

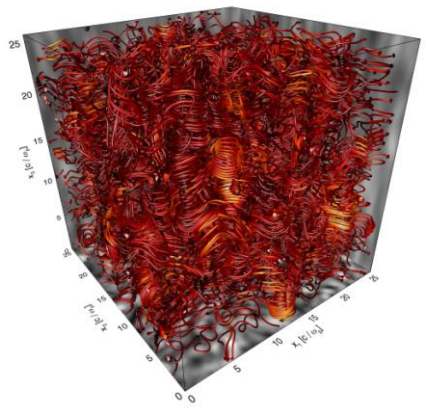

Figure 13.1 - Turbulent Magnetic Field Structure in the collision of an electron-positron plasma shell

[1]Activities performed in the frame of the Contract of Associated Laboratory, out of the Contract of Association Euratom/IST, by IPFN staff of the Group of Lasers and Plasmas

13.3. EFFECT OF RANDOM FREQUENCY FLUCTUATION IN MULTIPLE BEAMS ON LASER WAKE FIELD GENERATION

The next generation of ultra high intensity laser systems for laser driven fusion and plasma accelerator facilities will use multiple laser beam systems to achieve very high intensities. These beams may have small frequency mismatches, due to the separate optics involved. This may severely affect the wake field generation process in laser plasma based electron accelerators. *Effect of random frequency variation in multiple beam laser drivers on wake-field generation is studied using ensemble average technique (EAT)* (Figure 13.2). In EAT we take average over a large ensemble of simulation runs, which for random processes provides most probable results. OSIRIS, with a property of absolute reproducibility, is a very suitable candidate for EAT.

Analytical expression for the laser wakefield generation in 1D linear regime, incorporating the effect of random phase variation into the field amplitude, is deduced and compared with the simulation results obtained by EAT in the same regime. The results show that for the frequency fluctuation up to 5% the variation in wakefield amplitude is negligible. For fluctuation ~20 % the wake field amplitude variation in each run is appreciable, however, it reaches to a constant level after taking average over ~10 runs.

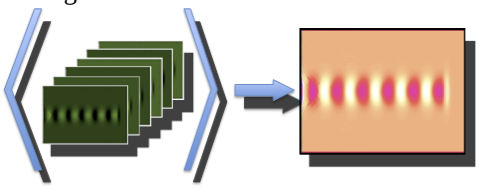

Figure 13.2 - Schematic of ensemble average technique

13.4. ENSEMBLE AVERAGE TECHNIQUE FOR THERMAL FLUCTUATIONS

Particle in Cell (PIC) simulation codes are usually noisy and require extra attention to reduce the noise. In presence of thermal fluctuations the noise level is more enhanced. The thermal effects can be significantly reduced by increasing the particle per cell (ppc) in the PIC simulations, however, this demands larger computational power and time. *We have worked on EAT to reduce the thermal noise using lesser computational power and time* (Figure 13.3).

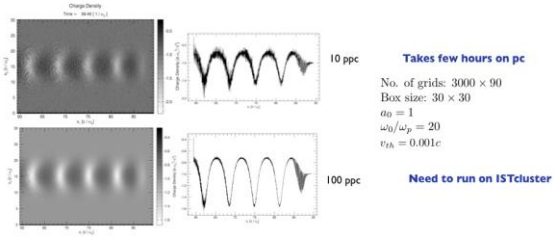

Figure 13.3 - Noise level in laser wake field generation simulations with 10 ppc and 100 ppc.

13.5. ION ACCELERATION FROM ULTRA INTENSE LASERS INTERACTING WITH SOLID HYDROGEN TARGETS: A PARAMETRIC STUDY OF THE ELI REGIME

High intensity laser systems (ELI, HIPER) are expected to reach intensities in excess of 10^{24} W/cm^2 opening the way to new regimes in laser based particle accelerators.

We have performed a large set of computer simulations modeling laser solid interactions in the ELI regime with the aim to make recommendations for the design of the facility (radiation shielding, safety procedure) and to guide acceleration experiments (experimental setup and recommended parameters) (Figure 13.4). After identifying the dominant acceleration mechanisms for the expected laser parameters we are able to give estimates of the expected particle energies dependent on the experimental parameters (laser energy, target composition and thickness), and to predict beam parameters and quality.

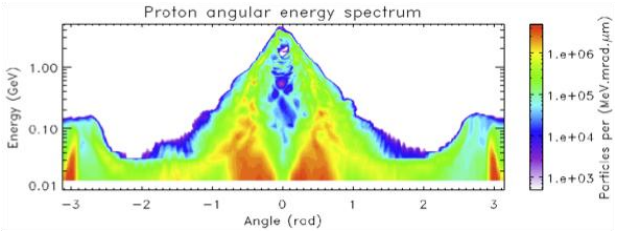

Figure 13.4 - Angular energy distribution of an ion beam resulting from laser solid interaction in the ELI regime.

13.6. ENABLING OSIRIS ON THE BLUEGENE ARCHITECTURE

With the allocation of 2'532'072 cpu-core hours on the Jugene Computer in Jülich, Germany for some of our projects arose the necessity to get OSIRIS ready to run on such machines. While OSIRIS was already perfectly prepared to run on world class parallel computer *it was necessary to make some adjustments to the code to account for some of the particularities of the Bluegene (B/G) architecture.* We have rewritten the setup of the MPI topology for OSIRIS to make effective use of the B/G torus network, by automatically adapting the simulation decomposition to the network partition at runtime. This largely increased the overall efficiency of the code for large number of cpu's. To make better use of the allocated resources we also rewrote the checkpoint facility in OSIRIS to allow for easy substitution of the file back-end. As a consequence we now use the sion back-end for OSIRIS simulations on the B/G architecture which greatly reduces overheads from disk I/O when writing/reading checkpoint information. Within the scope of the 2009 Extreme Scaling Workshop, we were given access to the full computing system, having achieved a strong scaling efficiency of over 80% on 294912 cores, starting from 4096 cores, making excellent use of this type of systems (Figure 13.5).

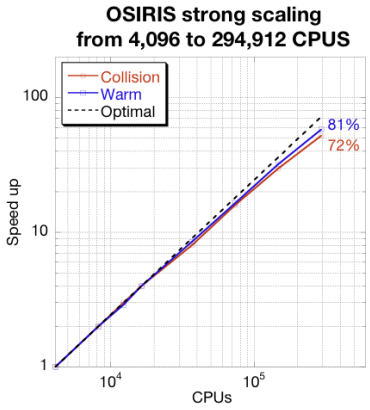

Figure 13.5 - Benchmark of the PIC code OSIRIS on the IBM Bluegene architecture up to 294'912 cpu's corresponding to the largest number of cores ever available on a single system as of 2009.

13.7. A FULL RELATIVISTIC PIC CODE IN CUDA ENABLED HARDWARE[2]

Particle in cell (PIC) fully relativistic kinetic codes for plasma simulation are computationally intensive, and new computing paradigms are required for one-to-one direct modeling of these scenarios. Continuing on last year's work, *we have implemented a fully relativistic 2D PIC code on a GPU using NVIDIA's C for CUDA.* The implementation was validated using a well-known benchmark problem of the Weibel instability in electron-positron plasmas (Figure 13.6). The main performance bottleneck is current deposition (approximately 71% of a simulation cycle), since it involves global scattering operations. We were able to avoid serializing this step by implementing a pseudo atomic add with floats. This implementation can be extended to include other kinds of atomic operations, as long as they have a neutral element and are commutative. The complete code performs significantly faster on a Tesla C1060 than on a single core of an Intel Xeon E5420.

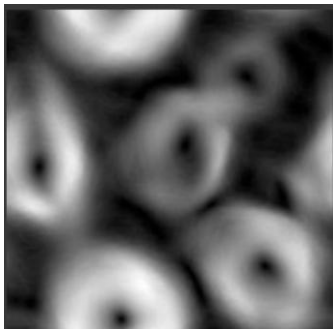

Figure 13.6 - 2D Weibel instability produced by our CUDA code. B12 intensity is depicted using direct visualization at interactive frame rates.

13.8. DIRECT VISUALIZATION IN PIC CODES

Visualization in particle-in-cell simulations can be a time consuming and computationally demanding task. By running the simulation on the GPU, the data is already available in video memory, and can readily be displayed, avoiding time consuming memory transfers from CPU to video memory. In this sense, *we have expanded our PIC implementation in CUDA to allow for the display and exploration of the resulting simulation data* (Figure 13.7). This expanded system is able to display millions of particles and also to produce several diagnostics (EM field, current, charge density) and other custom diagnostics at interactive frame rates.

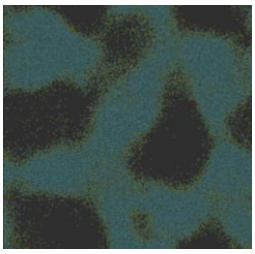

Figure 13.7 - Direct visualization of particle density during a 2D Weibel instability produced by our CUDA code. Electrons in cyan and positrons in yellow.

13.9. MAGNETIC FIELD AMPLIFICATION IN SUPERNOVA REMNANT SHOCKS BY THE NON-RESONANT KINETICALLY DRIVEN STREAMING INSTABILITY[3]

Very energetic Cosmic Rays (CR) ($\sim 10^{14}$ eV to 10^{15} eV) are thought to be accelerated in Supernova Remnant (SNR) Shocks. There is direct evidence that electrons are accelerated up to energies of 10^{14} eV at SNR sites, and the measured power law spectra of the CRs indicates Diffusive Shock Acceleration (DSA) as the most likely mechanism responsible for the acceleration. The acceleration of these particles up to energies of $\sim 10^{15}$ eV through the DSA mechanism requires the existence of magnetic fields much stronger than the typical B0 $\sim$ 3 μG; these strong fields have also recently been inferred from A mechanism for beam driven non-resonant magnetic field amplification has been proposed before. In this scenario, a very low density beam propagates parallel to a background magnetic field in the presence of a background plasma. The fastest-growing wavelength predicted by linear theory is much smaller than the Larmor radius for the beam ions, and thus the excited magnetic field does not affect the beam ions significantly.

The identification of the nonlinear saturation mechanism for the non-resonant streaming instability is analyzed using dHybrid, a fluid-electron kinetic ion code. Amplification factors of $B_{\perp}/B_{\parallel} \sim 10$, with local temporary peaks of $B_{\perp}/B_{\parallel} \sim 25$ are observable in the current simulations; similar results were also recently shown in the kinetic simulations, with reduced temporal and spatial scales, mass ratios and density ratios. The hybrid

[2]In collaboration with J. Madeiras Pereira (IST, INESC-ID)
[3]In collaboration with R. Bingham (RAL, UK), M. Pohl (Iowa, USA), J. Niemec (PAN, Poland)

simulation results presented (Figure 13.8) expand the current knowledge of the non-resonant streaming instability by extending the dynamical range under study, and by performing a detailed study of the instability under different driving regimes.

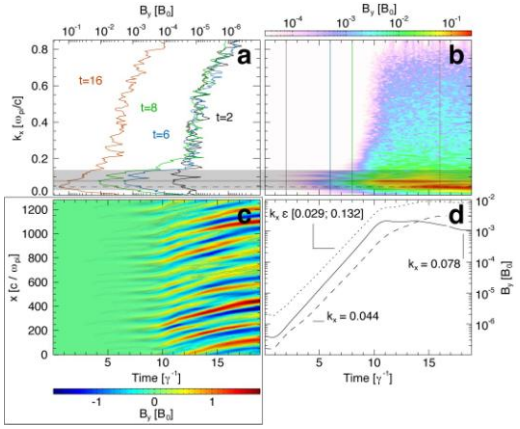

Figure 13.8 - Evolution of the perpendicular magnetic field component B_y in time. Frame a) shows lineouts of the power distribution in k space (frame b) at times: 2 γ^{-1} (black line), 6 γ^{-1} (blue line), 8 γ^{-1} (green line), and 16 γ^{-1} (red line). Frame d) shows the growth rates for k_x = 0.078 ω_{pi}/c (solid line), k_x = 0.044 ω_{pi}/c (dashed line), and for the 0.029<k_x<0.132 ω_{pi}/c high-growth band (dotted line). Frame b) is obtained by fourier transforming frame c) in the spatial dimension.

13.10. IMPLEMENTATION OF A PARTICLE-TRACKING ALGORITHM IN QUICKPIC[4]

QuickPIC is a reduced particle-in-cell code (PIC) used to examine both laser and plasma wakefield acceleration. This code leverages on the quasi-static approximation to reduce by up to three orders of magnitude the typical simulation times associated with stardard full PIC codes. Although detailed analysis of the dynamics of the accelerated particle bunches could be performed with the standard grid diagnostics, more in-depth research on the individual trajectory of each beam electron was not accessible. *A particle-tracking algorithm was thus implemented in QuickPIC,* opening novel perspectives for the use of this code in the research of radiation generation, and acceleration of polarized beams in wakefield accelerators.

The particle-tracking implementation consisted in the initialization of additional test-particle bunches. Similarly to regular particle beams, these are pushed through the Lorentz force, without, however, depositing any current. These beams were initialized in resemblance with the full PIC code OSIRIS, thus taking full advantage of the visualization infrastructure already in place to analyze OSIRIS simulations. Figure 13.9 shows an example of the trajectories of accelerated bunch particles in a laser wakefield accelerator QuickPIC simulation.

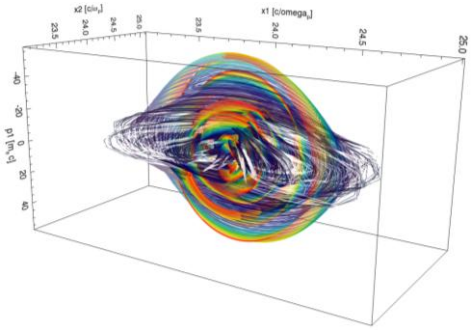

Figure 13.9 - Image of particles trajectories in the p1x2x1 phase-space from a QuickPIC simulation, using the VisXD visualization infrastructure.

13.11. POLARIZED BEAM ACCELERATION

For high-energy-physics (HEP) all the measurable quantities associated with the particle beams which are used in the experiments obey to tight constraints regarding their dimensions, emittance, and polarization (the average spin of the particle bunch). It has been shown that the dimensions, and the emittance of externally injected electron bunches may be preserved in wakefield acceleration. However, the practical use of wakefield accelerators as afterburners for HEP experiments, requires that the polarization of the accelerated bunches is also preserved. Resorting to the Thomas-Bargman-Michel-Telegdi (T-BMT) equations it was shown that wakefield accelerators preserve beam polarization. As a result, there is no fundamental restriction of the use of these type of accelerators in HEP applications.

An analytical model to investigate the acceleration of polarized beams was developed by considering the electro-magnetic field structure of the blowout regime in the T-BMT equations. It was shown that the depolarization was lower in externally-guided propagation regimes. In addition it was found that lower depolarization rates may be achieved with lower beam emittances. These conclusions were supported with QuickPIC simulations using particle-tracking. Since the spin does not interfere with the beam dynamics, the particle-tracking data was post-processed in a spin-tracking algorithm and compared with the analytical results.

13.12. LASER-PLASMA ACCELERATORS RIDE ON EINSTEIN'S SHOULDERS[5]

The ability to perform laser-wakefield accelerator (LWFA) simulations in relativistically moving frames is now fully implemented in OSIRIS (Figure 13.10). This allows for computational gains of several orders of magnitude, and dramatically changes the modeling of the current and the next generation experiments.

Using this technique, *we have designed and simulated self-guided stages up to 12 GeVs, and externally guided and injected stages up to 50 GeV*. These new kinds of numerical experiments enable us to understand the new physical processes involved, to optimize experimental

[4] In collaboration with W. B. Mori (UCLA,USA), and C.K. Huang (LANL,USA)
[5] In collaboration with W. B. Mori (UCLA, USA)

parameters, and to estimate the acceleration possible with the next generation of laser systems. The new results show that laser wakefield acceleration with near term lasers could lead to compact, less expensive infrastructures for fundamental science research, for new accelerator technology development, and might potentially lead to a future particle collider at very high energies.

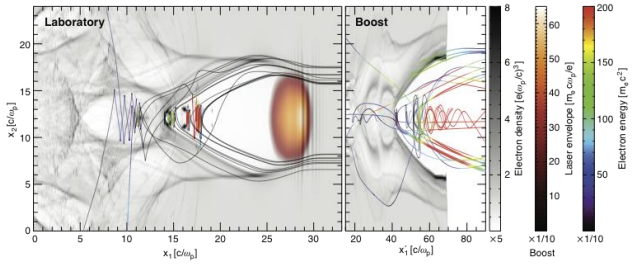

Figure 13.10 - Comparison between a laboratory and a boosted frame simulation. The spatial and time transformations lead to differences in the result interpretation. In the boosted frame shot shown, for instance, the injection is still occurring even after the laser had fully exited the plasma column.

13.13. MODELING LASER-WAKEFIELD ACCELERATION EXPERIMENTS IN OSIRIS[6]

LWFA experiments have recently started to explore alternative electron injection schemes, targeting improved control of the process and higher quality output beams. The state-of-the-art tools available in OSIRIS enabled the modeling and design support of these more advanced experiments, which typically require including additional physical processes in the code.

A first example is the ionization trapping scheme already explored with particle and laser beams (Figure 13.11). To model these experiments with OSIRIS, *the existing ionization module was expanded* to include additional atom types and to allow the follow up of individual electrons from each ionization level.

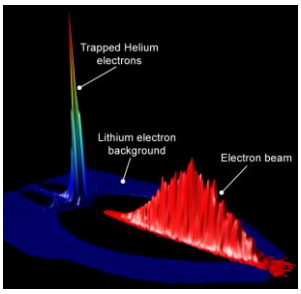

Figure 13.11 - Simulation of experiments performed at SLAC for the trapping of helium electrons in a beam driven plasma accelerator. A relativistic electron beam (red) propagates in a mix of lithium (97%) and helium (3%) gases. The lithium provides the electrons that generate the wakefield and the accelerating structure, while the helium electrons are trapped at the peak of the accelerating field.

current experiments with plasma lengths at the centimeter scale is now easily available. For example, quick parameter scans were performed for self-trapping experiments.

13.14. RELATIVISTIC COLLISIONLESS SHOCKS WITH STATE-OF-THE-ART PIC SIMULATIONS[7]

We have implemented several state-of-the-art tools available for full particle-in-cell (PIC) simulations to improve the modeling of astrophysical scenarios in OSIRIS. These tools involve higher precision field solvers, advanced current and field smoothing, dynamic load balancing for higher parallel efficiency, new hardware features, among others. The ongoing study of relativistic collisionless shocks in electron-ion unmagnetized plasmas was continued with ab-initio PIC simulations (Figure 13.12), and particle tracking was used to analyze in detail the particle dynamics and the acceleration process. We observed an energy growth in time that can be reproduced by a Fermi-like mechanism with a reduced number of scatterings, in which the time between collisions increases as the particle gains energy, and the average acceleration efficiency is not ideal.

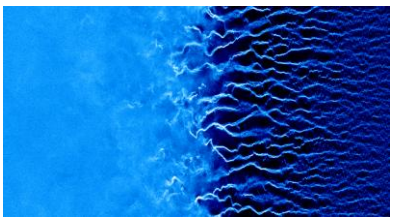

Figure 13.12 - Electron density in a relativistic shock in astrophysics. When two plasma regions cross each other, instabilities arise (density filaments) and a density compression (lighter region) is generated. It is believed that these shocks are at the origin of cosmic ray acceleration, the fastest particles yet observed in the Universe.

13.15. ASTROPHYSICS IN THE LABORATORY WITH FIREBALL BEAMS[8]

A new scheme to generate relativistic fireballs in the laboratory was also explored with relativistic electron-positron beams. This scheme provides an effective mean for the laboratory study of microphysics relevant to astrophysical scenarios. We showed that the current filamentation instability associated with some of these scenarios reaches saturation after only 10~cm of propagation in a typical laboratory plasma (Figure 13.13). The different regimes of the instability, from the purely transverse to the mixed mode filamentation, can be accessed by varying the background plasma density. The instability generates large local plasma gradients, intense transverse magnetic fields, and enhanced emission of radiation. We suggested that these effects may be observed experimentally for the first time.

[6] In collaboration with C. Joshi, W. B. Mori (UCLA, USA), and D. Froula (LLNL, USA)
[7] In collaboration with W. B. Mori (UCLA, USA)
[8] In collaboration with P. Muggli (USC, USA)

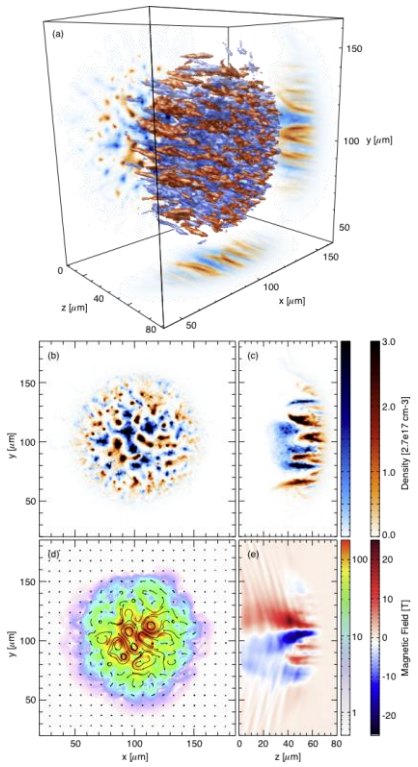

Figure 13.13 - Fireball beam after 10 cm propagation in a plasma with density 2.7x10^{18} cm^{-3}. The beam is made by overlapping two relativistic beams, one composed of electrons and the other of positrons. The Weibel instability leads to the fireball filamentation, with the generation of large magnetic fields, similarly to astrophysics scenarios.

13.16. GENERATION OF RELATIVISTIC SHOCKS IN FAST IGNITION SCENARIOS[9]

One of the critical issues for fast ignition of fusion targets is to understand/optimize the coupling of the ignition laser to the fast particles, and their transport in the mildly to high dense region of the target.

We have performed a series of two-dimensional (2D) PIC simulations in order to examine laser absorption and electron transport using ignition lasers with ultrahigh intensities, up to 5x10^{21} W/cm^2, and density gradients up to 1000 n_c. (Figure 13.14).

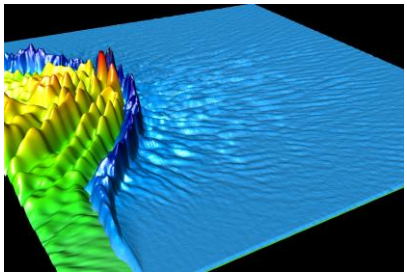

Figure 13.14 - Electron density (blue) of a fast ignition target irradiated by an ultrahigh intensity laser (green-red) illustrating the occurrence of strong filamentation and the generation of a relativistic shock structure

Our results indicate that the laser absorption is increased with increasing intensity and that the dynamics of the Weibel/streaming instabilities leads to an isotropization of the increased inward heat flux. This causes energy to be bottled up near the laser interaction point causing a shock to be launched. In fast ignition (both channel and cone guided) this shock and the associated heat flux need to propagate up a density gradient. The inclusion of the density gradient is observed to be crucial. As the shock moves to denser regions the Weibel/streaming instabilities become weaker, leading to a stronger energy release by the shock structure and to potentially higher efficiencies in the core. The observed shock dynamics can also be relevant to astrophysical scenarios, where Weibel-driven relativistic shocks propagate through different plasma density regions.

13.17. EFFICIENT RAMAN AMPLIFICATION INTO THE PETAWATT REGIME

In recent years, there has been considerable interest in obtaining ultrahigh laser intensities for several applications that range from fast ignition of fusion targets to ion acceleration. The use of the technique of Raman amplification in a plasma is seen as a promising approach, since plasma can tolerate much higher laser intensities (10^{17} W/cm^2 or more) than solid state devices.

We have studied the possibility of extending the Raman amplification scheme to ultrahigh intensities with multi-dimensional PIC simulations (Figure 13.15).

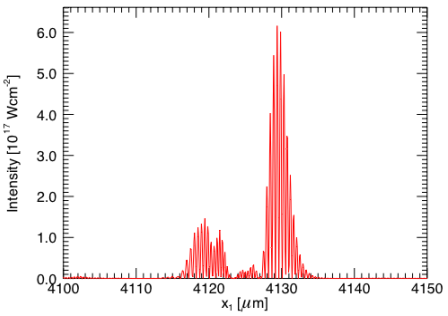

Figure 13.15 - Laser pulse Raman amplified to 20 PW in a 3D PIC simulation after the interaction with a 10 TW, 1 mm wide, 25 ps long pump pulse in a 4 mm plasma slab

Our results show that it is possible to control the multitude of nonlinear effects that can occur, such as probe saturation due to Raman forward scattering (RFS) and wakefield generation, breaking of the Raman backscattering (RBS) Langmuir wave that couples the pump and the probe, parasitic pump RBS, and transverse filamentation of both pump and probe pulses, by an appropriate choice of the laser and plasma parameters. In this narrow but definite parameter window it is possible to obtain efficient Raman amplification of a 10 TW, 1 mm wide, 25 ps long laser pulse up to 6 PW. Focusing of the amplified pulse to 1 micron spot sizes can lead to laser intensities of 6x10^{23} W/cm^2, opening the way to ultrahigh intensity laser-matter interactions.

[9] In collaboration with W. B. Mori (UCLA, USA), and C. Ren (URochester, USA)

13.18. NUMERICAL MODELING OF RADIATION FROM WEIBEL SCENARIOS

The Weibel instability is common in both laboratory and astrophysics scenarios. The study of the radiative signatures of this phenomenon is hence valuable for the interpretation of astrophysical and experimental observations. Leveraging on the numerical code developed in the past year to determine the radiation emitted by charged particles in PIC simulations (beyond the grid resolution), *we have studied the spectrum of radiation emitted by electrons in the magnetic field structures that arise from the Weibel instability* (Figure 13.16).

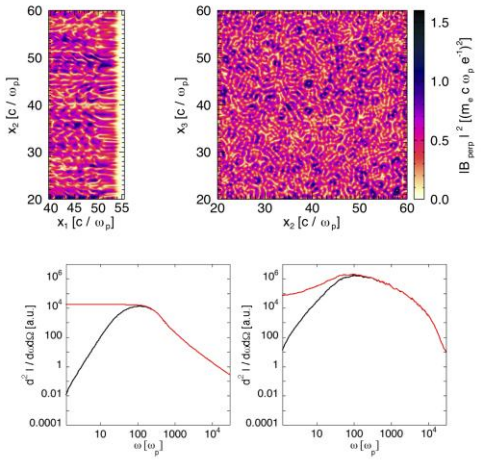

Figure 13.16 - In the upper figures, the perpendicular component of the magnetic field energy from a 3D Weibel scenario, taken at the peak of the instability, is presented in parallel (left pane) and perpendicular (right pane) planes to the flow propagation. At the bottom, the radiation spectrum emitted by electrons in electron/proton Weibel 2D scenario is presented, in the early (left) and the saturation (right) stages of the instability, with (black line) and without (red line) the inclusion of the Razin effect.

Scenarios where an electron-positron/proton plasma with a given bulk fluid velocity flows through a still plasma were explored through PIC simulations performed with the OSIRIS 2.0 framework. As the plasma flows cross, current filaments start growing which generate small-scale magnetic field structures (see top part of Figure 13.16). The evolution of these field structures, from their growth, during the early stages of the instability, up to their disintegration, during the saturation stage, determines the dynamics of the electrons, hence their radiation spectrum.

By determining the spectrum of radiation emitted up to certain time moments it is possible to establish a correlation between the evolution of the magnetic field energy spectral distribution and the electron radiation spectrum evolution (see bottom pane of Figure 13.16). In the lower frequency part of the spectrum, for instance, an increase in amplitude is observed as the characteristic size of the current filaments increases during the growth phase of the Weibel instability. The final spectrum power law index at lower frequencies was measured to be approximately in the range 2/3 to 1. The higher frequency part of the spectrum evolves towards a broken power law.

The effect of the medium on the radiation emitted by the electrons has also been studied and was modeled through the modification of the Liénard-Wiechert potentials to account for the Razin effect. This effect is characterized by a modification of the radiation beaming due to the presence of a medium with an index of refraction greater than that of the vacuum. It leads to a suppression of the beaming for emitted radiation of frequencies smaller than the Lorentz relativistic factor times the plasma frequency. This can be observed in the calculated spectra, where the inclusion of this effect (black line on the bottom of Figure 13.16) is shown to strongly reduce the energy emitted per unit of solid angle in the lower frequency region. Here the medium influence was modeled in an approximate manner by considering its density to be the initial density and initial results suggest that this effect may be affect significantly the spectrum shape in the lower frequency region.

13.19. COMPARISON OF RADIATION COOLING MODELS FOR PARTICLE-IN-CELL SIMULATIONS

Under extreme acceleration, charged particles can radiate strongly and the corresponding radiation damping/cooling can become important in the plasma energetics and dynamics. In particular, under the presence of ultra high intensity lasers or other intense electro/magnetic fields the motion of particles in the ultrarelativistic regime can be severely limited by radiation damping. The standard Particle-in-Cell (PIC) algorithms do not include radiation damping/cooling effects. Even though this is a well know mechanism, there is not yet a definite algorithm nor a standard technique to include radiation cooling in PIC codes. *We have compared several models for the calculation of radiation damping force,* with the goal of developing an algorithm for radiation damping in OSIRIS (Figure 13.17). We evaluate both the general numerical issues as well as the numerical implementation in the PIC algorithm. The results of the different models are compared with analytical models and standard results, and the relevance/advantages of each model are discussed.

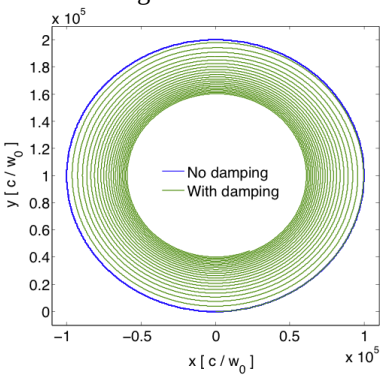

Figure 13.17 - Particle's trajectory in the constant magnetic field with and without radiation damping

13.20. ENHANCEMENT OF THE ELECTROMAGNETIC WEIBEL INSTABILITY DUE TO ION STREAMING

Fast Ignition (FI) relies on the propagation of the fast electrons which can create the ignition spark in the core of the pre-compressed target. One of the key issues in FI is the deposition of the beam energy into the core (overdense) required to ignite the FI target. It is well known that when a relativistic energetic beam propagates in a background plasma, background electrons provide for the return current in the opposite direction and it drives several plasma instabilities ranging from longitudinal modes (electrostatic instabilities) to transverse (electromagnetic instability) mode. Since it is cumbersome to analyze the coupling between the electrostatic and the electromagnetic mode, progress has been made achieved by considering the electrostatic and electromagnetic modes separately.

We have concentrated our work in the study of transverse electromagnetic mode. In these studies ion response was not examined. The motivation to include the ion response is associated with the influence of the ion streaming after the electron Weibel instability shutdown due for instance to strong electron heating. For this purpose, we have considered scenarios with counter streaming hot electrons and cold ions. The linear dispersion relation has been derived from relativistic theory by assuming waterbag distribution function in the momenta with the beam direction perpendicular to the wave vector of the unstable mode. The growth of electromagnetic instabilities due to ion response has been examined in this scenario. It was found that the inclusion of the ion response can lead to significant enhancement in the growth rates at high wave numbers (growing on the ion time scale) and prevents immediate shutdown of the Weibel instability (Figure 13.18).

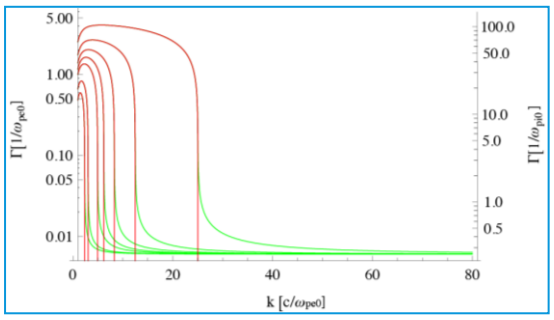

Figure 13.18 - Comparison between the growth rates of the Weibel instability with (green) and without (red) ion streaming. The growth rate is plotted for different temperatures of the stream. In this scenario $n_{e0} = n_{i0}$, $u_{e0} = -v_{xi0}$. and $T_i = 0$, where n_{e0}, u_{e0}, n_{i0} v_{xi0} are the density and velocity of the electron and ion respectively.

13.21. MAGNETIC FIELD GENERATION VIA THE KELVIN-HELMHOLTZ INSTABILITY

Collisionless plasma instabilities have been proposed as candidates to explain the strong magnetic fields required by models for non-thermal radiation emission in exotic astrophysical scenarios, such as AGN and GRBs. Since these extreme scenarios are usually associated with relativistic outflows, velocity-shears naturally emerge. These shears power the *Kelvin-Helmholtz instability* (KHI) and are caused by the strong and rapid variability of the ejecta.

In this work *we generalize previous relativistic collisionless KHI calculations to include arbitrary density jumps/flows and pressure effects.* The growth rates, the fastest growing modes, dependencies on density ratios and pressure effects, as predicted by the linear theory, are compared with 2D PIC simulations.

We are currently working on 3D PIC simulations in order to study the 3D effects of the instability, such as the magnetic dynamo. It is believed that the KH-induced turbulence may allow the magnetic dynamo to operate, and thus greatly amplify the magnetic fields.

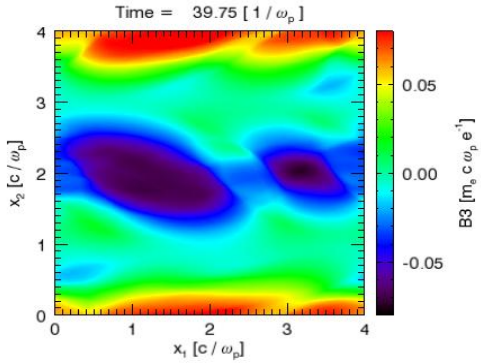

Figure 13.19 - 2D PIC simulation of the KHI: Magnetic field structures generated by the KHI in a tangential-discontinuity shear flow.

14. NEW RADIATION SOURCES FROM PLASMAS AND OPTICAL PHYSICS[1]

L.O. Silva (Head), J.M. Dias (Principal Investigator), N. Lemos and J. Berardo.

14.1. INTRODUCTION

The experimental work on new radiation sources from plasmas and optical physics was developed along the following lines of research:

- Optical modeling of the human eye;
- Betatron radiation from laser wakefield accelerators;
- Field ionization heating and plasma channel generation;
- Plasma refraction by a plasma channel.

14.2. OPTICAL MODELING OF THE HUMAN EYE[2]

With the development in the recent years of several new diagnostic tools of the optical properties of eye, with more precise biometric data, and with the new refractive surgeries methods, such as the corneal refractive surgeries and intra-ocular lens implantation, the discussion about the the study of the optical properties/capabilities of the human eye. This new biometric diagnostic techniques *in vivo*, such as aberrometry, corneal topography (Orbscan) and axial length measurements along the computational modeling of the eye allow us the possibility to model the optical properties of an eye of single individual. The customized modeling of the eye is essential for study eyes that not fit in the big datasets clinical studies where empiric statistical formulas are derived, such as SRK formula for the calculation of the intra-ocular lens power to be implanted in the eye. The Liou and Brennan anatomical correct model is the best candidate to be implement it in a ray-tracing software (ZEMAX©) that can enable us to perform detailed analysis the optical properties, like study the impact of small variation in vision acuity, of realistic eye (Figure 14.1). With this powerful ray-tracing software (ZEMAX©) it is also possible to introduce biometric data of a single individual into the eye optical model. For that the data from Orbscan topographer was reformatted to be introduced in the ZEMAX and reproduce the corneal surfaces shapes in the optical model along with data (axial lengths) from other diagnostics.

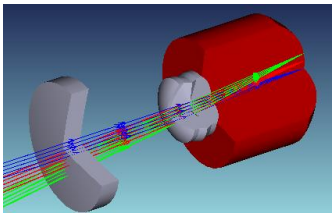

Figure 14.1 - ZEMAX Layout of the Liou & Brennan optical model with lens correction

An extensive comparison with the clinical data most preformed in order to validate the method and the capability of predicting an accurate intra-ocular lens power for each individual despite his clinical history.

14.3. BETATRON RADIATION FROM LASER WAKEFIELD ACCELERATORS[3]

The electrostatic forces in laser wakefield accelerator can drag electrons from the plasma and rapidly accelerate them and lead to transverse betatron motion, which gives rise to emission of hard X-rays in femtosecond duration pulses. The photon energy, which depends on the electron energy and betatron amplitude, is currently limited to spectra peaking in the 1 – 10 keV range. After performing an experiment in 2008 at the ASTRA-Gemini Laser facility at Rutherford Appleton Laboratory in a collaboration with the Strathclyde University Team *data analysis was preformed*. For ≈10 pC electrons bunches were produced intermittently in the range of 200-300 MeV. Intense beams of X-rays with ≈20% spectral bandwidth spectra and peaking at 40 KeV were emitted with the estimated peak brilliance $B_{peak} \approx 3.2 \times 10^{20}$ photons/(s mrad^2 mm^2 0.1% bandwidth) for a 10 fs pulse. This compact source of brilliant gamma rays may find use in medical imaging, medical isotope generation, homeland security and potentially probing nuclear phenomena. To prove the usefulness of the source we have demonstrated phase-contrast imaging in the 10 – 100 keV range (Figure 14.2).

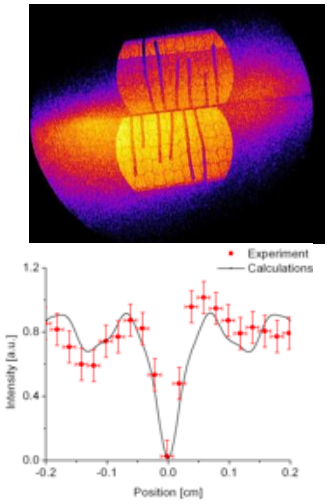

Figure 14.2 - Nickel grid phase–contrast image.

[1]Activities performed in the frame of the Contract of Associated Laboratory, out of the Contract of Association Euratom/IST, by IPFN staff of the Group of Lasers and Plasmas.
[2]In collaboration with F. Ribeiro (Hospital da Luz)
[3]In collaboration in experiment leaded by Jaroszynski DA and his team (Strathclyde)

For >400 MeV mono-energetic electron beams from a wakefield accelerator, we measure 10^9–10^{10} gamma-ray photons with spectra peaking in the 0.05-5 MeV range. The explanation for this is that the amplitude of the betatron oscillation can be resonantly enhanced when the electron beam simultaneously interacts with the laser pulse and the electrostatic field of the plasma bubble. This results in orders of magnitude increase in the radiation rate and photon energy. Since the X-ray detector was not able to obtain a spectrum for this regime another experiment is schedule for the beginning of 2010.

14.4. FIELD IONIZATION HEATING CAN GENERATE PLASMA CHANNELS SUITABLE FOR GUIDING

High-intensity (10^{18} W.cm^{-2}) laser guiding over lengths greater than a centimeter is one of the key issues for future laser-plasma accelerators and other applications, such as x-ray lasers and harmonic generators. In the plasma accelerator concept, an intense, ultrashort laser pulse interacts with a plasma of adequate electron density to produce high amplitude (hundreds of GV/m) plasma waves moving in the laser propagation direction at a velocity close to the speed of light. Since the strongest waves are generated at the focal spot of the laser pulses, the length of a plasma accelerator is, approximately, the Rayleigh length of the focusing optical system. The energy gains can be greatly enhanced by extending the interaction length beyond the Rayleigh length by using a guiding scheme, leading to energy gains up to GeV. Nowadays the most promising guiding schemes are based on preformed plasma waveguides and the most popular method uses a thermally driven laser-induce plasma expansion. A drawback of this method is the fact that uses long laser pulses (~10-100ps) to heat the plasma through inverse Bremsstrahlung (initial temperatures of tens of eV´s). This way it is necessary to use two laser systems to create a laser-plasma accelerator, one that produces long laser pulses to create a plasma channel and other that produces ultra-short high energy laser pulses (50-100 fs) to be guided in the channel creating the accelerating structure.

In this work *we show that ultra-short laser pulses (sub-picosecond) can heat the plasma to initial temperatures of tens of eV´s in order to create a hot plasma column that will expand into a plasma waveguide.* The heating mechanism is determined to be the related with some extra momentum that the electrons gain due to the Above threshold ionization (ATI) effect. In this case (as opposite to the long laser pulse regime) the inverse Bremsstrahlung heating has very little effect because the collisional frequency is reduced for large electron quiver velocities. Using this kind of heating mechanisms this method has a great advantage over the standard methods because it only uses one laser system to create a laser-plasma accelerator. This is accomplish by taking a small percentage of the pump beam to create the plasma channel and delaying the pump by a few femtoseconds to permit the creation of the channel.

To test this new method *we did a detailed study of the transverse dynamics and some preliminary evaluation of the optical guiding qualities of a plasma channel created by an ultra-short laser pulse* (Figure 14.3). By focusing a first laser pulse with 400 fs from the L2I laser chain on a gas jet (for three different gases, Ar, HE, and H), an 8 mm uniform plasma column was created, that expands after a few nanoseconds. We show that the plasma column expands into an on-axis parabolic density profile that acts as a waveguide suitable for guiding high intensity laser beams.

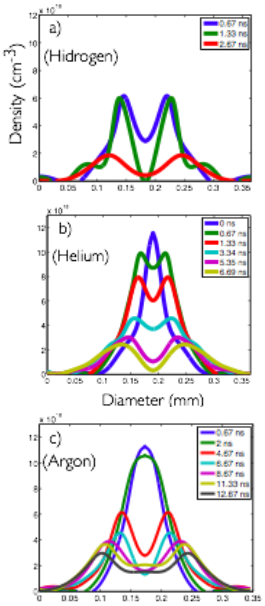

Figure 14.3 - Transverse time evolution of the plasma channel for three gases (Hydrogen, Helium and Argon)

A second laser pulse, focused at be beginning of the waveguide is injected into the plasma waveguide after an optimum delay in order to test the optical guiding of qualities of the waveguide. Preliminarily results indicate that there is guiding (Figure 14.4) but with low transmission coefficient that can be improved by solving some coupling problems at the channel entering.

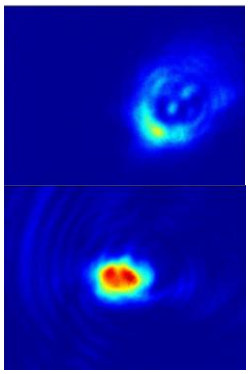

Figure 14.4 - Laser spot image at the plasma channel exit (left: without plasma channel; right: with plasma channel)

14.5. PLASMA REFRACTION BY A PLASMA CHANNEL

In the field of laser-plasma interaction experiments one of the main measurements its the electronic density. Some of the most common plasma density diagnostics are based on the plasma optical proprieties, like for example refractometry usually used qualitatively or interferometry usually used quantitatively. On this work, *it was proposed to use refractometry diagnostic in order to obtain quantitative results in opposition of what is normally used.* Studying the wave front deformation caused by the plasma was observed that the plasma acts like a convergent or a divergent lens depending of the electronic density profile of the plasma and it turns possible to know the position of the focal spots. Initially a relatively simple example with a Gaussian profile was performed to an experimental proof of principle in order to understand the physical phenomena. The simulation and experimental results were compared with theoretical values to pinpoint the focusing distance of the optical system. The data images acquired shows one focus before the plasma plan, a completely clean image on the plasma image plan and at last one plasma shadow after the plasma image plan. Measuring the distance between the focus and the plasma plan it enables to deduce the density profile of the plasma. Starting from this simple example we applied refractometry diagnostic to the plasma channel electronic density. With the plasma channel electronic density profile was observed, on simulations and experimentally, two focus before the plasma image plan, a completely clean image on the plasma image plan, and at last one focus after the plasma image plan (Figure 14.5). This clearly shows a signature of the plasma channel structure with the central core acting as a positive lens (lower plasma density profile) and the outer region a negative lens (higher plasma density).

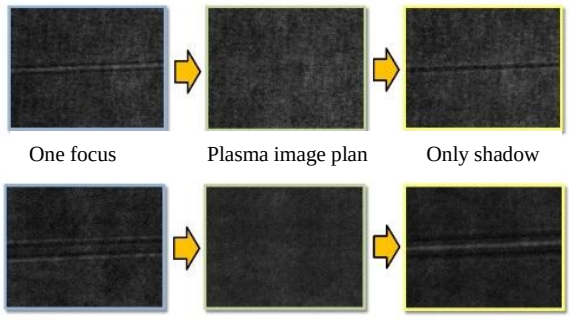

Figure 14.5 - From left to right images are: before, at and after the plasma image plan. The top images shows the plasma Gaussian density profile (one focus line before the plasma image plan) and the bottom images shows the channels density profile (two focus lines before and one focus line after the plasma image plan).

15. LASER-PLASMA ACCELERATORS AND APPLICATIONS[1]

L.O.Silva (Head), N.C. Lopes (Principal Investigator), C. Russo, R. Bendoyro, M. Hilbert and J. Jiang.

15.1. INTRODUCTION

The work in this field was developed along the following main topics:

- Development of long plasma channels for electron acceleration;
- Improvement of the reproducibility of a plasma source compatible with meter-scale LWPA;
- Automatic compensation system for the L2I laser facility;
- Study of the radiation shielding characteristics with Geant;
- Coupling of high-intensity lasers to plasma channels;
- The neutral gas guiding interface among LPA & FELs;
- The new design of compact undulator for tabletop FELs.

15.2. DEVELOPMENT OF LONG PLASMA CHANNELS FOR ELECTRON ACCELERATION

Plasma channels for electron acceleration are a key component for future laser-plasma accelerators. A guiding plasma channel allows to optimize the energy gain of one acceleration stage potentially enhancing the final electron beam emittance.

Previously we have developed and tested a set of new techniques to produce preformed plasma channels for high intensity lasers: structured gas cells, fast-risetime high-voltage discharges and simmer discharge. The combination of this three techniques in a gas cell 2.2 cm long resulted in the production of high-quality plasma channels with the profile adequate to guide low power laser beams focused to a beam diameter of 50 μm.

The plasma channels obtained with the 2.2 cm presented a plasma density of $2x10^{17}$ cm^{-3} on axis. This density is compatible with am accelerator dephasing length in excess of 10 cm and a maximum energy gain of about 8 GeV. *We have built a new gas cell with a length between electrodes of 8 cm* in order to evaluate the possibility to extend this plasma channeling technology to the 10 cm range, (Figure 15.1).

The gas cell was tested in the L2I plasma accelerators test bench, (Figure 15.2), in a one week time slot. These first tests were made using a gas cell with half of the ceramic elements. The reduction of the ceramic elements was decided to reduce the cost, to test the viability of longer cells (supported by modeling and previous experiments) and to reduce the probability of parasitic discharges (trough the gas feeding system).

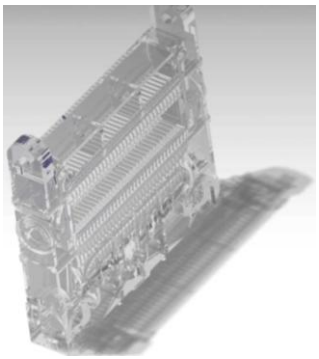

Figure 15.1 - Rendering of the 8 cm gas cell main body.

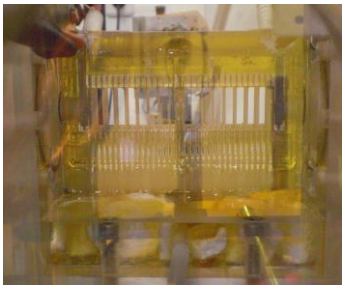

Figure 15.2 - Picture of the 8 cm gas cell mounted on the test bench

The device was tested using a slow rise low current discharge of 1 mA and a 100 ns high-voltage pulse (120 KV delivered trough 125 Ω impedance). It was possible to produce a straight plasma line measurable by interferometry. However, we could not avoid important parasitic discharges trough the gas feeding system. The reduction of current on the axial plasma changes its expansion dynamics and a plasma channel is no longer produced. The use of a 0.5 T axial magnetic field did not reduce the parasitic discharge significantly.

In conclusion, the path to increase the length of the plasma channels to the 10 cm range requires improvements of the experiment at different levels: change of the gas feeding geometry to reduce the probability of parasitic discharges, development of high-voltage (50 kV) switch in order to control the start of the simmer discharge and to increase the power of the main discharge by a factor of 2 by increasing the voltage to 200 kV and reducing the impedance to 100 Ω.

[1]Activities performed in the frame of the Contract of Associated Laboratory, out of the Contract of Association Euratom/IST, by IPFN staff of the Group of Lasers and Plasmas.

15.3. IMPROVEMENT OF THE REPRODUCIBILITY OF A PLASMA SOURCE COMPATIBLE WITH METER-SCALE LWPA

Recent theoretical work based on numerical simulation of laser wakefield plasma accelerators (LPWA) has shown that it is possible to accelerate electron bunches to the 60 GeV scale using a meter-long pre-formed plasma. Experimentally, energy gains of the order of 1 GeV have been demonstrated using 33 mm long plasma channels, formed by electrical discharges in a gas.

At GoLP, *we have demonstrated a plasma source based on a structured gas cell by producing plasma channels that are 20 mm long, with electron densities of the order of* 10^{19} cm^{-3}. The unique aspects of our technology are that it allows good optical access in the direction transverse to the laser propagation, requires no external laser triggering, and is extensible to much longer lengths.

Up to now, the principal obstacle in extending the length of the gas cell has been the degradation of the quality of the plasma channel. In fact, as the gap between the electrodes is increased, the physical mechanisms behind the electrical breakdown of the gas depart from the Townsend mechanism and become less homogeneous. Consequently, the path of the discharge becomes irregular.

We were able to successfully overcome this limitation by separating the process into two stages: plasma formation and plasma heating. By introducing a DC current-limited glow (pre-) discharge a few tens of milliseconds before the main discharge, a homogeneous weakly-ionized plasma is created. This "plasma line" significantly lowers the impedance between the electrodes. As a result, switching the main discharge leads in rapid heating. The free expansion of the plasma leads to plasma channels.

Our measurements using a 20 mm gas cell show that there is a substantial improvement in the reproducibility of the temporal evolution of both current and voltage (Figure 15.3). These results make a sound case on the feasibility of extending the current technology from the centimeter to the meter length scale.

15.4. AUTOMATIC COMPENSATION SYSTEM FOR THE L2I LASER FACILITY

High-power laser systems including L2I's are reported to suffer from pointing instability, mostly due to thermal effects. These occur typically in a slow time scale, ranging from a few minutes (the repetition rate of the L2I laser system at full power) to a few hours (the typical duration of an experimental run), and amount to a position uncertainty at the target of the order of a few hundred of micrometers. Such phenomena impose practical restrictions on the minimum workable dimensions of both the laser spot and the target itself.

In order to compensate this laser-pointing instability, *an automatic compensation system for the target area has been developed, tested and is currently being installed.* The position of the spot of the laser is measured at different positions using CCDs, and this information is then used to act upon motorized mirror mounts. This procedure runs continually at a maximum rate of 10 Hz, and guarantees the automatic correction of deviations in the laser pointing direction that occur in a time scale above one second.

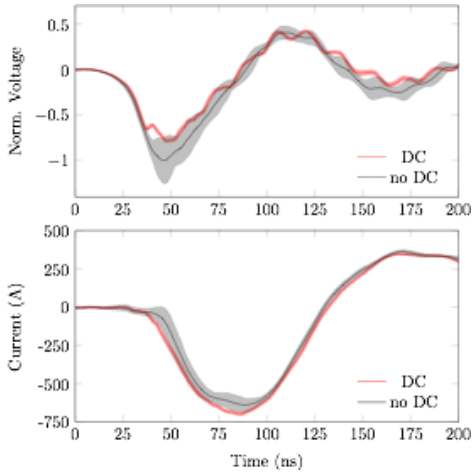

Figure 15.3 - Measurement of the temporal evolution of the voltage and the current of the electric discharge for hydrogen at a pressure of 500 mbar. The central solid lines corresponds to the average normalized voltage (top) and absolute current (bottom), while the shaded areas correspond to the 1-σ limit. The red (black) curves were obtained when the DC pre-discharge was enabled (disabled). Using the DC pre-discharge improves the reproducibility by a factor of 5.

15.5. STUDY OF THE RADIATION SHIELDING CHARACTERISTICS WITH GEANT

The ELI, as a user facility, needs to deliver accelerated particles at high repetition rates. Therefore, the acceleration of a large number of particles with energies up to 1 GeV diverging from the main beam (~0 degrees), as predicted by the Osiris simulations, poses a new challenge for beam production and delivery. Unlike conventional particle accelerators that benefit from a long history of progressive design evolution, the ELI approach has to conciliate the particle and the laser beams transport, the diagnostics and the shielding in a non-fixed layout, as this is a just new born technology. Since scaling the known shielding implementations is not an option, a full numerical simulation is the best approach. For this task it was chosen Geant 4, a highly versatile Monte Carlo simulation toolkit created in CERN.

The first step consisted of modeling a room and adding some virtual diagnostics to assess the shielding (Figure 15.4). Only a very simple layout was tested due to the inexistence of any facility sketch in the early preparatory phase. Particle shower generation, tracking and energy deposition were demonstrated. The second step was estimating the activation. This is especially relevant in a space where some of the materials choice will be dominated by their laser performance, rather than for their radioactive environment fitness.

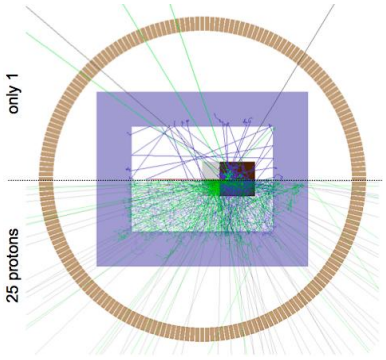

Figure 15.4 - Secondary particles shower generated by 5 GeV protons hitting a plastic and iron beam dump (center) surrounded by 1 m thick concrete walls and 200 radially distributed detectors.

15.6. COUPLING OF HIGH-INTENSITY LASERS TO PLASMA CHANNELS

Plasma channels created by electric discharges in a structured gas cell are able to guide intense laser pulses for distances many times longer than the Rayleigh length, as necessary to extend the acceleration length in a laser wake-field accelerator (LWFA). Nevertheless, in general, current state-of-the-art plasma channels cannot guide laser beams with a very small spot sizes (very high intensities) as required for an effective self-injection of electrons. However, the larger laser spot sizes these plasma channels can efficiently guide are adequate for long distances guiding (>10 cm), thus suitable for a very high electron energy gain.

In this work *we propose and tested with PIC simulations (using experimental parameters for lasers and channels), a scheme for the coupling of very high-intensity lasers to plasma channels.* In this scheme we tightly focused a high-power laser in a plasma in order to produce self-injection of electrons, but the plasma density is selected in a way that the critical power for self-focusing is smaller than the laser power ($P/P_c \gg 1$).

Figure 15.5 shows the beam radius evolution along the propagation direction for three set of laser and plasma parameters. In all cases the beams are focused to ~10 µm spot radius which is smaller than the ~35 µm matching propagation radius of the channel (horizontal dashed line). In all cases the beam intensity at waist is high enough to produce full cavitation of the plasma and self-injection of electrons in the bubble (Figure 15.6, (a)). In cases b) and c) the channel is not able to guide those unmatched beam radius, but, in case a) the enhanced self-focusing effect can compensate the beam diffraction collimating the beam radius to the channel propagation radius. At this point the channel start guiding the beam at lower intensities in a regime close to the blowout regime (Figure below, (b)), but with the peculiarity that already there are energetic electrons injected in the bubble.

This scheme shows the feasibility of a LWFA in which external injection of electrons is not required. Moreover, it is also possible to tune the relation between the self-injected charge and the energy gain, e.g. lower injected charge will lead to greater energy gain. Large scale simulation must be done in order to see the evolution of the accelerator structure for longer distances.

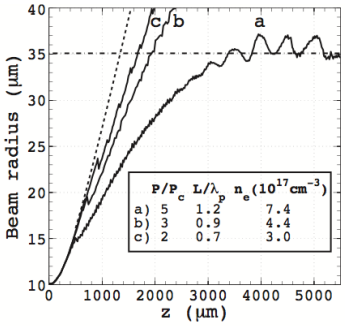

Figure 15.5 - Beam radius evolution for three set of laser and plasma parameters. Cases b) and c) show the general behavior in which the plasma channel is not able to guide a tightly focused (~10 µm) laser beam. Case a) shows that under certain conditions self-focusing can compensate beam diffraction collimating the beam to the channel propagation radius (~35 µm, horizontal dashed line). The vacuum evolution (dashed curve) is shown as a reference.

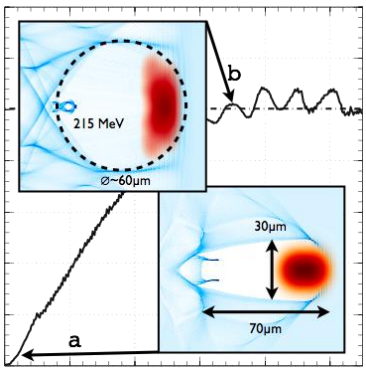

Figure 15.6 - Bubble evolution along beam propagation. Frames a) and b) show in blue the electron density and in red the beam position. Frame a) shows the full cavitation made in the plasma by the laser beam along with the self-injection of electrons. Frame b) shows the state of the bubble at the point of collimation with the channel, at this point the bubble have evolved to a spherical shape and the head of electron bunch already have an energy of 215 MeV.

15.7. THE NEUTRAL GAS GUIDING INTERFACE AMONG LPA & FELS

In this work, *we have explored the possibility to create a neutral gas guiding interface between a laser plasma accelerator (LPA) and a free-electron laser (FEL)* to concur the natural space charge blowout of the extremely high current density of electron bunches emitted from LPA. The idea is simple (Figure 15.7): while GeV, high current (>50 KA) electron beam injects into the neutral gas cell, the gas would be partially ionized via the field ionization, ion column and the configuration of electron space charge would confine and center the electron bunch through the unavoidable space between LPA & FEL.

We have used electrostatic kinetic model to study the

dynamics of electron beams in the neutral gas cell. From the results (Figure 15.8), we can conclude that with different gas pressure, it is plausible to guide the electron beam to propagate through variable distance (from 5cm to 20cm) in the gas cell, and keep the beam with acceptable diameter, in the meanwhile, greatly improved the beam pointing to the amplifier of the FEL.

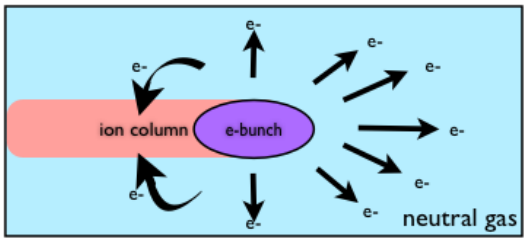

Figure 15.7 - PWFA based on relative e-beam field ionization

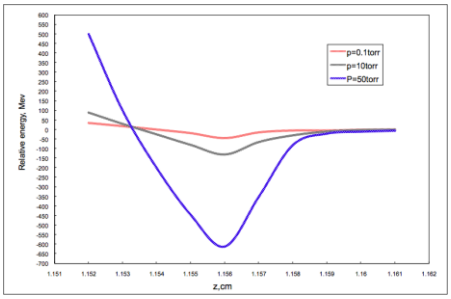

Figure 15.8 - Relative energy of electron bunch after gas cell at different pressure (the gas cell length=5 cm, electron bunch length=30 fs)

15.8. NEW DESIGN OF COMPACT UNDULATOR FOR TABLETOP FELS

In order to build tabletop LPA based FELs, an extreme compact undulator with high gain is required. *Our design is to use a pulse driven electro-magnetic scheme, to gain the high tunability (K=0~0.5) and high compactification* (Figure 15.9).

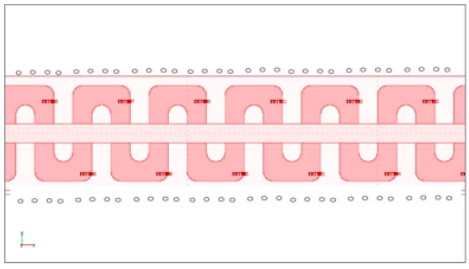

Figure 15.9 - Sketch of compact electro-magnetic undulator

Simply speaking, the design uses array of alloy part to guide the flux of pulse driven solenoid. During design, comsol-multiphysics was used, an FEA method simulation software to study the plausibility of the design. According to the results (Figure 15.10), our design can reach 10 Hz repetition rate with undulator parameter as high as 0.5 which is quite compatible for our LPA based FELs scheme.

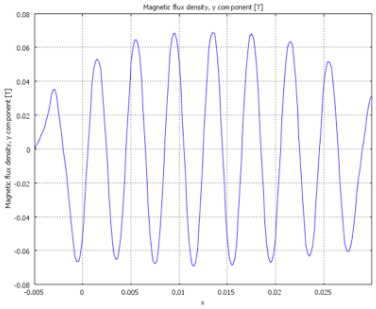

Figure 15.10 - The longitudinal magnetic flux density of one dipole during one driven pulse

16. HIGH INTENSITY LASER SCIENCE AND TECHNOLOGY[1]

L.O. Silva (Head), G. Figueira (Principal Investigator), T. Imran, J. Wemans, C. João, H. Pires, M. Fernandes

16.1. INTRODUCTION

The work on experimental high intensity laser science and technology was developed along the following lines of research:

- High energy diode-pumped ytterbium-based amplification;
- White-light continuum generation, characterization and optimization;
- Modelling of OPCPA using YCOB as the nonlinear gain medium;
- Participation in the development and characterization of the VULCAN 10 PW project;
- Spatio-temporal distortions and propagation of wavefront-aberrated beams in grating pairs;
- Evaluation of pump beam smoothing in a Ti:sapphire regenerative amplifier by using a diffractive optical element.

16.2. HIGH ENERGY DIODE-PUMPED YTTERBIUM-BASED AMPLIFICATION

The work done during 2009 represented an important step towards providing the Laboratory for Intense Lasers with a more efficient, compact, 100 mJ level pulse source. It is intended that in the short-term L2I will be capable of providing such pulse energies at repetition rates up to 100 times higher than the current status, either for laser-plasma experiments or as pump source for an optical parametric amplifier.

At the experimental level *we performed new tunability tests for the Yb:glass regenerative amplifier assembled the previous year*. The results show that it is possible to obtain mJ pulses with central wavelengths ranging from 1037 to 1052 nm for different seeds. Figure 16.1 presents the output pulse spectra for different cavity spectral tunings, with a seed centered at 1056.3 nm.

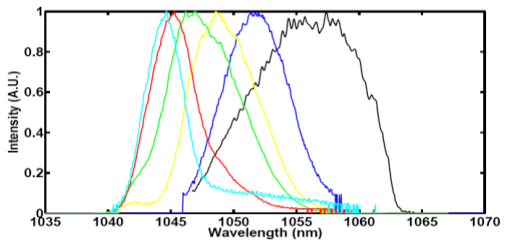

Figure 16.1 - Tunable spectral window for the study of tunability for different cavity spectral responses. Seed pulse spectrum is shown in black, other colours correspond to the output pulse spectra.

Currently, 100 mJ-level ytterbium-doped amplifiers with gains higher than 100 are based almost exclusively on Yb:YAG crystals, with operation at 1030 nm. Yb:YAG does have a small gain peak near 1050 nm, but it is not strong enough for efficient pulsed operation. In fact, we tested and measured experimentally the single pass gain for Yb:glass and Yb:CaF_2 at 1053 nm, and concluded that it would be very difficult to obtain gains ≥100 for an 8-pass amplifier with either medium. *We performed a new upgrade to the simulation code* and were able to identify Yb:KYW and Yb:KGW as the most promising alternatives for a future multipass amplifier. This will nonetheless require a change of the seed wavelength from 1053 nm to 1023–1040 nm.

We also performed several simulations for optimizing the performance of a hybrid Yb/Nd amplifier. This has allowed us to identify Yb:CaF_2 and the newer material Yb:CALGO as the most suitable materials for a laser chain based on an ytterbium pre-amplifier and neodymium amplifier. Figure 16.2 shows the calculated spectral intensity for the case of Yb:CALGO, evidencing a strong amplifier capability at 1053 nm.

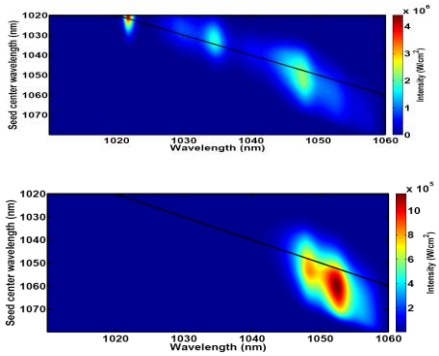

Figure 16.2 - Spectral intensity for an Yb/Nd hybrid chain using Yb:CALGO. Above: Output from Yb:CALGO pre-amplifier. Below: Final output from Nd:glass amplifier.

16.3. WHITE-LIGHT CONTINUUM GENERATION, CHARACTERIZATION AND OPTIMIZATION

The development of a broadband laser sources using the equipments and parameters of L2I was initiated, which will represent a new research field at this facility. We studied and evaluated the suitability to generate white-light continuum (WLC), a broadband spectrum from visible to infrared, in transparent solid media such as sapphire and fused silica, and investigated the required parameters. The study and characterization of WLC at L2I is the subject of several new trends in order to study few cycle laser pulses.

[1]Activities performed in the frame of the Contract of Associated Laboratory, out of the Contract of Association EURATOM/IST, by IPFN staff of the Group of Lasers and Plasmas.

The experimental advances in 2009 showed the promising results of WLC generation from the output of the Ti:sapphire regenerative amplifier, where we have used the mJ-level, 250 fs, 10 Hz pulses centered at 1053 nm to interact with fused silica glass and sapphire. In a typical experiment, a pulse energy of the order of 300 μJ is focused by a 400 mm focal length lens into a 10-12 mm thick solid material to generate WLC, which is then observed by a conventional CCD camera. The WLC beam has a central white-light part, and is surrounded by colored rings. The higher frequency light appears in the outermost ring, and lower frequency light forms the ring nearest the white-light portion. The resulting spectrum as detected by a broadband spectrometer (Ocean Optics) is a flat, octave spanning curve extending from 400 nm to 1100 nm, as (Figure 16.3).

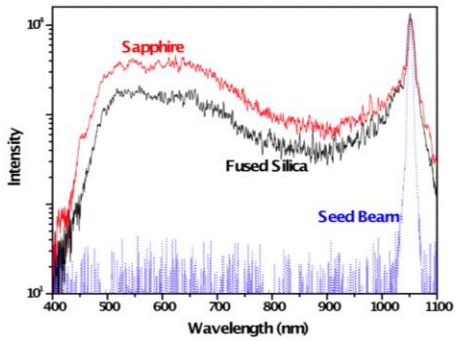

Figure 15.3 - Spectra of white-light continuum

In order to characterize the WLC spectrum, *we have decided to use a FROG (Frequency Resolved Optical gating) and XFROG (Cross-correlation FROG) diagnostic.* We have designed and installed the experimental setup for XFROG and FROG diagnostics as shown in Figure 16.4, and the XFROG beam alignment and image acquisition is under process.

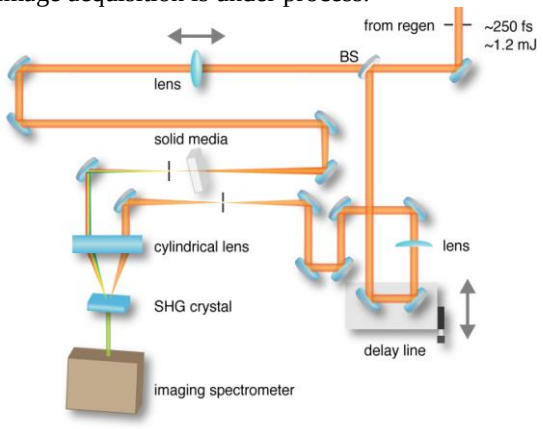

Figure 16.4 - Schematics of XFROG setup for characterizing the white-light continuum generation

16.4. MODELING OF OPCPA USING YCOB AS THE NONLINEAR GAIN MEDIUM

The work done during the year 2009, consisted in the *continuation of the OPCPA research line and laying the grounds for a new, more efficient diode-pumped OPCPA.* We investigated the feasibility of using the nonlinear crystal yttrium calcium oxyborate (YCOB) as the nonlinear gain medium for high power, high repetition rate parametric amplification. A simulation code using the crystal's Sellmeyer coefficients was used in an OPCPA stage with signal dispersion. Gain and amplification bandwidth show promising results. The numerical code was upgraded to work with biaxial crystals such as YCOB. Figure 16.5 shows the gain spectrum for a pump intensity of 1 GW/cm^2.

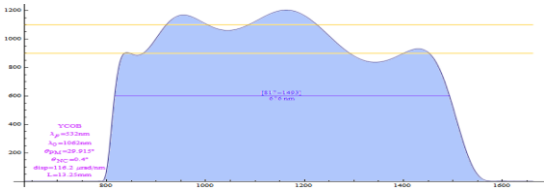

Figure 15.5 - Estimated gain spectrum for a 1 GW/cm^2 pump intensity

16.5. PARTICIPATION IN THE DEVELOPMENT AND CHARACTERIZATION OF THE VULCAN 10 PW PROJECT[2]

Currently the most powerful laser being built, the VULCAN 10 PW at the STFC Central Laser Facility (Chilton, United Kingdom) aims to deliver 300 J in 30 fs, with 10^{23} W/cm^2 focused intensity and 10^{10} contrast ratio. The laser is based on optically synchronized OPCPA stages, and will be the most powerful demonstration ever of this amplification concept. In 2009 *we started a collaboration with the VULCAN 10 PW team in order to participate in the development of temporal diagnostics and simulate the performance of the large amplification stages.*

In order to achieve the peak values expected, a complete characterization of the pulse structure is required. For the temporal characterization, the implementation of a spectral phase interferometry for direct electrical-field reconstruction (SPIDER) diagnostic has been planned since the start of the project. Although this diagnostic had already been built, as well as the software intended for its use in the front-end, it had never been effectively used. Therefore, it was tested using a MIRA 900 oscillator and, later, adapted for front-end usage. The nonlinear crystal was changed and the geometry was optimized for a better beam separation (Figure 16.6).

With the second phase of the 10 PW project starting in early 2010, simulation of the power amplifiers is planned so the future constraints are known when the time comes to design and purchase the parts for the experimental facility. In this way, extensive use of an amplification code developed by Marco Galimberti was started so that angular tolerances and consequences for non-optimal conditions

[2]In collaboration with Cristina Hernandez-Gomez, Marco Galimberti and Ian Musgrave (CLF/STFC, UK)

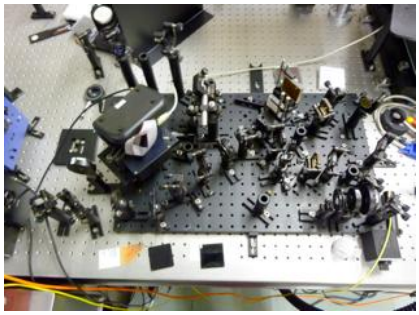

Figure 16.6 - View of the SPIDER diagnostic for the VULCAN 10 PW project.

16.6. SPATIO-TEMPORAL DISTORTIONS AND PROPAGATION OF WAVEFRONT-ABERRATED BEAMS IN GRATING PAIRS

We studied the propagation of spatially and temporally Gaussian beams with a finite wavefront curvature through grating compressors (Figure 16.7), using the simple and elegant formalism of Kostenbauder matrices. This approach is particularly adequate for determining the effect of deliberately introducing such perturbations in these beams in terms of the resulting spatio-temporal profile and changes to the peak intensity.

The results showed that for a well-aligned compressor the transform-limited pulse duration can still be achieved for an initial finite curvature, allowing the pre-compensation of commonly present low-order aberrations such as defocus and astigmatism.

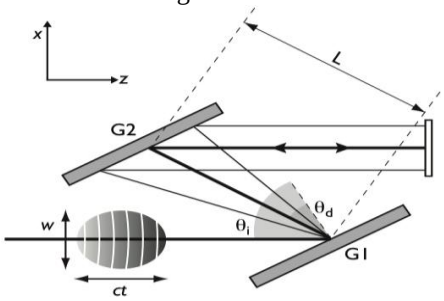

Figure 16.7 - General setup for the problem of compressing a chirped, non-collimated beam.

16.7. EVALUATION OF PUMP BEAM SMOOTHING IN A TI:SAPPHIRE REGENERATIVE AMPLIFIER BY USING A DIFFRACTIVE OPTICAL ELEMENT[3]

In Ti:sapphire-based regenerative or multipass amplifiers, the spatial quality of the pump beam is crucial for ensuring en efficient, damage-free amplification. This is particularly relevant for systems operating away from the peak of the gain medium, such as in our case, where the amplification wavelength is centered at 1053 nm.

The pump laser used at the L2I regenerative amplifier is a commercial, frequency-doubled q-switched Nd:YAG (Spectra Physics GCR-130), delivering up to 200 mJ at 532 nm. The current pump profile is rather inhomogeneous, which places the threshold for effective amplifier operation very near to the damage threshold of the Ti:sapphire crystal, leading to frequent optical damage. In collaboration with the French manufacturer SILIOS Technologies *we have evaluated the feasibility of introducing a beam-smoothing stage consisting of a specially engineered, large aperture diffractive optical element (DOE) coupled with an imaging lens.* The results (Figure 16.8) show a markedly improvement in the homogeneity of the beam profile, although at the cost of some added small-scale fluctuations, and extra complexity in the pump layout. For comparison purposes, in 2010 we will also evaluate a simpler approach based on image-relaying the frequency doubling crystal from the Nd:YAG laser onto the Ti:sapphire crystal surface.

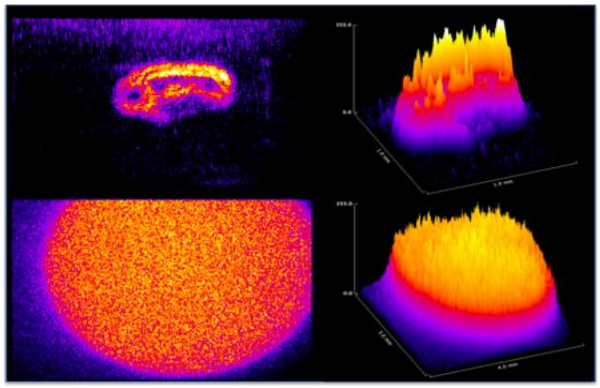

Figure 16.8 - Pump beam profile without (top) and with (bottom) using DOE smoothing.

[3] In collaboration with Thierry Berthou (SILIOS Technologies)

17. COHERENT XUV SOURCES AND APPLICATIONS[1]

L.O.Silva (Head), M. Fajardo (Principal Investigator), E. Abreu, A. Sardinha, JP Miranda

17.1. INTRODUCTION

The work on coherent XUV sources and applications was focused on:

- Optimization of soft x-ray amplifier by tailoring plasma hydrodynamics;
- Turning solid aluminium transparent by intense soft X-ray photoionization;
- Measurement of high harmonics polarization in an orthogonally polarized two-colour configuration;
- Diffraction-limited High Harmonic Generation;
- Generation of tunable EUV radiation.

17.2. OPTIMIZATION OF SOFT X-RAY AMPLIFIER BY TAILORING PLASMA HYDRODYNAMICS[2]

Plasma-based seeded soft X-ray lasers have the potential to generate a high-energy, highly coherent, short pulse beam. Owing to their high density, plasmas created by interaction of an intense laser with a solid target should store the highest amount of energy among all plasma amplifiers. However, to date output energy from seeded solid amplifiers remains as low as 60 nJ. With this work, *we demonstrated that careful tailoring of the plasma shape is crucial for extracting energy stored in the plasma.*

We have performed 2D hydrodynamic simulations of several transient collisional excitation plasmas based on early studies and experiments where 2D effects appeared, using the ARWEN code developed at UPM (Figure 17.1). A seeding experiment reported by Wang et al (2009) has been analyzed with our code, suggesting that the gain zone is very small because of deleterious hydrodynamic effects, and thus the output energy is intrinsically limited to values below 100 nJ. Simulations performed with wider plasmas corroborate this assumption.

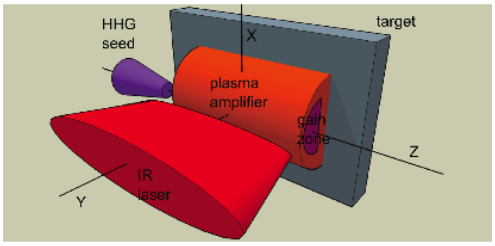

Figure 17.1 - Scheme of the simulations and the coordinate system used. HHG stands for High Harmonic Generation and indicates where the harmonics will be seeded in our scheme

Thus, *a geometry is proposed, increasing the width and decreasing the length of the plasma so as to ex- tract more energy and to dramatically increase the pumping efficiency.* With such tailored plasma, gain and pumping efficiency have been increased by nearly a factor of 10 as compared to the narrower plasma amplifiers studied, (Figure 17.2). With this geometry, energy as high as 22 µJ can be obtained with a 1-mm-wide plasma.

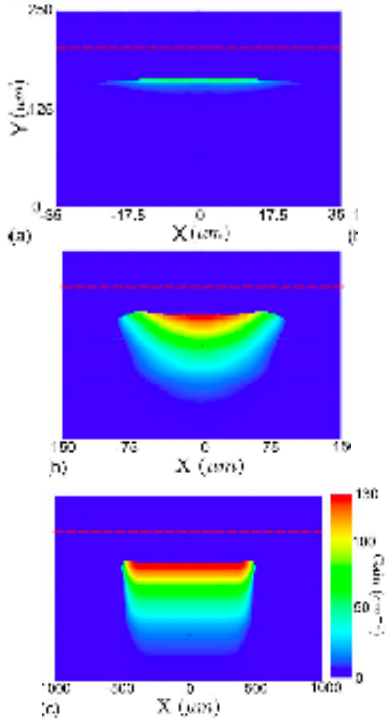

Figure 17.2 - Gain maps in false colors for 30 µm width plasma (left), 150 µm (center), and 1 mm (right). The pump lasers come from the bottom to the top.

17.3. TURNING SOLID ALUMINIUM TRANSPARENT BY INTENSE SOFT X-RAY PHOTOIONIZATION[3]

As extreme XUV laser intensities become available, new studies of laser-matter interaction become possible. *We took part in an experiment conducted by the "Peak brightness collaboration" at the VUV-FEL FLASH facility at DESY, aiming at investigating warm dense matter by XUV laser-solid interaction.*

Saturable absorption is a phenomenon readily seen in the optical and infrared wavelengths. It has never been observed in core-electron transitions owing to the short lifetime of the excited states involved and the high

[1]Activities performed in the frame of the Contract of Associated Laboratory, out of the Contract of Association Euratom/IST, by IPFN staff of the Group of Lasers and Plasmas.
[2]In collaboration with E. Oliva, P. Velarde (UPM, Spain), K. Cassou,D. Ros (LIXAM, France), S. Sebban, Ph. Zeitoun (LOA, France).
[3]In collaboration with Bob Nagler et al (the Peak Brightness Collaboration at DESY).

intensities of the soft X-rays needed. We measured saturable absorption of an L-shell transition in aluminium using record intensities over 1016 W cm−2 at a photon energy of 92 eV.

Transmission of thin aluminum thin foils reveal an induced transparency above an XUV fluence threshold, (Figure 17.3).

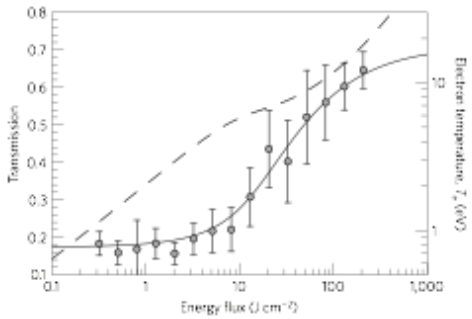

Figure 17.3 - Transmission of aluminium target as a function of fluence. The circles are the experimental data points with a 1σ error bar. The dashed curve is the predicted electron temperature in electronvolts (right y axis) in the valence band after the FEL pulse has passed, but before the L-shell holes are filled and the Auger recombination heats the band further.

From a consideration of the relevant timescales, by comparison to simulations we infer that immediately after the X-rays have passed, the sample is in an exotic state where all of the aluminium atoms have an L-shell hole, and the valence band has approximately a 9 eV temperature, whereas the atoms are still on their crystallographic positions. Subsequently, Auger decay heats the material to the warm dense matter regime, at around 25 eV temperatures. The method is an ideal candidate to study homogeneous warm dense matter, highly relevant to planetary science, astrophysics and inertial confinement fusion.

17.4. MEASUREMENT OF HIGH HARMONICS POLARIZATION IN AN ORTHOGONALLY POLARIZED TWO-COLOUR CONFIGURATION[4]

Since 2007 there has been considerable interest in producing harmonics in two-color fields, as Kim at al (2007) have shown a drastic increase in the efficiency of the Harmonic generation. However the actual mechanism involved with the increase in efficiency is not well understood. One simple theoretical model, the δ3 model, which is a simplified model of the atom using a 3D Dirac delta function to represent the atomic potential maintaining the symmetry of the central potential, has direct observables, such as the polarization of the generated harmonics in the mixed field. In that model, for the case of an orthogonally polarized two-colour fields scheme, the odd harmonics have the polarization of the fundamental field while the even harmonics have the polarization of the 2ω field.

We have been awarded in 2009 with Laserlab experimental beamtime at LOA to study the polarization of mixed field harmonics. A simple arrangement with a movable mirror could measure the reflectivity off a polarizing XUV mirror, followed by an XUV transmission grating, while direct measurement of the spectrum could also be made (Figure 17.4). The incident polarization onto the analyzer could easily be varied by changing the incident IR laser polarization.

Following the δ3 model expectations (odd and even harmonics polarizations respectively follow ω and 2ω polarizations) a 45º polarized ω beam would lead to observe in a two-colour arrangement a similar reflectivity for both odd and even harmonics (i.e. a soft line) as the ω and 2ω beams would present equal horizontal and vertical components. Our measurements clearly show that these expectations turned out to be totally inexact. Indeed, with the 45º polarized ω beam, oscillations of reflectivity and as a consequence of polarization are observed with higher vertical component for odd harmonics compared to even ones. Besides, these variations seem to be dependant of the order.

We have submitted a second round of experiments to explain these results, and determine wether the mixed field polarization is linear or elliptic. This result could have an important impact on the use of HHG for seeding in XUV free electron lasers, which have a fixed linear polarization.

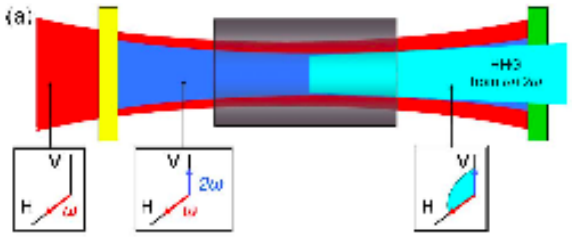

Figure 17.4 - Setup for the generation of even and odd harmonics. The polarization is measured using an XUV polarizer (45º multilayer and analyser)

17.5. DIFFRACTION-LIMITED HIGH HARMONIC GENERATION[5]

Imaging experiments of ultrafast phenomena of matter at nanometre-scale require intense, short pulse duration and diffraction-limited soft–X-ray beams, nowadays almost only provided by free-electron lasers. Here, *we focused on a table-top soft–X-ray source, which fulfils these fundamental criteria and in addition presents high temporal coherence, the high harmonics generated with a two-colour field (ω + 2ω).* These harmonics revealed to be free from aberration just by slightly spatially filtering the laser used for generation (ω). Indeed, the measured wavefront distortions, equal to λ/17 RMS at 44 nm, correspond to a diffraction-limited beam. This behaviour is explained by an additional spatial nonlinear filtering effect of the driving laser wavefront, induced here in our particular but simple geometrical configuration of generation by the 2ω component (Figure 17.5).

[4]In collaboration with G. Lambert, Ph. Zeitoun et al. (LOA, France).
[5]In collaboration with Lambert G, Douillet D, Gautier J, Rey G, Valentin C, Sebban S, Zeitoun Ph (LOA, France)

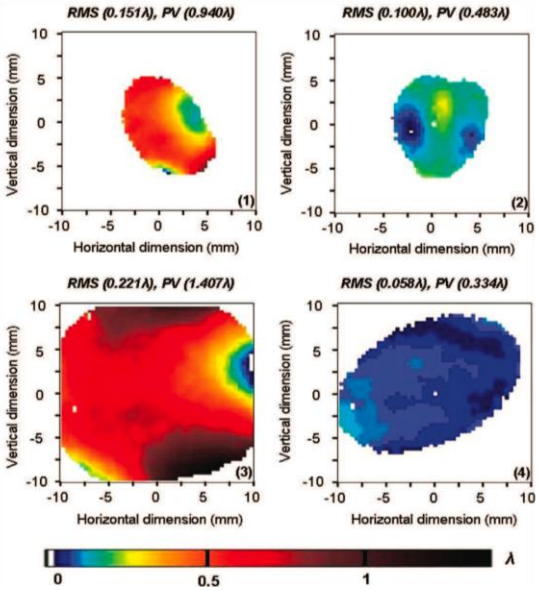

Figure 17.5 - Wavefront distortion amplitudes recorded on the wavefront sensor with ω of 37.5 nm and ω + 2ω of 44,5 nm. (1) ω technique with aperture of 20 nm, (2) ω technique with aperture of 15 nm. (3) ω + 2ω technique with full aperture beam 40 nm, (4) ω + 2ω technique with an aperture of 20 nm. RMS corresponding to Root Mean Square and PV corresponding to peak-to-valley.

17.6. GENERATION OF TUNABLE EUV RADIATION

X-ray lasers are a very useful tool producing a large quantity of data quickly and that can be used on many applications. Through seeding the X-ray laser (XRL) with a High Harmonic beam, the XRL will act as an amplifier of high-optical quality beam keeping the properties of the Harmonic while saturating at a shorter length. High Harmonics should however be tuned in order to match the wavelengths of the existing X-ray lasers. *We present the results of the generation of tunable high-order harmonics by changing the pulse compression.* We have obtained High harmonics up to the 51st order interacting a strong Nd-glass laser field with argon atoms in a gas cell. A shift of 13% around the central wavelength was observed allowing us to reach the Ne-like Mn and the Ne-like Fe lines via high harmonic generation (HHG) (Figure 17.6). A study of the linear chirp was also performed.

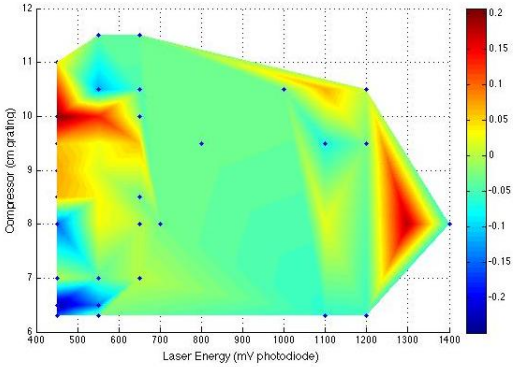

Figure 17.6 - Measured tunability of the HH radiation (a) Graphical representation of the variation in centimeters between the compressor gratings in function of the laser energy illustrating the average experimental Redshift/Blueshift in nanometers in the range 20-30 nanometers.

[6] In collaboration with Kozlova M (PALS), Rey G, Douillet D, Valentin C, Zeitoun Ph (LOA).

18. FAST IGNITION AND HIPER[1]

L.O. Silva (Head), J. R. Davies (Principal Investigator), P. K. Chauhan, K. Li, D. K. Singh

18.1. INTRODUCTION

Work on the HiPER preparatory phase project at IST increased considerably in 2009 with the hiring of 3 post-docs and participation in 3 HiPER experiments, one on each of the 3 major European laser facilities: RAL, PALS and LULI. Two post-docs started in May, one working on the theory of laser channeling and the other on the theory of ignition laser-plasma interactions. The third started in October and will work on HiPER experiments. They have been working on the interpretation and modeling of results from HiPER experiments, carried out this year and last year. The work on this topic was mainly developed along the following topics:

- HiPER experiment at RAL;
- HiPER experiment at PALS;
- PIC Modeling of Harmonic Emission as a Pre-Plasma Diagnostic;
- PIC Modeling of Laser Channeling.

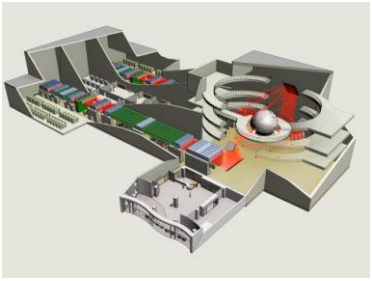

Figure 18.1 - Artistic impression of HiPER

18.2. HIPER EXPERIMENT AT RAL[2]

This experiment was carried out on Vulcan TAW in March and April to investigate laser channeling as an alternative to the use of a gold cone for fast ignition: the idea is to make a cone with a laser after the implosion rather than inserting one beforehand, avoiding problems with implosion asymmetry, high Z contamination and target fabrication. One of the CPA beams was stretched to 30 ps, long enough so that the laser ponderomotive force should open an almost empty channel in any underdense plasma. The other CPA beam was used to produce protons from thin metal foils for proton radiography. A 2 mm wide deuterium gas jet was used to provide plasmas with densities from 0.002 to 0.1 times the critical density, as would be found in the corona of an imploded ICF target. A wide range of diagnostics was used that confirmed the production of a straight channel, which was wider than the laser spot, all the way through the 2 mm long plasmas at all densities. Some results from the proton probing showing channel formation are given below.

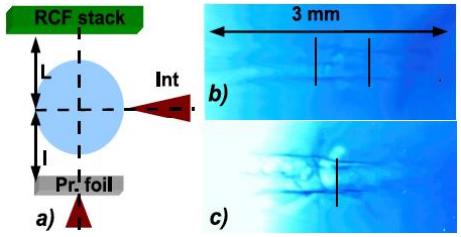

Figure 18.2 - The proton probing set-up used on the Vulcan TAW channeling experiment (a) and sample results for a 0.0002 nc deuterium gas jet at 100 ps (b) and 150 ps (c). Provided by G. Sarri (QUB)

18.3. HIPER EXPERIMENT AT PALS[3]

This experiment was carried out in September and was intended to measure the magnetic field in long pulse laser ablated plasmas, following on from our previous work on this subject [Davies J R, Fajardo M, Kozlová M, Mocek T, Polan J and Rus B Plasma Phys. Control. Fusion 2009 51 035013]. The PALS auxiliary beam was used in a line focus to produce 1 mm long plasma columns on plastic, aluminium and silver strips. To measure the magnetic field Faraday rotation of a third harmonic probe was measured by splitting the transmitted probe with a polarizing beam splitter cube and imaging each component onto a separate CCD. The PALS main beam was used to produce an XUV laser probe (21.2 nm) that was combined with the optical probe by using fused silica plates that transmitted the optical probe and reflected the XUV probe. Unfortunately, the silica plates severely limited the collection angle of the

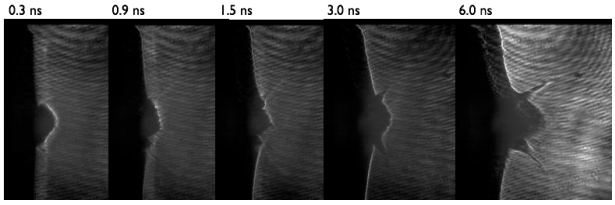

Figure 18.3 - A sequence of shadow/polarimetry images of the plasma formed on a silver target by the PALS auxiliary beam. Time 0 corresponds to the start of the 0.3 ns long pulse. Small-scale structure is visible at 0.9 ns and the formation of horn-like structures is clearly visible from 1.5 ns. The image is brighter on one side as a result of Faraday rotation.

[1]Activities performed in the frame of the Contract of Associated Laboratory, out of the Contract of Association Euratom/IST, by IPFN staff of the Group of Lasers and Plasmas.
[2]In collaboration with C Russo and J Jiang (IST).
[3]In collaboration with R. Bendoyro (IST).

optics, preventing us from seeing the region where a measurable magnetic field would be shadow images showing the plasma expansion and the development of horn-like structures in the plasmas at later times that were more pronounced for the higher Z targets. At the end of the experiment we removed the silica plates and obtained a series of higher quality images of the expansion of silver plasma, shown below, that show signs of filamentation and Faraday rotation. These results are still being analyzed.

18.4. HIPER EXPERIMENT AT LULI

This experiment was carried out on the PICO2000 laser in October and November to investigate fast electron generation at high laser contrast, lowering the pre-pulse by converting the laser to the second harmonic. This was intended as a follow on from the LULI HIPER experiment in 2008 where we deliberately increased the pre-pulse level to increase the pre-plasma. The data from this experiment are still being analyzed.

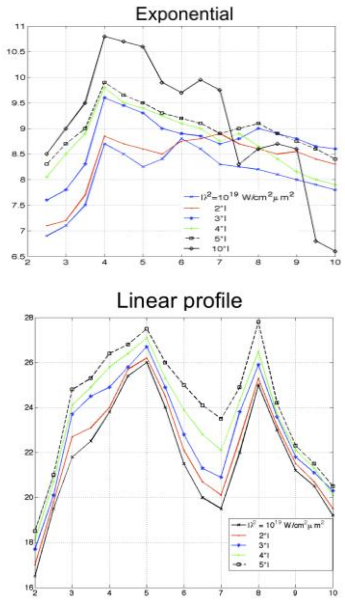

Figure 18.4 - The bandwidth of the 3rd harmonic in nm versus the pre-plasma scale length L in terms of the laser wavelength for exponential exp(-x/L) and linear 1-x/L profiles.

18.5. PIC MODELING OF HARMONIC EMISSION AS A PRE-PLASMA DIAGNOSTIC

In the LULI HiPER experiment in 2008 the bandwidth of harmonic emission was used as a diagnostic on the pre-plasma scale length, since self-phase modulation of the laser in the underdense plasma would be expected to give an increase in the bandwidth proportional to the scale length. To test this simple model *we carried out 2D PIC modeling using linear and exponential pre-plasma profiles for a wide range of scale lengths and laser intensities.* As the results below demonstrate, the simple model breaks down for scale lengths greater than about 4 λ, where the width of the harmonics starts to oscillate and varies considerably with the density profile and the laser intensity. This behavior was also seen in the red shift of the harmonics, the intensity of the harmonics and in the overall reflectivity and appears to be due to oscillations in the density profile caused by the laser. This shows that scale lengths greater than 4λ should be avoided for fast ignition in order to ensure a high degree of reproducibility. Unfortunately the LULI experiment in 2008 fell in this longer scale length regime.

18.6. PIC MODELING OF LASER CHANNELING

In the RAL HiPER experiment on channeling bubble-like structures were seen in the proton probing at the higher densities used, as illustrated by the image given below.

We have been studying the mechanisms behind the formation of these bubbles by PIC modeling. We have found from 2D modeling that they are caused by s-polarized radiation that leaks through the walls of the channel following relativistic self-focusing. This radiation is downshifted so that it becomes trapped in the void it makes in the plasma as a result of its ponderomotive force. This does not occur for p-polarization, apparently due to the lower reflectivity of p-polarized radiation. Limited 3D runs have shown that this phenomenon occurs only in the s-plane, where the radiation pressure makes holes in the channel walls, and that the bubbles are prolate spheroids. An example of the 3D results is shown below.

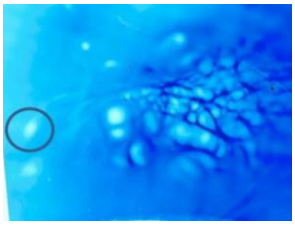

Figure 18.5 - Proton probing image from the Vulcan TAW channeling experiment for a 0.1n_{crit} deuterium gas jet 100 ps after the laser interaction, showing persistent bubble like structures. From G. Sarri (QUB).

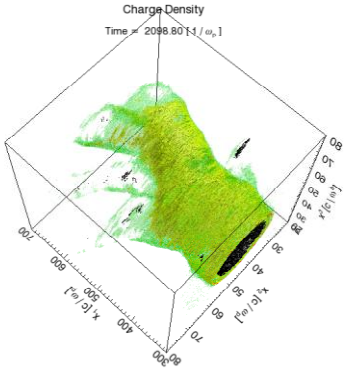

Figure 18.6 - Electron density contours from a 3D PIC code run 3 ps after the passage of a laser through a 0.1n_{crit} plasma. The yellow and green show where the density has increased and the black where the density has decreased. Elongated bubbles remain outside the channel in the plane where the laser was s-polarized.

19. PLASMA ENGINEERING LABORATORY[1]

C. M. Ferreira (Head), E. Tatarova and F. M. Dias (Principal Investigators), V. Guerra, J. Henriques, M. Pinheiro, E. Felizardo.

19.1. INTRODUCTION

Having in view environmental issues, the main activity of the "Environmental Plasma Engineering Laboratory" during 2009 was focused on experimental and theoretical investigations of microwave molecular plasmas over a large domain of operating conditions.

19.2. PLASMA TORCHES FOR ENVIRONMENTAL ISSUES[2]

High-density plasma torches provide suitable conditions to dissociate molecules in abatement systems and burn out chemical and biological warfare agents as well as to atomize materials. One of the main advantages of such microwave discharges at atmospheric pressure is that they make it possible to inject large power densities into the plasma and thus achieve high population densities of active species. Our work on microwave plasma torches and their applications was developed along the following main fields of investigation:

- Further improvement of the plasma torch experimental set-up; Building of "bubbling system" for Ar-Methanol plasma torch;
- Development of new experimental techniques for diagnostics of molecular plasmas – mass analyzer;
- Hydrogen production – decomposition of methanol (CH_3OH) by microwave plasmas.

Microwave plasma torches (2.45 GHz) operating at atmospheric pressure have been used to create plasma environment to decompose wood alcohol (methanol). To this end, the gas mixture of argon and methanol with or without water has been used to create the plasma. The plasma torch operating in Ar + CH_3OH is shown in (Figure 19.1). Mass and optical emission spectrometry have been applied as diagnostic tools. The optical emission spectrum in the range 250 – 700 nm has been detected. Mass spectroscopy has been used to detect the molecular hydrogen produced by methanol decomposition in argon plasma environment. Besides, H_2 and CO, which are the main reaction products of methanol (Figure 19.2) ($CH_3OH \rightarrow 2H_2 + CO$) decomposition process, H_2O, O_2 and N_2 have also been detected.

The experimental setup was built (Figure 19.3). The power is supplied by a microwave generator (0 – 2.0 kW) at 2.45 GHz. The microwave power was varied in the range 150 – 900W. The discharge takes place in a quartz tube open at one end (1.5 cm inner and 1.8 cm outer diameters, respectively). The total gas flow of 1000 sc cm (1.0 Slm) has a purity of 99.999%. Pure methanol is introduced into the discharge using bubbling of Ar through the alcohol at room temperature. Bubbling method allows one not to involve any additional energy in the process. The total gas flow is divided into two parts; one part is going through the quartz glass containing the alcohol to drag its molecules (bubbling). The resulting mixture (gas + alcohol) is united with the second part of the flow and then introduced into the quartz tube, where the discharge occurs.

Figure 19.1 - Argon – Methanol Plasma Torch

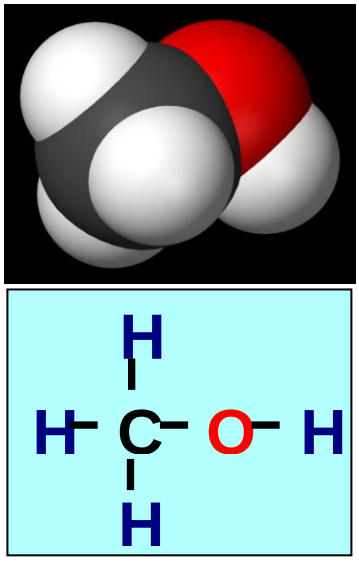

Figure 19.2 - Methanol (wood alcohol) molecular structure.

[1]Activities performed in the frame of the Contract of Associated Laboratory, out of the Contract of Association Euratom/IST, by IPFN staff of the Group of Gas Discharges and Gaseous Electronics.

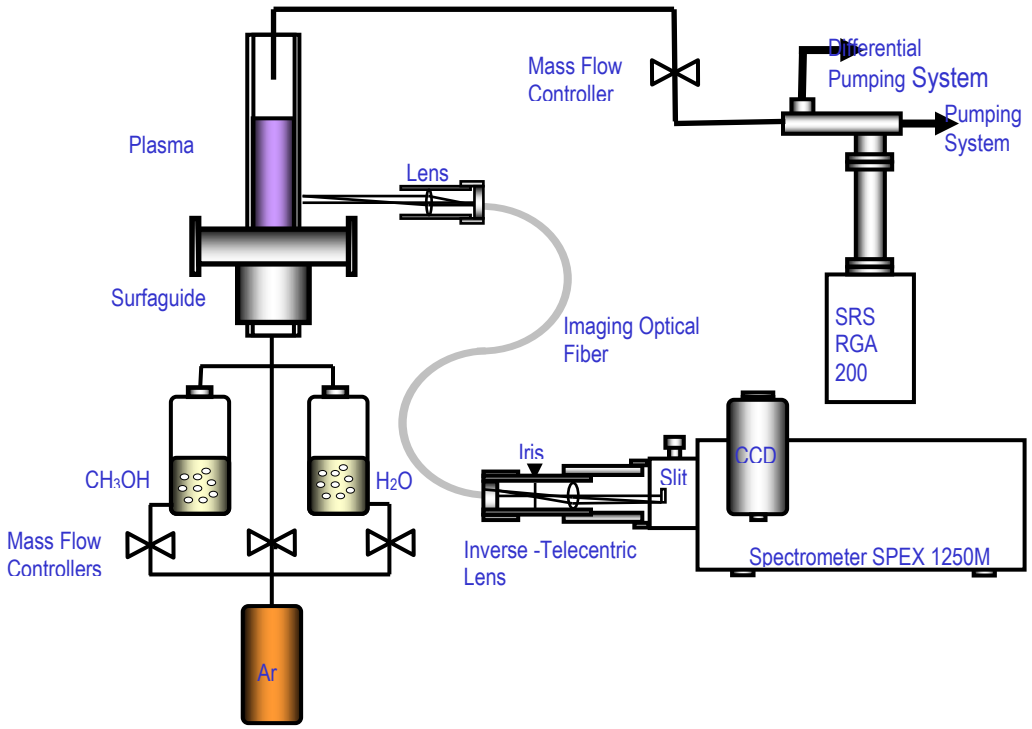

Figure 19.3 - Experimental setup

The influence of the fraction of Ar "bubbling flow" through the liquid methanol on the H_2 and CO partial pressures (at constant total Ar flow) (Figure 19.4). There is an increase of both partial pressures with the Ar fraction as far as H_2 and CO are the dissociation products of methanol according to the reaction: $CH_3OH \rightarrow 2H_2 + CO$.

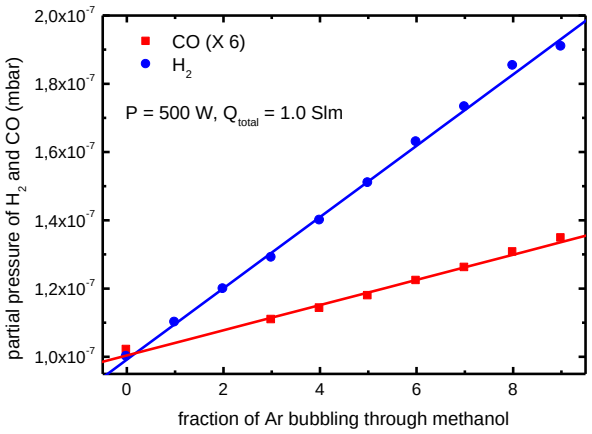

Figure 19.4 - Dependence of H_2 and CO production on the percentage (%) of Ar "bubbling flow" through the liquid methanol.

Obviously, H_2 production increases when Ar "bubbling flow" increases up to 9%. The same dependence for different total Ar flows is given in Figure 19.5. As seen, a small increase of hydrogen partial pressure is observed when the total Ar flow increases.

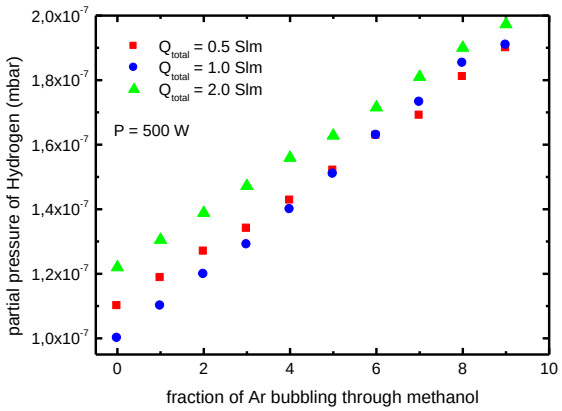

Figure 19.5 - H_2 pressure vs. (%) of "bubbling" Ar

The dependence of the H_2 flow on the power delivered to the launcher at constant total Ar flow (0.5 slm) and Ar "bubbling flow" (1%) is given in Figure 19.6. The dependence of H_2 flow on microwave power exhibits a sharp rise at nearly 300 W and then saturates at about 500 W. It should be noted that below 300 W the discharge is unstable, and distinct filaments appear.

The detected emission spectra demonstrate clearly an increase of the OH(A-X) band intensity when the percentage of methanol in the mixture is increased (Figure 19.7a). The emission of carbon atoms in the near UV range (240-300nm) indicates a significant increase with methanol amount in the mixture as seen in Figure 19.7b).

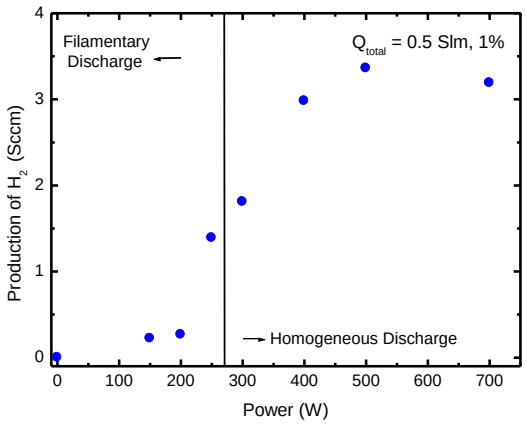

Figure 19.6 - H_2 flow dependence on the power.

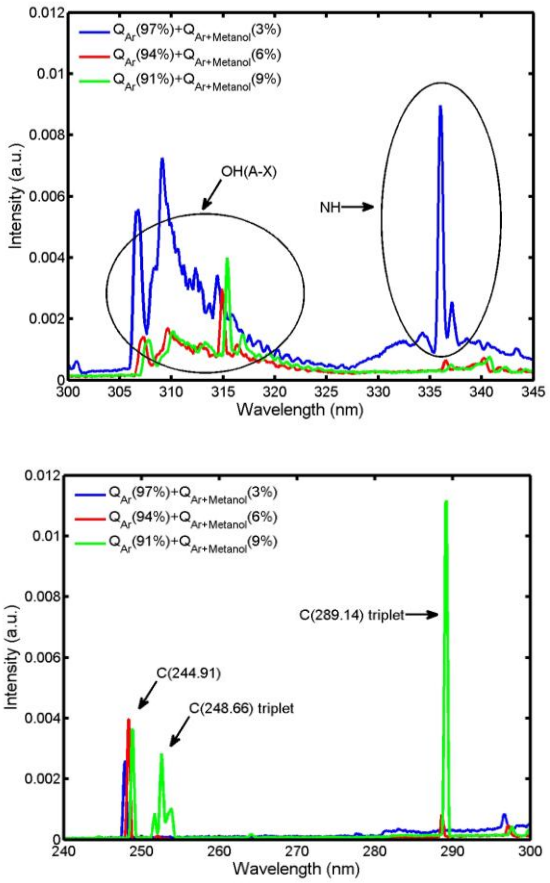

Figure 19.7 - Emission spectrum in (a) 300-345nm range and (b) 240-300 nm range.

19.3. HOT AND SUPER-HOT HYDROGEN ATOMS IN MICROWAVE PLASMA

Super-hot" (with kinetic energy ~ 4 - 8 eV) and "hot" (kinetic energy ~ 0.3 eV) hydrogen atoms were detected throughout the volume of a surface wave (500 MHz) generated H_2 plasma column, at pressure p = 0.01 mbar, from the analysis of the H_β, H_γ, H_δ, and H_ε emission line profiles. Population inversion between the levels 5→4 and 6→4 was detected. At pressure p = 0.2 mbar, super-hot atoms were not detected and the temperature of the hot atoms was found to increase with the upper level principal quantum number.

The surface wave discharge is created inside a Pyrex tube with internal and external radii of 2.25 cm and 2.5 cm, respectively, using a surfatron-based set-up (Figure 19.8). The microwave power, provided by a 500 MHz generator, was varied from 40 to 250 W. The background gas is injected into the tube at flow rates from 0.4 to 20 sccm under laminar gas flow conditions. The electron density decreases from about 2×10^{10} cm^{-3} at the beginning of the column to (1–2) × N_{cr} ($N_{cr} \approx 7\times10^{9}$ cm^{-3}) at its end. Calculated effective values of the microwave electric field intensity sustaining the discharge are in the range 1-7 V/cm. The temperature of the gas molecules was determined from measurements of the H_2 rotational temperature using the Q-branch of the Fulcher-α band [$d^3\Pi_u$ (v=0,1) → $a^3\Sigma_g^+$ (v=0,1)] in the 600 – 617 nm wavelength range. The measured profiles of the H_β, H_γ, H_δ, and H_ε lines are well fitted by single or two-Gaussian profiles (much better than by a Voigt profile). GRAMS/32® and Mat Lab-based software have both been used for this fitting.

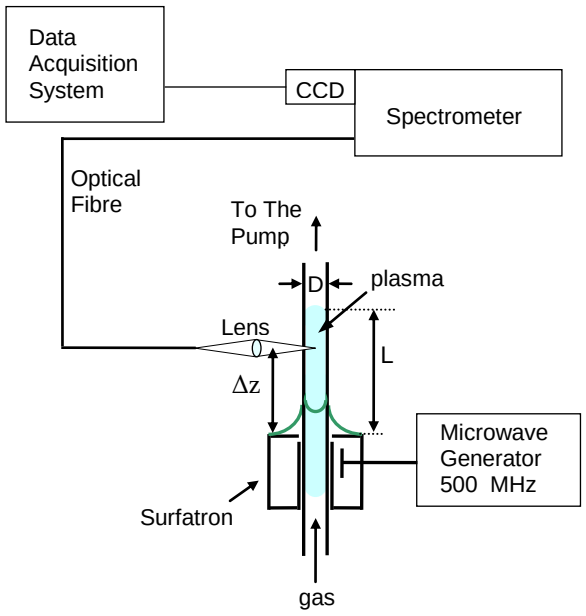

Figure 19.8 - Experimental setup

As a typical example, the H_δ and H_γ line profiles at axial distance Δz = 35 cm and pressure p = 0.01 mbar are shown in Figure 19.9. The H_β and H_ε line profiles have typically the same shape. Superimposed in Figure 18.9 are two Gaussian curves, a narrow and a broad one. These line profiles are symmetric with respect to the central wavelength. This type of spectrum reveals the existence of two groups of atoms, *viz.*, a "hot" group corresponding to the central peak, with a kinetic temperature of ~ 1,500 K (average kinetic energy ~ 0.2

eV), and a "super-hot" group corresponding to the broadened part, with a kinetic temperature of ~ 55,000 K (average kinetic energy ~ 8 eV).

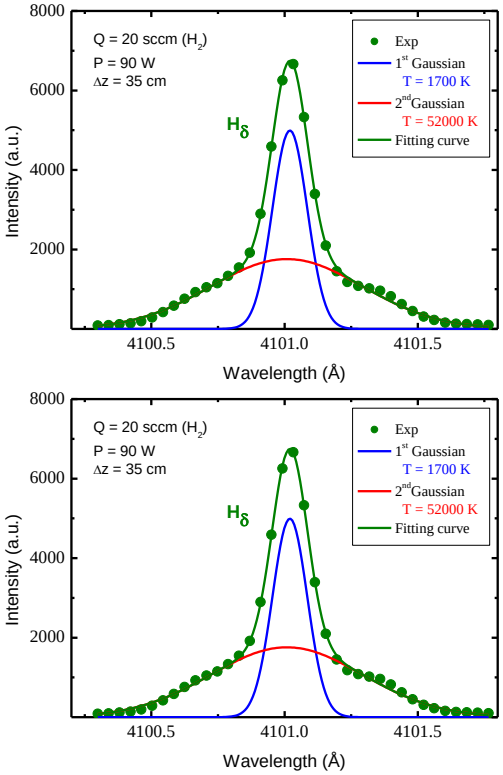

Figure 19.9 - Balmer lines emission profiles

The evolution of the Hγ line profile along the discharge is shown in Figure 19.10. The broader base starts to appear near the middle of the plasma column length and it expands towards the column end, where widely broadened wings are well established. The corresponding kinetic temperatures exhibit significant axial variations. The kinetic temperature of the super-hot component is ~ 25,000-30,000 K up to 20 cm axial distance and, then, steadily increases to ~ 60,000 K close to the end, at Δz = 40 cm, whereas the temperature corresponding to the sharp Gaussian peak decreases from ~ 1,800 K to ~ 1,400 K close to the end. The latter temperatures are about three times higher than the rotational temperature, which decreases from 600 K to 400 K along the plasma column. Note that the wall temperature, as measured by an infrared sensitive optical thermometer, is ~ 100 K below the rotational temperature.

Furthermore, *the radial variation of the Balmer line spectra has been investigated applying 2D imaging measurements.* To this end, a spectroscopic imaging system able to couple the plasma-emitted radiation into a SPEX 1250M spectrometer equipped with a nitrogen cooled CCD camera was used to measure radial profiles of emission intensities, and corresponding temperatures (Figure 19.11a,b) . Abel inversion has been applied to translate the side-on measurements to true radial profiles. The temperature of "hot" H atoms shows a small increase close to the wall while the "super hot" atoms temperature keeps approximately constant at about 50,300 K.

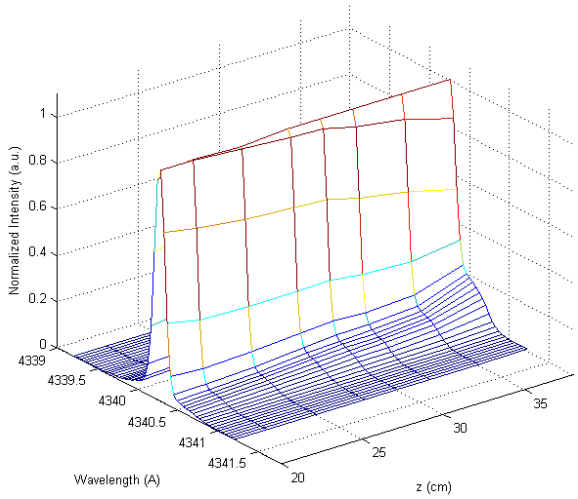

Figure 19.10 - Axial variation of Hγ line emission spectrum (p = 0.01 mbar; P = 90 W). The total discharge length is L = 45 cm.

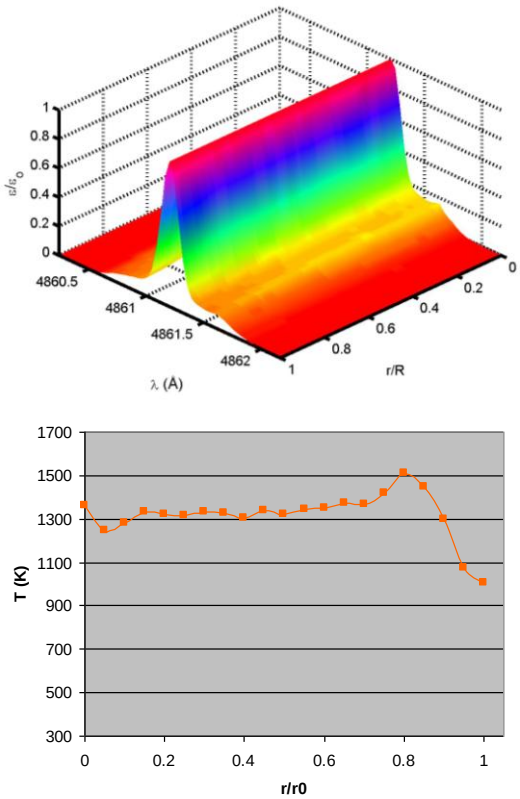

Figure 19.11 - Radial variation of (a) H_β line emission profile and (b) "hot" H atoms temperature..

The relative population distributions of the hot and super-hot components are shown in Figure 19.12(a,b) for Δz = 8 and 35 cm and 0.01 mbar pressure (the plot

represents the relative line intensity of each Gaussian component divided by the transition probability and the level degeneracy *vs.* the excitation energy of the level *n*). As seen, the super-hot component exhibits an inversion of population between the pairs of levels 5 - 4 and 6 – 4 away from the launcher, the same effect being not observed for the hot component. No population inversion is observed close to the launcher.

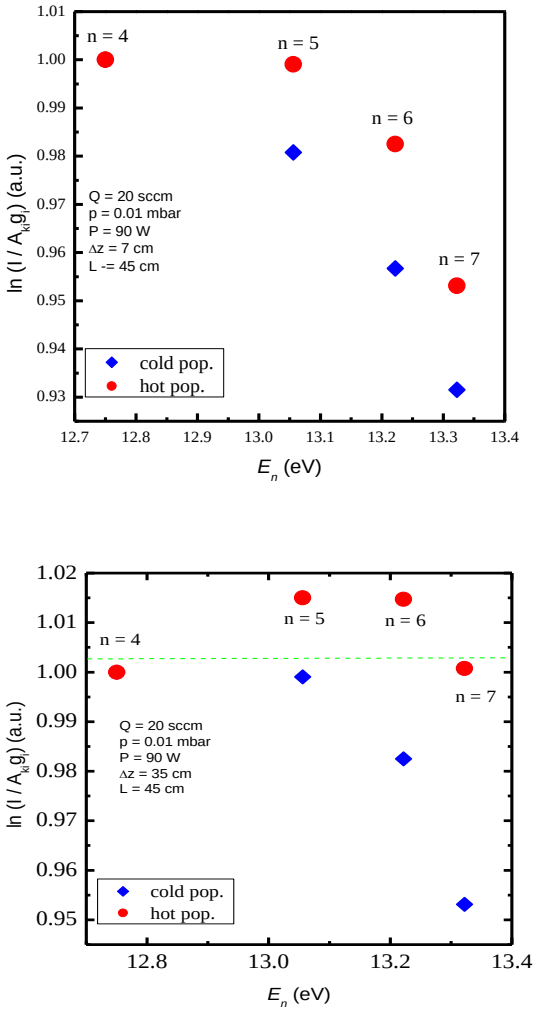

Figure 19.12 - Population distribution of "hot" and "super hot" at (a) Δz = 8 cm and (b) Δz = 35 cm.

When the pressure increases up to 0.2 mbar super-hot atoms disappear and the profiles become single-Gaussian. The temperatures of the single-Gaussian Balmer lines at 0.20 mbar and fixed distance increase with the upper level principal quantum number *n* as shown in Figure 19.13. This can not be due to the Stark effect. Linear Stark splitting caused by the microwave field somewhat broadens the Balmer lines [$n \rightarrow 2$] but estimations show this only introduces an error of ~ 5 – 50 K here. This increase in temperature with *n* can result from the generation of two groups of atoms by two different processes. The first one is dissociation by

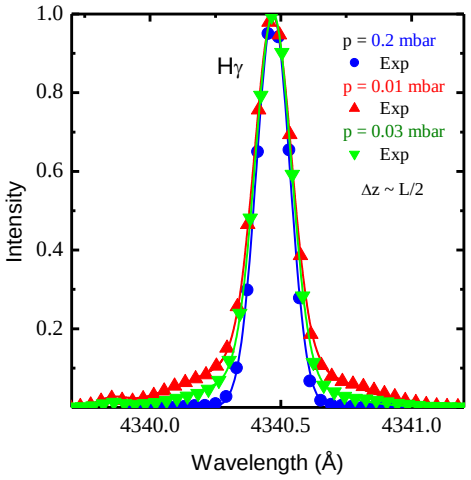

Figure 19.13 - Evolution of H_γ spectra with pressure.

electron impact with vibrationally excited molecules, which creates hot excited atoms: [H_2(X, v =1-4) + e $\rightarrow$ H_2^*(ε = 17 -19 eV) + e $\rightarrow$ H_{hot}(n=1) + H_{hot} (n=4-8) + e] (R1). Reactions (R1) are effective, due to the high electron and vibrational (T_{vib}) temperatures of H_2(X) molecules and the relatively large Frank-Condon coefficients. The second process is the excitation of "cold" atoms by direct electron impact: [H(1) +e $\rightarrow$ H($n\geq2$) +e] (R2). Therefore, two groups of radiating H (n>2) atoms are formed, with kinetic temperatures $T_{hot} \approx 0.32$ eV and $T_{cold} \approx T_{gas}$, respectively. The corresponding population distributions, N_n^{hot} and N_n^{cold}, have been calculated from a self-consistent model previously developed. The main radiative and collisional processes which populate and depopulate the various levels have been accounted for using a "single-quantum" approximation. The calculations show that the interplay of the relative contributions of (R1) and (R2) can produce an increase in the temperature of the ensemble (of both populations) when *n* increases. The sum of two Gaussian profiles, with no strong difference in temperatures T_{hot} and T_{cold} (at most a factor of ~ 8) and with different relative intensities, $I_n^{hot} = N_n^{hot}/(N_n^{hot} + N_n^{cold})$ and $I_n^{cold} = N_n^{cold}/(N_n^{hot} + N_n^{cold})$, can be approximated by a single Gaussian profile with an "ensemble" temperature, T_n, given by:

$$T_n = \left[\frac{\left(I_n^{hot}\right)^2}{T_{hot}} + \frac{\left(I_n^{cold}\right)^2}{T_{cold}} + 2\frac{I_n^{hot} \times I_n^{cold}}{\sqrt{T_{hot} T_{cold}}} \right]^{-1}$$

As I_n^{hot} increases from 0 to 1 T_n changes from T_{cold} to T_{hot}. Calculated kinetic temperatures of the levels n = 4-7 are shown in Figure 19.14 along with the experimental

ones.

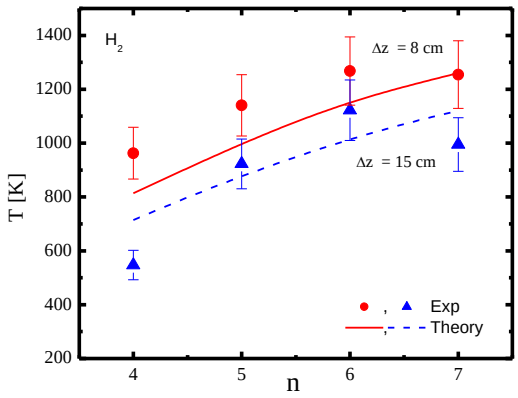

Figure 19.14 - Temperatures of H(n=4-7) vs upper level quantum number

20. NON-EQUILIBRIUM KINETICS AND SIMULATIONS OF PLASMAS AND AFTERGLOW PLASMAS[1]

C.M. Ferreira (Head), J. Loureiro (Principal Investigator), V. Guerra, P.A. Sá, C.D. Pintassilgo and M. Lino da Silva

20.1. INTRODUCTION

The research work carried out in 2009 falls into the following main lines of investigation:

- Kinetic modelling of low-pressure DC pulsed discharges in air;
- Simulation of Titan's atmosphere using a N_2 afterglow plasma with CH_4 addition in the post-discharge;
- Modelling of fundamental kinetic and radiative processes in low-pressure, high temperature plasmas;
- Study of Ar-O_2 and AR-O_2-N_2 afterglow plasmas for plasma sterilization and insight into elementary processes;
- Development of an Optical Emission Spectroscopy Diagnostic for electron density and temperature determinations

20.2. KINETIC MODELLING OF LOW-PRESSURE DC PULSED DISCHARGES IN AIR

A time-dependent kinetic model to study low-pressure (133 Pa and 210 Pa) pulsed discharges in N_2-O_2 for DC currents ranging from 20 to 80 mA, with a pulse duration in the range 0.1-1000 ms, has been developed. The model provides the temporal evolution of the heavy species along the pulse within this time interval. The coupling between vibrational and chemical kinetics has been also taken into account in the model. N_2-O_2 mixtures have also been the subject of our research in another specific situation in which oxygen is introduced in the post-discharge of a microwave discharge in pure N_2. This study includes a comparison with experimental measurements performed at the Laboratoire de Physique des Plasmas, Ecole Polytechnique, France and at Institute for Plasma Science and Technology, Greifswald, Germany.

20.3. SIMULATION OF TITAN'S ATMOSPHERE USING AN_2 AFTERGLOW PLASMA WITH CH_4 ADDITION IN THE POST-DISCHARGE

Titan's atmosphere using an afterglow plasma has been studied by considering a N_2 flowing microwave discharge with CH_4 addition in the post-discharge. Within this context, we have developed a kinetic model to simulate the afterglow of a flowing N_2 microwave discharge operating in the range 26.6-106.4 Pa, in which the methane is introduced downstream from the discharge with 2% percentage at 10^{-5}- 10^{-3} s. Also with the purpose of studying Titan's atmosphere we have started to develop a model describing capacitively coupled radio-frequency discharges in N_2-CH_4 mixtures. This second part of the work has been performed in collaboration with the Service d' Aéronomie from the University of Versailles St-Quentin, France.

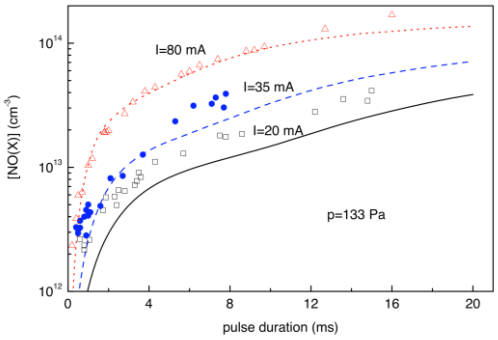

Figure 20.1 - Concentration of NO in a N_2-O_2 mixture.

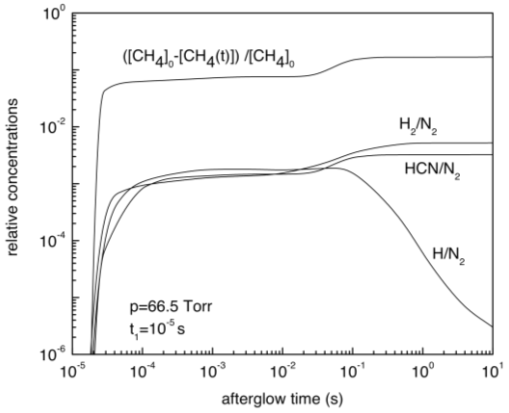

Figure 20.2 - Evolution of heavy particles in Titan's atmosphere.

20.4. MODELLING OF FUNDAMENTAL KINETIC AND RADIATIVE PROCESSES IN LOW-PRESSURE, HIGH TEMPERATURE PLASMAS

The research on the development of a multiquantum state-to-state model for the dissociation of nitrogen, with an emphasis on the effects of rotation, has been pursued. Namely, the influence of quasibound levels on the overall dissociation rate has been investigated. Quasibound levels are molecular levels which lie on a potential curve well, but also lie above the rotationless dissociation limit. In parellel, we pursued the development of a state-to-state model for O_2-O_2collisional dissociation, following the method previously developed for N_2-N_2 collisional dissociation.

[1]Activities performed in the frame of the Contract of Associated Laboratory, out of the Contract of Association EURATOM/IST, by IPFN staff of the Group of Gas Discharges and Gaseous Electronics.

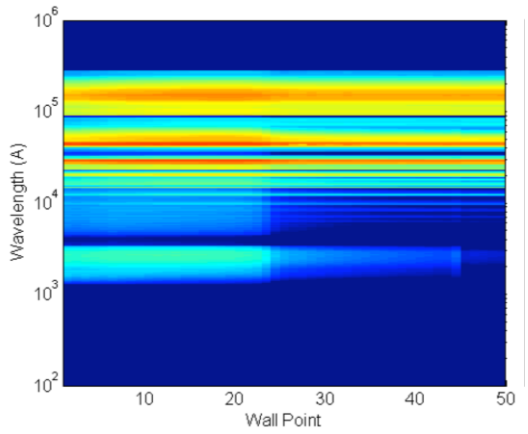

Figure 20.3 - Wall radiative heat flux for "Peak Dynamic Pressure" trajectory point in the EXOMARS spacecraft.

The other topic of research in this theme has been the atmospheric entry radiation. *A ray-tracing method allowing the calculation of the radiative heat fluxes impacting the walls of a spacecraft has been developped.* This model, coupled to the line-by-line in-house code SPARTAN, and its associated database, has been applied to: (i) the simulation of the radiation emitted from the entry of the NASA PHOENIX spacecraft, which was tracked by the European orbiter MARS EXPRESS; (ii) the entry of the future ESA EXOMARS spacecraft. In the scope of this last mission, the conclusions of our study were instrumental for the design of the spacecraft.

20.5. STUDY OF AR-O_2 AND AR-O_2-N_2 AFTERGLOW PLASMAS FOR PLASMA STERILIZATION AND INSIGHT INTO ELEMENTARY PROCESSES

Ar-O_2 plasmas are widely used in material processing and biomedical applications. For example, a post-discharge in Ar-O_2 has been successfully used as oxidizing media in deposition of oxide films, and the inactivation of bacterial spores have been achieved in the flowing afterglow of an Ar-O_2 microwave discharge. In Ar post-discharges the main sterilizing agents are believed to be the VUV photons (105-107 nm) emitted by the Ar atoms in the resonant states, whereas in Ar-O_2 mixtures this role is played by VUV photons and O atoms. In the Ar-O_2 system N_2 molecules can be also present as impurities, which makes possible the formation of UV emitting excited NO molecules. The enhanced UV emission in the Ar-O_2-N_2 can increase the sterilization efficiency of the system. As a matter of fact, the inactivation effectiveness of the Ar-O_2-N_2 ternary mixture has been recently investigated in a low pressure ICP discharge by Kylián et al.

The aim of our investigations is *to study the evolution of the densities of active species produced by flowing Ar-O_2 and Ar-O_2-N_2 microwave discharges in the discharge region and in the early-afterglow*, thus contributing to the understanding of the elementary processes occurring in these systems, in particular those responsible for plasma sterilization.

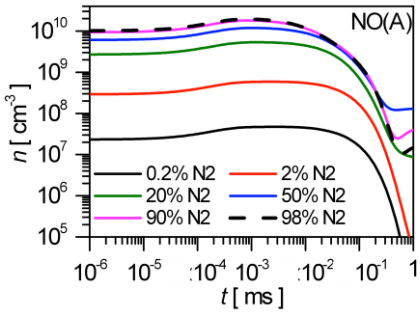

Figure 20.4 - Evolution of NO(A) in the afterglow of a discharge at f=2.45 GHz, p=2 Torr, with 2% of O_2.

20.6. DEVELOPMENT OF AN OPTICAL EMISSION SPECTROSCOPY DIAGNOSTIC FOR ELECTRON DENSITY AND TEMPERATURE DETERMINATIONS

A new method to experimentally determine the electron density (n_e) and the electron temperature (T_e) in the negative glow of a nitrogen pulsed discharge has been developed. The method is based on optical emission spectroscopy (OES) and consists on a variation and refinement of relatively similar schemes previously reported for different working conditions by other authors. The bottom line is the measurement of the emission intensities of the (0,0) bands of the first negative system at 391.44 nm and of the (0,2) bands of the second positive system at 380.49 nm.

The suggested procedure allows the establishment of the absolute values of n_e and T_e, as long as one calibration point is provided, such as the electron density at one specific discharge condition. If this calibration point is unavailable, the method nonetheless yields a qualitative dependence of T_e and n_e. Langmuir probe measurements confirmed and validate the OES results for n_e, thereby legitimizing the diagnostics technique developed. The interpretation of the results for T_e is slightly more complex, and in some circumstances an accurate determination of T_e may require further analysis.

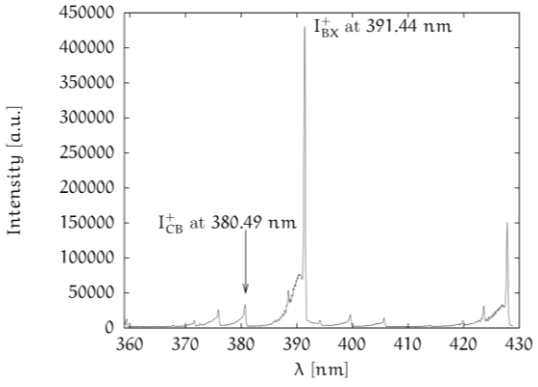

Figure 20.5 - Emission spectrum with the two bands of interest, for p=3.8 Torr, I=0.85 A, 6mm from the cathode.

21. MODELING OF PLASMA SOURCES[1]

C.M. Ferreira (Head), L.L. Alves (Principal Investigator), L. Marques, C. Pintassilgo, J. Gregório, J.S. Sousa and M. Santos.

21.1. INTRODUCTION

This project focuses on the modeling of different plasma sources, used in various applications (mainly with material processing and environmental control). The general goal is the *development of sophisticated simulation tools to describe and optimize, in an effective non-expensive way, the operation features of these plasma sources.*

In 2009, the staff of this project was reduced[2] which affected the execution and the scientific output of the project. The project contains the following research lines:

- Micro-plasma reactors;
- Microwave Micro-Plasma (MWMP) source;
- Micro-Cathode Sustained Discharge (MCSD);
- Microwave-driven plasma reactor operated by an axial injection torch;
- Capacitively coupled plasma reactor;
- Microwave discharges in nitrogen;
- Integrated Tokamak Modelling (ITM)[3].

21.2. MICRO-PLASMA REACTORS

We have continued to study atmospheric pressure micro-plasmas, created by electrical discharges in very small geometries (100's of microns) without glow-to-arc transition, in view of developing portable devices for flue gas treatment, biological decontamination or detection of heavy metal gaseous traces, in ambient air or aerosols.

21.3. MICROWAVE MICRO-PLASMA (MWMP) SOURCE

We have pursued studying an innovative plasma source for the production of atmospheric pressure micro-plasmas, in view of environmental applications. The device produces high-density (~10^{14}cm^{-3}), low-power (~10-100 W) plasmas in ambient air or in controlled environments (argon, helium), within the 50-200 µm end-gap of a microwave (2.45 GHz) microstrip-like line, by using a continuous wave excitation (thus ensuring a steady-state discharge regime). *A new source, corresponding to a standard microstrip line (Figure 21.1), was projected and built, yielding an improvement in power coupling.*

The MWMPs produced with these sources, and especially those produced in helium (as scheduled in the 2009-WP), were characterized experimentally using (i) electrical diagnostics of the power coupled to the sources, as a function of the gap size and of adjustable line lengths (with and without plasma, (Figure 21.2), allowing for the estimation of their quality factors; (ii) spatially-resolved emission spectroscopy measurements, to obtain rotational, vibrational and excitation temperatures (for helium, the rotational band of OH yielded T_{rot} ~ 350-550 K and the Boltzmann plot of emission lines indicated T_{exc} ~ 0.2-0.35 eV, for incident powers of 5-30 W); (iii) an imagery analysis (Figure 21.3), using a CCD camera coupled to an amplification system, to measure the volumes and to estimate the power densities with the different micro-plasmas (100 kW/cm^{-3} in air, 20 kW/cm^{-3} in helium, and 3 kW/cm^{-3} in argon).

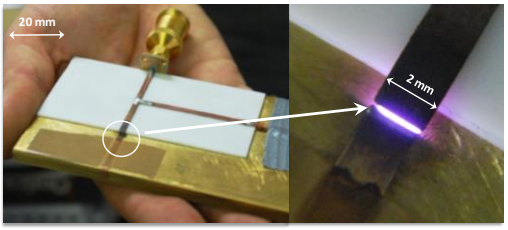

Figure 21.1 - Microscript line, producing an air plasma at 1W power.

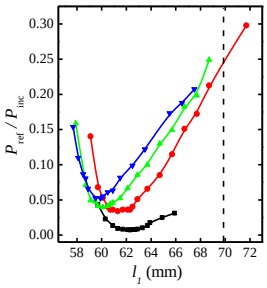

Figure 21.2 - Measured reduced reflected power, as a function of the adjustable transmission line-length, for a micro-wave source with plasma (at 50-µm gap size) and for the following coupled powers (in watts): 47 (black curve), 73 (red), 97 (green), and 125 (blue). The vertical broken line marks the value of l_1 obtained for the same source without plasma.

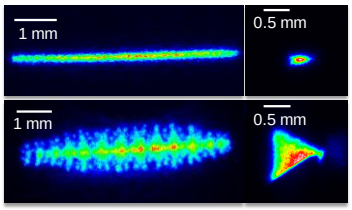

Figure 21.3 - Front view (left) and side view (right) of atmospheric pressure MWMPs in air (top, at 32 W coupled power) and in argon (down, at 13 W coupled power) for a 50 µm gap size.

[1]Activities performed in the frame of the Contract of Associated Laboratory, out of the Contract of Association Euratom/IST, by IPFN staff of the Group of Gas Discharges and Gaseous Electronics.
[2]After the departure of Dr. R. Alvarez.
[3]Work performed in collaboration with J.P. Bizarro et al (with the Group of Theory and Modelling, IPFN/IST, Lisbon, Portugal).

The MWMPs were also characterized, as a function of the axial electron density, gap size, and average gas temperature, using numerical simulation tools. These were (i) the commercial code CST Microwave Studio®, to obtain the distribution of the electromagnetic field within the sources (Figure 21.4); (ii) a one-dimensional stationary fluid code, applied to argon, coupling different calculation modules: transport, for charged particles and electron mean energy; electromagnetic, for the microwave field; kinetic, for the 4s argon species; and now also thermal (as scheduled in the 2009-WP), for neutral gas heating. The model predicts plasma power densities between 1–5 kW cm^{-3}, in good agreement with measurements for comparable work conditions (Figure 21.5).

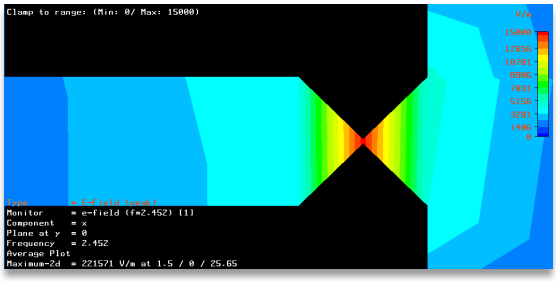

Figure 21.4 - Contour-plot of the modulus of the axial-component with the microwave electric field (CST-simulations).

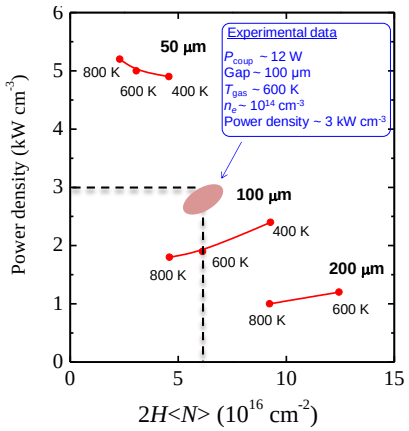

Figure 21.5 - Plasma power density, as a function of the product 'average gas density times gap size', calculated at $5x10^{13}$ cm^{-3} on-axis electron density, for different values of average gas temperatures and gap sizes. The oval region locates the measured power density.

21.4. MICRO-CATHODE SUSTAINED DISCHARGE (MCSD)

We continued our work on a micro-discharge reactor, which uses a micro-hollow cathode discharge (MHCD), running in $He/O_2/NO$ mixtures at atmospheric pressure, to generate a stable glow discharge of larger volume between the MHCD and a third electrode, placed at a distance of some mm's from the MHCD. This 3-electrode configuration is the so-called micro-cathode sustained discharge (MCSD), which is basically a positive column with low value of the reduced electric field (5-10 Td) and gas temperature (300-375 K). *We have now started using arrays of MCSDs (Figure 21.6) to enhance the production of intense fluxes of $O_2(a^1\Delta)$ metastables.*

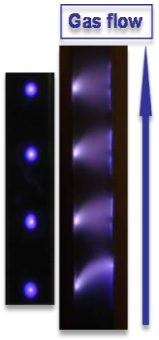

Figure 21.6 - Photo of an array of MCSDs.

As scheduled in the 2009-WP, *we have measured the gas temperature* (using the high resolution spectra of the O_2 atmospheric band at 760 nm), *the density of* $O_2(a^1\Delta)$ (using IR emission at 25cm downstream from the MCSD), *and the density profiles with* O_3 (using UV absorption spectroscopy) *and with O* (using TALIF spectroscopy measurements), *as a function of flux, gas mixture composition, and discharge current.* By using an array of MCSDs we have obtained $O_2(a^1\Delta)$ fluxes above 40 mmol/h, corresponding to densities higher than $4x10^{16}$ cm^3 (Figure 21.7). Arrays of MCSD, allowing the production at atmospheric pressure of $O_2(a^1\Delta)$ and O_3 densities between 10^{13} and 10^{16} cm^{-3}, with an easily tunable ratio, appear to be very useful tools to study in detail the reactivity of these species with DNA constituents. We have shown that Adenine, Thymine and Cytosine constituents are effectively oxidized by O_3, while $O_2(a^1\Delta)$ only reacts with 2'-deoxyguanosine (dGuo). A more detailed study on the reactivity of $O_2(a^1\Delta)$ and O_3 with aqueous DNA solutions is currently in progress.

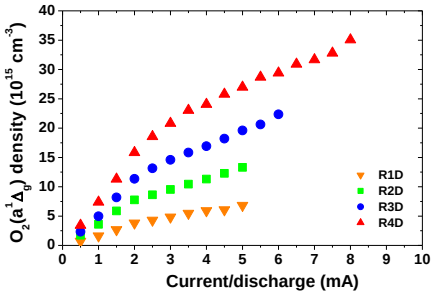

Figure 21.7 - Density of $O_2(a^1\Delta)$, as a function of the discharge current, obtained at atmospheric pressure for a gas mixture flow Q(He/O2/NO) = 10000/400/4.2 sccm, using arrays of MCSDs with 1 (orange curve), 2 (green), 3 (blue) and 4 (red) discharges.

21.5. MICROWAVE-DRIVEN PLASMA REACTOR OPERATED BY AN AXIAL INJECTION TORCH

We have continued analyzing a microwave-driven (2.45 GHz) plasma reactor (cylindrical chamber with 55 mm radius and 150 mm height), *operated by an Axial Injection*

Torch (AIT). The torch (connected to a coaxial waveguide with 5.3 mm and 14.5 mm inner and outer radii, respectively) creates atmospheric plasmas in different pure gases (argon, helium, nitrogen) or gas mixtures (e.g. air), over a wide range of powers (300−3,000 W) and flow-rates (0.5−13 L min^{-1}), producing very hot flows of plasma species (electron temperatures around 20,000 K and gas temperatures between 2,000−6,000 K). We began to study the transport of the radiation within the plasma created by the AIT-reactor device, using the radiative heat transfer equation in the Eddington (small anisotropy) approximation. Due to the lack of manpower, the work could not evolve towards new collaborations and applications (heat transfer, material deposition, bio-treatments), as announced in the 2009 Work Plan (WP).

21.6. CAPACITIVELY COUPLED PLASMA REACTOR

We have continued to study low-pressure (0.05-2 Torr) capacitively coupled radio-frequency (CCRF) nitrogen discharges (13.56 MHz), produced within cylindrical parallel-plate reactors (~6 cm radius and ~3-5 cm height). Our motivation is the analysis of the chemistry of Titan's atmosphere, using CCRF discharges in nitrogen / methane mixtures (for CH_4 concentrations up to 2%). These discharges are used to simulate the atmosphere of Titan at laboratory scale, by successfully producing, in gas phase, dust particles analogue to Titan's aerosols-tholins. Although the 2009-WP scheduled the modeling of N_2-CH_4 discharges, only N_2 plasmas were studied due to manpower limitations.

Simulations used a hybrid calculation code that solves a two-dimensional time-dependent fluid model (coupling the charged particle and the electron mean energy transport equations to Poisson's equation), which resort to lookup-tables for the electron parameters obtained from the two-term homogeneous electron Boltzmann equation (yielding the electron energy distribution function in the presence of inelastic and superelastic collisions, involving both electronically and vibrationally excited states), coupled to a quasi-homogeneous collisional-radiative model for the populations of electrons, positive ions N_2^+, and N_4^+, vibrationally excited ground-state molecules $N_2(X^1\Sigma_g^+$, v=0–45), and electronically excited molecules $N_2(A^3\Sigma_u^+$, $B^3\Pi_g$, $C^3\Pi_u$, $a^1\Sigma_u$, $a^1\Pi_g$, $w^1\Delta_u$, $a^1\Sigma_g^+$). We have initiated a modification of this simulation tool so as to ensure full coupling between its fluid and kinetic modules. Calculation results (Figure 21.8) were compared with new measurements of the electron density, the self-bias voltage, the power coupled, and the intensity of the radiative transitions with the first negative system [FNS-00, N_2^+(B,v=0)–N_2^+(X,v=0)] and the second positive system [SPS-02,N_2(C,v=0)–N_2(B,v=2)], at various pressures and coupled powers (Figure 21.9). As scheduled in the 2009-WP, we have updated some mechanisms with the nitrogen kinetics, in order to quantitatively reproduce spectroscopic measurements.

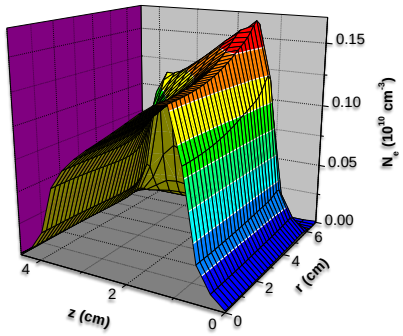

Figure 21.8 - Time-average spatial profile of the electron density for the CCRF discharge, at 10W coupled power and 0.5mbar pressure.

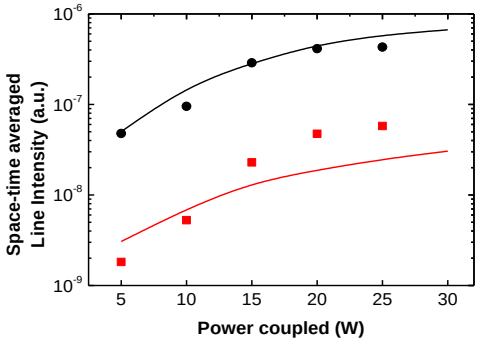

Figure 21.9 - Calculations (curves) and measurements (points) of the space-time average line-intensity transitions with the first negative system (red) and the second positive system (black) of nitrogen plasma produced by a CCRF discharge, as a function of the power coupled, at 1.5mbar pressure.

21.7. MICROWAVE DISCHARGES IN NITROGEN

By combining optical emission spectroscopy (OES) measurements with a non-equilibrium kinetic model, describing the intensity of the observed radiative transitions, one obtains a powerful diagnostic tool for the electron density and temperature with a plasma. We have analyzed the line intensities with the FNS-00 [N_2^+(B,v=0)–N_2^+(X,v=0) at 391.4 nm] and the SPS-25 [N_2(C,v=2)–N_2(B,v=5) at 394.3 nm] of nitrogen plasmas, produced by low-pressure (0.3-0.7 Torr) surface-wave (2.45 GHz) discharges, within a 8 mm diameter quartz tube, at ~55 W power and ~100 mm axial length. OES diagnostics use an optical fiber coupled to a 0.5m focal monochromator, equipped with a 1200 grooves/mm grating (0.2nm spectral resolution and 185-930 nm spectral sensitivity). The kinetic model is essentially the same used in the study of CCRF discharges, which now further includes the N(^{4}S, ^{2}D, ^{2}P) atomic states and the N_2^+(X,B) ion states. The evolution of the line intensities, with variations in the electron density and the gas pressure (Figure 21.10), was used as guideline to propose a correction upon some model parameters, and so ensure a very good comparison between calculation results and optical measurements (for electron densities ~4-7x10^{11} cm^{-3} and temperatures ~3 eV).

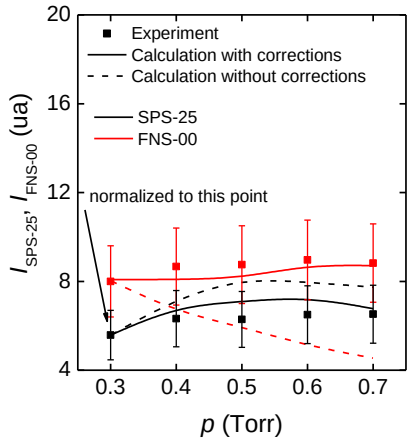

Figure 21.10 - Calculations (curves) and measurements (points) of the line-intensity transitions with the first negative system (red) and the second positive system (black) of nitrogen plasma produced by a surface-wave discharge, as a function of pressure, at 4-7x10^{11}cm^{-3} electron densities (corresponding to 4-7 W cm^{-1} powers per unit length).The solid (dashed) curves are the result of simulations with (without) model corrections.

21.8. INTEGRATED TOKAMAK MODELLING (ITM)

As announced in the 2009-WP, we started to participate in some Integrated Tokamak Modeling (ITM-EFDA) tasks, related with the development of Consistent Physical Objects (CPOs) and with the Verification and Validation (V&V) of case-study solutions for the European Transport Solver (ETS) code. In particular, we have collaborated in:

- *Development of a schema/xsd and of the corresponding xml file to describe a set of V&V tests;*
- *Development of a Python script for automatic generation of ETS xml input files from a V&V xml description;*
- *Development of an ETS V&V test version based on the solver_test and the new eq_ets_test version (August 2009), that reads ETS V&V input data files.*

22. QUANTUM PLASMAS[1]

J.T. Mendonça (Head), A.M. Martins, D. Resendes, S. Mota, H. Terças.

22.1. INTRODUCTION

Our main activities during this year focusing on the study of the properties of cold atoms con_ned in magneto-optical traps (MOT). Our work consists in *both theoretical and experimental investigations of the collective effects of cold atoms that are due to the multiple scattering of light, which is responsible for the occurrence of long-range interactions in those systems.* Although these effects have been identified among the physicists as one of the most critical mechanisms that prevents atoms of cooling further, a very reduced effort has been put within the atom physics community to better understand and describe their physical properties. *Based on hydrodynamical and kinetic theories, we propose a powerful and interdisciplinary approach to the collective properties of these systems. We also explore the analogies between plasmas and Bose-Einstein condensates.*

22.2. DRIVEN INSTABILITIES IN MAGNETO-OPTICAL TRAPS

In a previous work, we have suggested that a the atoms confined in MOTs can be regarded as a one-component plasma, where the effective charge is due to the multiple scattering of light and is given in terms of the basic parameters of the trap. *We make use of such an interesting analogy and establish a model to describe an instability mechanism that had been reported experimentally in the past.* Our model describes the coupling between two fundamental hydrodynamical modes of the system: the center-of-mass (or dipole) oscillation, ω_{CM}, and the plasma oscillation, ω_P . The dynamics of this coupling is mastered by the following equation:

$$\frac{d^2A_2}{dr^2} + \left[\nu + 2\varepsilon\cos(2r)\right]A_2 + \varepsilon\sin(2r)\frac{dA_2}{dr} = 0, \qquad (1)$$

where $\xi=2u_1\bullet\nabla\ln B_2$ is a free coupling parameter and describes the amplitude of the center-of-mass oscillation. Here, $2r=\omega_{CM}\ t+\phi$, $\nu=4\omega^2_p/\omega^2_{CM}$ and $\varepsilon=\xi/\omega_{CM}$ are dimensionless variables. Describing the parameters of the dynamics in terms of the basic MOT parameters (the detuning δ and magnetic field gradient ∇B), we naturally recover the stability criteria for what had been identified as a "self sustained oscillation", illustrated in Figure 22.1. Our results suggest that the instability may be rooted in a parametric excitation of the plasma frequency, that become unstable for sufficiently large modulations of the center-of-mass oscillation.

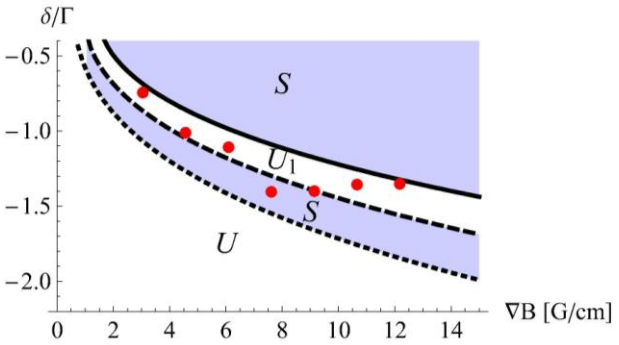

Figure 22.1 - The shadowed (light) regions are stable (unstable). The red dots represent the experimental threshold.

22.3. TWO-STREAM INSTABILITY INBOSE-EINSTEIN CONDESATES

Motivated by the experimental realization of collisions between two clouds of Bose-Einstein condensates, *we proposed that an instability mechanism may explain the formation of patterns in the scattering images.* We use a quantum kinetic description of the Bose-Einstein condensate and derive the following transport equation:

$$i\hbar\left(\frac{\partial}{\partial t}+\frac{\hbar}{m}k.\nabla\right)W = \int\frac{dq}{(2\pi)^3}\int\frac{d\Omega}{2\pi}V(q,\Omega) \times\left[W_- - W_+\right]\exp\left(-i\Omega t + iq.r\right)) \qquad (2)$$

where $W_\pm=W(\omega\pm\Omega/2, k\pm q/2)$ and

$$V(q,\Omega = \int dr\int dt V(r,t)\exp(-iq.r+i\Omega t) \qquad (3)$$

stands for the double Fourier transform of the total potential $V = V_0 +V_{SC}$. After linearization, we can obtain the following dispersion relation for the sound waves (also referred to as Bogoliubov waves) in the two-stream configuration

$$1-\frac{K^2}{2}\left\{\frac{1}{\beta^2\left(\tilde{\Omega}+K\right)^2-K^4}+\frac{1}{\beta^2\left(\tilde{\Omega}+K\right)^2-K^4}\right\}=0 \qquad (4)$$

where we have defined the normalized quantities $\Omega=\Omega/\omega_0$, $K = hq/mu_B$, and the dimensionless parameter $\beta= v_0/u_B$. Here, $\omega_0= u_Bk_0$ represents the 'resonance' frequency. The parameter β defines a sonic number, the Mach number at T=0. It measures if the beam flow is either subsonic ($\beta< 1$) or supersonic ($\beta>1$). Figure 22.2 shows the growing rates fro different values of the parameter β.

[1]Activities performed in the frame of the Contract of Associated Laboratory, out of the Contract of Association Euratom/IST, by IPFN staff of the Group of Lasers and Plasmas.

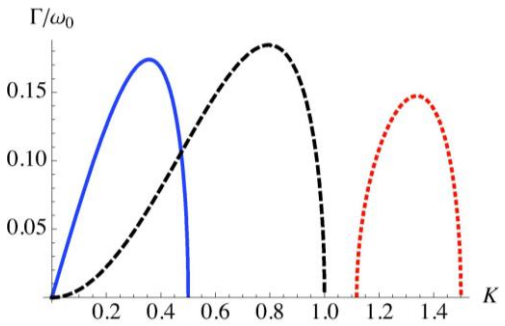

Figure 22.2 - (Color Online) Normalized wave growth rate $\Gamma=Im(\Omega)/\omega_0$, for different values of β. Blue full line, $\beta=0.5$, black dashed line, $\beta=1.0$, and red dotted line, $\beta=1.5$. The maximum growth rate, corresponding to the most unstable mode, occurs for $\beta=1$ and $K\approx0.8$.

23. FUNDAMENTAL PHYSICS IN SPACE[1]

L.O. Silva (Head), O. Bertolami (Deputy Head), T. Barreiro, C. Carvalho, A.M. Martins, J. Paramos, C. Bastos.

23.1. INTRODUCTION

The research activity of this project was focused in 2009 on:

- Generalized *f*(R) theories;
- Non-commutative quantum mechanics and cosmology;
- Unparticle and ungravity physics;
- Mass-varying models;
- Experiments in space.

23.2. GENERALIZED *F*(R) THEORIES

Generalized *f*(R) theories present an extension to General Relativity, where the space-time curvature displays a non-minimal coupling to matter, together with a non-linear pure curvature term in the action functional.

The fundamental issues of stability and the validity of the strong, weak, dominant and null energy conditions were addressed, and it was shown that this theory satisfies these physical requisites for suitable forms of the non-trivial terms involving the curvature. Furthermore, through the modified dynamics ensuing from this non-minimal gravitational coupling, it was shown that known dark matter density profiles may be mimicked, thus explaining the flattening of the galaxy rotation curves.

23.3. NON-COMMUTATIVE QUANTUM MECHANICS AND COSMOLOGY

Another interesting prospect lies in the possibility of quantum effects arising due to the manifestation of a meaningful non-commutative quantum mechanics. *Several work was developed within this context, including the formulation of a non-commutative cosmology, stability conditions for a non-commutative scalar field coupled to gravity, the study of the structure of black holes and the study of astrophysical objects such as main-sequence stars, white dwarfs and neutron stars in a noncommutative context.*

23.4. UNPARTICLE AND UNGRAVITY PHYSICS

Recently, the possibility of the existance of a "hidden" sector of scale-invariant particles within the Standard Model was advanced: the so-called Unparticles. A possible gravitational coupling of these novel particles leads to corrections to the gravitational field, adequately dubbed as Ungravity.

The effect of this hypothetical modification of gravitation was studied in the context of the available solar observables, with competitive constraints obtained for the fundamental parameters of the theory. Further constraints on Unparticle long range forces were obtained from Big Bang nucleosynthesis bounds on the variation of the gravitational coupling.

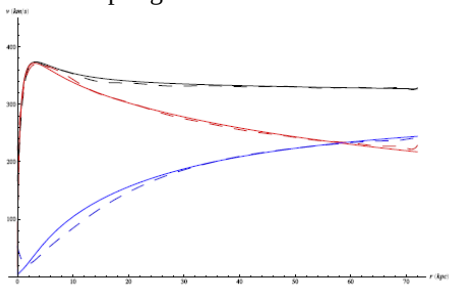

Figure 23.1 - NGC 5846 galaxy rotation curve with fit (dashed) arising from a power-law coupling of matter with curvature.

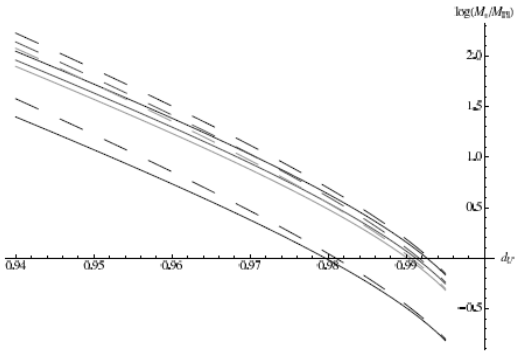

Figure 23.2 - Bounds on the characteristic Ungravity mass scale as a function of the scaling dimension, derived from solar observables

23.5. MASS-VARYING MODELS

The implications of the existence of mass-varying particles or fields was also addressed, including its stability and thermodynamic conditions.

23.6. EXPERIMENTS IN SPACE

Our group has also remained involved in the interesting prospect of *conducting experiments in space to test the fundamental underlying principles of physics,* including tests of General Relativity, Lorentz invariance, Equivalence Principle and confirming the observed anomalous acceleration of the Pioneer 10 and 11 spacecraft. This drives our *participation in the international collaboration in the Gravity Advanced Package* team, which aims to design an instrument package to be

Flown onboard a outer Solar System mission. Other possibilities were also addressed, including *the feasibility of resorting to the Galileo Navigation Satellite System to probe gravity or instaling a fundamental physics instrument on the International Space Station.*

[1]Activities performed in the frame of the Contract of Associated Laboratory, out of the Contract of Association Euratom/IST, by IPFN staff of the Group of Lasers and Plasmas.

24. PUBLICATIONS, LABORATORIAL PROTOTYPES, PRIZES AND AWARDS

24.1. MAGNETIC FUSION

24.1.1. Publications in Books

- Varandas C., *"Contribuições da energia nuclear para uma sociedade sem CO_2",* A energia da razão por uma sociedade com menos CO_2, F. Ramôa Ribeiro (Coord), Universidade Técnica de Lisboa/Gradiva Publicações, S.A., pag. 103, 2009.

24.1.2. Publications in refereed scientific journals (publications in ISI)

- Abel IG, BN Breizman, SE Sharapov and JET-EFDA contributors *"Resonant excitation of shear Alfvén perturbations by trapped energetic ions in a tokamak",* Physics of Plasmas, 16, 102506, 2009

- Alonso J.A., P. Andrew, A. Neto, J.L. de Pablos, E. de la Cal, H. Fernandes, W. Fundamenski, C. Hidalgo, G. Kocsis, A. Murari, G. Petravich, R.A. Pitts, L. Rios, C. Silva and EFDA-JET contributors, *"Fast visible imaging of ELM-wall interactions on JET"*, J. Nucl. Materials, 390-391 (2009) 797

- Araújo T. and R. Vilela Mendes, *"Innovation and self-organization in a multi-agent model"* Advances in Complex Systems 12, 233 (2009)

- Baranov Yu F, I Jenkins, B Alper, CD Challis, S Conroy, V Kiptily, J Ongena, S Popovichev, P Smeulders, E Surrey, K-D Zastrow and JET-EFDA contributors *"Anomalous and classical neutral beam fast ion diffusion on JET",* Plasma Physics and Controlled Fusion, 51, 4, 044004, 2009

- Bonheure G., J. Mlynar, A. Murari, C. Giroud, P. Belo, L. Bertalot, S. Popovichev and JET-EFDA Contributors, *"A novel method for trace tritium transport studies",* Nuclear Fusion 49, 085025 (2009)

- Briolle F., R. Lima, V. I. Man'ko and R. Vilela Mendes, *"A tomographic analysis of reflectometry data I: Component factorization";* Measurement Science and Technology 20, 105501 (2009)

- Briolle F., R. Lima and R. Vilela Mendes, *"Tomographic analysis of reflectometry data II: the phase derivative"* Measurement Science and Technology 20, 105502 (2009)

- Carlen E. and R. Vilela Mendes, *"Signal reconstruction by random sampling in chirp space"* Nonlinear Dynamics 56, 223 (2009)

- Cipriano F., H. Ouerdiane and R. Vilela Mendes, *"Stochastic solution of a KPP-type nonlinear fractional differential equation",* Fractional Calculus and Applied Analysis 12, 47 (2009)

- Chapman IT, CG Gimblett, MP Gryaznevich, TC Hender, DF Howell, YQ Liu, SD Pinches and JET EFDA Contributors *"Stability of the resistive wall mode in JET",* Plasma Physics and Controlled Fusion, 51, 5, 055015, 2009

- Chankin AV, DP Coster, G Corrigan, SK Erents, W Fundamenski, A Kallenbach, K Lackner, J Neuhauser, R Pitts, the ASDEX Upgrade Team and JET-EFDA Contributors *"Fluid code simulations of radial electric field in the scrape-off layer of JET",* Plasma Physics and Controlled Fusion, 51, 6, 065022, 2009

- Coelho R. and D. Alves, "*Real time Lock-in amplifier implementation using a Kalman filter for quasi-periodic signal processing in fusion plasma diagnostics"*, IEEE Trans. Plasma Science 37, 164, (2009)

- Coelho R. and D. Alves, "*Real-time data processing and magnetic field pitch angle estimation of the JET motional Stark effect diagnostic based on Kalman filtering"*, Rev. Sci. Instrum. 80, 063504, (2009)

- Crombé K, Y Andrew, TM Biewer, E Blanco, PC de Vries, C. Giroud, NC Hawkes, A Meigs, T Tala, M von Hellermann, K-D Zastrow and JET EFDA Contributors *"Radial electric field in JET advanced tokamak scenarios with toroidal field ripple",* Plasma Physics and Controlled Fusion, 51, 5, 055005, 2009

- Eester Van D, E Lerche, Y Andrew, TM Biewer, A Casati, K Crombé, E de la Luna, G Ericsson, R Felton, L Giacomelli, C Giroud, N Hawkes, C Hellesen, A Hjalmarsson, E Joffrin, J Källne, V Kiptily, P Lomas, P Mantica, A Marinoni, M-L Mayoral, J Ongena, M-E Puiatti, M Santala, S Sharapov, M Valisa and JET-EFDA contributors *"JET (^{3}He)-D scenarios relying on RF heating: survey of selected recent experiments",* Plasma Physics and Controlled Fusion, 51, 4, 044007, 2009

- Ekedahl A, K Rantamäki, M Goniche, J Mailloux, V Petrzilka, B Alper, Y Baranov, V Basiuk, P Beaumont, G Corrigan, L Delpech, K Erents, G Granucci, N Hawkes, J Hobirk, F Imbeaux, E Joffrin, K Kirov, T Loarer, D McDonald, MFF Nave, I Nunes, J Ongena, V Parail, F Piccolo, E Rachlew, C Silva, A Sirinelli, M Stamp, K-D Zastrow and JET-EFDA contributors *"Effect of gas injection during LH wave coupling at ITER-relevant plasma-wall distances in JET"*, Plasma Physics and Controlled Fusion, 51, 4, 044001, 2009

- Eriksson L-G, T Hellsten, MFF Nave, J Brzozowski, K Holmström, T Johnson, J Ongena, K-D Zastrow and JET-EFDA contributors *"Toroidal rotation in RF heated JET plasmas",* Plasma Physics and Controlled Fusion, 51, 4, 044008, 2009

- Estrada T, T Happel, L Eliseev, D López-Bruna, E Ascasíbar, E Blanco, L Cupido, J M Fontdecaba, C Hidalgo, R Jiménez-Gómez, L Krupnik, M Liniers, M E Manso, K J McCarthy, F Medina, A Melnikov, B van Milligen, M Ochando, I Pastor, M Pedrosa, F L Tabarés, D Tafalla and TJ-II Team, "Sheared flows and transition to improved confinement regime in the TJ-II stellarator", *Plasma Physics and Controlled Fusion, 51 12 4015 (2009).*

- Ford OP, J. Svensson, A Boboc, DC McDonald and JET EFDA contributors *"Experimental verification of relativistic finite temperature polarimetry effects at JET",* Plasma Physics and Controlled Fusion, 51, 6, 065004, 2009

- Gomes R.B., H. Fernandes, C. Silva, A. Sarakovskis, T. Pereira, J. Figueiredo, B. Carvalho, A. Soares, P. Duarte, C. Varandas, O. Lielausis, A. Klyukin, E. Platacis, I. Tale, A. Alekseyv, "*Liquid gallium jet–plasma interaction studies in ISTTOK tokamak"*, J. Nucl. Materials, 390-391, 938, 2009

- Goniche M, A Ekedahl, J Mailloux, V Petrzilka, K Rantamäki, P Belo, G Corrigan, L Delpech, K Erents, P Jacquet, K Kirov, M-L Mayoral, J Ongena, C Portafaix, M Stamp, K-D Zastrow and JET EFDA contributors *"SOL characterization and LH coupling measurements on JET in ITER-relevant conditions",* Plasma Physics and Controlled Fusion, 51, 4, 044002, 2009

- Gryaznevich M., G. Van Oost, P. Peleman, J. Brotankova, R. Dejarnac, E. Dufkova, I. Ďuran, M. Hron, J. Sentkerestiova, J. Stöckel, V. Weinzettl, J. Zajac, L.A. Berni, E. Del Bosco, J.G. Ferreira, F.J.R. Simões, M. Berta, D. Dunai, B. Tál, S. Zoletnik, A. Malaquias, G. Mank, H. Figueiredo, Y. Kuznetsov, L. Ruchko, H. Hegazy, A. Ovsyannikov, E. Sukhov, G.M. Vorobjev, N. Dreval, A. Singh, V. Budaev, G. Kirnev, N. Kirneva, B. Kuteev, A. Melnikov, D. Nurov, M. Sokolov, V. Vershkov, A. Talebitaher, P. Khorshid, R. Gonzales, I. El Chama Neto, A.W. Kraemer-Flecken, V. Soldatov, B. Brotas, P. Carvalho, R. Coelho, A. Duarte, H. Fernandes, J. Figueiredo, A. Fonseca, R. Gomes, I. Nedzelski, A. Neto, G. Ramos, J. Santos, C. Silva, D. Valcárcel, C.R. Gutierrez Tapia, L.I. Krupnik, L. Petrov, M. Kolokoltsov, J. Herrera, M. Nieto-Perez, A. Czarnecka, P. Balan, A. Sharnin and V. Pavlov, "*Results of Joint Experiments and other IAEA activities on research using small tokamaks"*, Nucl. Fusion 49 (2009) 104026

- Hidalgo C., M. A. Pedrosa, C. Silva, D. Carralero, E. Ascasibar, B. A. Carreras, T. Estrada, F. Tabares, D. Tafalla, J. Guasp, M. Liniers, A. Lopez-Fraguas, B. van Milligen and M. A. Ochando, "*Multi-scale physics mechanisms and spontaneous edge transport bifurcations in fusion plasmas"*, Europhys. Lett., 87 (2009) 55002

- Hoang G. T., A. Bécoulet, J. Jacquinot, J. F. Artaud, Y. S. Bae, B. Beaumont, J. H. Belo, G. Berger-By, J. P. S. Bizarro, P. Bonoli, M. H. Cho, J. Decker, L. Delpech, A. Ekedahl, J. Garcia, G. Giruzzi, M. Goniche, C. Gormezano, D. Guilhem, J. Hillairet, F. Imbeaux, F. Kazarian, C. Kessel, S. H. Kim, J. G. Kwak, J. H. Jeong, J. B. Lister, X. Litaudon, R. Magne, S. Milora, F. Mirizzi, W. Namkung, J. M. Noterdaeme, S. I. Park, R. Parker, Y. Peysson, D. Rasmussen, P. K. Sharma, M. Schneider, E. Synakowski, A. Tanga, A. Tuccillo and Y. X. Wan, *"A lower-hybrid current drive system for ITER",* Nuclear Fusion 49, 075001 (2009)

- Kiptily V.G., C.P. Perez von Thun, S.D. Pinches, S.E. Sharapov, D. Borba, F.E. Cecil, D. Darrow, V. Goloborod'ko, T. Craciunescu, T. Johnson, F. Nabais**,** M. Reich, A. Salmi, V. Yavorskij, M. Cecconello, G. Gorini, P. Lomas, A. Murari, V. Parail, S. Popovichev, G. Saibene, R. Sartori, D.B. Syme, M. Tardocchi, P. de Vries, V.L. Zoita and JET-EFDA Contributors; *"Recent progress in fast ion studies on JET";* Nuclear Fusion 49, 065030 (2009)

- Kirov KK, M-L Mayoral, J Mailloux, Yu Baranov, L Colas, A Ekedahl, K Erents, M Goniche, A Korotkov, P Morgan, V Petrzilka, J Ongena, K Rantamäki, M Stamp and JET EFDA contributors *"Effects of ICRF induced density modifications on LH wave coupling at JET",* Plasma Physics and Controlled Fusion, 51, 4, 044003, 2009

- Krasilnikov AV, D Van Eester, E Lerche, J Ongena, VN Amosov, T Biewer, G Bonheure, K Crombe, G Ericsson, B Esposito, L Giacomelli, C Hellesen, A Hjalmarsson, S Jachmich, J Kallne, Yu A Kaschuck, V Kiptily, H Leggate, J Mailloux, D Marocco, M-L Mayoral, S Popovichev, M Riva, M Santala, M Stamp, V Vdovin, A Walden and JET EFDA Task Force Heating and JET EFDA contributors *"Fundamental ion cyclotron resonance heating of JET deuterium plasmas",* Plasma Physics and Controlled Fusion, 51, 4, 044005, 2009

- Kurinskiy P., V. Chakin, A. Moeslang, R. Rolli, A. A. Goraieb, H. Harsch, E. Alves, N. Franco, *"Characterisation of titanium beryllides with different microstructure"*, Fusion Engineering and Design, Volume: 84, Issue: 7-11,Pages: 1136-1139, 2009

- Lerche E, D Van Eester, A Krasilnikov, J Onjena, P Lamalle and JET EFDA contributors *"Modelling of D majority ICRH at JET: impact of absorption at the Doppler-shifted resonance",* Plasma Physics and Controlled Fusion, 51, 4, 044006, 2009

- Lehnen M., S.S. Abdullaev, G. Arnoux, S.A. Bozhenkov, M.W. Jakubowski, V.V. Plyusnin, R. Jaspers, V. Riccardo, U. Samm, JET EFDA Contributors, The TEXTOR Team, "*Runaway generation during disruptions in JET and TEXTOR",* J. Nucl. Materials, 390-391 (2009) 740

- Martins J. F., J. A. Dente, A. J. Pires and R. Vilela Mendes, *"From controlled dynamical systems to context-dependent grammars: A connectionist approach"*, Engineering Applications of Artificial Intelligence 22,192-200, (2009)

- Murari A., J. Vega, G. Vagliasindi, J.A. Alonso, D. Alves, R. Coelho, S. DeFiore, J. Farthing, C. Hidalgo, G.A. Rattá, JET-EFDA Contributors, "*Recent developments in data mining and soft computing for JET with a view on ITER",* Fusion Engineering and Design 84, 1372 (2009)

- Nedzelskiy I.S., C. Silva, H. Fernandes, C. Hidalgo, *"Retarding field energy analyzers for ion temperature*

measurements in the boundary plasmas of the tokamak ISTTOK and TJ-II stellarator", Problems of At. Science and Tech. (Plasma Physics), 1, 174 (2009).

- Neto A, Sartori F, Piccolo F, et al., *"Linux Real Time Framework for Fusion Devices"*, Fusion Engineering and Design 84 (7-11): 1408-1411 Jun 2009

- Neto A., C. Silva, J. Sousa, H. Fernandes, C. Hidalgo, J.L. Pablos, S. Salasca, J. Travère and J. B. Lister, "*ITER CODAC interface for the visible and infra-red wide angle viewing cameras"*, Fusion Engineering and Design, 84 (2009) 1412

- Nunes D., R. Mateus, I.D. Nogueira, P.A. Carvalho, J.B. Correia, N. Shohoji, R.B. Gomes, H. Fernandes, C. Silva, N. Franco, E. Alves, *"Microstructural evolution in tungsten and copper probes under hydrogen irradiation at ISTTOK"*, J. Nucl. Materials, 390-391 (2009) 1039

- Paley JI, J. Berrino, S. Coda, N. Cruz, B.P. Duval, F. Felici, T.P. Goodman, Y. Martin, J.M. Moret, F. Piras, A.P. Rodrigues, B. Santos, C.A.F. Varandas and the TCV Team, "*Real time control of plasmas and ECRH systems on TCV*", IOP Publishing and International Atomic Energy Agency Nuclear Fusion Vol. 49 Nr. 8 (2009).

- Parail V., P. Belo, P. Boerner, X. Bonnin, G. Corrigan, D. Coster, J. Ferreira, A. Foster, L. Garzotti, G.M.D. Hogeweij, W. Houlberg, F. Imbeaux, J. Johner, F. Kochl, V. Kotov, L. Lauro-Taroni, X. Litaudon, J. Lonnroth1, G. Pereverzev, Y. Peysson, G. Saibene, R. Sartori, M. Schneider, G. Sips, P. Strand, G. Tardini, M. Valovic, S. Wiesen, M. Wischmeier, R. Zagorski, JET EFDA contributors and EU ITM Task Force, *"Integrated modelling of ITER reference scenarios"*, Nuclear Fusion 49, 075030 (2009)

- Rodrigues P. and J. P. S. Bizarro, *"Noniterative reconstruction of tokamak equilibria"*, Physics of Plasmas 16, 022505 (2009).

- Saarelma S, A Alfier, MNA Beurskens, R Coelho, HR Koslowski, Y Liang, I Nunes and JET EFDA contributors *"MHD stability analysis of small ELM regimes in JET",* Plasma Physics and Controlled Fusion, 51, 5, 035001, 2009

- Salasca S., B. Esposito, Y. Corre, M. Davi, C. Dechelle, G. Brolatti, D. Marocco, F. Moro, L. Petrizzi, E. De La Calc, C. Hidalgo, A. Manzanares, J.L. De Pablos, S. Recsei, S. Tulipan, A. Neto, C. Silva, L. Bertalot, C. Walker, C. Ingesson, "*Development of equatorial visible/infrared wide angle viewing system and radial neutron camera for ITER",* Fusion Engineering and Design, 84 (2009) 1689

- Sánchez J. et al, J. Sánchez , M. Acedo, A. Alonso, J. Alonso, P. Alvarez , E. Ascasíbar, A. Baciero, R. Balbín, L. Barrera, E. Blanco, J. Botija, A. de Bustos, E. de la Cal, I. Calvo, A. Cappa, J.M. Carmona, D. Carralero, R. Carrasco, B.A. Carreras, F. Castejón , R. Castro, G. Catalán, A.A. Chmyga, M. Chamorro, L. Eliseev, L. Esteban, T. Estrada, A. Fernández, R. Fernández-Gavilán, J.A. Ferreira, J.M. Fontdecaba, C. Fuentes, L. García, I. García-Cortés, R. García-Gómez, J.M. García-Regaña, J. Guasp, L. Guimarais, T. Happel, J. Hernanz, J. Herranz, C. Hidalgo, J.A. Jiménez, A. Jiménez-Denche, R. Jiménez-Gómez, D. Jiménez-Rey, I. Kirpitchev, A.D. Komarov, A.S. Kozachok, L. Krupnik, F. Lapayese, M. Liniers, D. López-Bruna, A. López-Fraguas, J. López-Rázola, A. López-Sánchez , S. Lysenko [3], G. Marcon , F. Martín , V. Maurin [3], K.J. McCarthy , F. Medina , M. Medrano , A.V. Melnikov [3], P. Méndez , B. van Milligen , E. Mirones , I.S. Nedzelskiy [5], M. Ochando , J. Olivares , J.L. de Pablos , L. Pacios , I. Pastor , M.A. Pedrosa , A. de la Peña , A. Pereira , G. Pérez , D. Pérez-Risco , A. Petrov [3], S. Petrov [6], A. Portas , D. Pretty , D. Rapisarda , G. Rattá , J.M. Reynolds [7], E. Rincón , L. Ríos , C. Rodríguez , J.A. Romero , A. Ros , A. Salas , M. Sánchez , E. Sánchez , E. Sánchez-Sarabia , K. Sarksian [8], J.A. Sebastián , C. Silva [5], S. Schchepetov [8], N. Skvortsova [8], E.R. Solano , A. Soleto , F. Tabarés , D. Tafalla , A. Tarancón [7], Yu. Taschev [5], J. Tera , A. Tolkachev , V. Tribaldos , V.I. Vargas , J. Vega , G. Velasco , J.L. Velasco [7], M. Weber , G. Wolfers and B. Zurro, "*Confinement transitions in TJ-II under Li-coated wall conditions"*, Nucl. Fusion 49 (2009) 104018

- Sassenberg K, M. Maraschek, PJ Mc Carthy, H. Zohm, R Bilato, W Bobkov, S Da Graça, A Flaws, M Garcia-Muñoz, S Günter, V Igochine, P Lauber, MJ Mantsinen, P Piovesan and the ASDEX Upgrade Team *"Stability of toroidicity induced shear Alfvén eigenmodes in ASDEX Upgrade",* Plasma Physics and Controlled Fusion, 51, 6, 065003, 2009

- Silva C., W. Fundamenski, A. Alonso, B. Gonçalves, C. Hidalgo, M. A. Pedrosa, R. A Pitts, M. Stamp and JET-EFDA contributors, "*Reciprocating probe measurements of ELM filaments on JET"*, Plasma Phys. Control. Fusion, 51 (2009) 105001

- Silva C., B. Gonçalves, C. Hidalgo, M.A. Pedrosa, W. Fundamenski, M. Stamp, R.A. Pitts and JET-EFDA contributors, "*Intermittent transport in the JET far-SOL"*, J. Nucl. Materials, 390-391 (2009) 355

- Silva C., P. Duarte, H. Fernandes, H. Figueiredo, I. Nedzelskij, C. Hidalgo and M. A. Pedrosa, "*Characterization of geodesic acoustic modes in the ISTTOK edge plasma"*, Plasma Phys. Control. Fusion, 51 (2009) 085009

- Sunden E. Andersson, H.Sjostrand, S.Conroy, G.Ericsson, M.Gatu Johnson, L.Giacomelli, C. Hellesen, A.Hjalmarsson, E.Ronchi, M.Weiszflog, J.K¨allne, G.Gorini, M.Tardocchi, A.Combo, N.Cruz, A.Batista, R.Pereira, R.Fortuna, J.Sousa, S.Popovichev, *"The thin-foil magnetic proton recoil neutron spectrometer MPRu at JET"*, Nuclear Instruments and Methods in Physics Research, A 610 (2009), 682–699.

- Tala T., K.-D. Zastrow, J. Ferreira, P. Mantica, A.G. Peeters, G. Tardini, M. Brix, G. Corrigan, C. Giroud, V. Naulin, D. Strintzi and JET-EFDA contributors, *"Evidence of inward toroidal momentum convection in the JET tokamak";* Physical Review Letters, 102, 075001, (2009).

- Tardini G., J. Ferreira, P. Mantica, A.G. Peeters, T. Tala, K.D. Zastrow, M. Brix, C. Giroud, G.V. Pereverzev and JET-EFDA contributors, *"Angular momentum studies with NBI Modulation in JET";* Nuclear Fusion 49, 085010 (2009).

- Valcárcel DF, A. Neto , J. Sousa , B.B. Carvalho, H. Fernandes, J.C. Fortunato, A.S. Gouveia, A.J.N. Batista, A.G. Fernandes, M. Correia, T. Pereira, I.S. Carvalho, A.S. Duarte, C.A.F. Varandas, M. Hron, F. Janky, J. Pisacka, "*An ATCA Embedded Data Acquisition and Control System for the Compass Tokamak"*, Journal of Fusion Engineering and Design, 84, 1901–1904 (2009).

- Vilela Mendes R., *"Stochastic solutions of some nonlinear partial differential equations"* Stochastics 81, 279 (2009)

- Vilela Mendes R., *"A fractional calculus interpretation of the fractional volatility model"* Nonlinear Dynamics 55, 395-399 (2009)

- Vilela Mendes R., *"Universal families and quantum control in infinite dimensions"* Physics Letters A 373, 2529 (2009)

- Xu G.S., V. Naulin, W. Fundamenski, C. Hidalgo, J.A. Alonso, C. Silva, B. Gonçalves, A.H. Nielsen, J. Juul Rasmussen, S.I. Krasheninnikov, B.N. Wan, M. Stamp and JET EFDA Contributors, "*Blob/hole formation and zonal-flow generation in the edge plasma of the JET tokamak"*, Nucl. Fusion, 49 (2009) 092002

- Wright G.M., A. W. Kleyn, E. Alves, L. C. Alves, N. P. Barradas, G. J. van Rooij, A. J. van Lange, A. E. Shumack, J. Westerhout, R. S. Al, W. A. J. Vijvers, B. de Groot, M. J. van de Pol, H. J. van der Meiden, J. Rapp, N. J. L. Cardozo, J. *"Hydrogenic retention in tungsten exposed to ITER divertor relevant plasma flux densities"*, Nucl. Materials, 390-391 (2009) 610

- Zohm H., J. Adamek, C. Angioni, G. Antar, C.V. Atanasiu, M. Balden, W. Becker, K. Behler, K. Behringer, A. Bergmann, T. Bertoncelli, R. Bilato, V. Bobkov, J. Boom, A. Bottino, M. Brambilla, F. Braun, M. Brüdgam, A. Buhler, A. Chankin, I. Classen, G.D. Conway, D.P. Coster, P. de Marné, R. D'Inca, R. Drube, R. Dux, T. Eich, K. Engelhardt, B. Esposito, H.-U. Fahrbach, L. Fattorini, J. Fink, R. Fischer, A. Flaws, M. Foley, C. Forest, J.C. Fuchs, K. Gál, M. García Muñoz, M. Gemisic Adamov, L. Giannone, T. Görler, S. Gori, S. da Graça, G. Granucci, H. Greuner, O. Gruber, A. Gude, S. Günter, G. Haas, D. Hahn, J. Harhausen, T. Hauff, B. Heinemann, A. Herrmann, N. Hicks, J. Hobirk, M. Hölzl, D. Holtum, C. Hopf, L. Horton, M. Huart, V. Igochine, M. Janzer, F. Jenko, A. Kallenbach, S. Kálvin, O. Kardaun, M. Kaufmann, M. Kick, A. Kirk, H.-J. Klingshirn, G. Koscis, H. Kollotzek, C. Konz, K. Krieger, T. Kurki-Suonio, B. Kurzan, K. Lackner, P.T. Lang, B. Langer, P. Lauber, M. Laux, F. Leuterer, J. Likonen, L. Liu, A. Lohs, T. Lunt, A. Lyssoivan, C.F. Maggi, A. Manini, K. Mank, M.-E. Manso, M. Mantsinen, M. Maraschek, P. Martin, M. Mayer, P. McCarthy, K. McCormick, H. Meister, F. Meo, P. Merkel, R. Merkel, V. Mertens, F. Merz, H. Meyer, A. Mlynek, F. Monaco, H.-W. Müller, M. Münich, H. Murmann, G. Neu, R. Neu, J. Neuhauser, B. Nold, J.-M. Noterdaeme, G. Pautasso, G. Pereverzev, E. Poli, S. Potzel, M. Püschel, T. Pütterich, R. Pugno, G. Raupp, M. Reich, B. Reiter, T. Ribeiro, R. Riedl, V. Rohde, J. Roth, M. Rott, F. Ryter, W. Sandmann, J. Santos, K. Sassenberg, P. Sauter, A. Scarabosio, G. Schall, H.-B. Schilling, J. Schirmer, A. Schmid, K. Schmid, W. Schneider, G. Schramm, R. Schrittwieser, W. Schustereder, J. Schweinzer, S. Schweizer, B. Scott, U. Seidel, M. Sempf, F. Serra, M. Sertoli, M. Siccinio, A. Sigalov, A. Silva, A.C.C. Sips, E. Speth, A. Stäbler, R. Stadler, K.-H. Steuer, J. Stober, B. Streibl, E. Strumberger, W. Suttrop, G. Tardini, C. Tichmann, W. Treutterer, C. Tröster, L. Urso, E. Vainonen-Ahlgren, P. Varela, L. Vermare, F. Volpe, D. Wagner, C. Wigger, M. Wischmeier, E. Wolfrum, E. Würsching, D. Yadikin, Q. Yu, D. Zasche, T. Zehetbauer and M. Zilker, *"Overview of ASDEX Upgrade results",* Nuclear Fusion 49, 104009 (2009).

24.1.3. Publications/Contributions in Conferences and Workshops

24.1.3.1. Invited Talks

- Alves E., L.C. Alves, N P Barradas, R. Mateus, P.A. Carvalho, G.M. Wright, "*Influence of temperature and plasma composition on deuterium retention in refractory metals"*, 18th International Conference on Ion Beam Analyses, Cambridge 7-11 September 2009

- Borba D., Nuclear Fusion, "*A limitless environmentally responsible source of energy",* Invited paper to the Nuclear Fission, Nuclear Fusion and the Environment Symposium, 42nd IUPAC Congress: Chemistry Solutions, 2-7 August, (2009)

- Kendl A., Tiago Ribeiro and Bruce D. Scott, *"Turbulence in the Edge of Magnetized Plasmas: Emergent Structures and Transport"*, Workshop on Electric Fields, Turbulence and Self-organization in Magnetized Plasmas, (EFTSOMP July), Sofia, Bulgaria, (2009)

- Lehnen M., A. Alonso, G. Arnoux, S.A. Bozhenkov, S. Brezinsek, T. Eich, K.H. Finken, A. Huber, S. Jachmich, U. Kruezi, P.D. Morgan, V.V. Plyusnin, C. Reux, V. Riccardo, G. Sergienko, M.F. Stamp and JET EFDA contributors, "*First experiments on massive gas injection at JET - consequences for disruption mitigation in JET and ITER"*, Plenary Talk, 36th EPS Conference on Plasma Physics, Sofia, Bulgaria O2.001 (2009)

- Loureiro N. F., *"An efficient iterative semi-implicit numerical scheme for fluid models"*, Plasmas, Computation & Mathematics workshop, University of Cumbria, Ambleside, UK, (2009)

- Loureiro N. F., *"Current sheet instability and formation of plasmoid chains",* International Conference on the Numerical Simulation of Plasmas, Lisbon, Portugal, (2009)

- Lyssoivan A., R. Koch, J.-M. Noterdaeme, V. Philipps, N. Ashikawa, Y.D. Bae, B. Beaumont, A. Becoulet, V. Bobkov, S. Bremond, E. de la Cal, D. Douai, H.G. Esser, E. Gauthier, M. Graham, D.A. Hartmann, J. Hu, J.G. Kwak, R. Laengner, P.U. Lamalle, E. Lerche, F. Louche, O. Marchuk, M.-L.

Mayoral, V.E. Moiseenko, I. Monakhov, M. Nightingale, J. Ongena, M.K. Paul, R. Pitts, V. Plyusnin, V. Rohde, F.C. Schüller, G. Sergienko, M. Shimada, B. Unterberg, D. Van Eester, M. Van Schoor, G. Van Wassenhove, M. Vervier, E.D. Volkov, T. Wauters, R. Weynants, Y. Zhao, the TEXTOR Team, the TORE SUPRA Team, the ASDEX Upgrade Team, JET EFDA Contributors, the URAGAN-2M Team, the LHD Team, the EAST Team and the KSTAR Team, "*ICRF Wall Conditioning: Present Status and Developments for Future Superconducting Fusion Machines"*, Invited Talk, 18th Topical Conference on Radio Frequency Power in Plasmas, Gent, Belgium, June 2009

- Nedzelskiy I. S., C. Silva, P. Duarte, H. Fernandes, "*Mass-sensitive ion probe for plasma boundary characterization on the tokamak ISTTOK"*, IWEP2009, September 21-23, 2009, Innsbruck, Austria

- Nedzelskiy I.S., "*HIBP and non-traditional HIBP applications"*, Joint Li Beam Diagnostic Meeting, November 19-20, 2009, Budapest, Hungary

- Scott B., A. Kendl and T. Ribeiro, *"Nonlinear Dynamics in the Tokamak Edge",* 12th International Workshop on Plasma Edge Theory in Fusion Devices, September, Rostov Veliky, Russia, (2009)

- Silva. A,*"Overview of the microwave reflectometry system for Compass"*, with contributions from IPFN Reflectometry Group, IPP CZ and IRE Kharkov, Ukraine, COMPASS programmatic meeting, Prague, Czech Republic, April 2009.

- Silva C., P. Duarte, H. Fernandes, H. Figueiredo, I. Nedzelskij, C. Hidalgo, M.A. Pedrosa, "*Experimental evidence of coupling between local turbulent transport and large scale fluctuations in the ISTTOK edge plasma"*, 2nd EFDA Transport Topic Group meeting, Culham Science Centre, England, September 2009

- Silva C., *"Divertor Physics Studies on COMPASS",* COMPASS programmatic meeting, Prague, Czech Republic, April 2009

- Varandas CAF, *"Research and development physics and technology issues towards fusion energy",* 4th International Conference on Frontiers of Plasma Physics and Technology, April 6-10, Kathmandu, Nepal, 2009.

- Vilela Mendes R., *"Stochastic solutions of charged kinetic equations",* Workshop on Kinetics and Statistical Methods for Complex Particle Systems (Lisbon, July 20-24 2009)

- Vilela Mendes R., *"Stochastic volatility: models and questions"* Complexity, Mathematics and Socio-Economic Problems (Bielefeld, September 1-11, 2009) "Cooperation, punishment, emergence of governnent and the tragedy of authorities"

- Vilela Mendes R., *"Fractional stochastic processes: Finite and infinite dimensions"*, International Conference on Stochastic Analysis and Applications (Hammamet, October 12-17, 2009)

24.1.3.1. Oral Contributions

- Alves E., "*Post-mortem analysis and simulation",* (JW9-FT-3.47) Task Force Fusion Technology Monitoring Meeting, 01-04 December 2009, JET Culham Science Centre

- Alves E., L. C. Alves, , N. P. Barradas, R. Mateus, P. A. Carvalho, G. M. Wright, "*Influence of temperature and composition on deuterium retention in refractory metals",* 19th International Conference on Ion Beam Analysis, Cambridge, United Kingdon, September 7 -11, 2009

- Baranov Y., K. Kirov, M. Goniche, J. Mailloux, M.-L. Mayoral, J. Ongena, M. F. F. Nave and JET EFDA Contributors, *"LH power modulation experiment on JET",* 18th Topical Conference on Radio Frequency Power in Plasmas, Gent, Belgium, 22nd to 24th , June , (2009)

- Basiuk V., P.Börner, D.Coster, J.Ferreira, A.Figueiredo, P.Huyn, G.Huysmans,F.Imbeaux, I.Ivanova-Stanik, D.Kalupin, S.Moradi, G.Pereverzev, D.Reiter, R.Stankiewicz, P.Strand, M.Tokar, D.Twarog, R.Zagorski and ITM-TF contributors, *"European Transport Solver"*, 13th European Fusion Theory Conference, 12-15 October 2009, Riga, Latvia

- Beaumont B., J. H. Belo, J. P. S. Bizarro, P. Bonoli, M. H. Cho, F. Kazarian, C. Kessel, S. H. Kim, J. G. Kwak, J. H. Jeong, J. B. Lister, S. Milora, F. Mirizzi, R. Maggiora, D. Milanesio, W. Namkung, J. M. Noterdaeme, S. I. Park, R. Parker, D. Rasmussen, P. K. Sharma, A. Tanga, A. Tuccillo, and Y. X. Wan, *"A Lower Hybrid Current Drive System for ITER and High Power CW Klystron Development",* 18th Topical Conference on Radio Frequency Power in Plasmas, Gent, Belgium, 22nd to 24th , June , (2009)

- Beurskens M A, T.H. Osborne, L.D. Horton, L. Frassinetti, R. Groebner, A. Leonard, P. Lomas, I Nunes, S. Saarelma, P.B. Snyder, I. Balboa, B. Bray, K. Crombe, J Flanagan, C. Giroud, E Giovannozzi, M Kempenaars, N. Kohen, A. Loarte, J. Lonnroth, E. de la Luna, G. Maddison, C. Maggi, D. McDonald, G. McKee, R. Pasqualotto, G. Saibene, R. Sartori, E. Solano, W. Suttrop, E. Wolfrum, M. Walsh, Z. Yan, L. Zabeo, D. Zarzoso, *"Pedestal identity studies in JET, DIII-D and implications for ITER",* 36th EPS Conference on Plasma Physics, Sofia, Bulgaria, (2009)

- Bizarro J.P.S., J. S. Ferreira, X. Litaudon, T. J. J. Tala, and JET EFDA Contributors, *"ITB oscillations in fully non-inductive advanced tokamaks"*, 4th International Conference on the Frontiers of Plasma Physics and Technology, Kathmandu (2009)

- Carvalho B.B., A.J.N. Batista, M. Correia, A. Neto, H. Fernandes, B. Gonçalves, J. Sousa, "*Reconfigurable ATCA Hardware for Plasma Control and Data Acquisition*". Seventh IAEA Technical Meeting (IAEA-TM) on Control, Data Acquisition, and Remote Participation for Fusion Research, 15 - 19 June 2009, Aix-en-Provence, France

- Duarte A.S., B. Santos, T. Pereira, B.B. Carvalho, H. Fernandes, A. Neto, F. Janky, P. Cahyna, J. Písack, M. Hron, "*FireSignal Application Node for Subsystem Control*", Seventh IAEA Technical Meeting (IAEA-TM) on Control, Data Acquisition, and Remote Participation for Fusion Research, 15 - 19 June 2009, Aix-en-Provence, France

- Fernandes A.M., R.C. Pereira, J. Sousa, A. Neto, P. Carvalho, A.J.N. Batista, B. B. Carvalho, C.A.F. Varandas, M. Tardocchi, G. Gorini and JET-EFDA Contributors, "*Parallel processing method for high-speed real time digital pulse processing for gamma-ray spectroscopy*", Seventh IAEA Technical Meeting (IAEA-TM) on Control, Data Acquisition, and Remote Participation for Fusion Research, 15 - 19 June 2009, Aix-en-Provence, France

- Gonçalves, J. Sousa, A. Batista, R. Pereira, M. Correia, A. Neto, B. Carvalho, H. Fernandes, C.A.F. Varandas, "*ATCA Advanced Control and Data acquisition systems for fusion experiments*". 16th IEEE NPSS Real-Time Conference, May 10-15, 2009, Beijing.

- Gonçalves B., J. Sousa, C.A.F. Varandas and IPFN Control and Data Acquisition Team, "*Real-time control of fusion reactors*", 14th International Conference on Emerging Nuclear Energy Systems, Ericeira, Portugal, 29th June – 3rd July, 2009

- Heuraux S., F. Clairet, F. da Silva, "*An X-mode reflectometry study on the reflection point for the density profile reconstruction",* Reflectometry Workshop for fusion plasma diagnostics, IRW9, Lisbon, May 2009.

- Janky F., T. Pereira, B. Santos, M. Hron, "*Vacuum Control and Gas Handling for COMPASS Tokamak*", 18th Week of Doctoral Students, Charles University, Prague, June 2 - 5, 2009

- Lehnen M., A. Alonso, G. Arnoux, S.A. Bozhenkov, S. Brezinsek, T. Eich, K.H. Finken, A. Huber, S. Jachmich, U. Kruezi, P.D. Morgan, V.V. Plyusnin, C. Reux, V. Riccardo, G. Sergienko, M.F. Stamp and JET EFDA contributors *"First experiments on massive gas injection at JET - consequences for disruption mitigation in JET and ITER",* 36th EPS Conference on Plasma Physics, Sofia, Bulgaria, (2009)

- Loureiro N. F., D. A. Uzdensky, A. A. Schekochihin, S. C. Cowley and T. A. Yousef, *"The effect of two-dimensional turbulence on resistive MHD reconnection",* APS-DPP09 Meeting, Atlanta, Georgia, USA, (2009)

- Mayoral M.-L., J. Ongena, A. Argouarch, Yu. Baranov, T. Blackman, V. Bobkov, R. Budny, L. Colas, A. Czarnecka, L. Delpech, F. Durodié, A. Ekedahl, M. Gauthier, M. Goniche, R. Goulding, M.Graham, J. Hillairet, S.Huygen, P. Jacquet, T. Johnson, K. Kiptily, K. Kirov, M. Laxaback, E. Lerche, J. Mailloux, I. Monakhov, M.F.F. Nave, M. Nightingale, V. Plyusnin, V. Petrzilka, F. Rimini, D. Van Eester, A. Whitehurst, E. Wooldridge, M. Vancken and JET-EFDA Contributors, *"Overview of Recent Results on Heating and Current Drive in the JET Tokamak",* 18th Topical Conference on Radio Frequency Power in Plasmas, Gent, Belgium, 22nd to 24th , June , (2009)

- Mayoral M.-L., J. Ongena, A. Argouarch, T. Blackman, V. Bobkov, G. Calabrò, F. Durodié, D. Frigione, R. Goulding, M.Graham, S. Huygen, P. Jacquet, E. Lerche, I. Monakhov, M.F.F. Nave, I. Nunes, M. Nightingale, F. Rimini, C. Sozzi, D. Van Eester, M. Vrancken, A. Whitehurst, E. Wooldridge and JET-EFDA Contributors, *"ICRF heating: the JET experience and prospect for ITER",* 36th EPS Conference on Plasma Physics, Sofia, Bulgaria, (2009)

- McDonald DC, M Beurskens, C Maggi, J Hobirk, I Nunes, B Alper, M Baruzzo, A Brett, M Brix, P Buratti, P C de Vries, C D Challis, O P Ford, C Giroud, D Howell, E Joffrin,, G P Maddison, S Saarelma, I Voitsekhovitch, L Zabeo and JET-EFDA contributors, *"Confinement and ETB studies of JET hybrid discharges",* 12th International Workshop on "H-mode Physics and Transport Barriers", Princeton, USA, (2009)

- Nave M.F.F., *"Intrinsic rotation at JET",* Transport &Confinement ITPA meeting in Naka, on March 31-April 2, (2009)

- Nedzelskiy I. S., C. Silva, P. Duarte, H. Fernandes, *"Mass-sensitive ion probe for plasma boundary characterization on the tokamak ISTTOK",* IWEP2009, September 21-23, 2009, Innsbruck, Austria

- Nedzelski I. S., *"HIBP and non-traditional HIBP applications",* Joint Li Beam Diagnostic Meeting, November 19-20, 2009, Budapest, Hungary

- Neto, et al., "*MARTe: a Multi-platform Real-time framework*", 16th IEEE NPSS Real-Time Conference, May 10-15, 2009, Beijing.

- Nunes D., V. Livramento, J.B. Correia, K. Hanada, P.A. Carvalho, R. Mateus, N. Shohoji, H. Fernandes, C. Silva, E. Alves, E.Osawa, "*Consolidation of Cu-nDiamond nanocomposites; hot extrusion vs spark plasma sintering*", Materiais 2009, 5-8 April 2009, Lisbon, Portugal

- Pereira T., F. Janky, B. Santos, H. Alves, P. Cahyna, M. Hron, J. Sousa, H. Fernandes, "*Subsystems Control on the COMPASS tokamak*", Seventh IAEA Technical Meeting (IAEA-TM) on Control, Data Acquisition, and Remote Participation for Fusion Research, 15 - 19 June 2009, Aix-en-Provence, France

- Ribeiro T.T. and B. Scott, *"On deformation-free geometry for turbulence computations",* 21st International Conference on Numerical Simulation of Plasmas, Lisbon, October 6-9, (2009)

- Ribeiro T.T., *"Addressing the geometric deformation on turbulence computations",* Max-Planck-Institut fuer Plasmaphysik Greifswald-Garching Theory Meeting, Sellin, Germany, November, 2009

- Rodríguez-Pascual M., B.D. Scott, T.T. Ribeiro, F. Castejón, R. Mayo, "*gGEM: a gyrofluid model to be used on distributed platforms",* 21st International Conference on

Numerical Simulation of Plasmas, Lisbon, October 6-9, (2009)

- Ruchko L., A. G. Elfimov, R. M. O. Galvão, C. M. Teixeira, J. I. Elizondo, E. Sanada, M. E. Manso and A. Silva, *"Registration of Alfvén wave resonances in the TCABR tokamak by the new frequency scanning reflectometer",* 10º Encontro Brasileiro de Física dos Plasmas, 26 -29 November, Maresias SP, Brasil (2009).

- Santos J., L. Guimarãis, C. Amador, M. Manso, and the IPFN and ASDEX Upgrade Teams, *"Status of the demonstration of Reflectometry based plasma position control on ASDEX Upgrade",* Reflectometry Workshop for fusion plasma diagnostics, IRW9, Lisbon, May 2009.

- Santos J., C. Amador, L. Guimarãis, M. Manso, W. Treutterer, M. Zilker, ASDEX Upgrade Team, " *Real Time Data Acquisition for Reflectometry on ASDEX Upgrade",* 10º Encontro Brasileiro de Física dos Plasmas, 26 -29 November, Maresias SP, Brasil (2009).

- Sartori R, Y Andrew, M Kempenaars, P J Lomas, D MC Donald , E de la Luna , G Saibene , A Loarte, I Nunes, *"L-H and H=1 access experiments in JET and implications for ITER",* 12th International Workshop on "H-mode Physics and Transport Barriers", Princeton, USA, (2009)

- Schubert M., F. Clairet, F. da Silva, T. Gerbaud, E. Gusakov, S. Heuraux and R. Sabot, "*Full wave test of analytical theory for fixed frequency fluctuation reflectometr*y", Reflectometry Workshop for fusion plasma diagnostics, IRW9, Lisbon, May 2009.

- Silva A. *"Overview of the microwave reflectometry system for Compass",* Reflectometry Workshop for fusion plasma diagnostics, IRW9, Lisbon, May 2009.

- Silva F. da, S.Heuraux, T. Ribeiro and B. Scott, "*Development of a 2D full-wave JE-FDTD Maxwell X-mode code for reflectometry simulation",* Reflectometry Workshop for fusion plasma diagnostics, IRW9, Lisbon, May 2009.

- Silva F. da, S. Heuraux, T. Ribeiro, B. Scott, *"Development of a 2D full-wave JE-FDTD Maxwell X-mode code for reflectometry simulation",* Reflectometry Workshop for fusion plasma diagnostics, IRW9, Lisbon, May 2009.

- Sirinelli A, Alper B, Fessey J, Walsh M J, Bottereau C, Clairet F, Cupido L, Meneses L, Sabot R EURATOM/UKAEA Fusion, Culham Science Centre, "*Design of a fast-sweep profile reflectometry system on JET",* Reflectometry Workshop for fusion plasma diagnostics, IRW9, Lisbon, May 2009.

- Solano E.R., P.J. Lomas, B. Alper, G. Xu, Y. Andrew, A. Boboc, L. Barrera, P. Belo, M.N.A. Beurskens, M. Brix, K. Crombe, E. de la Luna, S. Devaux, T. Eich, S. Gerasimov, C. Giroud, D. Harting, D. Howell, A. Huber, G. Kocsis, A. Korotkov, A. Lopez-Fraguas, M. F. F. Nave, C. Pérez Von Thun, E. Rachlew, F. Rimini, S. Saarelma, A. Sirinelli, L. Zabeo, D. Zarzoso and JET EFDA contributors, *"High Temperature Pedestals in JET and confined current filaments",* Reflectometry Workshop for fusion plasma diagnostics, IRW9, Lisbon, May 2009.

- Strand P., R. Coelho, D. Coster, L.G. Eriksson, *"Simulation & high performance computing - building a predictive capability for Fusion",* Seventh IAEA Technical Meeting (IAEA-TM) on Control, Data Acquisition, and Remote Participation for Fusion Research, 15 - 19 June 2009, Aix-en-Provence, France

- Tala T., J. Ferreira, P. Mantica, D. Strintzi, G. Tardini, K.-D. Zastrow, M. Brix, G. Corrigan, C. Giroud, L. Hackett, I. Jenkins, T. Johnson, J. Lönnroth, V. Naulin, V. Parail, A.G. Peeters, A. Salmi, M. Tsalas, T. Versloot, P.C. de Vries and JET-EFDA contributors, *"NBI Modulation Experiments to Study Momentum Transport on JET + Status of TC-15",* 2nd ITPA Transport and Confinement ITPA Group Meeting, Naka, Japan, 2009

- Teixeira C. M. O., L. F. Ruchko, A. G. Elfimov, A. Silva, J. I. Elizondo, M. E. Manso, E. Sanada, R. M. O. Galvão, *"TCABR reflectometry system firsts results",* 10º Encontro Brasileiro de Física dos Plasmas, 26 -29 November, Maresias SP, Brasil (2009).

- Varela P., *"Status of plasma-position reflectometry for ITER",* Reflectometry Workshop for fusion plasma diagnostics, IRW9, Lisbon, May 2009.

- Vicente J., S.I. Lashkul, M. Tendler, S.V. Shatalin, E.O. Vekshina, A.V. Sidorov, and L.A. Esipov, *"Blobs at the high field side of tokamaks",* 19th International Toki Conference on Advanced Physics in Plasma and Fusion Research, December, Toki City, Gifu, Japan (2009).

- Vilela Mendes R., *"A stochastic approach to the solution and simulation of plasma kinetic equations",* 21st International Conference on Numerical Simulation of Plasmas, Lisbon, October 6-9, (2009)

- Vilela Mendes R., *"Universal families and quantum control in infinite dimensions",* Coherence, Control, and Dissipation, (Minneapolis, March 2-6, 2009)

24.1.3.2. Posters

9th International Symposium on Fusion Nuclear Technology, ISFNT 2009, Dalian, China, 2009

- Gutiérrez C. González, C. Damiani , M. Irving , J-P. Friconneau , A. Tesini , I. Ribeiro , A. Vale *,"ITER Transfer Cask System: status of design, issues and future developments"*

11th IAEA Technical Meeting on Energetic Particles In Magnetic Confinement Systems, September 21-23, 2009, Kyiv, Ukraine

- Jakubowski L., J. Zebrowski, V.V. Plyusnin, K. Malinowski, M.J. Sadowski, M. Rabinski, H. Fernandes, C. Silva, P. Duarte, *"A Detection Method for Direct Measurements of Fast Electrons via Cherenkov Effect in the ISTTOK Tokamak"*

- Nabais F., V. Kiptily, S. Pinches, S. Sharapov and JET-EFDA contributors, *"Fast Ion Redistribution and Losses in the Advanced Tokamak Scenario"*

- Plyusnin V.V., V.G. Kiptily, I. H. Coffey, J. Mailloux, M.-L. Mayoral, P. C. de Vries, J. Ongena and JET EFDA contributors, *"Enhancement of metal impurities release due to fast ions loss in JET"*

36th EPS Conference on Plasma Phys. Sofia, Bulgaria, (2009).

- Angelis De R, Orsitto F, Brix M, Hawkes N, Rachlew E, Botrugno A, Buratti P, Fonseca A, Howell D, Pericoli V, Tudisco O, JET-EFDA Contributors "*Current profile measurements in JET advanced tokamak scenarios"*

- Belo P., V. Parail, E. R. Solano, G Corrigan, C. Giroud, J. Spence, P. J. Lomas and JET EFDA contributors , *"Effect of the initial ELM on impurity transport in hot ion H mode plasma"*

- Bernardo J., Y. Andrew, K. Crombé, S. Reyes Cortes, G. Saibene, T.M. Biewer, J. Ferreira, N.C. Hawkes, I. Jenkins, E. de la Luna, D. McDonald, I. Nunes, A. Salmi and JET EFDA contributors, *"Highly spatially resolved measurements of JET edge toroidal rotation in Type-I ELMy H-mode plasmas"*

- Crombe K, Andrew Y, Biewer T M, Blanco E, Brix M, de Vries P, Fonseca A, Giroud C, Hawkes N C, Joffrin E, Mantica P, Meigs A, Naulin V, Pinches S, Rachlew E, Tala T, Whiteford A, JET-EFDA contributors, *"Influence of rotational shear on triggering and sustainment of internal transport barriers on JET"*

- Figueiredo A. C. A., J. Ferreira, Y. Andrew, F. Nabais, V. Naulin, A. Sirinelli and JET-EFDA contributors; *"Measurement and qualitative interpretation of the radial scale of turbulence in JET plasmas"*

- Graves J, I. Chapman, S. Coda, K. Crombe, L.-G. Eriksson, T. Johnson, R. Koslowski, M. Lennholm, M. -L. Mayoral, I. Nunes, *"Sawtooth control mechanism in JET using off-axis toroidally propagating ICRF"*

- Hobirk J, F. Imbeaux, F. Crisanti, P. Buratti, C. Challis, E. Joffrin, B. Alper, Y. Andrew, P. Beaumont, M. Beurskens, D. Frigione, J. Garcia, C. Giroud, N. Hawkes, D. Howell, I. Jenkins, D. Keeling, M. Kempenaars, H. Leggate, P. Lotte, E. de la Luna, G. Maddison, P. Mantica, C. Mazzotta, D. McDonald, A. Meigs, I. Nunes, F. Orsitto, E. Rachlew, F. Rimini, M. Schneider, A.C.C. Sips, J. K. Stober, W. Studholme, T. Tala, M. Tsalas, I. Voitsekhovich, P.C. de Vries, *"Improved Confinement in JET hybrid discharges"*

- Kirov K. K., Yu. Baranov, J. Mailloux, M.F.F.Nave, J. Ongena and JET EFDA contributors, *"LH Wave Absorption and Current Drive Studies by Application of Modulated LHCD at JET"*

- Kocsis G., J.A.Alonso, B.Alper, G.Arnoux, G.Cseh, J.Figueiredo, D.Frigione, L.Garzotti, J.Hobirk, S.Kalvin, M.Lampert, P.T.Lang, G.Petravich, T.Szepesi, R.Wenninger, *"Pellet cloud distribution and dynamics for different plasma scenarios in ASDEX Upgrade and JET"*

- Lang P. T., A. Alonso, B. Alper, A. Boboc, S. Devaux, T. Eich, R.Felton, D. Frigione, K. Gal, L. Garzotti, A. Geraud, S. Gerasimov, M. Goniche, J. Hillairet, J. Hobirk, S. H. Hong, K. M. Kin, G. Kocsis, R. Koslowski, Y. Liang, T. Loarer, A. Loarte, P. J. Lomas, M. Maraschek, H. W. Muller, Y. S. Na, M.f. F. Nave, I. Nunes, G. Petravich, F. Poli, G. Saibene, R. Sartori, H. Thomsen, M. Tsalas, M. Valovic, R. Wenninger and JET EFDA contributers, *"Pellet fuelling and ELM triggering investigations at JET"*

- Lazzaro E., S.Nowak, S. Cirant, R.Coelho, *"Self-consistent Determination of Magnetic Islands Frequency in ν and $1/\nu$ Neoclassical Viscous Regimes"*

- Lazzaro E., S.Nowak, S. Cirant, R.Coelho, P.Buratti, *"Rotation and Stability of Magnetic Islands in Neoclassical Viscous Regimes"*

- Maddison GP, C.Giroud, K.McCormick, A.Alonso, B.Alper, Y.Andrew, G.Arnoux, P.Belo, M.Beurskens, A.Boboc, S.Brezinsek, M.Brix, I.Coffey, E.de la Luna, P.de Vries, S.Devaux, T.Eich, R.Felton, W.Fundamenski, D.Harting, J.Hobirk, A.Huber, S.Jachmich, I.Jenkins, E.Joffrin, A.Kallenbach, M.Kempenaars, M.Lehnen, T.Loarer, D.McDonald, A.Meigs, P.Morgan, J.Ongena, F.Rimini, A.Sirinelli, M.Stamp, G.Telesca, H.Thomsen, I.Voitsekhovitch, *"Impurity-seeding experiments on JET in preparation for the ITER-like wall"*

- Maget P., H. Lutgens, R. Coelho, B. Alper, M. Brix, P. Buratti, R.J. Buttery, E. De la Luna, N. Hawkes, I. Jenkins, C. Challis, C. Giroud, *"Modelling of (2,1) NTM threshold in JET"*

- Mailloux J., X. Litaudon, P. de Vries, B. Alper, Yu. Baranov, M. Baruzzo, M. Brix, P. Buratti, G. Calabro, R. Cesario, C.D. Challis, K. Crombe, O. Ford, D. Frigione, J. Garcia, C. Giroud, D. Howell, Ph. Jacquet, I. Jenkins, E. Joffrin, K. Kirov, P. Maget, D. C. McDonald, V. Pericoli-Ridolfini, V. Plyusnin, F. Rimini, F. Sartori, M. Schneider, S. Sharapov, C. Sozzi, I. Voitsekovitch, L. Zabeo, M. K. Zedda, and JET-EFDA contributors, "*Development of a steady-state scenario in JET with dimensionless parameters approaching ITER target values"*

- McCormick K, G.Maddison, C.Giroud, A.Alonso, B.Alper, Y.Andrew, G.Arnoux, P.Belo, M.Beurskens, A.Boboc, S.Brezinsek, M.Brix, J.Bucalossi, I.Coffey, E.de la Luna, P.de Vries, S.Devaux, T.Eich, R.Felton, W.Fundamenski, D.Harting, J.Hobirk, A.Huber, S.Jachmich, I.Jenkins, E.Joffrin, M.Kempenaars, M.Lehnen, T.Loarer, P.Lomas, D.McDonald, A.Meigs, P.Morgan, F.Rimini, A.Sirinelli, M.Stamp, G.Telesca, H.Thomsen, I.Voitsekhovitch, *"High target-plate recycling and degradation of confinement on JET"*

- Nave M.F.F., T. Johnson, L.-D. Eriksson, C. Giroud, K. Crombe, M.-L. Mayoral, J. Ongena, A. Salmi, T. Tala, M.

Tsalas and JET EFDA contributors, *"The influence of magnetic field ripple on JET Intrinsic Rotation"*

- Nunes I, P J Lomas, G Saibene, T Eich, G Arnoux, E de La Luna and JET EFDA contributors, "*Divertor power handling assessment for baseline scenario operation in JET in preparation for the ILW"*

- Petrzilka V, G. Corrigan, P. Belo, A. Ekedahl, M. Goniche, P. Jacquet, J. Mailloux, J. Ongena, V. Parail, *"Scrape-off-layer variations during Lower Hybrid ionization and ELMs"*

- *Silva C., P. Duarte, H. Fernandes, H. Figueiredo, I. Nedzelskij, C. Hidalgo, M.A. Pedrosa,* "Characterization of geodesic acoustic modes in the ISTTOK edge plasma"

- Solano E.R., P.J. Lomas, B. Alper, G. Xu, Y. Andrew, A. Boboc, L. Barrera, P. Belo, M.N.A. Beurskens, M. Brix, K. Crombe, E. de la Luna, S. Devaux, T. Eich, S. Gerasimov, C. Giroud, D. Harting, D. Howell, A. Huber, G. Kocsis, A. Korotkov, A. Lopez-Fraguas, M. F. F. Nave, C. Perez Von Thun, E. Rachlew, F. Rimini, S. Saarelma, A. Sirinelli, L. Zabeo and JET EFDA contributors, *"High Temperature Pedestals in hot ion H-mode in JET: overview of recent results"*

- Soldatov S, Fonseca A, Liang Y, Fessey J, Sirinelli A, Kramer-Flecken A, Van Oost G, JET-EFDA contributors EURATOM/UKAEA Fusion, "*Results of reflectometry studies on ELM dynamics in JET* "

- Valisa M, C Angioni , L Carraro I Coffey, I Predebon, ME Puiatti, L Lauro Taroni, B Alper, P. Belo, C Giroud , D Van Eester, E Lerche, V Naulin, T Tala, M Tsala and JET EFDA contributors, *"Radio-frequency power injection and impurity profile control in JET"*

EFTSOMP2009 (Satellite meeting of EPS), Sofia, Bulgaria, 6th July, (2009)

- Solano ER, P. J. Lomas, B. Alper, Y. Andrew, L. Barrera, P. Belo, M. Beurskens, M. Brix, K. Crombe, E. de la Luna, S. Devaux, T. Eich, J. Flanagan, O. Ford, S. Gerasimov, C. Giroud, D. Hartman, D. Howell, A. Huber, G. Huysmans, T. Johnson, M. Kempenaars, A. Korotkov, A. Lopez-Fraguas, J. Lonnroth, M. F. F. Nave, V. Parail, C. PÃ©rez Von Thun, E. Rachlew, F. Rimini, S. Saarelma, S. Sharapov, A. Sirinelli, I. Voitsekhovitch, G. Xu, L. Zabeo and JET EFDA contributors, *"Observation of confined current ribbon in hot ion H-mode in JET"*

18th Topical Conference on Radio Frequency Power in Plasmas, Gent (2009)

- Guilhem D., J. Achard, J. Belo, B. Bertrand, Z. Bej, Ph. Bibet, C. Brun, M. Chantant, E. Delmas, L. Delpech, Y. Doceul, A. Ekedahl, C. Goletto, M. Goniche, J.C. Hatchressian, M. Houry, P. Joubert, M. Lipa, S. Madeleine, A. Martinez, S. Poli, D. Raulin, A. Saille, B. Soler, D. Thouvenin, J.M. Verger, K. Vulliez, B. Zago, *"Passive Active Multi-Junction 3,7 GHZ launcher for Tore Supra Long pulse experiments: manufacturing process and tests"*

12th International Workshop on "H-mode Physics and Transport Barriers", Princeton, USA, (2009)

- Nunes I, P J Lomas, D C McDonald, G Saibene, R Sartori, M Beurskens, G Arnoux, T Eich, C Giroud, S Heureux, E de la Luna, G Maddison, A C C Sips, H Thomsen, T W Versloot and JET EFDA contributors, *"Pedestal parameters at high plasma current at JET"*

- Tala T., J. Ferreira, P. Mantica, D. Strintzi, M. Brix, G. Corrigan, C. Giroud, L. Hackett, I. Jenkins, T. Johnson, J. Lonnroth, V. Naulin, V. Parail, A.G. Peeters, A. Salmi, G. Tardini, M. Tsalas, T. Versloot, P.C. de Vries, K.-D. Zastrow and JET-EFDA contributors, *"NBI Modulation Experiments to Study Momentum Transport on JET"*

14th International Symposium on Laser-Aided Plasma Diagnostics, Treviso, Italy, (2009)

- Alonso M. P. et al., "Thomson Scattering Diagnostic for the TCABR tokamak"

IBA- 19, United Kingdon, September, 7 -11, 2009.

- Alves E., L.C. Alves, N P Barradas, R. Mateus, P.Carvalho, J.P.Coad, A. M. Widdowson, J. Likonen, S. Koivuranta**,** *Erosion and re-deposition processes in JET tiles studied with ion beams*

16th IEEE NPSS Real-Time Conference, May 10-15, 2009, Beijing.

- Alves D., R. Coelho, A. Klein, T. Panis, A. Murari and JET-EFDA contributors, *"A Real-Time Synchronous Detector for the TAE Antenna Diagnostic at JET"*

Seventh IAEA Technical Meeting (IAEA-TM) on Control, Data Acquisition, and Remote Participation for Fusion Research, 15 - 19 June 2009, Aix-en-Provence, France

- Zabeo L., F. Sartori, A. Neto, F. Piccolo, D. Alves, R. Vitelli, A. Barbalace, G. De Tommasi, and JET-EFDA contributors, *"Continuous data recording on fast real-time systems"*

12th International Workshop on Plasma Facing Materials and Components for Fusion Applications, 11-14 May 2009, Jülich, Germany (book of abstracts P127).

- Mateus R., A.M. Deus, P.A. Carvalho, D. Nunes, J.B. Correia, N. Shohoji, H. Fernandes, C. Silva, N. Barradas, L.C. Alves, *"Deuterium retention in tungsten at high temperatures"*

- Nunes D., V. Livramento, J.B. Correia, P.A. Carvalho, R. Mateus, N. Shohoji, H. Fernandes, C. Silva, L.C. Alves, K. Hanada, E.Osawa, "*A study of Cu/Graphite and Cu/Diamond interfaces reinforced with chromium"*

6-10 September 2009, Glasgow, United Kingdom.

- Mateus R., A.M. Deus, P.A. Carvalho, D. Nunes, J.B. Correia, N. Shohoji, H. Fernandes, C. Silva, N.P. Barradas, L.C. Alves, E. Alves, G.M. Wright, *"Microstructural changes in tungsten exposed at high temperatures"*

18th International Conference on Ion Beam Analyses, Cambridge 7-11 September 2009

- Alves E., L.C. Alves, N P Barradas, R. Mateus, P.A. Carvalho, G.M. Wright, *Erosion and re-deposition processes in JET poloidal tiles studied with ion beams*

- Barradas N. P., R Mateus, M. Fonseca, M.A. Reis, K. Lorenz, I. Vickridge, Thin film depth *profiling using simultaneous particle backscattering and nuclear resonance profiling*

1st International Conference on Frontiers in Diagnostic Technologies, Frascati, 25-27 November 2009

- Jakubowski L., K. Malinowski, M.J. Sadowski, J. Zebrowski, V.V. Plyusnin, M. Rabinski, H. Fernandes, C. Silva, P. Duarte, and M.J. Jakubowski, *"Study of electron beams within ISTTOK tokamak by means of a multi-channel Cherenkov detector; their correlation with hard X-rays"*

European Congress and Exhibition on Advanced Materials and Processes, 6-10 September, Glasgow, UK.

- Mateus R., A.M. Deus, P.A. Carvalho, D. Nunes, J.B. Correia, N. Shohoji, H. Fernandes, C. Silva, N. Barradas, L.C. Alves, E. Alves, *Deuterium retention studies in tungsten*.

- Nunes D., V. Livramento,,J.B. Correia, P.A. Carvalho, R. Mateus, N. Shohoji, H. Fernandes, C. Silva, L.C. Alves, E.Osawa, *A study of Cu/Graphite and Cu/Diamond interfaces reinforced with chromium*.

21st International Conference on Numerical Simulation of Plasmas 2009 ICNSP 09, Lisbon, October, 2009

- Silva F. da et al., "*A numerical study of forward- and back-scattering signatures on Doppler reflectometry signals*"

- Heuraux S., E. Z. Gusakov, A. Yu Popov, F. da Silva, M. Irzak, *"Simulations on the role of the resonance of the probing on the reflectometry measurements in fluctuating plasma"*

- Stankiewicz R., D. P. Coster, A. Figueiredo, D. Kalupin, G.Pereverzov, M. Tokar, D. Twaróg, R. Zagorski, "Verification of *the European Transport Solver for Transport Barrier"*

Seventh IAEA Technical Meeting (IAEA-TM) on Control, Data Acquisition, and Remote Participation for Fusion Research, 15 - 19 June 2009, Aix-en-Provence, France

- Valcárcel D.F., A.S. Duarte, A. Neto, I.S. Carvalho, B.B. Carvalho, H. Fernandes, J. Sousa, F. Sartori, F. Janky, P. Cahyna, M. Hron, R. Pánek, "*Real-Time Software for the Compass Tokamak Plasma Control*".

16th IEEE NPSS Real-Time Conference, May 10-15, 2009, Beijing.

- Batista A.J.N. et al., "*ATCA Control System Hardware for the Plasma Vertical Stabilization in the JET Tokamak"*

- Pereira R.C. et al., "*ATCA Fast Data Acquisition & Processing System for JET Gamma-Ray Cameras Upgrade Diagnostic"*

24.1.4. International Reports

- Baião D., Medina F., Ochando M., Varandas C., *"Feasibility of the Two Filters Method in TJ-II for Electron Temperature Measurements in High Density Plasmas"*, Editorial Ciemat, ISSN: 1135-9420, 1191, December 2009

- Crombé K., Y. Andrew, T.M. Biewer, E. Blanco, M. Brix, P. de Vries, A. Fonseca, C. Giroud, N.C. Hawkes, E. Joffrin, P. Mantica, A. Meigs, V. Naulin, S. Pinches, E. Rachlew, T. Tala, A. Whiteford and JET EFDA contributors, *Influence of Rotational Shear on Triggering and Sustainment of Internal Transport Barriers on JET,* EFDA–JET–CP(09)06/29, 2009.

- Figueiredo A.C.A., J. Ferreira, Y. Andrew, F. Nabais, V. Naulin, A. Sirinelli and JET EFDA contributors, *Measurement and Qualitative Interpretation of the Radial Scale of Turbulence in JET Plasmas*, EFDA–JET–CP(09)06/32, 2009.

- Soldatova S., A. Fonseca, Y. Liangb, J. Fesseyc, A. Sirinellic, A. Krämer-Fleckenb, G. Van Oost1 and JET-EFDA contributors, *Results of reflectometry studies on ELM dynamics in JET,* EFDA–JET–CP(09)06/39, 2009.

24.1.5. Laboratorial Prototypes

- Batista A.J.N., et al, "*192-channel galvanic isolated ATCA Control and Data Acquisition System for the Plasma Vertical Stabilization in the JET Tokamak".*

- Batista A.J.N., et al, "*448-channel galvanic isolated ATCA Control and Data Acquisition System for the Plasma Vertical Stabilization in the COMPASS Tokamak".*

- Pereira R.C. et al, *"24-channel 250 MHz 13-bit ATCA Data Acquisition and Pulse Processing System for the Gamma-ray Camera (DNGG) diagnostic at JET-EFDA".*

- Pereira R.C. et al, *"8-channel 400 MHz 14-bit ATCA Data Acquisition and Pulse Processing System for the Gamma-ray Spectroscopy (GRS) diagnostics at JET-EFDA".*

- Cupido L. "*Hybrid frequency synthesizer/swept frequency generator"* First generation of PLL boards and first version of the FPGA ramp generator assembled together and loaded with a novel FPGA configuration controlling software; to be applied on Reflectometry system for COMPASS.

- Cupido L. "*Advanced Swept Reflectometers equipped with TCPIP remote control and network communications using in house adopted solutions for frequency translator and proprietary ramp generators".* Application:/ JET KG10 reflectometers

- Meneses L., L. Cupido, *"Frequency Translator by Double Frequency Conversion"* Description: Novel layout to generate the frequency translation by double frequency conversion to guarantee the intermediate frequency (IF); Application: JET KG10 reflectometers

24.1.6. Computational codes

- Cruz N., "*HTTP Interface and Control Software for JET Diagnostics - Upgrade*", installed in the KK3f and KG8B diagnostics at the JET-EFDA Tokamak.

- Cruz N., "*MDSPlus Interface and Control Software for TCV Diagnostics and Control Systems*", installed in the Advanced Plasma Control System at TCV, Switzerland, Tokamak.

- Fernandes A. et al, "*Verilog code for Real-time Parallelized Pulse Processing and Data Acquisition for Gamma Spectroscopy*", applied in the Neutron Camera (DNGG) and Gamma-ray Spectroscopy (GRS) systems at JET-EFDA.

- Neto A. et al, "*MARTE - Multi-platform Real-time Framework*" installed at the JET-EFDA, UK and COMPASS, Prague tokamaks.

- Rodrigues P., *"Control and Signal processing Software for the Real Time control system of the PHA-V X-Ray diagnostic of TCV". Installed in the TCV tokamak, Lausanne.*

- Rodrigues P., *"DSP Real Time Control software for Advanced Plasma Control"* installed in the TCV tokamak, Lausanne.

- Santos B. et al, "*Software for Sub-systems control on the COMPASS tokamak*" installed at the COMPASS, Prague tokamak.

- Varela P. and L. Meneses *"automatic calibration of Kg8b heterodyne signals on JET".*

- Varela P. *"Automatic density profile inversion from Lower X mode cutoff"*

24.1.7. PhD. Thesis

- *Sílvia Ramos* "MHD and fast particle mode studies using fast frequency hopping reflectometers on the ASDEX Upgrade tokamak"

- Rui Barrocas Gomes, *"Interaction of a liquid gallium jet with the ISTTOK edge plasma"*

- Teresa Isabel Picoto Pena Madeira Amorim PhD, *"Soft-X-ray Pulse Height Analysis studies on the TCV tokamak"*

- Paula Belo, *"Numerical Simulations of Recycling Impurity Screening on JET".*

24.1.8. Master thesis

- Sérgio Martins Simões Dias, *"Controlo dinâmico com CANBUS de fresadora CNC para objectos alares de grandes dimensões"*, supervised by Bernardo Brotas de Carvalho.

- Diana Filipa Apolónia Medeiro Baião, *"Preliminary studies to implement a new electron temperature diagnostic for the TJ-II plasmas heated with energetic neutral beams"*

- Gama J., *"Nonlinear growth of Neoclassical Tearing modes in a Tokamak Plasma".*

24.1.9. Prizes

- André Cabrita Neto won the prize with its work "MARTe: a Multi-platform Real-time Framework" during the conference held in Beijing, China on 11-15 May 2009. The RT2009 Outstanding Student Awards honored the best student submission accepted for oral presentation and the best student submission accepted for poster. The award is based on the quality of the work as described in the paper submitted. About 200 researchers attended the conference. The awarded work is related with the JET Vertical Stabilization Project where IPFN ATCA solutions are used.

24.1.10. Organizing Committees of Conferences

- Organization of the 17th Real Time Conference, RT2010, which be held from May 24th to May 28th, 2010 at the Instituto Superior Técnico.

- An agreement of a joint project with National Instruments is foreseen. The joint project aims at building an ITER-relevant generic control and data acquisition system.

- The GMD organized the **"**9th International Reflectometry Workshop for Fusion Plasma Diagnostics, IRW9, held in Lisbon, May 2009.

- The GTM organized the 21st International Conference on Numerical Simulation of Plasmas 2009 (October 6-9 2009, Lisbon)

24.1.11. Education and training

- The Group will organize and lecture the Control and Data Acquisition module of the Joint European Doctorate in Fusion Science and Engineering in 2010.

- Three Group members are expected to graduate and obtain a PhD in 2010.

24.2. TECHNOLOGIES OF PLASMAS AND LASERS

24.2.1. Publications in refereed scientific journals

- Abreu R. de and V. Guerra, *"Special relativity as a simple geometry problem"*, Eur. J. Phys. 30, 229 (2009).

- Alves L.L., S. Letout and C. Boisse-Laporte, *"Modeling of surface-wave discharges with cylindrical symmetry"*, Phys. Rev. E 79, 016403 1-18 (2009).

- Alves L.L., R. Álvarez, L. Marques, S. Rubio, A. Rodero and M.C. Quintero, *"Modeling of an axial injection torch"* Eur. Phys. J.: Appl. Phys. 46, 21001 1-10 (2009).

- Atzeni S., A. Schiavi and J. R. Davies, *"Stopping and scattering of relativistic electron beams in dense plasmas and requirements for fast ignition"*, Plasma Phys. Control. Fusion 51 015016 (2009).

- Atzeni S et al, *"Studies on targets for inertial fusion ignition demonstration at the HiPER facility",* Nucl. Fusion 49 055008 (2009)

- Bastos C., O. Bertolami, N. C. Dias and J. N. Prata, *"Noncommutative Quantum Mechanics and Quantum Cosmology",* Int. J. Mod. Phys. A 24, 2741 (2009)

- Bastos C, O. Bertolami, N. C. Dias and J. N. Prata, *"Black Holes and Phase Space Noncommutativity"* to appear in Phys. Rev. D, arXiv:0907.1818 [gr-qc]

- Bernardini A. E. and O. Bertolami *"On the stability of mass varying particle lumps"* to appear in Phys. Rev. D, arXiv:0909.1541 [gr-qc]
- Bento M. C. and O. Bertolami, *"Dark energy and the Rutherford-Soddy radiative decay law",* Phys. Lett. B 675, 231 (2009)
- Bento M. C., A. E. Bernardini and O. Bertolami, *"Coupling dark energy with Standard Model states"*, J. Phys. Conf. Ser. 174, 012060, 2009.
- Bertolami O. and A.D. Zarro, *"Stability conditions for a noncommutative scalar field coupled to gravity",* Lett. B 673, 83, 2009 [arXiv:0812.4607 [hep-th]].
- Bertolami O., C. Carvalho, and J.N. Laia, *"A new source for a braneworld cosmological constant from a modified gravity model in the bulk",* Nuclear Phys., B 807, 56, 2009 [arXiv:0805.1546 [hep-th]].
- Bertolami O. and N. M. C. Santos *"Constraints on unparticle long range forces from big bang nucleosynthesis bounds on the variation of the gravitational coupling",* Phys. Rev. D 79, 127702 (2009)
- Bertolami O., J. Páramos and P. Santos, *"Astrophysical constrains on Ungravity inspired models",* Phys. Rev. D 80, 022001 (2009)
- Bertolami O. and M. C. Sequeira, *"Energy conditions and stability in f(R) theories of gravity with non-minimal coupling to matter",* Phys. Rev. D 79, 104010 (2009)
- Bertolami O. and F. S. N. Lobo, *"Time and Causation",* NeuroQuantol. 7, 1 (2009)
- Bertolami O. and C. A. D. Zarro, *"Stability conditions for a noncommutative scalar field coupled to Gravity",* Phys. Lett. B 673, 83 (2009)
- Bertolami O., *"The Cosmological constant problem: A User's guide"* to appear in Int. J. Mod. Phys. D, arXiv:0905.3110 [gr-qc]
- Bonifacio P.M., C.H.-T. Wang, J.T. Mendonça and R. Bingham, *"Dephasing of a non-relativistic quantum particle due to a conformally fluctuating space-time",* Class. Quant. Grav., 26**,** 145013 (2009).
- Brussard G, et al, "*Electro-optic Measurement of Terahertz Pulse Energy"*, Review of Scientific Instruments (2009) vol. 80 (11) pp. 113103
- Cardoso L et al, *"Increased bandwidth optical parametric amplification of supercontinuum pulses with angular dispersion",* Opt. Letters 34, 1369 (2009).
- Christophe B. et al., *"Odyssey: a Solar System Mission",* Exper. Astron. 23, 529 (2009)
- Davies J R et al, *"Filamented plasmas in laser ablation of solids",* Plasma Phys. Control. Fusion 51 035013 (2009)
- Davies JR, *"Laser absorption by overdense plasmas in the relativistic regime",* Plasma Phys. Control. Fusion 51 014006 (2009)
- Fang F et al, *"Pump depletion limited evolution of the relativistic plasma wave-front in a forced laser-wakefield accelerator",* Plasma Phys. Control. Fusion 51, 024003(2009)
- Ferreira C. M, E. Tatarova, J. Henriques and F. M. Dias, *"Modelling of large-scale microwave plasma sources"* (Review paper)**,** J. Phys. D: Appl. Phys. 42, 194016-1-15 (2009)
- Froula D et al, *"Measurements of the critical power for self-injection of electrons in a laser wakefield accelerator"* Phys. Rev. Letters 103 (221): Art. No. 215006 Nov. 2009
- Gregório J., O. Leroy, P. Leprince, L.L. Alves and C. Boisse-Laporte, *"Design of a Microwave Micro-Plasma Source at Atmospheric-Pressure",* IEEE Trans. Plasma Sci. Special issue on Atmospheric-pressure plasmas: science and applications 37, 797-808 (2009).
- Gregório J., C. Boisse-Laporte and L.L. Alves, *"Fluid modelling of a microwave micro-plasma at atmospheric pressure",* Eur. Phys. J.: Appl. Phys. 49, 13102 1-4 (2010).
- Guerra V., K. Kutasi, M. Lino da Silva, P. A. Sá and J. Loureiro, *"Kinetic simulation of discharges and afterglows in molecular gases",* High Temperature Material Processes (Begell House) 14(1) 135 (2010).
- Isola L. M., B. J. Gómez and V. Guerra, *"Determination of the electron temperature and density in the negative glow of a nitrogen pulsed discharge using optical emission spectroscopy"*, J. Phys D: Appl. Phys. 43, 015202 (2010).
- *Kirby N et al., "*Transverse emittance and current of multi-GeV trapped electrons in a plasma wakefield accelerator"*, Physical Review Special Topics: Accelerators and Beams, 12, 051302.*
- Kneip S et al, *"Near-GeV Acceleration of Electrons by a Nonlinear Plasma Wave Driven by a Self-Guided Laser Pulse"*, Physical Review Letters 103, 035002 (2009);
- Kutasi K., C. D. Pintassilgo and J. Loureiro, *"An overview of modelling of low-pressure post-discharge systems used for plasma sterilization"* Journal of Physics: Conference Series 162(1), 012008 (2009).
- Lallement L., A. Rhallabi, C. Cardinaud, M.C. Peignon-Fernandez and L.L. Alves, *"Global model and diagnostic of a low-pressure SF6/Ar inductively coupled plasma",* Plasma Sources Sci. Technol. 18, 025001 1-10 (2009).

- Lambert et al, *"An optimized kHz two-colour high harmonic source for seeding free-electron lasers and plasma-based soft x-ray lasers",* New Journal of Physics, 11, 083033 (2009)

- Last I et al, *"dt nuclear fusion within a single Coulomb exploding composite nanodroplet"*, European Physical Journal D 54, 71 (2009);

- Lemos, N et al, *Design and characterization of supersonic nozzles for loose focus laser-plasma interactions*, Review of Scientific Instruments (2009) vol. 80 (10) pp. 103301

- Marques L., H.M. Pinto, A.C. Fernandes, O. Banakh, F. Vaz and M.M.D. Ramos, *"Optical properties of titanium oxycarbide thin films"*, Applied Surface Science 255, 5615 (2009).

- Marques L., S. Carvalho, F. Vaz, M.M.D. Ramos and L. Rebouta, *"Ab initio study of the properties of Ti1-x-ySixAlyN solid solution"*, Vaccum (2009), [DOI: 10.1016/j.vacuum.2009.03.011].

- Martins A.M., V. Vieira, J. T. Mendonça and A. Guerreiro, *"Temporal interferometer for trapped electrons",* submitted to Phys. Rev. A (2009).

- Martins A.A. e M.J. Pinheiro, "Fluidic electrodynamics: Approach to electromagnetic propulsion," Phys. Fluids 21, 097103 (2009) (7 pages) ; doi:10.1063/1.3236802

- Martins SF et al, *"Ion dynamics and acceleration in relativistic shocks",* Astrophysical Journal Letters 695, L189-L193 (2009);

- Mendonça JT, *"Laser wakefield acceleration in the Tetawatt regime",* Plasma Physics and Controlled Fusion, 51, 2, 024007, 2009

- Mendonça JT, *"Plasmons with orbital angular momentum",* Physics of Plasmas, 16, 112103, 2009

- Mendonça J.T., *"Laser acceleration in the Peta-Watt regime"* (invited paper), Plasma Phys. Controll. Fusion, 51, 024007 (2009).

- Mendonça J.T., J. Loureiro and H. Terças, *"Electromagnetic waves in Rydberg plasmas"*, J. Plasma Phys., 75, 713 (2009).

- Mendonça, J.T. *"Photon Landau damping of relativistic plasma waves"*, Proceed. SPIE, (2009).

- Mendonça J.T., B. Thidé and H. Then, *"Stimulated Raman and Brillouin backscattering of collimated beams carrying orbital angular momentum"*, Phys. Rev. Lett., 102, 185005 (2009).

- Mendonça J.T., *"Time Refraction in Expanding Plasma"*, New J. Phys., 11, 013029 (2009).

- Mendonça J.T., P.K. Shukla and R. Bingham, *"Nonlinear excitation of zonal flows by Rossby wave turbulence"*, New J. Phys., 11, 073038 (2009).

- Mendonça J.T and S. Eliezer, *"Nuclear and particle physics with ultraintense lasers"*, in Applications of Laser-Plasma Interactions, edited by S. Eliezer and K. Mima, CRC Press, Taylor and Francis, Boca Raton (2009), pages 143-179.

- Mendonça J.T., *"Acceleration of Photons and Quasi-Particles"*, in Laser-Plasma Interactions, edited by D.A. Jaroszynski, R. Bingham and R.A. Cairns, CRC Press, Taylor and Francis, Boca Raton (2009), pages 219-229.

- Mendonça J.T., *"New effects in quantum vacuum: photon undulator and transition radiation"*, J. Phys. A: Math.Theor, 42, 375403 (2009).

- Mendonça J.T., S. Ali and B. Thidé, *"Plasmons with orbital angular momentum"*, Phys. Plasmas, 16, 112103 (2009).

- Mendonça J. T., J. Loureiro and H. Terças, *"Waves in Rydberg plasmas"*, Journal of Plasma Physics 75(6), 713 (2009).

- Mocek T, Rus B, Kozlova M, et al., *"Plasma-based X-ray laser at 21 nm for multidisciplinary applications",* European Physical Journal D 54: 439 (2009)

- Mrázková M., P. Vašina, V. Kudrle, A. Tálský, C. D. Pintassilgo and V. Guerra, *"On the nitrogen addition into nitrogen post-discharges",* J. Phys. D: Appl. Phys. 42, 075202 (2009).

- Nagler B et al, *"Turning solid aluminium transparent by intense soft X-ray photoionization"*, Nature Physics 5, 693 (2009)

- Nelson, AJ et al, *"Soft x-ray free electron laser microfocus for exploring matter under extreme conditions"*, Optics Express 17(20), 18271 (2009)

- Norreys PA et al, *"Intense laser-plasma interactions: New frontiers in high energy density physics",* Physics of Plasmas 16, 041002 (2009);

- Norreys PA et al, *"Recent fast electron energy transport experiments relevant to fast ignition inertial fusion",* Nucl. Fusion 49, 104023 (2009)

- Oliva E et al, *"Optimization of soft x-ray amplifier by tailoring plasma hydrodynamics"*, Optics Letters, Vol. 34, Issue 17, pp. 2640-2642 (2009)

- Peano F, J Vieira, R Mulas, G Coppa, R Bingham and LO Silva *"Prospects for all-optical ultrafast muon acceleration",* Plasma Physics and Controlled Fusion, 51, 2, 024006, 2009

- Peano F et al, *"Statistical kinetic treatment of relativistic binary collisions"*, Physical Review E 79, 025701(R) (2009);

- Peano F et al, *"Prospects for all-optical ultrafast muon acceleration"*, Plasma Physics and Controlled Fusion 51, 024006 (2009);

- Pinheiro M. J., "*On Newton's third law",* arXiv:0901.3726v1 [physics.class-ph], 2009

- Ping Y, et al, *"Development of a nanosecond-laser-pumped Raman amplifier for short laser pulses in plasma",* Physics of Plasmas 16(12): Art. No. 123113 Dec 2009

- Pintassilgo C. D., O. Guaitella and A. Rousseau, *"Heavy species kinetics in low-pressure dc pulased discharges in air"* Plasma Sources Science and Technology 18, 025005, 2009.

- Pintassilgo C. D. and J. Loureiro*,"Production of hyrocarbons and nitriles using a N_2-CH_4 and afterglow plasma for simulation of Titan's atmosphere"*, Planetary and Space Science 57(13), 1621, 2009.

- Pinto H. M., J. Coutinho, M. M. D. Ramos, F. Vaz and L. Marques, *"First principles study of point defects in titanium oxycarbide"*, Mat. Sci. & Eng. B, 2009 [DOI: 10.1016/j.mseb.2009.08.011].

- Ravasio et al, *Single-shot diffractive imaging with a table-top femtosecond soft X-ray laser-harmonics sources*, Physical Review Letters, 103, 028104, 2009.

- Romeiras, F.J., *"Exact travelling wave solutions of the generalized Bretherton equation",* Applied Mathematics and Computation, 215 (2009) 1791-1805.

- Serbeto A., L. F. Monteiro, K. H. Tsui and J. T. Mendonça, *"Quantum plasma fluid model for high-gain free-electron lasers"*, Plasma Phys. Controll. Fusion, 51**,** 124024, 2009.

- Silva LO et al, *"Laser electron acceleration with 10 PW lasers"*, Compte Rendus Physique 10, 167 (2009); (Invited paper)

- Silva M. Lino da, J. Loureiro and V. Guerra, *"Nonequilibrium dissociation and recombination rates in nitrogen: From shock waves to discharge conditions",* Chemical Physics 358(1-2), 123 (2009).

- Silva M. Lino da, V. Guerra and J. Loureiro, *"A Review of Non-Equilibrium Dissociation Rates and Models for Atmospheric Entry Studies"*, Plasma Sources Sci. Technol. 18, 034023 (2009).

- Shukla PK *"Generation of wakefields by electromagnetic waves in a magnetized electron-position-ion plasma",* Plasma Physics and Controlled Fusion, 51, 2, 024013, 2009.

- Shukla N,et al, *"Nonlinear electromagnetic wave equations for superdense magnetized plasmas",* Physics of Plasmas 16(8): Art. No. 089904 AUG 2009

- Shukla N, Shukla PK, Stenflo L, *"Magnetization of a warm plasma by the non-stationary ponderomotive force of an electromagnetic wave",* Physical Review E 80(2): Art. No. 027401, Aug 2009

- Sousa J. Santos, G. Bauville, B. Lacour, V. Puech and M. Touzeau, *"Atmospheric Pressure Generation of $O_2(a^1\Delta_g)$ by Microplasmas"*, Eur. Phys. J.: Appl. Phys. 47, 22807, 2009.

- Sun J, Gallacher J, Brussaard G, Lemos N, Issac R, Huang Z, Dias JM, Jaroszynski D, *Electro-optic measurement of terahertz pulse energy*, Review of Scientific Instruments 80 (11): 113103, 2009

- Tanimoto T et al, *"Measurements of fast electron scaling generated by petawatt laser systems",* Phys. Plasmas 16 062703, 2009

- Tatarova E., E. Felizardo, F. M. Dias, M. Lino da Silva, C. M. Ferreira and B. Gordiets, *"Hot and super-hot hydrogen atoms in microwave plasma"*, Appl. Phys. Lett. 95, 181503 - 1-3, 2009.

- Tatarova E., F. M. Dias and C. M. Ferreira, *"Hot hydrogen atoms in a water-vapor microwave plasma source"*, Int. J. Hydrogen Energy 34, 9585-9590, 2009.

- Terças H., J.T. Mendonça and G.R.M. Robb, *"Two-stream instability of quasi-one-dimensional Bose-Einstein condensates"*, Phys. Rev. A, 79, 065601, 2009.

- Trines RMGM, CD Murphy, KL Lancaster, O Chekhlov, PA Norreys, R Bingham, JT Mendonça, LO Silva, SPD Mangles, C Kamperidis, A Thomas, K Krushelnick and Z Najmudin, *"Photon acceleration and modulational instability during wakefield excitation using long laser pulses",* Plasma Physics and Controlled Fusion, 51, 2, 024008, 2009.

- Trines RMGM et al, *"Applications of the wave kinetic approach: From laser wakefields to drift wave turbulence",* Physics of Plasmas 16, 055904, 2009;

- Trines R et al, *"Photon acceleration and modulational instability during wakefield excitation using long laser pulses"*, Plasma Physics and Controlled Fusion 51, 024008, 2009;

- Tonge J et al, *"A simulation study of fast ignition with ultrahigh intensity lasers"*, Physics of Plasmas 16, 056311, 2009;

- Tzoufras M et al, *"Beam loading by electrons in nonlinear plasma wakes"*, Physics of Plasmas 16, 056705, 2009;

- Turyshev S. G. et al., *"Advancing fundamental physics with the Laser Astrometric Test of Relativity",* Exp. Ast. 10.1007/s10686-009-9170-9, 2009.

- Weigand R., J.T. Mendonça and H. Crespo, *"Cascaded non-degenerate four-wave-mixing technique for high-power single-cycle pulse synthesis in the visible and ultraviolet ranges"*, Phys. Rev. A, 79, 063838 (2009).

- Willingale L, et al, *"Characterization of High-Intensity Laser Propagation in the Relativistic Transparent Regime through Measurements of Energetic Proton Beams",*, Phys. Rev. Lett. 102, (12), 125002, 2009.

- Wijtvliet R., E. Felizardo, E. Tatarova, F. M. Dias, C. M. Ferreira, S. Nijdam, E. Veldhuizen, and G. Kroesen, *"Spectroscopic investigation of wave driven microwave plasmas",* J. Appl. Phys. 106**,** 103301, 2009.

- Wolf P. et al., *"Quantum physics exploring gravity in the outer solar system: the SAGAS project"* Exper. Astron. 23, 651 (2009)

24.2.2. Contributions in Conferences and Workshops

Colloquium on Scientific and Fundamental Aspects of the Galileo Programme, Padua, Italy, 14-16 October 2009

- Páramos J. and O. Bertolami, *"The Galileo satellite constellation and modifications to the inverse-square law for Gravitation",* arXiv:0910.3413 [gr-qc].

Invisible Universe International Conference, Paris, 29 June-3 July 2009

- Bertolami O. and M. C. Sequeira, *"Modified theories of Gravity with non-minimal curvature-matter coupling",* arXiv:0910.3876 [gr-qc],

- Bertolami O. and C. A. D. Zarro, *"Stability conditions for a noncommutative scalar field coupled to gravity via the positive energy theorem",* arXiv:0910.3886 [hep-th]

31st International Electric Propulsion Conference, University of Michigan • Ann Arbor, Michigan • USA, September 20 – 24, 2009.

- Mota S., D.P. Resendes and L. Cupido, *"Plasma Reflectometry Applied to Plume Density Measurements of Electric Propulsion Thrusters"*

36th EPS Conference on Plasma Physics, Sofia, Bulgaria 2009,

- Bendoyro R. A., C. Russo, M. Hilbert, J. Jiang, G. Figueira, F. Fiúza, R. Fonseca, L. O. Silva, N. C. Lopes, "*Coupling of high-intensity lasers to plasma channels"*

- Cardoso L., M. Marti, N. C. Lopes, "*Secondary radiation from multi-GeV protons generated in laser-solid interactions in ELI, L. PIC modeling of ion acceleration with laser intensities in excess of 1024 W/cm2"*

- Felizardo E., E. Tatarova, F.M. Dias, C.M. Ferreira and B. Gordiets, *"Microwave Air-Water Plasma Torch, Experiment and Theory"*

- Fiúza F, Martins SF, Fonseca RA, Joshi C, Silva LO, "*High brilliance synchrotron radiation from the plasma magnetic mode"*

- Fonseca RA, Martins SF, Abreu P, Fiúza F, Silva LO, "*Using state of the art processing units for hardware acceleration of PIC codes"*

- Gargaté L, Fonseca RA, Niemiec J, Bingham R, Silva LO, "*Magnetic field amplification and saturation mechanisms for the non-resonant Bell instability in astrophysical shocks"*

- Henriques J., F.M. Dias, E. Tatarova, and C.M. Ferreira, *"Hot Hydrogen Atoms in a Microwave Ar – N2 – H2 Wave Driven Plasma Torch"*, Proceed. p. 2.112.

- Kneip S, Nagel SR, Martins SF, Bellei C, Cheklov O, Clarke RJ, Dangor AE, Delerue N, Divall EJ, Doucas G, Ertel K, Fiúza F, Fonseca RA, Foster P, Hawkes SJ, Heathcote R, Hooker CJ, Krushelnick K, Mori WB, Palmer C, Ta Phuoc K, Rajeev P, Schreiber J, Streeter MJV, Urner D, Vieira J, Silva LO, Najmudin Z, "*Near GeV acceleration of electrons by a non-linear plasma wave driven by a self-guided laser pulse, Mangles SPD"*

- Jiang J., C. Russo, F. Fiúza, R. A. Fonseca, M. Fajardo, L. O. Silva, N. C.Lopes, "*Compact HHG seeded Free-Electron-Laser based on laser-plasma"*

- Lemos N., J. Berardo, J. M. Dias, R. Onofrei, N. C. Lopes, G. Figueira, F. Fiuza, L.O. Silva, R. C. Issac, D. A. Jaroszynski, "*Plasma waveguides created by ultra-short laser pulses"*

- Martins SF, Fonseca RA, Mori WB, Silva LO, "*Ion dynamics and acceleration in relativistic shocks"*

- Martins JL, Martins SF, Fonseca RA, Silva LO, "*Numerical modeling of radiation in Weibel turbulence"*

- Russo C., R. A. Bendoyro, M. Hilbert, J. Jiang, G. Figueira, N. C. Lopes, "*Improving the reproducibility of plasma channels formed by electric discharges in structured gas cells"*

- Soural I., V. Guerra, M. Lino da Silva, P. A. Sá and F. Krčma, *"The Importance of Discharge Current in the Formation of the Pink Afterglow of a Nitrogen DC Discharge"*, Conference Abstracts 33E P-2.103

- Vieira J, Fonseca RA, Silva LO, Huang C, Mori WB, "*Spin precession of electron beams in plasma based acceleration"*

7th International Workshop on Microwave Discharges: Fundamentals and Applications, Hamamatsu, Japan 2009

- Dias F.M., E. Tatarova, E. Felizardo, J. Henriques and C.M. Ferreira, *"Microwave Plasmas Torches Driven by Surface Waves"*

62nd Gaseous Electronics Conference, Saratoga Springs, NY, USA 2009

- Alves L.L., R. Álvarez, L. Marques, S.J. Rubio, A. Rodero and M.C. Quintero, *"Modeling of a microwave plasma torch"* Bull. Am. Phys. Soc. 54, 44 (2009).

- Alves L.L., V. Guerra, C. Lopez and J. Cotrino, *"Line intensities in nitrogen low-pressure microwave discharges"*, Bull. Am. Phys. Soc. 54, 34, 2009.

- Felizardo E., E. Tatarova, F. M. Dias, M. Lino da Silva, C. M. Ferreira and B. Gordiets, *"Super Hot Hydrogen Atoms in Microwave Plasmas"*, Bull. Am. Phys. Soc. 54 (12), 36, 2009.

- Felizardo E., M. Pencheva, E. Benova, F. M. Dias, and E. Tatarova, *"Microwave Argon Plasma Torch"*, Bull. Am. Phys. Soc. 54 (12), 46 (2009)

- Gregório J., C. Boisse-Laporte and L.L. Alves *"Fluid modeling of a microwave micro-plasma at atmospheric pressure"*, Bull. Am. Phys. Soc. 54, 44 (2009).

- Gregório J., O. Leroy, P. Leprince, C. Boisse-Laporte and L.L. Alves, *"Microwave micro-plasma sources at atmospheric pressure"*, Bull. Am. Phys. Soc. 54, 44 (2009).

- Henriques J., F.M. Dias, E. Tatarova, and C.M. Ferreira, *"Wave Driven Ar – N2 – H2 Plasma Torch"*, Bull. Am. Phys. Soc. 54 (12), 47 (2009).

- Marques L., C.D. Pintassilgo, L.L. Alves, G. Alcouffe and G. Cernogora, *"Modeling of capacitively coupled radio-frequency discharges in nitrogen"*, Bull. Am. Phys. Soc. 54, 39 (2009).

- Sousa J. Santos, G. Bauville, B. Lacour, P. Jeanney, L. Magne and V. Puech, *"Spectroscopic Investigations of an Atmospheric Pressure Singlet Oxygen Plasma Source"*, Bull. Am. Phys. Soc. 54, 43 (2009).

5th International Workshop on Fundamentals and Applications of Microplasmas, San Diego, California, USA 2009.

- Gregório J., L.L. Alves, P. Leprince, O. Leroy and C. Boisse-Laporte, *"Study of a microwave micro-plasma reactor at atmospheric pressure"*

- Gregório J., C.Boisse-Laporte and L.L.Alves, *"Fluid modeling of microwave micro-plasmas at atmospheric pressure"*

17th International Colloquium on Plasma Processes (Société Française du Vide, ed.), Marseille, France 2009

- Alves L.L., R. Álvarez and L. Marques, *"Modelling of an axial injection torch"*

- Gregório J., C.Boisse-Laporte and L.L.Alves, *"Modelling of microwave micro-plasmas at atmospheric pressure"*

- Marques L., C.D. Pintassilgo, G. Alcouffe, G. Cernogora e L.L.Alves, *"Modelling of capacitively coupled radio-frequency discharges in nitrogen"*

- Sarrette J. P., S. Cousty, N. Merbahi, A. Nègre-Salvayre, F. Clément, J. Santos Sousa and V. Puech, *"Observation of Antibacterial Effects Obtained at Atmospheric and Reduced Pressures in Afterglow Conditions"*

29th ICPIG, International Conference on Phenomena in Ionized Gases, Cancun, Mexico, July 2009.

- Guerra V., "*Atom recombination at surfaces"*

- Kutasi K., V. Guerra, P. Sá and J. Loureiro, "UV Radiation in Ar-O_2, N_2-O_2 and Ar-O_2-N_2 Microwave Discharges and Post-discharges"

- Marques L., C.D. Pintassilgo, G. Alcouffe, G.Cernogora and L.L. Alves, *"Modelling of capacitively coupled radio-frequency discharges in nitrogen"*

- Pintassilgo C. D., V. Guerra, O. Guaitella and A. Rousseau, *"Study of an afterglow of a low-pressure dc pulsed discharge in air"*

IX International Conference on Atomic and Molecular Pulsed Lasers, Tomsk, Russia 2009.

- Lacour B., X. Aubert, G. Bauville, F. Carlin, C. Levy, V. Martin, V. Puech and J. Santos Sousa, *"Microbiological Efficiencies of Excilamps and Flash-lamps: Comparison and Perspectives"*

VIIth International Workshop on Microwave Discharges: Fundamental and Applications, Hamamatsu, Japan 2009

- Alves L.L., R. Álvarez and L. Marques, *"Modelling of an axial injection torch"*

- Gregório J., C.Boisse-Laporte and L.L.Alves, *"Modelling of microwave micro-plasmas at atmospheric pressure"*

21st International Conference on Numerical Simulation of Plasmas, Lisbon, Portugal 2009

- Abreu P, Fonseca RA, Pereira JM, Silva LO, "*PIC codes in new processors: a full relativistic PIC code in CUDA enabled hardware with real-time visualization"*

- Fiuza F, Fonseca RA, Silva LO, Tonge J, May J, Mori WB, "*Numerical techniques for large-scale PIC simulations of fast ignition"*

- Gargaté L, Fonseca RA, Bingham R, Silva LO, "*dHybrid: a 3D kinetic ion fluid electron code for space and astrophysical plasma simulations"*

- Gregório J., C.Boisse-Laporte and L.L.Alves *"Fast time-relaxation algorithm to solve plasma fluid-equations"*, CD-Proceed. P2.035.

- Martins JL, Martins SF, Fonseca RA, Silva LO, "*Full radiation calculations based on PIC particle tracking"*

- Marti M, Vranic M, Cardoso L, Lopes N, Fonseca RA, Silva LO, "*Ion acceleration from ultra intense lasers interacting with solid hydrogen targets: a parametric study of the ELI regime"*

- Martins SF, Fonseca RA, Lu W, Mori WB, Silva LO, "*Ultra-fast full-PIC simulations of LWFA in boosted frames"*

- Pathak VB, Martins JL, Fonseca RA, Silva LO, "*Assessing the role of bandwidth effects and frequency fluctuation in laser wake field generation with ensemble averaged PIC simulations"*

- Vieira J, Fonseca RA, Silva LO, Huang C, Mori WB, "*Examining electron beam spin conditioning using particle-tracking simulations in QuickPIC"*

19th International Symposium on Plasma Chemistry), ISPC-19 Bochum, Germany, July 2009.

- Kutasi K., V. Guerra, P. A. Sá and J. Loureiro, *"Active Species in Ar-O2 and Ar-O2-N2 Flowing Microwave Discharges and Post-discharges"*

2nd ICAPT (2th International Conference on Advanced Plasma Technologies), Piran, Slovenia, September 2009.

- Kutasi K., V. Guerra, P. A. Sá e J. Loureiro, *"O-atoms in Ar-O_2 surface wave microwave discharges and post-discharges"*

3rd European Conference for Aero-Space Sciences, 6-9 Jul 2009, Versailles, France.

- Le Quang D., Lino da Silva M., and Dudeck M., *"Non Equilibrium Plasma Flows in a Low-Pressure Supersonic Arcjet Facility"*

47th AIAA Aerospace Sciences Meeting, 5-8 Jan 2009, Orlando, Florida, USA.

- Lino da Silva M., Sobbia R., and Witasse O., *"Radiative Trail of the PHOENIX Entry"*, AIAA paper 2009-1032

9th International School for Space Simulations, Paris (France), 2nd-10th July 2009

- Alves E. P., L. Gargaté, R. A. Fonseca, R. Bingham, L. O. Silva, "*Mini-Magnetospheres: High-Energy Particle Deflection"*

Particle Accelerator Conference, Vancouver, Canada, May 4-8 2009

- Lu W, Martins SF, Lu W, Joshi C, Mori WB, "*Improving the reliability of a LWFA with ionization induced trapping*"

- Martins JL, Martins SF, Fonseca RA, Silva LO, Joshi C, Mori WB, "*Emission of collimated x-ray radiation in laser-wakefield experiments using particle tracking in PIC simulations"*

- Martins SF, Fonseca RA, Lu W, Mori WB, Silva LO, "*Boosted frame PIC simulations of LWFA: Towards the energy frontier"*

- Tsung FS, Martins SF, Tsung F, Joshi C, Mori WB, "*Acceleration of ions via a shock compression in a critical density plasma using a CO2 laser"*

KITP Conference: Nonlinear Processes in Astrophysical Plasmas: Particle Acceleration, Magnetic Field Amplification, and Radiation Signatures, Santa Barbara, California, USA, September 28 - October 2, 2009

- Gargaté L., R. A. Fonseca, J. Niemiec, M. Pohl, R. Bingham, L. O. Silva, "*Hybrid simulations of the saturation phase of the non-resonant Bell instability"*

- Martins JL, Martins SF, Fonseca RA, Silva LO, "*Radiation in Weibel/Current Filamentation Turbulence"*

Inertial Fusion Science and Applications (IFSA), San Francisco (USA), September, 2009

- Fiuza F, Fonseca RA, Silva LO, Tonge J, May J, Mori WB, and Ren C, "*On the role of relativistic shocks in fast ignitor scenarios"*

- May J, Tonge J, Mori WB, Fiuza F, Fonseca RA, and Silva LO, "*Investigations into the mechanism of electron acceleration by high intensity lasers at sharp matter interfaces"*

- Tonge J, May J, Mori WB, Fiuza F, Fonseca RA, and Silva LO, "*On the Advantages of Fast Ignition with Ultra High Intensity Lasers"*

51th Annual Meeting of the Division of Plasma Physics, Atlanta, 2009

- Kirkwood R.K, Y. Ping, S.C. Wilks, N. Meezan, P. Michel, E.A. Williams, D. Clark, L.J. Suter, O.L. Landen, N.J. Fisch, E.O. Valeo, V. Malkin, J. Wurtele, T.L. Wang, S.F. Martins, C. Joshi, "*Light Amplification by Seeded Stimulated Raman Scattering of a Crossing Beam and Its Saturation as is Relevant to Ignition Experiments"*

- Fiuza F, Fonseca RA, Silva LO, Tonge J, May J, Mori WB, Ren C, "*On the role of relativistic shocks in fast ignition"*

- Tonge J, May J, Mori WB, Fiuza F, Fonseca RA, Silva LO, Ren C, "*On the Advantages of Fast Ignition with Ultra-High Intensity Lasers"*

- A. Pak, K.A. Marsh, S.F. Martins, W. Lu, W.B. Mori, C. Joshi, "*Injection and Trapping of Tunnel Ionized Electrons into Laser Produced Wakes"*

- May J, Tonge J, Mori WB, Fiuza F, Fonseca RA, Silva LO, Ren C, "*Electron Acceleration by High Intensity Lasers at Sharp Matter Interfaces"*

- Martins JL, Martins SF, Fonseca RA, Silva LO, "*Radiation emission in electron/proton Weibel scenarios"*

- Gargaté L, Fonseca RA, Niemiec J, Bingham R, Silva LO, "*The nonlinear phase of the non-resonant cosmic ray-driven Bell instability"*

- Kneip S, Mangles SPD, Palmer CAJ, Nagel SR, Bellei C, Schreiber J, Najmudin Z, McGuffey C, Chvykov V, Dollar F, Huntington C, Kalintchenko G, Maksimchuk G, Matsuoka T, Thomas AGR, Yanovsky V, Krushelnick K,

Martins JL, Martins SF, Fonseca RA, Silva LO, Ta Phuoc K, "*Laser Plasma Wiggler"*

- Silva LO, Fiuza F, Martins SF, Fonseca RA, Joshi C, "*Harnessing the plasma magnetic mode for the generation of brilliant synchrotron radiation"*

- Fonseca RA, Martins SF, Abreu P, Martins JL, Fiuza F, Vieira J, Silva LO, Decyk VK, Tsung F, Tonge J, Mori WB, "*New features in OSIRIS 2.0"*

- Vieira J, Fonseca RA, Silva LO, Huang C, Mori WB, "*Acceleration of polarized electron beams in plasma-based accelerators"*

- Pathak VB, Martins JL, Fonseca RA, Silva LO, "*Effect of frequency and phase fluctuations in multi laser beam systems on wakefield excitation"*

- Decyk VK, Singh TV, Abreu P, Fonseca RA, Silva LO, "*Designing Particle-in-Cell Algorithms for Advanced Computer Architectures: Application to GPUs"*

- Vranic M., J. L. Martins and L. O. Silva, "*Comparison of radiaton cooling models for particle-in-cell simulations"*

Light at Extreme Intensities, Brasov, Oct. 2009

- Celso P. João, João Wemans, Gonçalo Figueira, "*Numerical model for a hybrid Yb/Nd laser chain at 1053 nm"*

- Figueira Gonçalo, Tayyab Imran, "*Efficient white-light continuum generation in transparent solid media using ~ 250 fs, 1053 nm laser pulses"*

- Lemos N., J. Berardo, N. C. Lopes, G. Figueira, F. Fiuza, D. A. Jaroszynski,, L. O. Silva, and J. M. Dias , "*Ultra-short laser pulses generate plasma channels suitable for guiding high intensity laser beams"*

- Pires Hugo, Luis Cardoso, João Wemans, Gonçalo Figueira, "*OPCPA modeling using YCOB as the non-linear crystal"*

- Sardinha A., M. Fajardo, E. Abreu, J. Miranda, G Figueira, T. Imran, J. M. Dias, N. Lemos, N. Lopes, R. Bendoyro, R. Onofrei, Ph. Zeitoun, G. Rey, D. Douilllet, M. Kozlova, "*Generation of tunable High-order Harmonics"*

31st International Free Electron Laser Conference, Liverpool, UK, 23-28 May 2009

- Jiang J., N. C. Lopes, "*Neutral gas aided electron propagation in free electron lasers"*

Laser and Plasma Workshop 2009, Kardamili, Greece, June 2009

- Lemos N., J. Berardo, N. C. Lopes, G. Figueira, F. Fiúza, D. A. Jaroszynski, L. O. Silva, J. M. Dias, "*Field ionization heating can generate plasma channels suitable for guiding"*

- Lemos N., J. Berardo, N. C. Lopes, G. Figueira, F. Fiuza, D. A. Jaroszynski, L. O. Silva, and J. M. Dias, "*Field ionization can generate plasma channel suitable for guiding"*

- Russo C., R. A. Bendoyro, M. Hilbert, J. Jiang, G. Figueira, N. C. Lopes, "*Improving the reproducility of plasma channels formed by electric discharges in structured gas cells"*

36th International Conference on Plasma Science (ICOPS09),May 31 – June 5, 2009, San Diego, California, US

- Lopes N. C. , C. Russo, R. A. Bendoyro, M. Hilbert, J. Jiang, C. E. Clayton, F. Fang, "*Plasma Channels for Multi-Gev Laser-Plasma Accelerators Using Discharges in Structured Gas Cells"*

7th International Workshop on Microwave Discharges: Fundamentals and Applications, 5, Hamana-Iake, Japan, September 2009.

- Guerra V., K Kutasi, P. A. Sá, and J. Loureiro, *"Kinetic Modeling of a Ar-O_2 Flowing Afterglow for Plasma Sterilization"*

International School on True-Nano Plasma Science and Technology, Shizuoka University, Japão, Setembro de 2009.

- Guerra V., *"Dark sates and energy transfers in the nitrogen pink afterglow"*

17th Symposium on Application of Plasma Processes & Visegrad Workshop on Research of Plasma Physics (SAPP XVII), Slovakia, January 2009.

- Kutasi K., V. Guerra, J. Loureiro, C. D. Pintassilgo and Paulo Sá, *"Plasma Sterilization: the Applicability of Discharge and Post-discharge Plasmas for Medical Sterilization"*

24.2.2.1. Papers in conference proceedings

- Clayton CE et al, "*Towards a compact 0.1-10 MeV broadband betatron photon source"*, Proceedings of SPIE (2009) vol. 7359 pp. 735902

- Fiuza F and Silva LO, "*Short-wavelength plasma undulators"*, AIP CONFERENCES PROCEEDINGS 1086: 561 JAN 2009;

- Fiuza F et al, "*Short-wavelength magnetic structures from the plasma magnetic mode and their applications"*, Proceedings of SPIE (2009) vol. 7359 pp. 73590J

- Martins SF et al, "*Boosted frame PIC simulations of LWFA: Towards the energy frontier"*, Particle Accelerator Conference, Vancouver, Canada.

- Martins JL et al, "*Radiation post-processing in PIC codes",* Proceedings of SPIE (2009) vol. 7359 pp. 73590V

- Martins SF, Vieira J, Fiuza F, Fonseca RA, Huang C, Lu W, Mori WB, Trines R, Norreys P, and Silva LO, "*Numerical simulations of LWFA for the next generation of laser systems"*, AIP Conference Proceedings 1086: 285 JAN 2009;

- Martins SF, Fonseca RA, Lu W, Mori WB, Silva LO, "*Boosted frame PIC simulations of LWFA: Towards the energy frontier"*, Particle Accelerator Conference proceedings (in press)

- Martins SF, Fonseca RA, Lu W, Mori WB, Silva LO, "*Exploring the future of laser-plasma acceleration with massively parallel simulations in OSIRIS"*, First International Conference "Light at Extreme Intensities" LEI'09 (in press)

- Paul K, Huang C, Bruhwiler DL, Mori WB, Tsung FS, Cormier-Michel E, Geddes CGR, Cowan B, Cary JR, Esarey E, Fonseca RA, Martins SF, Silva LO, "*Benchmarking the codes VORPAL, OSIRIS, and QuickPIC with Laser Wakefield Acceleration Simulations"*, AIP Conference Proceedings 1086: Art. No. 315 2009

- Shukla N, Moselem WM and Shukla PK, "*Electrostatic Solitary waves in multi-competent non-thermal plasma"*, J. Plasma Fusion Res. series 8: Art. No. 0302 Sep 2009

24.2.2.2.Invited talks

- Alves L.L., J.Gregório, O.Leroy, P.Leprince and C.Boisse-Laporte, *"Microwave micro-plasma sources at atmospheric pressure: simulation and experiment"*, Proceed. VIIth International Workshop on Microwave Discharges: Fundamentals and Applications, Hamamatsu, Japan 2009 (to be published).

- Davies JR, "*Discussion Panel on Key Uncertainties and Future Development Paths for the Various Approaches to Ignition"*, ULIS 2009, May 2009, Frascati, Italy, with Dunne M, Batani D and Roth M.

- Davies JR, "*Resistive Magnetic Field Generation by Fast Electrons: Conditions for Magnetic Collimation"*, 7th Direct Drive and Fast Ignition Workshop, May 2009, Prague, Czech Republic.

- Fajardo M, "*Tabletop Ultra Intense XUV Sources"*, 1st Porto Workshop on Sources of Super-intense and Ultrashort Laser Pulses, 26-28 Oct 2009

- Felizardo E., F. M. Dias, E. Tatarova, G. Ferreira, J. Henriques, and C. M. Ferreira, *"Microwave plasma torches driven by surface waves for bacteria treatment"*, in "Plasma for Environmental Issues" (E. Tatarova, A. Ricard and E. Benova, eds.) Artgraf, Sofia 2009, pp. 159-168.

- Fiuza F, "*Short-wavelength magnetic structures from the plasma magnetic mode and its applications"*, SPIE Conference Optics and Optoelectronics, Prague (Czech Republic), APR 2009

- Fonseca RA, "*Aceleradores Laser-Plasma a caminho da Fronteira de Energia: 10 GeV e mais além"*: um projecto aprovado no âmbito da DECI – DEISA Extreme Computing Initiative", Encontro Ciência em Portugal - Ciência 2009, Lisboa, Portugal, July 2009.

- Fonseca RA, "*Numerical modeling with Petaflop machines: making direct contact between experiment and simulation, Plasma"*, Computation and Mathematics Meeting, Ambleside, Cumbria, UK, July 2009.

- Gargaté L, "*Nonlinear evolution of the cosmic ray-driven Bell instability"*, Plasmas, Computation & Mathematics Workshop, 2009, Ambleside

- Gordiets B., E. Tatarova , E.Felizardo, J. Henriques , F. M. Dias, and C. M. Ferreira, *"Microwave Air Plasma Torch"*, Proceed. 2nd Workshop on "Plasmas for Environmental Issues", 36th EPS Conference on Plasma Physics, July 2009, Sofia, Bulgaria (to appear)

- Guerra V., K Kutasi, P. A. Sá, and J. Loureiro, *"Kinetic Modeling of a Ar-O_2 Flowing Afterglow for Plasma Sterilization"*, MD – 7: 7th International Workshop on Microwave Discharges: Fundamentals and Applications, 5, Hamana-Iake, Japan, September 2009.

- Guerra V., "*Atom recombination at surfaces", XXIX ICPIG* (29th International Conference on Phenomena in Ionized Gases), Cancún, México, Julho de 2009.

- Guerra V., *"Dark sates and energy transfers in the nitrogen pink afterglow"*, International School on True-Nano Plasma Science and Technology, Shizuoka University, Japão, Setembro de 2009.

- Kutasi K., V. Guerra, J. Loureiro, C. D. Pintassilgo and Paulo Sá, *"Plasma Sterilization: the Applicability of Discharge and Post-discharge Plasmas for Medical Sterilization"*, 17th Symposium on Application of Plasma Processes & Visegrad Workshop on Research of Plasma Physics (SAPP XVII), pages 31-34, Hotel Máj, Liptovský Ján, Low Tatras, Slovakia, January 2009.

- Kutasi K., V. Guerra, P. Sá and J. Loureiro, *"UV Radiation in Ar-O_2, N_2-O_2 and Ar-O_2-N_2 Microwave Discharges and Post-discharges"*, 29th International Conference on Phenomena in Ionized Gases (XXIXth ICPIG), PA16-1 – Topical Invited Lectures TA109, Cancún, Mexico, July 2009.

- Lopes NC, "*Laser-plasma electron acceleration at ELI, Light at Extreme Intensities"*, Brasov, Romania, October 2009

- Martins JL, "*Radiation post-processing in PIC codes"*, SPIE Europe Optics + Optoelectronics: Harnessing Relativistic Plasma Waves as Novel Radiation Sources from Terahertz to X-Rays and Beyond, Prague, Czech Republic, April 20–24 2009

- Martins SF, "*Boosted frame PIC simulations of LWFA: ultra-fast modeling of current experiments and first studies of acceleration towards the energy frontier"*, APS-Division of Plasma Physics, Atlanta, GA, USA.

- Martins SF, "*Exploring the future of laser-plasma acceleration with massively parallel simulations in OSIRIS, Light at Extreme Intensities*", Scientific opportunities and

technological issues of the Extreme Light Infrastructure, Romania.

- Martins SF, "*OSIRIS simulations of laser wakefield accelerators: boosted frame, particle injection methods, and radiation"*, 10th International Computational Accelerator Physics Conference, San Francisco, CA, USA.

- Martins SF, "*Particle Acceleration in Astrophysical Plasmas, Kavli Institute for Theoretical Physics"*, Santa Barbara, CA, USA, (2009).

- Silva LO, "*Extreme Plasma Physics"*, 10th Brazilian Meeting on Plasma Physics, November 2009 (Plenary Talk)

- Silva LO, "*Laser electron acceleration: moving towards the energy frontier"*, 36th European Physical Society Conference on Plasma Physics, Sofia (Bulgaria), July 2009 (Plenary Talk)

- Silva LO, "*Relativistic shock formation, ion acceleration, and the prospects for laboratory experiments"*, 12th Marcel Grossmann Meeting, Paris, July 2009

- Silva LO, "*Relativistic shocks with ultra intense beams and in GRBS"*, Second International Conference on High Energy Density Physics, Austin, May 2009

- Silva LO, "*Laser Plasma Accelerators towards the energy frontier with transformative simulations"*, DEISA Extreme Computing/DEISA PRACE Symposium 2009 "HPC Infrastructures for Petascale Applications", Amsterdam (Netherlands), May 2009

- Silva LO, "*Radiation from self-injected beams in the blow-out regime with multi-PW lasers, Harnessing Relativistic Plasmas Waves as Novel Radiation Sources from THz to X-rays and beyond"*, SPIE Europe Conference, Prague (Czech Republic), April 2009

- Silva LO, "*Laser electron acceleration with multi-PW lasers"*, 1st Dresden Exchange oN Laser-plasma Interaction ThEory 09, Dresden (Germany), April 2009

24.2.2.3. Oral Comunications

- Alves E. P., L. Gargaté, R. A. Fonseca, R. Bingham, R. Bamford, L. O. Silva, "*Mini-Magnetospheres: High-Energy Particle Deflection"*, Mini-Magnetosphere Team Meeting, Swedish Institute for Space Physics (Kiruna, Sweden), 18th-21st March 2009.

- Davies J R, "*Experimental studies of fast ignition physics"*, ULIS 2009, May 2009, Frascati, Italy

- Dias F. M., J. Henriques, E. Felizardo, E. Tatarova, and C. M. Ferreira, "*Microwave plasma torches driven by surface waves"*, Proceed. VIIth International Workshop on Microwave Discharges: Fundamentals and Applications, Hamamatsu, Japan 2009 (to be published).

- Gregório J., O.Leroy, P.Leprince, L.L.Alves and C.Boisse-Laporte, *"Microwave micro-plasma sources at atmospheric pressure: experiments and simulations"*, Proceed. 17th International Colloquium on Plasma Processes (Société Française du Vide, ed.), Marseille, France 2009, p.6.

- Guerra V., P. A. Sá and J. Loureiro, *"Self-consistent Kinetic Modeling of Ar-O_2 Discharges"*, 36th European Physical Society (EPS) Conference on Plasma Physics, Europhysics Conference Abstracts **33E** O-4.036 – oral communication), Sofia, Bulgaria, June 29-July 3, 2009.

- Martins SF et al, "*Laser-Plasma Accelerators and the Energy Frontier"*, Laser Plasma Accelerator Workshop, Kardamyli, Greece, June (2009).

- Martins SF et al, "*Boosted frame PIC simulations of LWFA: Towards the energy frontier"*, Particle Accelerator Conference, Vancouver, Canada, May (2009)

- Sousa J. Santos, G. Bauville, B. Lacour, V. Puech, M. Touzeau and J.-L. Ravanat, *"Microplasmas Production of Singlet Oxygen at Atmospheric Pressure for DNA Oxidation"*, 5th International Workshop on Fundamentals and Applications of Microplasmas, San Diego, California, USA 2009.

- Sousa J. Santos, G. Bauville, B. Lacour, V. Puech, M. Touzeau and J.-L. Ravanat, *"Atmospheric Pressure Generation of Singlet Oxygen by Arrays of Microplasmas for DNA Oxidation"*, 62nd Gaseous Electronics Conference, Saratoga Springs, NY, USA 2009; Bull. Am. Phys. Soc. **54**, 64 (2009).

- Tatarova E., E. Felizardo, F. M. Dias, B. Gordiets and C.M. Ferreira, *"Hot and Super-Hot Atoms in Microwave Plasmas"*, Proceed. 36th EPS Conference on Plasma Physics, July 2009, Sofia, Bulgaria.

24.2.3. Numerical codes

- Alves L.L. and V. Guerra, Kinetic model for OES transitions in nitrogen plasmas.

- Gregório J. and L.L. Alves, 1D fluid model for Microwave Micro-Plasmas (including thermal description).

- Numerical code for low-pressure, microwave hydrogen plasmas – hot and super-hot atom generation and excited state population distribution.

- Generation of synthetic Balmer (H_γ, H_δ, H_ε, H_ζ, H_η) line spectra taking into account Doppler, Stark, van der Waals , instrumental and fine structure broadening.

- Numerical code for Abel inversion of radially resolved measurement of the Balmer H_γ line.

- Numerical code developed in MatLab to handle phase and amplitude signals collected by an intereferogram setup to determine wave characteristics.

- Numerical code for the kinetics of Ar - O2 – N2 plasma mixtures.

- Numerical code STS2 for the simulation of high-speed shocks using the state-to-state approach.

- Numerical code SPARTAN for the simulation of radiation from nonequilibrium high-T plasmas.

- 1D fluid model for Microwave Micro-Plasmas (including thermal description).

- Kinetic model for OES transitions in nitrogen plasmas.

24.2.4. Laboratorial Prototypes

- Water–Methanol atmospheric pressure plasmas torch (system for argon bubbling through methanol).

- 2D imaging system for radially resolved measurements of "super hot" hydrogen atoms in hydrogen microwave plasmas.

- Mass analyser setup for measurements of H_2 production.

- Atmospheric plasma torches driven by surface waves - Setup for dispersion characteristics measurements.

24.2.5. Technical Reports

- M. Lino da Silva: EXOMARS Phase B2: Simulation of the Radiative Flowfield Surrounding the EXOMARS Spacecraft

24.2.6. Advisory Boards

- Ferreira C. M., member of the Scientific Council for Exact Sciences and Engineering of the *Fundação para a Ciência e a Tecnologia (FCT).*

- Alves LL, Programme National en Nanosciences et Nanotechnologies (PNANO), consultant on Plasma modelling and simulation for material treatment, Agence Nationale de la Recherche (ANR), France

24.2.7. Board of Scientific Journals

- Alves LL, European Physical Journal – Applied Physics (EDP Sciences, ed.), Associated Editor (Section "Plasmas discharges and processes")

24.2.8. Organizing Committees of Conferences

- Tatarova E., chair Organizing Committee of the 2nd Wokshop on "Plasmas for Environmental Issues", a satellite meeting of the 36th EPS Conference on Plasma Physics, Sofia, Bulgaria, July 2009.

- Alves LL, member of the Program Committee of the 21st ICNSP, International Conference on the Numerical Simulation of Plasmas, Lisbon, 6-9 October 2009

- Alves LL, member of the International Scientific Committee of the CIP, International Colloquium on Plasma Processes, Marseille, 22-26 June 2009

- Guerra V., member of the International Organizing Committee of the 2nd Wokshop on "Plasmas for Environmental Issues", a satellite meeting of the 36th EPS Conference on Plasma Physics, Sofia, Bulgaria, July 2009.

- Guerra V., member of the International Scientific Committee of ESCAMPIG

- Guerra V., member of the International Scientific Committee of European Plasma Conference HTTP

- Guerra V., member of the International Scientific Committee of SPIG- Summer School and International Symposium on the Physics of Ionized Gases.

- Spring School in Advanced Computing TACC @ IST

- Participation in the organization of the LEI Conference as part of WP9 in the ELI-PP project

24.2.9. Supervision and training of students

- Edgar Felizardo, *"Experimental investigation of hydrogen containing plasmas",* PhD student at IST; Supervisor: Tatarova E.

- Mariana Pencheva, *"Modelling of surface wave discharges at high pressure"*, PhD student at Sofia University; Supervisor: Tatarova E. and Benova E.

- Kaloyan Pavlov, *"Experiments on atmospheric pressure surface wave discharges",* MSc student at Sofia University; Supervisors: Tatarova E. and Benova E.

- José Gregório, *"Micro-wave system for the production of mini-plasmas at atmospheric pressure",* PhD student (FCT-SFRH/BD/29294/2006), Supervisors: Alves LL and Boisse-Laporte C

- João Santos e Sousa, *"Micro-hollow cathode discharges for the production of intense flows of reactive species",* PhD student (FCT-SFRH/BD/28668/2006), Supervisors: Alves LL and Puech V

- Miguel Santos, *"Transporte de radiação numa tocha a plasma",* BSc student (BII IPFN/IST-FCT), Supervisor: Alves LLRui Tomás, "Modelização de uma tocha microndas a plasma", MSc student (BIC with FCT-SFRH/BD/28668/2006), Supervisor: Alves LL

24.2.10. Participation in the Scientific Committee of Conferences and Workshops

- M. Fajardo, Since 2006: Scientific Board for Workshop Radiative Properties of Hot Dense Matter, R. W. Lee e S. Rose. Next edition 2010, Marbella

- M. Fajardo, 2009: LEI 2009 Light at Extreme Intensities, Scientific opportunities and technological issues of the Extreme Light Infrastructure, October 16 - 21, 2009, Brasov, Romania

- M. Fajardo, Organizing Committee Co-chair and International Scientific Committee member 2009: Scientific Committee of 2nd International Conference on Ultra-Intense Laser Interaction Sciences (ULIS), Frascati, Italy, May 2009

- M. Fajardo, 2009: International Program Committee of "X-ray Free Electron Laser High Energy Density Science workshop" March 2009, St Catherine's College Oxford

- R. A. Fonseca, Chairman of the 21st International Conference on Numerical Simulation of Plasmas, ICNSP'09 (http://icnsp09.ist.utl.pt/)

- L. O. Silva, chairman of the Spring School in Advanced Computing TACC @ IST, May 2009

- L. O. Silva, Member of the Selection Committee of the John Dawson PhD Thesis Prize on Laser and Plasma Accelerators 2009

- L. O. Silva, Member of the Scientific Committee of the 20th International Conference on the Numerical Simulation of Plasmas, October 2009

- L. O. Silva, Member of the International Advisory Committee of Coulomb 09 - Ions Acceleration with high Power Lasers: Physics and Applications, Senigallia (Italy), June 2009

- L. O. SIlva, Member of the Programme Committee, Harnessing Relativistic Plasmas Waves as Novel Radiation Sources from THz to X-rays and beyond, SPIE Europe Conference, Prague (Czech Republic), April 2009

- L. O. Silva, Member of the Programme Committee of the 2nd Symposium on Laser-Driven Relativistic Plasmas applied to Science, Industry and Medicine, Kyoto (Japan), January 2009

24.2.11. Patents

- Fiuza F and Silva LO, Apparatus and method for the generation of synchrotron radiation in plasmas, PT104198, 2008 (granted 2009)

24.2.12. PhD thesis completed

- J. Wemans, Ytterbium-doped laser materials pumped by diodes, Instituto Superior Técnico, Supervisor: Gonçalo Figueira. Sep. 2009

- L. Gargaté, Hybrid Simulations and Theory of Artificial Magnetospheres and Particle Acceleration in Laboratory and Space Plasmas, Instituto Superior Técnico, Supervisor: L. O. Silva, July 2009

24.2.13. MSc thesis completed

- Celso P. João, Novos materiais para amplificadores laser: amplificadores de itérbio bombeados por díodos, Supervisor: Gonçalo Figueira. Jun. 2009.

24.2.14. Board of Scientific Journals and Editor

- Figueira G., Assistant Editorial Director at "Gazeta de Física"

- 2009 ELI Courier, IOP Publishing ISSN 2041-9023. Chief Editor P. Antici., Editorial committee: A. Dujardin, M. Fajardo, K. Osvay, C. Russo

- Fonseca R. A., L. L. Alves, J. P. Bizarro, Guest Editors for IEEE Transactions on Plasma Science, Special Issue on Numerical Simulation of Plasmas

24.2.15. Projects/funding awarded in 2009

- Figueira G. (PI), FCT project PTDC/FIS/71101/2006 (after re-evaluation), Jan. 2009-Dec. 2010

- Silva L.O. (PI), NVIDIA Professorship Awards, in-kind grant, Jan 2009- Dec 2009

- Silva L.O. (PI), LIMA, DECI Award of 1.5 M cpu hours for BlueGene/P in Jülich

24.2.16. Individual fellowships awarded in 2009

- Hugo Pires, PhD fellowship from FCT (start 2009)

- Fajardo M., Poste d'accueil de Direction Générale Adjointe à la Recherche (14 scholarships/year for Ecole Polytechnique) Invited sénior scientist, Laboratoire d'Optique Appliquée, 2009-2010

- Gargaté L. was awarded a Postdoctoral Research Associate Fellowship from Princeton University, Department of Astrophysical Sciences

- Vranic M., PhD fellowship from FCT (start 2010)

24.2.17. Refereeing of journal papers and Popular accounts of research in the media

- Several members of the group are regular reviewers of papers submitted to J. Phys. D: Appl. Phys., Plasma Sources Sci. Technol., J. Appl. Phys., Int. J. Hydrogen Energy, Plasma Phys. Controlled Fusion, etc.

- For paper in Nature Physics (transparent aluminium) in several portuguese and international newspapers.

- For APS fellowship in several portuguese newspapers, including i and Correio da Manhã.

- For DEISA award for computing time in Jugene (Jülich) in newspaper "Público".

- Press release of the APS Division of Plasma Physics for the talk of S. Martins on the boosted frame simulations as one of the highlights of the meeting.

- The cover image of this report has been used in the 2010 calendar for the ANL supercomputer center.

- Fiuza F and Silva LO, High-intensity synchrotron radiation from compact magnetic-plasma structures, SPIE newsroom, JUN 2009.

24.2.18. Short-term visitors

- F. Krausz (LMU and MPQ), D. Jarozinski (Strathclyde), R. Bingham (RAL and Strathclyde), M. Dieckmann (Bochum), J. Hein (FSU Jena), V. Decyk (UCLA), F. Tsung (UCLA), M. Tzoufras (Oxford), B. Afeyan (Polymath), J. Kindel (U Nevada), A. Stockem (Bochum), P. V. Nickles (MBI), C.

Mendes (Salamanca), G. Lambert (LOA), P. Norreys (RAL), K. Lancaster (RAL), R. Scott (RAL), F. Perez (LULI), J. Santos (CELIA)

24.2.19. Long-term visitors

- A. Sgattoni (Bologna U)

24.2.20. Other activities

- G. Figueira, coordinator of Corporate Image Office of IPFN. Development of institutional webpage, stationery, promotional and recruitment material.

- M. Marti participated in the Scalasca Performance Analysis Toolset, Amsterdam, The Netherlands, November 3 -4, 2009

- M. Marti and S. Martins participated in the JSC Blue Gene/P Extreme Scaling Workshop, Jüich, Germany, October 26 - 28, 2009